University Library

A gateway to Melbourne's research publications

Minerva Access is the Institutional Repository of The University of Melbourne

Author/s:
Wibawa, Rachelia Raissa

Title:
Legionella pneumophila: from amoeba to macrophage metabolism

Date:
2020

Persistent Link:
https://hdl.handle.net/11343/252840

Terms and Conditions:
Terms and Conditions: Copyright in works deposited in Minerva Access is retained by the copyright owner. The work may not be altered without permission from the copyright owner. Readers may only download, print and save electronic copies of whole works for their own personal non-commercial use. Any use that exceeds these limits requires permission from the copyright owner. Attribution is essential when quoting or paraphrasing from these works.

Legionella pneumophila: from amoeba to macrophage metabolism

Rachelia Raissa Wibawa

0000-0002-5173-5053

Doctor of Philosophy

May 2020

Faculty of Medicine, Dentistry, and Health Sciences

Department of Microbiology and Immunology

Submitted in total fulfilment for the degree of
Doctor of Philosophy

ABSTRACT

Legionella pneumophila is an aquatic bacterium that has emerged as an accidental human pathogen. Within the aquatic environment, *L. pneumophila* has evolved virulence factors to survive predation by environmental amoebae. These virulence factors are hypothesised to allow the adaptation of the bacteria to replicate in human alveolar macrophages. During infection, *L. pneumophila* forms a replicative vacuole termed the *Legionella*-containing vacuole (LCV) that sustains the bacterial intracellular replication. Establishment of the LCV requires the Dot/Icm type IV secretion system (T4SS), that secretes over 330 bacterial proteins termed effectors into the infected host cell in order to manipulate host processes and facilitate bacterial replication. Despite their central role in LCV biogenesis, to date most effector proteins remain uncharacterised. Therefore, to aid in the characterisation of Dot/Icm effector proteins, in this study, we generated large genomic region mutants. To date, we have created nine genomic deletion mutants (ΔA-ΔI), as well as two multiple-region deletion mutants (ΔFGHI and ΔDFGHI) in *L. pneumophila*, resulting in the deletion of 68 effector genes and 138 non-effector genes.

These mutants were then used to identify the genomic regions important for bacterial replication *in vitro* and *in vivo.* Despite the loss of up to 42 effector-encoding genes, all mutants can replicate efficiently in THP1 macrophages. Meanwhile, in the protozoan host, at least six mutants showed a severe replication defect. Interestingly, in the mouse model, four mutants displayed an unexpected increase in bacterial burden, while one mutant showed a reduction in bacterial replication. Surprisingly, two of the mutants showing an increase in bacterial load in the mouse model were unable to replicate in *Acanthamoeba castellanii*. Together, these highlight the difference in requirements to survive in different hosts. This also suggests that the large effector repertoire of the Dot/Icm T4SS effectors likely evolved to enable an intracellular lifestyle in a diverse range of hosts.

Finally, the mutants were also used to identify a Dot/Icm effector protein that degraded host *GAPDH* mRNA. RNA sequencing of infected cells revealed that *L. pneumophila* downregulated multiple host glycolytic mRNAs which depended on a particular Dot/Icm

effector. Taken together, this project has used mutants carrying large genomic deletions to identify genetic regions important for bacterial replication, as well as those manipulating host immune defence.

DECLARATION

This is to certify that:

i. This thesis comprises only my original work towards the Doctor of Philosophy except where indicated in the preface

ii. Due acknowledgement has been made in the text to all other material used

iii. This thesis is fewer than 100,000 words in length, exclusive of tables, maps, bibliographies and appendices

Rachelia Raissa Wibawa
Department of Microbiology and Immunology
The University of Melbourne

PREFACE

In accordance with the regulations of the University of Melbourne, I acknowledge that some of the work presented in this thesis was collaborative. Specifically:

- In chapter 3, the generation of large genomic region mutants was conducted in collaboration with Pengfei Li.
- In chapter 3, the replication of mutants in *Acanthamoeba castellanii* was performed by Pengfei Li.
- In chapter 3, whole genome sequencing and SNP calling were performed by Dr Sacha Pidot.
- In chapter 4, the replication of Δ*legC4* and cytokine response against Δ*legC4* in C57BL/6 mice were performed by Dr Garrett Ng.
- In chapters 4 and 5, ΔE1, ΔE2, ΔE3, ΔE4, ΔE2-1, ΔE2-2, ΔE2-3, and Δ*legC4* strains were created by Dr Kathleen McCaffrey.
- In chapter 4, Δ*lpw_04831,* Δ*lpw_04841,* Δ*lpw_04851,* and Δ*lpw_04861* were created by Pengfei Li.
- In chapter 5, all QRT-PCR experiments and sample preparation for the RNAseq were performed by Dr Kathleen McCaffrey.
- In chapter 5, RNA sequencing was performed by the Australian Genome Research Facility (AGRF).
- In chapter 5, the genome alignment and read count generation for RNA sequencing data was performed by Dr Dane Vassiliadis.

The remainder of this thesis comprises of only my original work.

This thesis also contains material that is published or is currently in preparation for publication:

Li P, Wibawa RR, Ong SY, Pidot S, Stinear T, Pasricha S, Hartland EL (2020). Large genomic region deletions in *Legionella pneumophila* identifies new genes influencing bacterial replication and *Acanthamoeba castellanii* encystment.

McCaffrey K, Wibawa RR, Ng GZ, Pasricha S, Hartland EL (2020). *Legionella pneumophila* Dot/Icm T4SS effector LegC4 degrades a subset of host mRNAs enriched for glycolytic enzymes.

ACKNOWLEDGMENTS

Firstly, I would like to thank Liz for the opportunity she has given me to undertake projects in her lab since I was a third-year undergraduate student, and allowed me to do more projects in Honours and PhD. I am really grateful for your trust in me. I am also grateful for your supervision, guidance and for giving me ideas especially when my project was yielding negative results throughout my second and third years. Thank you so much for your patience and kindness. Also, thank you for the examples of hard work and integrity. I am very lucky to have you as my supervisor.

I also want to thank my co-supervisor Shiv for your supervision and mentoring since I first started in the lab. I really appreciate your supervision and guidance throughout my project. I am really grateful for your optimism, creativity, and ability to think out of the box. Thank you so much for teaching me not only academic/technical skills, but also life skills, how to balance work and life, and how to cope when things go wrong. I have really learned a lot from you, and I think I will never become the scientist I am today without your guidance. I am really thankful to have you as my supervisor; I really don't think I can go through my PhD if it were not for you. Also special thanks to your husband Dane for helping with the RNA-seq analysis!

Thank you also to Kitty, who has kindly allowed me to join her in the LegC4 project. Thank you so much for your help and patience, especially with RNA techniques and QRT-PCR. Also, thank you for sharing your wisdom and insightful knowledge. You have been very generous with your time and knowledge. Thank you also for helping in reading and correcting my thesis. Thank you for showing me how to properly build an argument and how to use words more efficiently.

I also want to thank Ying for your guidance in the *Legionella* work. You are very knowledgeable about *Legionella* and are really good with technical skills. Thank you for your patience whenever I ask too many questions. Thank you for helping me to develop accurate lab skills. I still remember doing replication assays side by side with you so many times, until my hideous error bars shrink. I also want to thank you for your help in reading and correcting my thesis. I think my thesis would have been an embarrassment if it were

not for your help. Thank you also for the occasional ride home, so that I don't get kidnapped after late days in the lab.

Thank you also to Ian, who has allowed me to do the mouse work in his lab. Thank you for your generosity and suggestions for the work. Thank you for allowing me to have the experience in animal work, I really don't think my PhD will ever be complete without your help.

I would also like to thank Garrett, who has guided me through the animal experiment world. I am really lucky to have you around. You are one of the most efficient and knowledgeable person that I know. Thank you for your patience, especially when I ask too many questions. Thank you so much for your generosity with time and knowledge. I really do appreciate your suggestions and guidance. Also, thank you for sparing your time to read and correct my thesis, and help transforming my incoherent paragraphs into more solid arguments.

Thank you also to my PhD committee, Jason, Hayley, and Cristina. You all have been really helpful and fantastic. Thank you so much for your time, ideas, and suggestions. I would never have reached this stage if it were not for your help.

I also want to thank Pengfei, with whom I share the large genomic deletion mutants project. Thank you for working your magic hands in cloning, without your help this project will never have finished. Thank you also for the discussions regarding our project and life in general. I really appreciate having you around. Your hardworking attitude is an inspiration for me especially when I feel lazy and unmotivated.

I also want to thank my PhD buddies, Pengfei, Yoges, Linda, and Jiyao. You guys have made my PhD journey much more fun! Thank you for the friendship, for the spontaneous coffee run, the gatherings, and dinners after a tiring day at work.

Thank you also to all Hartland/Van Driel lab members for welcoming me in the lab and providing a great environment to work in. Thank you Cristina, Gina, Tania, Ying Z, Clare, Vicki, Max, Nick, Abdou, Jac, Josh, Anastasia, Victoria, Wendy, Markus, Andrew, Sarah, Jackie, and Manal, for your presence in the lab. I am really lucky to have you all as my labmates. It is a real pleasure to work with smart and passionate people like you.

Thank you also for the lab social events; the birthday celebrations, lab lunches, and occasional morning teas.

Last but not least, I want to thank my family and friends for your ongoing support throughout my PhD. Thank you for listening to my complaints and for bearing with me, especially when I was stressed and grumpy. Adit, thank you for being such a hardworking and successful person. I am really proud of you and am looking up to you whenever I feel tired with life. Dion and Michael, thank you for being my sources of joy. Even though you are annoying, it is fun to talk to you. Thank you also for the random jokes and dog pictures. Papi, mami, terima kasih sudah menyekolahkan aku ke Australia. Terima kasih juga karena papi mami selalu mendengarkan dan mensupport aku ketika ada masalah. Juga terima kasih untuk doa papi mami, aku yakin aku tidak akan bisa menyelesaikan PhD ini kalau bukan karena papi dan mami.

ABBREVIATIONS

The following abbreviations are used throughout the thesis:

%	Percentage
~	Approximately
°C	Degrees Celcius
A_{600}	Absorbance at 600 nm
ACES	N-(2-acetamido)-2-aminoethanesulfonic acid
ADP	Adenosine diphosphate
AEC	Airway epithelial cell
AIM2	Absent in melanoma 2
ALDO	Aldolase
AM	Alveolar macrophage
ARF	ADP ribosylation factor
ASC	Apoptosis-associated speck-like protein containing CARD domain
ATP	Adenosine triphosphate
BCYE	Black charcoal yeast extract
Bp	Base pair
CARD	Caspase recruitment domain
Cas	Caspase
cDC	Conventional dendritic cell
CFU	Colony-forming unit
CRISPR	Clustered regularly interspaced short palindromic repeats
DC	Dendritic cell
Da	Dalton
dH_2O	Distilled water
DNA	Deoxyribonucleic acid
dNTP	Deoxynucleotide triphosphate
DMSO	Dimethyl sulfoxide
ENO	Enolase
ER	Endoplasmic reticulum
FBP1	Fructose bisphosphatase 1

FBS	Foetal bovine serum
G6PD	Glucose-6-phosphate dehydrogenase
GAP	GTPase activating protein
GAPDH	Glyceraldehyde 3-phosphate dehydrogenase
GDP	Guanosine diphosphate
GEF	Guanine nucleotide exchange factor
GPI	Glucose-6-phosphate isomerase
GTP	Guanosine triphosphate
h	Hour
HA	Haemagglutinin
HK	Hexokinase
hpi	Hour post-infection
IFN	Interferon
IκB	Inhibitor of NF-κB
IL	Interleukin
kDa	Kilodalton
kbp	Kilo base pair
LAMP-1	Lysosomal-associated membrane protein 1
LB	Luria-Bertani
LCV	*Legionella*-containing vacuole
LDH	Lactate dehydrogenase
LFC	Log_2 fold change
LPS	Lipopolysaccharide
LRR	Leucine-rich repeat
MAPK	Mitogen-activated protein kinase
Mbp	Mega base pair
MC	Monocyte-derived cell
MHC	Major histocompatibility complex
Min	Minute
MOI	Multiplicity of infection
MPI	Mannose phosphate isomerase
mRNA	Messenger RNA

MyD88	Myeloid differentiation primary response gene 88
NAD	Nicotinamide adenosine dinucleotide
NADP	Nicotinamide adenosine dinucleotide phosphate
NK	Natural killer
NF-κB	Nuclear factor kappa-light-chain-enhancer of activated B cells
NLR	Nod-like receptor
NLRC	Nod-like receptor CARD domain containing
NLRP	Nod-like receptor pyrin domain containing
Nm	Nanometer
OD	Optical density
OD_{600}	Optical density at 600 nm
OXPHOS	Oxidative phosphorylation
PADJ	Adjusted p-value
PAMP	Pathogen-associated molecular pattern
PCA	Principal component analysis
PCR	Polymerase chain reaction
PDH	Pyruvate dehydrogenase
PFK	Phosphofructokinase
PI3K	Phosphatidylinositol-3 kinase
PI(3)P	Phosphatidylinositol (3) phosphate
$PI(3,4)P_2$	Phosphatidylinositol (3,4) bisphosphate
$PI(3,4,5)P_3$	Phosphatidylinositol (3,4,5) triphosphate
PI(4)P	Phosphatidylinositol (4) phosphate
$PI(4,5)P_2$	Phosphatidylinositol (4,5) bisphosphate
PGK	Phosphoglycerate kinase
PK	Pyruvate kinase
PRR	Pattern recognition receptor
QRT-PCR	Quantitative real-time PCR
RNA	Ribonucleic acid
RNAseq	RNA sequencing
rRNA	Ribosomal RNA
RT	Room temperature

SEM	Standard error of the mean
siRNA	Short interfering RNA
SNARE	Soluble N-ethylmaleimide-sensitive factor activating protein receptor
snRNA	Small non-coding RNA
snRNP	Small non-coding ribonucleoprotein
T1SS	Type 1 secretion system
T2SS	Type 2 secretion system
T4SS	Type 4 secretion system
Tat	Twin arginine translocation
TCA	Tricarboxylic acid
TLR	Toll-like receptor
TNF	Tumour necrosis factor
V	Volt
v/v	Volume/volume
w/v	Weight/volume
WT	Wild type

TABLE OF CONTENTS

ABSTRACT ..... **i**
DECLARATION ..... **iii**
PREFACE ..... **iv**
ACKNOWLEDGMENTS ..... **vi**
ABBREVIATIONS ..... **ix**
TABLE OF CONTENTS ..... **xiii**
LIST OF TABLES AND FIGURES ..... **xvii**
Chapter 1 Literature Review **1**
1.1 Historical background **1**
1.2 *Legionella spp* **1**
1.3 Legionellosis **2**
1.3.1 Clinical manifestations 2
1.3.2 Epidemiology and risk factors 3
1.4 Ecology of *Legionella spp* **4**
1.5 Genome of *Legionella spp* **5**
1.6 *L. pneumophila* infection strategy **7**
1.6.1. Entry into host cells 7
1.6.2. Legionella-containing vacuole (LCV) formation 8
1.6.3 Exit from host cells 12
1.7 Immunity to *L. pneumophila* infection **13**
1.7.1 Pattern recognition receptors (PRRs) 13
1.7.2 Immune cell response 16
1.7.3 Cytokine response 18
1.8 Secretion systems of *L. pneumophila* **20**
1.8.1. Lss type 1 secretion system (T1SS) 20
1.8.2 Lsp type 2 secretion system (T2SS) 21
1.8.3 Type 4 secretion systems (T4SSs) 22
1.9 Modulation of host processes by Dot/Icm effectors **24**
1.9.1 Dot/Icm effectors and avoidance of phagosome acidification 24
1.9.2 Dot/Icm effectors and PI lipid tailoring 24
1.9.3 Dot/Icm effectors in ER remodelling and small GTPase modulation 25
1.9.4 Dot/Icm effectors and host immune response 27

1.9.5 Dot/Icm effectors and host cell death 28
1.10 Aims of this study **30**
Chapter 2 Materials and Methods **33**
2.1 Chemicals and reagents **33**
2.2 Bacterial strains, media, and growth conditions **33**
2.3 DNA isolation, purification, and sequencing **34**
2.3.1 Bacterial genomic DNA (gDNA) extraction 34
2.3.2 Plasmid DNA extraction 34
2.3.3 DNA purification 34
2.3.4 Quantification of DNA concentration 34
2.3.5 DNA sequencing 34
2.4 DNA manipulation **35**
2.4.1 Polymerase Chain Reaction (PCR) 35
2.4.2 DNA gel electrophoresis 35
2.4.3 DNA restriction digest and ligation 35
2.4.4 Transformation of E. coli 36
2.5 Genetic manipulation of *L. pneumophila* **36**
2.5.1 Transformation of L. pneumophila 36
2.5.2 L. pneumophila mutants construction 37
2.5.3 Ectopic expression of effector proteins in L. pneumophila 38
2.6 Whole genome sequencing of *L. pneumophila* **38**
2.7 Growth curve of *L. pneumophila* **39**
2.8 Cell culture **39**
2.9 *L. pneumophila* replication assay **40**
2.9.1 L. pneumophila replication assay in THP1 macrophages 40
2.9.2 L. pneumophila replication assay in A. castellanii 40
2.10 TEM-1 β-lactamase translocation assay **41**
2.11 Cell viability assay **41**
2.12 Immunofluorescence **42**
2.13 Quantitative real time (QRT)-PCR **43**
2.14 RNA sequencing **44**
2.15 Animals and animal experiments **44**
2.15.1 Mice 44
2.15.2 Intranasal infection and organ harvesting 45

2.15.3 Preparation of lungs for CFU counting 45
2.16 Flow cytometry **45**
2.16.1 Preparation of cell suspension 46
2.16.2 Staining of phagocyte panel 46
2.16.3 Staining of lymphocyte panel 46
2.17 Cytometric bead array (CBA) **47**
2.18 Bioinformatics prediction and phylogenetic analysis **47**
2.19 Data analysis **48**
Chapter 3 Identification of *L. pneumophila* 130b genes important for *in vitro* infection **67**
3.1 Introduction **67**
3.2 Results **69**
3.2.1 Towards an effector-less mutant library in L. pneumophila 130b 69
3.2.2 Generation of marker-less deletion mutants 70
3.2.3 Growth rate of mutant strains under axenic condition 72
3.2.4 Dot/Icm T4SS functionality in mutant strains 73
3.2.5 Replication of L. pneumophila mutants in THP1 macrophages 74
3.2.6 Replication of L. pneumophila mutants in Acanthamoeba castellanii 74
3.3 Discussion **75**
Chapter 4 Identification of *L. pneumophila* effector regions modulating survival under immune pressure **95**
4.1 Introduction **95**
4.2 Results **97**
4.2.1 Replication of L. pneumophila mutants in IFNγ-stimulated macrophages 97
4.2.2 Viability of THP1 macrophages infected with L. pneumophila mutants 98
4.2.3 L. pneumophila mutants showed a variable phenotype in A-strain mice 99
4.2.4 L. pneumophila ΔFGHI mutant infection did not alter the host pulmonary immune response 100
4.2.5 Lpw_04861 enhanced L. pneumophila clearance from the lungs 100
4.2.6 Regions E1, E3, and E4 were important for L. pneumophila survival in lungs 102
4.2.7 LegC4 enhanced host cytokine response against L. pneumophila infection in A-strain but not C57BL/6 mice 102
4.3 Discussion **103**

Chapter 5 Characterization of the *Legionella pneumophila* Dot/Icm T4SS-effector protein LegC4 137

5.1 Introduction 137

5.2 Results 138

5.2.1 LegC4 downregulates host GAPDH mRNA levels during L. pneumophila infection. 138

5.2.2 GAPDH mRNA downregulation was not due to decreased bacterial fitness 139

5.2.3 LegC4 is translocated by the Dot/Icm T4SS into the host cytosol 139

5.2.4 Bioinformatics analysis of LegC4 140

5.2.5 LegC4 alters the host cell transcriptome during infection 140

5.2.6 LegC4 downregulates genes involved in glucose metabolism 142

5.3 Discussion 143

Chapter 6 Perspective 161

REFERENCES 167

Appendix 1. List of genes deleted in each genomic region and their homologs in Philadelphia-1 strain. 195

LIST OF TABLES AND FIGURES

Figure 1.1. The intracellular lifestyle of *L. pneumophila.* 31
Figure 1.2. Electron micrograph of *L. pneumophila*-infected macrophage..... 32
Table 2.1. Bacterial strains used in this study 49
Table 2.2. Plasmids used in this study..... 51
Table 2.3. Oligonucleotides used in this study..... 53
Table 2.4. Thermocycler reactions used in this study 62
Table 2.5. Buffers used in this study 64
Table 2.6. Antibodies for phagocyte staining panel 65
Table 2.7. Antibodies for lymphocyte staining panel..... 66
Table 3.1. List of designed genomic regions..... 79
Table 3.2. Location, size, and composition of the deleted genomic regions..... 80
Table 3.3. List of SNPs in *L. pneumophila* genomic region mutants..... 81
Table 3.4. Summary of *L. pneumophila* mutants replication phenotype 82
Figure 3.1. Effector-less mutant library design in *L. pneumophila* 130b genome. 83
Figure 3.2. Generation of marker-less deletion mutants. 84
Figure 3.3. Comparison of deleted regions in 130b vs Philadelphia. 90
Figure 3.4. Growth rate of the mutants *in vitro.* 91
Figure 3.5. Functionality of the Dot/Icm T4SS in the mutants. 92
Figure 3.6. Replication of *L. pneumophila* mutants in THP1 macrophages. 93
Figure 3.7. Replication of *L. pneumophila* mutants in *Acanthamoeba castellanii*. 94
Table 4.1. List of SNPs in Δ*lpw_04861* 110
Table 4.2. Sub-regions of genomic region E. 111
Figure 4.1. *L. pneumophila* mutants replicate proficiently in IFNγ-stimulated THP1 macrophages. 113
Figure 4.2. Cells infected with ΔE mutant showed enhanced viability at 48 h post-infection. 115
Figure 4.3. Mutants showed variable phenotypes in A-strain mice..... 117
Figure 4.4. ΔFGHI infection resulted in similar host cytokine response compared to WT infection. 118
Figure 4.5. ΔFGHI displayed no alteration in lung immune response. 120
Figure 4.6. Lpw_04861 may influence the clearance of *L. pneumophila* from A-strain mice lungs. 122
Figure 4.7. Lpw_04861 may influence host cytokine response. 123
Figure 4.8. Infection with ΔB induced an increase in lung phagocyte infiltrate. 125
Figure 4.9. Phylogeny of Lpw_04861. 127
Figure 4.10. Regions E1, E3, and E4 were important for bacterial survival in lungs. . 129
Figure 4.11. LegC4 did not alter *L. pneumophila* survival at day 3 post-infection in A-strain mice. 131
Figure 4.12. LegC4 did not alter aflagellated *L. pneumophila* survival in WT C57BL/6 mice 133
Figure 4.13. LegC4 enhanced host IFNγ production during infection of A-strain mice. 134

Figure 4.14. LegC4 did not influence host cytokine production during infection of WT C57BL/6 mice 136
Table 5.1. Sub-deletions of region E2 147
Table 5.2. List of genes commonly upregulated in Δ*legC4*, ΔE, and Δ*dotA* 148
Figure 5.1. Downregulation of host *GAPDH* mRNA during *L. pneumophila* infection. 151
Figure 5.2. LegC4 downregulates host *GAPDH* mRNA during infection. 152
Figure 5.3. Trans-complementation of LegC4 rescued *GAPDH* downregulation phenotype. 153
Figure 5.4. Δ*legC4* efficiently replicates in THP1 macrophages. 154
Figure 5.5. LegC4 was translocated to host cytosol by the Dot/Icm T4SS. 155
Figure 5.6. *L. pneumophila* alters host transcriptome dependently on LegC4. 158
Figure 5.7. Genes involved in glucose metabolism were upregulated in mutant-infected cells. 159
Figure 5.8. Genes involved in host glycolysis/gluconeogenesis pathway were upregulated in Δ*legC4*-infected cells. 160
Table 6.1. Comparison of *L. pneumophila* mutants phenotypes in different hosts 166

Chapter 1
Literature Review

1.1 Historical background

During the summer of 1976, at the American Legion Convention, an outbreak of severe pneumonia occurred. This disease, termed Legionnaires' disease, affected 182 people, of which 147 people required hospitalization, and 29 people eventually succumbed to the disease (1). A novel Gram-negative bacterium was ultimately isolated in guinea pigs inoculated with patient samples, and subsequently 101 out of 111 tested patients were positive for serum antibody to this bacterium (2). Due to the unique DNA sequence and biochemical characteristics of this novel bacterium, a new family *Legionella*ceae and a new genus *Legionella* were described. In addition, the Legionnaires' disease bacterium was then named *Legionella pneumophila* (3).

Following the discovery of *L. pneumophila*, previous unexplained outbreaks of respiratory disease and sporadic pneumonia cases were retrospectively investigated. In 1965, an outbreak of 81 cases of respiratory illness occurred in Columbia, in which 2 patients died. Examination of stored patient serum revealed the presence of anti-*L. pneumophila* antibody in 21 out of 23 tested samples (2). Additionally, in 1968, 144 people contracted a mysterious respiratory illness in Pontiac, Ohio, characterized with febrile fever and 'flu'-like symptoms. 31 out of 37 patient samples tested also confirmed the presence of anti-*L. pneumophila* antibody (2, 4). Inoculation of guinea pigs with *L. pneumophila* subsequently confirmed the role of this bacterium in the Pontiac outbreak (5).

1.2 *Legionella spp*

Legionella spp are classified into the class gamma-proteobacteria (3). *Legionella spp* comprise Gram-negative rod-shaped bacteria sized between 2-3 μm in length, although a long filamentous form of approximately 50 μm may occasionally be found. The width of

the bacilli ranges between 0.3-0.4 μm (2, 6). *L. pneumophila* also possesses a single polar flagellum, as well as pili, to aid in the bacterial motility and adherence to surfaces (6-9).

Four decades after the discovery of *L. pneumophila*, new *Legionella* species are being continuously described. Currently, with the recent discovery of *Legionella qingyii*, there are 65 species and 80 serogroups of *Legionella* (10-12). However, not all species have been demonstrated to infect humans. In Europe, *L. pneumophila* causes over 90% of *Legionella* infections, whereas in USA, 60% of *Legionella* infections were caused by this species. Further, *L. pneumophila* serogroups 1 and 6 are responsible for more than 60% of *Legionella* infections (13-16). Uniquely, in Australia and New Zealand, 30-50% of *Legionella* cases are caused by *Legionella longbeacheae* (17, 18).

The high prevalence of *L. pneumophila* in clinical samples may partly be caused by the high abundance of *L. pneumophila* in the environment compared to other *Legionella* species. In Europe, non-pneumophila species only made up less than 20% of total *Legionella* isolated from various environmental sources (19-22). Furthermore, in the USA, *L. pneumophila* makes up approximately 53% of environmental *Legionella* species (23). However, despite comprising of only 28% of total environmental *Legionella*, *L. pneumophila* serogroup 1 was responsible for 95% of clinical cases in France (19), suggesting that the virulence of this serogroup also contributes to its increased clinical prevalence.

1.3 Legionellosis

1.3.1 Clinical manifestations

Legionellosis is the umbrella term for diseases caused by *Legionella spp.* This disease may present as a severe atypical pneumonia termed Legionnaires' disease or a less severe disease called Pontiac fever (24). Additionally, in rare occasions, *Legionella spp* also cause septic arthritis, endocarditis, and other soft tissue inflammation (25-29). After exposure to *Legionella spp*, the incubation period ranges from 2-14 days, and possibly

longer in immunocompromised people. The clinical manifestation of Legionnaires' pneumonia may resemble other bacterial pneumonia. There is no specific defining symptom of Legionnaires' disease, as symptoms range from fever, coughing, shortness of breath, myalgia, headache, confusion, diarrhea, and loss of appetite (24, 30). While these symptoms are similar to other nosocomial pneumonia diseases, Legionnaires' disease typically presents more gastrointestinal and neurological symptoms (31). On the other hand, the milder form of legionellosis, Pontiac fever, is characterised with milder symptoms, such as fever, chills, headache, and myalgia (4, 5). Currently it is unclear why legionellosis can manifest in two different diseases. However, it is hypothesized that the inoculation dose, *Legionella* species, and the host immune conditions may contribute to this distinction.

1.3.2 Epidemiology and risk factors

Legionellosis is currently included in the national disease surveillance system of multiple countries, including Australia, USA, Canada, New Zealand, Japan, as well as members of the European Union. The worldwide incidence of legionellosis is approximately 4-25 cases per one million population (13, 17, 18, 32). However, legionellosis is considered underdiagnosed, partly due to the lack of specific symptoms and the tendency to treat pneumonia cases empirically without testing for *Legionella* (14, 24, 31, 33). Noteworthy, over 60% of community-acquired pneumonia patients were not tested for any bacterial pathogen that caused atypical pneumonia (34). Furthermore, perhaps due to the lack of diagnosis and case definition, surveillance of legionellosis is neglected in other countries, therefore the worldwide incidence is currently uncertain (24).

The incidence of legionellosis peaks in the late summer to autumn months, possibly due to the higher relative humidity and warmer temperature (13, 18, 24). Indeed, higher humidity increased *L. pneumophila* survival in aerosols (35-37). In addition, warmer weather improved *L. pneumophila* survival in the aquatic environment (38). Interestingly, in Australia, in addition to the autumn (April-May) peak, an extra peak in spring (October) associated with *L. longbeacheae* infections was also observed, perhaps due to the correlation of spring and increased contact with contaminated gardening soil as, unlike

other *Legionella spp, L. longbeacheae* naturally resides in soil (18). Over 60% of legionellosis cases affected males, and 75-91% of legionellosis cases occur in people older than 50 years of age (13, 18, 24). In addition to age, risk factors for legionellosis include both current and history of smoking, diabetes, chronic obstructive pulmonary disease (COPD), chronic organ disease, heart failure, current immunosuppressant therapy, and alcohol abuse (11, 14, 39).

Legionellosis is associated with a substantial economic and health burden. The median cost for each hospitalized legionellosis patient in the USA is $26,000-$38,000 (40). The hospitalization rate for Legionnaires' disease is 95%, and approximately 44% patients in the USA develop a more severe disease, requiring intensive care (14). Furthermore, Legionnaires' disease is considered one of the top five infectious diseases with high population and individual disease burden (41). Worldwide, the mortality rate of Legionnaires' disease ranges from 4-22% (13, 14, 18, 20, 32). Together, these demonstrate that legionellosis is a significant burden to public health.

1.4 Ecology of *Legionella spp*

Legionella spp are naturally found in various aquatic environments, such as rivers, lakes, and cooling towers of air conditioning systems (19-22). While free-living *L. pneumophila* can survive in tap water for at least one year, there is no evidence of bacterial replication in the absence of other microbes (42). *Legionella spp* are also often found in biofilms (43). Biofilms constitute a community of one or more species of microbes that adheres to a particular surface. Through microbial secretions, nutrients can be sequestered and concentrated within biofilms (44).

While the microbial composition of *Legionella* biofilms is currently unclear, it is known that *L. pneumophila* co-exists with free-living amoeba (FLA) in biofilms, such as *Acanthamoeba spp, Naegleria spp, Vermamoeba spp,* and *Stenamoeba spp* (45-47). In laboratory-made biofilms where these FLAs are absent, *L. pneumophila* is unable to replicate, although the bacteria can remain viable for at least one month (48, 49). FLAs typically prey on bacteria. Upon predation, *L. pneumophila* can resist killing and replicate

intracellularly within these amoebae (50). Incubation of amoebae with the viable but not culturable (VBNC) form of *L. pneumophila,* which is induced under stressful conditions such as nutrient starvation, restored bacterial replication, suggesting that amoebae provide nutrients and a replicative niche for environmental *L. pneumophila* (51-53). Additionally, the intracellular replication in amoebae also enhanced the survival of *L. pneumophila* in the presence of biocides, ultraviolet (UV) light, chlorine, and heat (54-57).

Amoebae may also contribute to the transmission of *L. pneumophila*. Upon infection with *L. pneumophila*, amoebae releases *L. pneumophila*-containing vesicles of respirable sizes to the environment, suggesting the possibility that these vesicles can enhance bacterial transmission (58, 59). These vesicles are estimated to contain up to 1,365 live bacteria, and may protect the bacteria from environmental challenges and enhance resistance to biocides (58, 60). As such, it is generally thought that amoebae act as a reservoir and 'Trojan horse' of environmental *L. pneumophila* (61).

The survival of *L. pneumophila* in protozoan hosts is also thought to allow *L. pneumophila* to infect humans. Notably, the intracellular replication of *L. pneumophila* in amoebae and human cells are highly similar, as the same virulence factors facilitate the bacterial replication in similar fashion (62, 63). In addition, *L. pneumophila* displays enhanced virulence in human cells after passaging through amoebae (64). For example, *L. pneumophila* recovered after infection with *Vermamoeba vermiformis* (previously known as *Hartmanella vermiformis* (65)) were more infectious and lethal than agar medium-grown *L. pneumophila* during infection of mice (66). Together, these suggest that the virulence factors that evolved during the adaptation of *L. pneumophila* to living in the protozoan host contribute to bacterial virulence in human hosts.

1.5 Genome of *Legionella spp*

Legionella spp possess one circular chromosome sized between 2.7-4.9 Mbp, with an average G+C content of 34-51% (67-71). Some species or strains of *Legionella,* such as *L. dumoffii, L. jamestowniensis,* and *L. pneumophila* strains Paris and Lens, also carry plasmids, whereas others, such as *L. pneumophila* 130b strain, do not (67, 69).

Additionally, *Legionella* may also carry episomal or plasmid-like mobile elements which can either be integrated in the chromosome or carried in plasmid (67, 68).

The genomes of *Legionella spp* display high diversity and plasticity. Only 6% of orthologous genes in the pan-genome of 58 species are present in the core genome (72). Furthermore, studies have suggested that the *Legionella spp* pan-genome remains "open", implying that the pan-genome will grow larger with the increase in sequenced strains or species (72, 73). Indeed, compared to the analysis of 38 or 43 *Legionella spp* genomes, analysis of 80 *Legionella spp* genomes resulted in a larger number of orthologous clusters, but a smaller percentage of these genes is conserved amongst these 80 species (72-74). Multiple factors may contribute to the genome diversity. Firstly, numerous mobile genetic elements, insertion sequences, and transposases are present in the *Legionella spp* genomes (67-69, 72, 75). These elements may facilitate the movement of genetic elements throughout the genome, thus creating diversity. Secondly, mutations may also contribute to the diversification. For instance, several *Legionella* species underwent gene pseudogenization through nonsense mutation acquisition (74). Thirdly, genetic recombination also plays a major role in the diversification of *Legionella spp* genome (73, 75, 76). For instance, genome analysis of 69 outbreak-associated *Legionella spp* isolates in Spain revealed that 16 recombination events were responsible for 98% of single nucleotide polymorphisms (SNPs) diversity (76). Uniquely, while a significant level of homologous recombination occurred between strains of the same species, there is little recombination between different clades of *Legionella spp*, perhaps suggesting an inter-clade barrier to DNA exchange (73).

Foreign DNA may be incorporated into the genome of *L. pneumophila* through horizontal gene transfer (HGT). Multiple studies have reported the presence of genomic regions within the *Legionella spp* genomes with distinct G+C content, suggesting that these regions may be acquired from organisms of different species (67-69, 72, 74). Frequent HGT also leads to the reduction of the G+C content as genome size increases (77). Consistently, analysis of multiple *Legionella* species showed that the size of the genome was inversely correlated with the G+C content, suggesting frequent HGT (72). Finally, multiple eukaryotic domains or eukaryotic-like proteins typically not found in the

prokaryotic genomes were also found in the genomes of *Legionella spp* (67, 72, 74). For instance, a recent study discovered 184 eukaryotic small GTPases in the pan-genome of 58 *Legionella spp* sequences, 149 of which were exclusively found in *Legionella spp* and eukaryotes. Phylogenetic analysis then revealed the acquisition of 16 *Legionella spp* Rab GTPases from protozoa (72). In addition to the small GTPases, genes encoding for proteins containing eukaryotic domains, such as F-box, U-box, or ankyrin domains were also found in the genome of *Legionella spp*. These eukaryotic domains may also be present in multiple combinations, thus improving the diversity of *Legionella spp* genome (72, 74).

1.6 *L. pneumophila* infection strategy

After entry into the host cells, *L. pneumophila* forms a specialized vacuole termed *Legionella*-containing vacuole (LCV) where the bacteria can replicate to a high titer before exiting the host cells (**Figure 1.1**). This section details the processes that occur during the intracellular lifestyle of *L. pneumophila*.

1.6.1. Entry into host cells

In mammals, the alveolar macrophages are considered the primary replication niche of *L. pneumophila* (78, 79). *L. pneumophila* enters macrophages via conventional phagocytosis (80), although another type of phagocytosis, termed coiling phagocytosis, has also been reported (81). This is a unique process in which microbes are internalized via unilateral, coiling pseudopods, resulting in the engulfment of the bacteria in phagosomes (82). The complement system has also been reported to aid in the entry of *L. pneumophila* (83). The action of complement 3 (C3) leads to opsonization of the bacteria, which are then internalized through complement receptors (CRs) (84). Antibodies to CR1 and CR3 reduced the uptake of *L. pneumophila* into monocytes (83). While the level of complement components in the lungs are low during naïve conditions, exposure to LPS increases the expression of complement in the lungs, including C3, perhaps suggesting a role for this process during advanced stages of infection (85, 86).

Phosphatidylinositol-3-kinase (PI3K) is known to be important for the closure of phagosomes during phagocytosis (87). However, the importance of PI3K in *L. pneumophila* phagocytosis is currently unclear. One study found that pharmacological inhibition of PI3K using either LY294002 or wortmannin led to a reduction in the phagocytosis of non-opsonized *L. pneumophila* during infection of J774A.1 murine macrophage cell line. Cells deficient in the PI3K p85 (*p85*$^{-/-}$) also displayed reduced uptake of *L. pneumophila* (88). However, other studies showed that wortmannin inhibition only reduced the phagocytosis of avirulent *L. pneumophila*, not WT *L. pneumophila* in *Dictyostelium discoideum*, a commonly used protozoan model host for *L. pneumophila*, as well as in human and murine macrophages regardless of whether the bacteria were opsonized (89-91). Furthermore, in *D. discoideum* mutants lacking PI3K, no reduction in WT *L. pneumophila* entry was observed, although avirulent *L. pneumophila* were defective in entry (91).

L. pneumophila is also able to infect HeLa cells and other non-professional phagocytes, thus suggesting that the entry is a product of host-pathogen interaction (92). Indeed, bacterial mutants lacking the LetA/S two-component system regulator were defective for entry into macrophages (93). Defect in this regulator led to a reduced transition into the infectious form of *L. pneumophila*, consequently reducing the expression of multiple virulence genes (94, 95). The *L. pneumophila* proteins RtxA, EnhC, LpnE, and HtpB, have also been shown to influence *L. pneumophila* entry (96-100). In addition, LvhB2, another *L. pneumophila* protein encoded in a locus termed *lvh*, was shown to be important for bacterial entry at 30°C, but not 37°C (101). Consistently, the mobile genetic element p45 of *L. pneumophila* strain Philadelphia-1, which carries the *lvh* locus, was also shown to contribute to the bacterial entry (102). Whatever the means of entry, the processes that lead to formation of the *Legionella*-containing vacuoles (LCVs) appear to be similar in different cell types and hosts.

1.6.2. Legionella-containing vacuole (LCV) formation

1.6.2.1 Avoidance of phagosome maturation

Upon entry, *L. pneumophila* is initially encapsulated inside a phagosome. Traditionally, the phagosome progressively acquires markers which signify the maturation of the bacteria-containing vacuole into phagolysosome. Mature phagolysosomes then degrade the bacteria through the actions of hydrolytic enzymes and acidic pH (103, 104). Once internalised, *L. pneumophila* forms a replicative niche termed the *Legionella*-containing vacuole (LCV) (**Figure 1.2**). In contrast to normal phagosomes, the LCV maintains a neutral physiological pH indicating the avoidance of progression into an acidic phagolysosome (105, 106). Further, unlike traditional phagosomes, the LCV avoids the acquisition of late-endosomal markers such as the lysosomal-associated membrane protein-1 (LAMP-1) and cathepsin D, but retains some early endosomal markers such as the Early Endosomal Antigen (EEA) 1 (107, 108). The mechanisms of LCV formation have been widely studied and are described in detail throughout this chapter.

1.6.2.2 Phosphoinositide (PI) lipid conversion

The phosphoinositides (PIs) are phospholipids that make up approximately 10% of eukaryotic membranes. These lipids are composed of two fatty acid chains connected via glycerol to an inositol head group. The head group of PI lipids contains three free hydroxyl groups at positions 3, 4, and 5, that can be phosphorylated. Phosphorylation and de-phosphorylation of these residues occur via the PI-metabolizing enzymes PI-kinases and PI-phosphatases. Together with small GTPases, PI lipids recruit proteins with PI-binding motifs, establish the cellular organelle identity, and regulate membrane dynamics (109).

Extensive live cell imaging during *L. pneumophila* infection of *D. discoideum* clearly demonstrates the subversion of PI lipids by WT but not avirulent *L. pneumophila* (110). Upon entry into the host cells, regardless of the virulence, all phagosomes are covered in $PI(3,4,5)P_3$, a marker of signal transduction and phagocytosis. Within one minute of entry, $PI(3,4,5)P_3$ is replaced by PI(3)P in phagosomes containing either WT or avirulent *L. pneumophila*. PI(3)P signifies the endocytic pathway, and vesicles with PI(3)P are destined for phagosome maturation (110). However, by 2 hours post-infection, WT

L. pneumophila LCV, but not those containing avirulent mutants, has lost PI(3)P and instead acquired PI(4)P, a marker of the secretory pathway (110, 111).

After its acquisition, PI(4)P is maintained on the LCV throughout infection, and functions to dock bacterial proteins, such as SidM/DrrA, SidC, and LotA, which are important for the next stage of intracellular replication (91, 110, 112-114). Despite the absence of comprehensive live imaging studies of PI lipid conversion in macrophages, SidC has also been shown to anchor to the LCV via PI(4)P (115), suggesting that similar conversion also happens in mammalian cells.

1.6.2.3 Endoplasmic reticulum (ER) remodelling and vesicle recruitment

In addition to the avoidance of phagosome maturation and the conversion of PI lipid, LCV formation also involves an extensive remodelling of the host endoplasmic reticulum (ER). The ER is responsible for protein and lipid synthesis, and exists in three morphologies: tubules, sheets, and the nuclear envelope. Traditionally, after synthesis in ER, proteins are packaged in vesicles destined to the Golgi apparatus, where sorting and distribution occurs (116). Approximately 20 to 40 minutes after infection with *L. pneumophila*, the LCV associates with tubular ER proteins reticulon 4 (Rtn4) and atlastin 3 (Atl3), suggesting the recruitment of tubular ER to the LCV (117, 118). Despite this early recruitment, the importance of Rtn4 and Atl3 has only been demonstrated at later stage of infection to allow the expansion of LCV and accommodate bacterial replication (119).

In addition to the tubular ER proteins, the small GTPases Rab1 and Arf1 are found on the LCV, where they mediate the recruitment of ER-derived vesicles to the LCV (107, 120). These small GTPases are key regulators that act as 'molecular switches' to regulate cargo selection and vesicle formation, transport, tethering, uncoating, and fusion (121). To execute these functions, small GTPases, such as Rab1, cycle between active (GTP-bound) and inactive (GDP-bound) forms. A GDP dissociation inhibitor (GDI) dissociation factor (GDF) facilitates the insertion of GDP-bound GTPases to the target membrane. Following this, guanine exchange factors (GEFs) convert the GTPases into the active GTP-bound

state. Active GTPases can recruit effectors to mediate appropriate functions (121). For instance, to allow vesicle movement, active GTP-bound Ypt31/32, a homolog of Rab11 in yeast, recruits the motor protein myosin (122). After this function is executed, GTPase activating proteins (GAPs) convert the GTPases back into the inactive GDP-bound state. GDFs can then extract the inactive GTPases and later facilitate the insertion of inactive GTPase into the next target membrane (121).

During *L. pneumophila* infection, vesicles from ER exit sites are recruited to the LCV in a process that is dependent on host small GTPases (107, 120, 123). Rab1 GTPase is one of the first proteins recruited to the LCV (123, 124). Rab1 mediates the recruitment of host proteins required for membrane fusion, such as the soluble N-ethylmaleimide sensitive fusion attachment protein receptors (SNAREs) (121). Disruption of Rab1 leads to a delay in Sec22b vesicular SNARE (v-SNARE) recruitment and reduced LCV biogenesis, as well as impaired *L. pneumophila* replication (123). At ER exit sites, the GTPase Sar1 recruits coat protein complex-II (COP-II) coat protein, v-SNAREs such as Sec22b, and other Sar1 effectors to form vesicles destined for the Golgi (125). Inhibition of Sar1 by an inactivating mutation leads to reduced recruitment of the v-SNARE Sec22b to the LCV (123). The v-SNARE Sec22b binds to target SNARE (t-SNARE) such as syntaxin on the LCV membrane, leading to trans-SNARE complex formation and subsequently the attachment and fusion of vesicles to the target compartment (126, 127). Consequently, inactivation of Sar1 also reduces the tethering and fusion of ER vesicles to the LCV and subsequently reduced *L. pneumophila* replication (123, 128). The GTPase Arf1 is responsible for the assembly of COP-I. After fusion, COP-II coat is removed and replaced with COP-I coat dependent on Arf1. As such, continuous vesicle production depends on Sar1-COP-II/Arf1-COP-I interactions. Consequently, silencing of Arf1 leads to reduced recruitment of ER proteins such as Sec22b, and impaired LCV biogenesis and *L. pneumophila* replication (120, 123).

By 30 minutes post-infection, approximately 60% of WT *L. pneumophila* LCVs were associated with ER vesicles and mitochondria (**Figure 1.1**). The ER vesicles flatten and densely surround the LCV, resulting in a very narrow free area of less than 500 Å. This may also hinder the fusion of acidic vesicles to the LCV (129). By 6 hours after infection,

ER vesicles are no longer visible (129). However, resident ER proteins such as glucose-6-phosphatase can be found in the LCV, suggesting that the vesicles have fully fused with the LCV (128). Additionally, ribosomes appear on the cytoplasmic face of the LCV, suggesting fusion with rough ER (**Figure 1.1**) (129). Following the ER vesicle fusions, the LCV membrane acquires a similar thickness to the Endoplasmic Reticulum (ER) membrane (129, 130). As infection progresses, the LCV transitions from a tight to a spacious compartment to accommodate bacterial replication. The host ER tubular proteins, Atl3 and Rtn4, are important to allow expansion of the LCV and subsequent bacterial replication (119).

1.6.2.4 Accumulation of poly-ubiquitinated proteins on the LCV

The cytoplasmic face of the LCV is also covered in poly-ubiquitinated proteins (**Figure 1.1**), which is believed to support intracellular replication (131). Staining with FK-2 antibody, which recognizes both mono- and poly-ubiquitin chains, showed that only cells infected with WT *L. pneumophila* produce a high level of staining of the LCV (132, 133). In addition, recruitment of eukaryotic ubiquitin ligases required for ubiquitination to the LCV has been observed, suggesting the importance of this process to LCV biogenesis (134).

1.6.3 Exit from host cells

The final step of infection is exit of the host cells and infection of other cells. Prior to cell egress, the LCV is lysed, leading to the presence of *L. pneumophila* in the cytosol. At 12 h post-infection of U937 macrophages, 71% of LCV were disrupted, and by 18 hours, 77% of infected macrophages harboured cytosolic bacteria. This number increased to 99% at 24 h post-infection (135). After 24 h, cell death occurs, leading to the release of bacteria (136, 137).

The timing of egress is governed by bacterial numbers and nutrient availability. The *Legionella* quorum sensing (Lqs) proteins are implicated in the regulation of a biphasic

life cycle. When the bacteria reached the post-exponential stage, a transition to the transmissive state occurs, where multiple virulence genes are upregulated (138). Mutants lacking the *lqs* gene cluster displayed reduced cytotoxicity in both macrophages and amoebae, suggesting reduced bacterial egress (139). In addition to the bacterial number, nutrient starvation also activates the stringent response, leading to the upregulation of virulence traits (140-143), which may then facilitate bacterial egress. For example, mutants lacking the iron importer LbtP display an early egress despite not reaching the same bacterial numbers as WT *L. pneumophila* (144).

There are several proposed mechanisms of *L. pneumophila* egress. Firstly, host cell death may facilitate *L. pneumophila* exit from the host cells. Flagella biosynthesis is upregulated during the *L. pneumophila* transmissive stage (140). In mammalian cells, flagella may trigger host Nod-like receptor (NLR) family CARD domain containing 4 (NLRC4) inflammasome assembly, leading to pyroptosis and bacterial exit from the cells during infection (145). However, upon entry, *L. pneumophila* still possess flagella. As such, pyroptosis due to flagella can also occur at early time points prior to bacterial replication and can be observed at high infectious dose in cell culture (145, 146). In addition to pyroptosis, a non-inflammatory type of host cell death, apoptosis, occurs at 48 h and 96 h post-infection with *L. pneumophila*, and is hypothesized to aid in the bacterial egress (147). Infection with *L. pneumophila* also triggered mitochondrial damage, as shown by the release of cytochrome-c, leading to apoptosis at 24 h post-infection (148).

1.7 Immunity to *L. pneumophila* infection

1.7.1 Pattern recognition receptors (PRRs)

1.7.1.1 Toll-like receptors (TLRs)

To enable immune defence against infection, the mammalian cells recognize pathogen-associated molecular patterns (PAMPs) via pattern recognition receptors (PRRs). This

leads to the activation of immune signaling cascades and the transcription of pro-inflammatory and anti-microbial genes. The Toll-like receptors (TLRs) are one of the PRR classes implicated during *L. pneumophila* infection. TLRs are expressed in immune cells such as macrophages, DCs, and neutrophils, as well as other cell types such as fibroblasts, endothelial, and epithelial cells (149). There are 10 TLR classes in humans (TLR1-10), and 12 TLR classes in mice (TLR1-9, 11-13). Each class of TLR engages distinct sets of PAMPs. Upon PAMP recognition, all TLRs, except TLR3, signal through MyD88, resulting in the activation of immune signalling pathways such as NFκB, AP-1, and MAPK, and subsequently the secretion of pro-inflammatory cytokines (150, 151).

During *L. pneumophila* infection, TLR2, 5, and 9 respectively recognize the bacterial cell wall components, flagellin, and unmethylated DNA (152-155). Despite the ability of TLR4 to recognize bacterial LPS, TLR4 is not activated by *L. pneumophila* LPS, perhaps due to the long lipid A fatty acid chain, high hydrophobicity, and unique sugar component (156). Consequently, *Tlr4*$^{-/-}$ mice displayed no reduction in either bacterial clearance or secretion of the pro-inflammatory cytokines IL12 and TNFα, suggesting that TLR4 is dispensable for host defence against *L. pneumophila* (157, 158). Mice deficient in TLR2 displayed reduced bacterial clearance during infection with *L. pneumophila*. Consistently, a modest reduction in cytokine secretion and immune cell recruitment was observed, suggesting a protective role for TLR2 (159, 160). TLR5-deficient mice show a severe defect in neutrophil recruitment upon *L. pneumophila* infection (155). In humans, a stop codon polymorphism in the *TLR5* gene rendered TLR5 unable to recognize flagellin, and this was associated with increased susceptibility to legionellosis (161). Together, these findings demonstrate the importance of TLR5 in protection against *L. pneumophila* infection. In contrast, deficiency in TLR9 does not have any significant effect on bacterial clearance and cytokine secretion (162).

TLR2, 5, and 9 signal through MyD88. Consistent with the protective roles of TLR2 and TLR5 in *L. pneumophila* infection, MyD88-deficient mice were unable to clear *L. pneumophila*. Furthermore, these mice also displayed reduced cytokine secretion and neutrophil recruitment, as well as dissemination of the bacteria to the lymph nodes and spleen (159, 160, 162, 163). The impact of MyD88 deficiency is more pronounced than

the deficiency in either TLR2, 5, or 9 (163). Additionally, combinatorial deletions of TLR2, 5, or 9 do not produce similar impact to MyD88 deficiency (162), suggesting that other MyD88-dependent responses are also important for host immunity against *L. pneumophila* infection.

1.7.1.2 Nod-like receptors (NLRs)

In addition to the TLRs, the Nod-like receptors (NLRs) are also involved in host immunity against *L. pneumophila*. NLRs are cytosolic PRRs which upon recognition of PAMPs may form the multi-protein complex inflammasome together with other adapter proteins. ASC is a key adapter protein in inflammasome assembly, however, not all inflammasomes require ASC (164). For instance, upon recognition of flagella, the NLR family, apoptosis inhibitor protein 5 (Naip5) heterodimerizes with NLRC4, thus forming the NLRC4 inflammasome. Activation of the NLRC4 inflammasome leads to the cleavage of pro-caspase-1 into active caspase-1. This leads to the activation of Gasdermin D, a pore-forming host protein that causes an inflammatory cell death termed pyroptosis, and aids the secretion of IL1β and IL18 (165).

The NLRC4/Naip5 inflammasome mediates restriction of *L. pneumophila* upon recognition of *L. pneumophila* flagellin during both *in vitro* and *in vivo* murine infection (166-170). While the Dot/Icm T4SS is also required for the restriction, the pore-forming agent lysteriolysin O from *Listeria monocytogenes* can compensate the lack of Dot/Icm T4SS, suggesting that the pore-forming ability, rather than the effector translocation, is important for the restriction, presumably suggesting the role of Dot/Icm T4SS in mediating the entry of flagella to the cell cytosol from the LCV (167). Furthermore, unlike WT macrophages, infection of *Naip5*$^{-/-}$ macrophages do not lead to pyroptosis (167-169). NLRC4 inflammasome-mediated activation of caspase-1 also activates caspase-7. Deficiency in caspase-7 results in reduced bacterial clearance and pyroptosis, thus demonstrating the role of caspase-7 in NLRC4-driven response against *L. pneumophila* (171).

Caspase-1 is also activated through NLRC4-independent pathways. Upon *L. pneumophila* infection, the NLR family Pyrin domain containing 3 (NLRP3) inflammasome can activate caspase-1 via ASC (172). However, *Asc*$^{-/-}$ BMDMs can efficiently clear *L. pneumophila* despite the absence of IL1β secretion, suggesting that the bacterial clearance is primarily mediated by pyroptosis (169). Interestingly, while caspase-1 deficient macrophages displayed reduced clearance of *L. pneumophila*, the phenotype is weaker than NLRC4- or Naip5-deficient mice, suggesting the presence of caspase-1-independent NLRC4-mediated clearance of *L. pneumophila* (169, 170).

A recent study demonstrated that in the absence of caspase-1 and caspase-11, NLRC4 inflammasome can alternatively be assembled via ASC (173). Consequently, BMDMs deficient in caspase-1, caspase-11, and ASC displayed similar phenotype as *Nlrc4*$^{-/-}$ BMDMs, suggesting that NLRC4 response against *L. pneumophila* is mediated through ASC and caspase-1 (173). Following the alternative activation, an increase in caspase-8 activity was observed, and silencing or deletion of caspase-8 in the absence of caspase-1 or caspase-11 led to reduced bacterial clearance, suggesting that NLRC4/ASC inflammasome acts through caspase-8 (173, 174). However, this alternative activation is only observed when caspase-1 or gasdermin-D is silenced, perhaps suggesting that the NLRC4/Naip5 protection against *L. pneumophila* is mediated primarily by caspase-1-dependent response (173). Alternative activation of the NLRC4-ASC-caspase-8 inflammasome leads to the activation of caspase-7, and subsequently pyroptosis and bacterial clearance (174).

1.7.2 Immune cell response

Alveolar macrophages (AMs) are resident macrophages in the lungs. AMs are considered as the primary cell type infected by *L. pneumophila* upon inhalation of contaminated aerosols (79). Upon infection, AMs secrete pro-inflammatory cytokines, such as IL-1, TNFα, and IL-6, leading to the recruitment of other immune cells to the lungs (163, 175-177). Secretion of IL-1 also stimulates uninfected bystander cells to secrete pro-inflammatory cytokines such as TNFα and IL12 (177). Stimulation of AMs with TNFα also enhances the bactericidal properties of these cells, thus improving the clearance of

L. pneumophila (175). As such, while AMs may seem ineffective against *L. pneumophila* infection due to their role as the bacterial replicative niche, these cells also play an important role during immunity against the bacteria by executing anti-bacterial, surveillance, and paracrine functions.

Cytokine secretion by infected and bystander cells leads to the recruitment of immune cells, such as neutrophils, monocytes, NK cells, and T cells. Neutrophils are recruited to the lungs during *L. pneumophila* infection by pro-inflammatory cytokines and chemokines, such as the C-X-C motif ligand 2 (CXCL2) family chemokines and IL1α (79, 178-180). Defects in neutrophil recruitment are associated with a higher *L. pneumophila* burden (163, 180-182). Furthermore, neutrophil-depleted mice are unable to clear *L. pneumophila* and eventually succumb to the disease (182, 183). Interestingly, upon phagocytosis of *L. pneumophila* by neutrophils, Dot/Icm effectors are translocated (79). However, there is no evidence of LCV formation or *L. pneumophila* replication in neutrophils. Neutrophils phagocytose *L. pneumophila* and produce reactive oxygen species (ROS), and deficiency in ROS production leads to an increase in bacterial burden in neutrophils, thus demonstrating the role of ROS in bacterial clearance from neutrophils (175). Additionally, neutrophils secrete pro-inflammatory cytokines, such as TNFα, IL-1α, IL17A, and IL12, which stimulate other cells bactericidal activity and cytokine secretion (175, 180, 184).

Monocytes are also recruited to the lungs during *L. pneumophila* infection, leading to either differentiation into phagocytic cells termed monocyte-derived cells (MCs) or the maintenance of a non-differentiated state (177, 180, 185). The recruitment of monocytes into the lungs is dependent on the chemokine receptor CCR2 (186). Deficiency in CCR2 leads to reduced clearance of *L. pneumophila*, suggesting the importance of monocytes in response against *L. pneumophila* (185). While blood monocytes or monocyte cell lines are often used as an *in vitro* model of *L. pneumophila* infection , there is no Dot/Icm translocation into monocytes during *in vivo* infection, perhaps suggesting that monocytes do not facilitate *L. pneumophila* replication (79). In addition, MCs serve as the major source of IL-12, which induces the production of IFNγ, a cytokine important for *L. pneumophila* clearance, by T cells and NK cells (180, 185).

1.7.3 Cytokine response

During *L. pneumophila* infection, a robust pro-inflammatory cytokine response is correlated with bacterial clearance. During *L. pneumophila* infection, high levels of TNFα, IL-1, IL-12, and IFNγ are observed. Patients receiving anti-TNFα therapy are more susceptible to *L. pneumophila* infection (39), and, similarly, TNFα is also important for *L. pneumophila* clearance in the murine model of *L. pneumophila* infection, where the depletion of TNFα in the lungs exacerbates *L. pneumophila* infection (187). Furthermore, mice deficient in TNFα receptor 1 (TNFR1) display a severe reduction in *L. pneumophila* clearance, suggesting the importance of TNFα signalling. Interestingly, deficiency in TNFR2 does not negatively impact clearance, although excess neutrophil recruitment was observed, perhaps suggesting the different roles of the two TNF receptors during *L. pneumophila* infection (175, 188). TNFα also enhances the bactericidal capacity of BMDMs, leading to increased fusion of LCV with the lysosomal compartments (175).

L. pneumophila can inhibit host protein translation, leading to a reduction of TNFα secretion by infected macrophages (177, 189). However, in response to this inhibition, global induction in pro-inflammatory mRNAs occurs, leading to the production of IL-1α and IL-1β in a MyD88-dependent manner (177, 189, 190). IL-1 production subsequently stimulates the production of other pro-inflammatory cytokines, such as TNFα, IL-12, and IL-6 by uninfected bystander cells (177, 189). In addition, bypassing this translation inhibition means IL-1α is further important for *L. pneumophila* clearance and neutrophil recruitment (176, 191). While the role of IL-1β in *L. pneumophila* clearance is less prominent than IL-1α (191), IL-1β stimulates the production of CXCL1 and CXCL2 chemokines from alveolar epithelial cells, which later are important for neutrophil recruitment (181).

During *L. pneumophila* infection, IL-12 is produced by monocytes, MCs, as well as dendritic cells (154, 180, 192). Neutralization of IL-12 reduces *L. pneumophila* clearance from A-strain mice (193). In addition, IL-12 also stimulates the secretion of IFNγ from NK cells and T cells (185, 192). IFNγ is vital for the clearance of *L. pneumophila,* as mice deficient in IFNγ or the IFNγ receptor IFNGR fail to control *L. pneumophila* (185, 192,

194). IFNγ enhances the bactericidal activity of MCs, but not neutrophils or AMs (185). The absence of IFNγ-mediated enhancement of AM bactericidal activity may be explained by the downregulation of IFNGR from AMs during infection, as constitutively expressing IFNGR in AMs reduces bacterial burden (195). Similar to AMs, IFNGR is also downregulated in BMDMs upon *L. pneumophila* infection (195). However, IFNγ treatment still enhances the clearance of *L. pneumophila* from macrophages and monocytes *in vitro* (196-198).

IFNγ treatment enhances the transcription of IFN-stimulated genes (ISGs). These include the interferon-inducible GTPases, such as the guanylate binding protein (GBP), immunity-related GTPase (IRG), myxovirus resistance proteins (MX), and very large interferon-inducible GTPase (VLIG) (199). One study showed that IRG1 (*Acod1*) is sufficient for *L. pneumophila* control, as *Acod1*$^{-/-}$ deficient BMDMs displayed similar bacterial burden to *Ifnar*$^{-/-}$ BMDMs (200). However, another study showed that IRG1 alone cannot account for the IFNγ-mediated restriction of *L. pneumophila*. Instead, the knock-out of six genes encoding for IRG1, IRG family M protein 1 (IRGM1), IRGM3, inducible nitric oxide synthase (iNOS), NADPH oxidase 2 (NOX2), and caspase-11 are required to achieve a complete loss in the IFNγ-mediated restriction of *L. pneumophila*, suggesting the roles of these six genes in IFNγ response to *L. pneumophila* (201).

In addition to IRGs, GBPs have also been shown to play a role during the murine immune response to *L. pneumophila* infection. In particular, the GBPs encoded in chromosome 3 (*Gbp*^{chr3}, GBP1, 2, 3, 5, and 7) promotes non-conventional caspase-11 activation and pyroptosis (202-204). Caspase-11 recognizes cytosolic LPS, however, the LCV protects *L. pneumophila* LPS from caspase-11 recognition (205). Furthermore, the LPS of *L. pneumophila* possesses a long and unique structure which may be harder to recognise by host PRR (156). Upon IFN stimulation, GBP^{chr3} co-localize with *L. pneumophila* to promote the lysis of *L. pneumophila* (203, 206). This is hypothesised to unravel the *L. pneumophila* LPS to expose caspase-11 binding sites, leading to the non-conventional activation of caspase-11 inflammasome and pyroptosis (204). GBP^{chr3}-mediated *L. pneumophila* lysis also leads to the release of bacterial DNA, leading to the activation of cytosolic DNA sensor such as cyclic GMP-AMP synthase (cGAS) (203). However,

the loss of LCV integrity is likely contributed through another factor, as *Gbp*^{chr3} knock-out alone did not compromise the LCV integrity (203, 206). Consistently, *Gbp*$^{chr3-/-}$ BMDMs only display a modest reduction in bacterial clearance (203, 204).

1.8 Secretion systems of *L. pneumophila*

Bacterial secretion systems are commonly employed by various pathogenic bacteria, such as the pathogenic *E. coli*, *Salmonella* species and *Yersinia* species, to secrete bacterial virulence factors into the host cells to enable infection. The *L. pneumophila* genome encodes for four secretion systems; one type 1 secretion system (T1SS), one type 2 secretion system (T2SS), and at least two type 4 secretion systems (T4SS) (67-70, 207-209).

1.8.1. Lss type 1 secretion system (T1SS)

The T1SS encompasses a transmembrane apparatus used to secrete substrates into the extracellular space (210). This secretion system is commonly used by pathogenic bacteria such as the uropathogenic *E. coli* (UPEC) and *Pseudomonas aeruginosa* to secrete pore-forming toxins (211, 212). In fact, many of the known pore-forming toxins, often characterized by having an RTX motif, are secreted through T1SS (209, 213). In UPEC, this apparatus consists of HlyA-D, with HlyA as the secreted pore-forming toxin. HlyC acts as an acyltransferase which activates HlyA. Meanwhile, HlyB and D are involved in the secretion process itself. In addition, another protein encoded separately from the *hly* operon, TolC, is also vital for the functionality of the T1SS. Altogether, these proteins form an apparatus similar to that of the ATP-binding cassette (ABC) transporter (213).

During a search of *L. pneumophila* strain Corby genome, a set of genes which exhibited significant similarity to an ABC transporter system was identified (214). These genes, comprising *lssXYZABD*, were later shown to share homology with the T1SS of UPEC, *Salmonella typhii* and *Vibrio cholera* (209). *L. pneumophila* mutants lacking a component of the T1SS, TolC, displayed reduced replication in both mammalian and protozoan hosts,

perhaps suggesting that the T1SS plays a role in bacterial pathogenesis (215, 216). As the ability of the *lss* mutants to recruit ER marker was comparable to WT *L. pneumophila*, the T1SS may be important in early infection (217). Consistent with this, the T1SS substrate RtxA, is essential for *L. pneumophila* entry into the host cell (96, 217-219).

1.8.2 Lsp type 2 secretion system (T2SS)

Similar to the T1SS, T2SS also secretes substrates to the extracellular space (210). T2SSs rely on two different mechanisms; the Sec and Tat pathways to translocate proteins across the inner bacterial membrane into the periplasmic space (220). Sec and Tat are two major ways utilized by bacteria to transport proteins across the cytoplasmic membrane. Sec typically transports unfolded proteins, whereas Tat transports them in folded state (221). Genomic analysis has revealed the presence of both Sec and Tat systems in *L. pneumophila* (67, 68), and mutation of *tatB* resulted in decreased levels of some, but not all, T2SS substrate (222), indicating the functionality of both systems.

Genomic analysis shows that *L. pneumophila* possesses a complete T2SS apparatus (67, 68, 223, 224). The T2SS consists of 12 components, LspC-M, and Lsp O. LspD forms the tip of the secretion system, and is anchored via LspC to the inner membrane protein channel that is composed of LspF, LspL, and LspM. The pseudopilins, consisting of LspG-K, aids in the translocation of substrates through LspO. Finally, LspE acts as a cytoplasmic ATPase (224, 225). The lack of functional T2SS led to a significant reduction in replication in amoebae and macrophages, indicating the importance of this system during *L. pneumophila* infection (223, 226, 227).

In silico analysis predicts the presence of 60 T2SS effectors in *L. pneumophila* genome (228). To date, 25 of these predicted substrates have been confirmed through the analysis of *lsp* mutant compared to WT *L. pneumophila* culture supernatant (223, 224, 226, 229, 230). Of these, while at least five proteins were shown to be important for replication in amoebae, only ChiA and NttE were shown to contribute to *L. pneumophila* survival in mammalian hosts (228, 231-234). Interestingly, the culture supernatant analysis revealed that IcmX and LvrE, components of two distinct T4SS in *L. pneumophila*, as well as

VirK, a homologue of the T4SS component in *Agrobacterium tumefaciens* were only found in the supernatant when the T2SS was fully functional (228). This suggests that the T2SS might have a relationship with the T4SS. In addition, LegP, which was one of the proteins identified in the analysis (228), was also reported to be a T4SS substrate, suggesting the possibility that proteins could be secreted through different secretion systems (224).

1.8.3 Type 4 secretion systems (T4SSs)

1.8.3.1 Lvh T4SS

The Lvh T4SS is encoded in the *lvh* locus and consists of 11 genes with high homology to the *virB/D* secretion system of *Agrobacterium tumefaciens* (235). The *lvh* locus has a higher G+C content than the rest of the genome, suggesting acquisition via HGT (67, 235). Different strains of *L. pneumophila* carry the *lvh* locus in different ways. For instance, the *lvh* locus of strain 130b is encoded chromosomally (69), whereas the Philadelphia-1 carries this locus in the p45 mobile genetic element (68). Not all *L. pneumophila* strain possess the Lvh T4SS. For instance, *L. pneumophila* strain Corby does not have this secretion system (71). The Lvh T4SS is dispensable for *L. pneumophila* replication in either macrophages or amoebae (235). However, under stressful condition and in the absence of a functional Dot/Icm T4SS, the Lvh T4SS can translocate several Dot/Icm effectors, leading to the rescue of bacterial entry, intracellular replication, and avoidance of phagosomal maturation (236, 237).

1.8.3.2 Dot/Icm T4SS

The Dot/Icm locus was first discovered during a screening for mutants defective in replication by two different groups (208, 238). Two distinct loci defective in replication were called either Dot for **d**efect in **o**rganelle **t**rafficking or Icm for **i**ntra**c**ellular **m**ultiplication locus (208, 238). Mutants lacking these loci were unable to avoid phagosome acidification and could not recruit components of endoplasmic reticulum

(239, 240). Further analysis suggested that the components from both the *dot* and *icm* groups of genes, many of which were predicted transmembrane proteins, shared homology with the conjugal plasmid transfer apparatus (241).

It was later shown that the apparatus was able to transfer plasmid DNA to both *L. pneumophila* and *E. coli* recipients (242, 243). This machinery was then found to translocate a *L. pneumophila* protein called RalF thus showing that this set of genes indeed encodes for a functional protein secretion system (244). Analysis of 58 *Legionella spp* species revealed that despite a high diversity between genomes, genes encoding for the Dot/Icm T4SS components were highly conserved, thus confirming the universal importance of this T4SS for replication of *Legionella spp* in multiple hosts (72, 74). There are 26 components of the Dot/Icm T4SS. DotC, DotD, DotF, DotG, and DotH form a core transmembrane subcomplex. DotL, DotM, DotN, IcmS, IcmW, and LvgA form the *Legionella* type 4 coupling proteins (LT4CP) subcomplex (245). To allow efficient protein translocation, the Dot/Icm is localized to the polar ends of the bacteria, which depends on DotU and IcmF (246).

The proteins secreted and translocated into the host cell cytosol by the Dot/Icm T4SS are termed Dot/Icm effector proteins. The discovery and characterisation of Dot/Icm T4SS effector proteins has been a major focus of research for many laboratories focusing on *L. pneumophila* infection. Identification of Dot/Icm effectors has been done through either screening of proteins that bind to the Dot/Icm apparatus using the yeast genetic system or by testing empirically using translocation assays (247-250). In addition, bioinformatics has also been used to identify C-terminal signal sequences thought to be important for translocation (251-253). Finally, within the genome of *L. pneumophila*, multiple genes encoding for eukaryotic-like proteins and eukaryotic domain-containing proteins were found (67, 72). These proteins are hypothesized to be Dot/Icm effectors, as they may be secreted into the host cell to mediate the manipulation of host processes. However, empiric evidence of the translocation via Dot/Icm T4SS has only been provided for a subset of these proteins (72, 254). Nonetheless, these efforts have led to the identification of over 330 putative effector proteins. These effectors manipulate various

eukaryotic cell processes, such as vesicle trafficking, protein translation, apoptosis and stress responses (255-257).

1.9 Modulation of host processes by Dot/Icm effectors

1.9.1 Dot/Icm effectors and avoidance of phagosome acidification

Mutants lacking a functional Dot/Icm T4SS are unable to avoid phagosome maturation and acquire late endosomal markers such as LAMP1. Several Dot/Icm effectors have been reported to promote the avoidance of phagosome maturation. For instance, the Dot/Icm effector SidK inhibits VatA, a host vacuolar H^+-ATPase (v-ATPase) involved in the acidification of phagosomes (258). In addition, the Dot/Icm effectors SetA, LtpM, and RavD, localize to the LCV as well as the early and late endosomes, where they are hypothesized to interfere with the endosomal trafficking (259-263). LtpM possesses glucosyltransferase activity, through which it blocks the microtubule-dependent movement of endosomes, possibly leading to reduced endosome fusion with LCV (261). While the mechanism of action of RavD remains unknown, *ravD* mutants display a significant increase in LAMP1 late endosomal marker acquisition compared to WT *L. pneumophila*, suggesting the role of this effector in the avoidance of phagosome maturation (262). Finally, VipD localizes to the endosome where it exhibits a phospholipase activity which catalyses the removal of PI(3)P from the endosome and, subsequently, efficient avoidance of recruitment of the endosomal protein Rab5 (264).

1.9.2 Dot/Icm effectors and PI lipid tailoring

The Dot/Icm effectors play a prominent role in the conversion of PI lipids, as mutants lacking a functional Dot/Icm T4SS reside in vacuoles containing PI(3)P, whereas WT *L. pneumophila* LCV is enriched for PI(4)P (110). At least four Dot/Icm effectors act as PI-metabolizing enzymes. LppA is a PI phosphatase which can facilitate the formation of PI(4)P from $PI(3,4,5)P_3$, $PI(3,4)P_2$, or $PI(4,5)P_2$ *in vitro*. However, LppA does not appear to influence PI composition on LCV. Rather, LppA improves *L. pneumophila*

intracellular replication by removing phytate (265). Another effector, SidP, acts as PI(3)-phosphatase, leading to the conversion of PI(3,5,)P_2 into PI(5)P, or PI(3)P into PI. The ability of SidP to remove PI(3)P is hypothesized to aid in phagosome maturation evasion, however the role of SidP during infection is currently unknown (263).

The Dot/Icm effector LepB was recently found to be a PI-3-kinase, which converts PI(3)P into PI(3,4)P_2 (266). PI(3,4)P_2 can later be used as a substrate by another effector, SidF, to generate PI(4)P through its CX_5R protein-tyrosine phosphatase motif (266, 267). In addition to this role, SidF may also work together with the host PI(5)-phosphatase inositol polyphosphate-5-phosphatase (OCRL) to generate PI(4)P from PI(3,4,5)P_3. The deletion of SidF leads to a reduction in SidC recruitment to the LCV, suggesting reduced PI(4)P availability on the LCV (267). However, *sidF* mutants do not display any reduction in bacterial replication (268), perhaps due to the presence of other Dot/Icm effectors involved in PI tailoring. Bioinformatics analysis revealed that over 400 *L. pneumophila* proteins possessed CX_5R motifs, suggesting the presence of more proteins with PI-phosphatase activity (267). In addition to the PI-metabolizing enzymes, *L. pneumophila* also acquires PI(4)P-rich vesicles from the trans-Golgi in a Dot/Icm-dependent manner (111). However, the effector responsible for this phenotype has yet to be identified. Finally, to maintain the PI(4)P-rich composition of LCV, *L. pneumophila* may also avoid the acquisition of PI(3)P-rich vesicles from endosomes and retrograde trafficking. A Dot/Icm effector protein, RidL, modulates Rab7 GTPase to prevent the acquisition of vesicles from the retrograde (Golgi-ER) trafficking pathway (269).

1.9.3 Dot/Icm effectors in ER remodelling and small GTPase modulation

The Dot/Icm effectors are important in ER remodelling. Mutants lacking a functional Dot/Icm T4SS are unable to recruit ER-derived vesicles (107, 208, 270). The association of the tubular ER protein Rtn4 is dependent on the Sde family effectors, which consists of three effectors located in close proximity SdeA, SdeB, and SdeC. The loss of all three Sde proteins leads to a reduction in Rtn4 association with LCV, however, this can be rescued by the expression of SdeB or SdeC alone, suggesting that the three proteins act redundantly (118). The effector protein Ceg9 can interact with Rtn4 to form a tripartite

complex with Atl3 on the LCV (117). However, Ceg9 is not important for the recruitment of Rtn4 (118), suggesting that it may play a role in the modulation of Rtn4 on the LCV. In addition to the recruitment of Rtn4, WT *L. pneumophila* infection leads to a structural change in Rtn4, characterized by the presence of a higher molecular weight form. This structural change is dependent on the Dot/Icm T4SS, and is associated with five other effectors, Lpg0112, Lem10, SidJ, Lpg2244, and Lpg2248, that drive the high molecular weight version of Rtn4. Additionally, mutants lacking Sde family proteins show an alteration in LCV morphology, as well as premature rough ER association (118). However, the consequence of this for bacterial intracellular replication remain unknown.

Many Dot/Icm effectors are involved in the manipulation of host small GTPases. For instance, the effector protein RalF contains a Sec7 homology domain, commonly found in GEFs. RalF recruits the small GTPase Arf1 to the LCV and acts as GEF for Arf1 (120). Other Dot/Icm effectors target host Rab1 GTPase. The Dot/Icm effector SidM/DrrA is implicated in recruiting and activating host Rab1 (271-273). SidM/DrrA possesses a GDI-displacement factor (GDF) activity which can displace the endogenous Rab1 GDI and recruit Rab1 to the LCV. The GEF domain of SidM/DrrA then mediates the activation of Rab1 (271, 274). Another study later found that the GEF activity of SidM/DrrA alone can displace Rab1 GDI, therefore the importance of the GDF domain of SidM/DrrA is questionable (275). SidM/DrrA also mediates AMPylation of Rab1, which hinders GAP-mediated inactivation of Rab1 (276). Despite these exciting actions of SidM/DrrA *in vitro*, deletion of *sidM* does not lead to any significant replication defect or any defect in LCV biogenesis (272). This suggests the presence of other effectors which may compensate the loss of SidM by executing similar functions.

In addition to SidM/DrrA, other effectors (DrrB-E, LspE, LvgA, SidC, SdcA, SdeA, SdeB, SdeC, SdeD, SidE, and LidA) are all involved in the recruitment of Rab1 to the LCV (273). SidC and its paralogue SdcA are anchored to the LCV via PI(4)P binding, where they promote the recruitment of ER vesicles (114, 115). SidC ubiquitinates Rab1, leading to increased recruitment of Rab1 to the LCV (277). Additionally, a member of SidE family protein, SdeA, ubiquitinates Rab1 using its arginine-specific ADP-ribosyltransferase motif (R-S-EXE), possibly leading to the recruitment of Rab1 to the

LCV (278). On the other hand, LidA protects active GTP-bound Rab1 from inactivation by GAP proteins (279), but the loss of LidA does not lead to any significant reduction in replication, other than a modest reduction in Rab1-positive LCVs, again suggesting the presence of functionally redundant effectors (272). Another effector, WipB, is functionally similar to LidA, and a Δ*wipB*Δ*lidA* double mutant strain displays an attenuation in ER-vesicle recruitment and *L. pneumophila* replication (280). However, this attenuation is modest, suggesting the presence of other effectors that may execute similar function.

Key to the role of Rab1 is the cycling between active and inactive forms (121). In addition to effectors activating Rab1, there are also Dot/Icm effectors that inactivate Rab1. The effector protein SidD can remove AMP from Rab1, which allows access for GAP proteins to inactivate Rab1 (281, 282). Furthermore, the Dot/Icm effector LepB acts as a GAP that converts GTP-bound Rab1 to the inactive GDP-bound Rab1 (271). The effector protein AnkX mediates the phosphocholination of Rab1 to hinder GAP-mediated inactivation (283, 284). However, another effector protein, Lem3, removes this modification hence enabling access to inactivate Rab1 (285).

In addition to the Arf1, Sar1, and Rab1 GTPases, other GTPases, such as Ran and Rap are found on the LCV (286-289), suggesting that *L. pneumophila* may be modulating multiple GTPases including those not directly involved in the ER-Golgi (anterograde) trafficking pathway. For instance, the Dot/Icm effector protein LegG1 targets Ran GTPase, leading to microtubule polymerization and increased LCV motility. This interaction is important for *L. pneumophila* replication, as *legG1* mutants displayed attenuated replication in BMDMs (290).

1.9.4 Dot/Icm effectors and host immune response

Although *L. pneumophila* is a pathogen of amoebae, and as such has not evolved with a mammalian immune system, several effector proteins inadvertently influence host cell immune responses. For example, *L. pneumophila* can dampen the host NFκB response to

allow efficient infection. NFκB activation results in pro-inflammatory cytokine production, such as TNFα, important for the clearance of *L. pneumophila* (175, 187, 291).

The Dot/Icm effector proteins MavC and RavD can dampen host NFκB responses (292, 293). MavC acts as a trans-glutaminase that covalently modifies the host E2 ubiquitin-conjugating enzyme, UBE2N, with a unique ubiquitin linkage that is unusable by the host (292). E2 enzymes work in concert with E3 ubiquitin ligases to synthesize ubiquitin chains (294). The modification of host UBE2N inhibits its activity, resulting in the loss of K63 poly-ubiquitin chains, and subsequently the K48-linked ubiquitination and degradation of IκB. This leads to the inhibition of NFκB activation during early infection (292). Interestingly, MavC can be inhibited by another Dot/Icm effector, Lpg2149, which competes with ubiquitin to bind MavC (295). However, the relevance of this inhibition during infection requires more investigation. Another effector, RavD is a deubiquitinase (DUB) that hydrolyzes linear ubiquitin chains. RavD localizes to the LCV via PI(3)P/PI(4)P interactions and reduces the amount of linear ubiquitin chains on the LCV. Deletion of *ravD* leads to increased degradation of IκB, suggesting a role for RavD in inhibition of the NFκB pathway (293). However, it is currently unclear how the reduction in linear ubiquitin chain leads to inhibition of the NFκB pathway.

In addition to the NFκB pathway, *L. pneumophila* also inhibits the host translation, leading to the inhibition of cytokine production. There are at least seven Dot/Icm effectors (Lgt1-3, SidI, SidL, LegK4, and Lpg1489) that can inhibit host translation (177, 296-298). This inhibition leads to a reduced cytokine response from infected cells. However, mutants lacking all seven effectors still display translation inhibition compared to the Δ*dotA* mutant, suggesting the presence of other effectors modulating this process (176).

1.9.5 Dot/Icm effectors and host cell death

While amoebae can undergo programmed cell death, the molecular mechanism is currently unclear. Nonetheless, the signalling leading up to apoptosis is likely to be different from that of mammalian cells, as amoebae lacks mammalian proteins involved

in apoptosis, such as caspases (299-301). In addition, amoebae also lacks the mammalian immune signalling that may result in apoptosis, such as the NFκB signalling pathway.

Several Dot/Icm effectors were shown to reduce host apoptosis through the modulation of NFκB signalling pathway. Despite an initial inhibition of host NFκB, this response is later activated. WT *L. pneumophila* infection resulted in a sustained NFκB activation in a Dot/Icm T4SS dependent manner. Transfection of a library of tagged Dot/Icm revealed that 13 Dot/Icm effectors can induce prolonged NFκB activation, leading to the transcription of anti-apoptotic BCL2 family proteins (302-304). Of these 13 Dot/Icm effectors, two effectors, LnaB and LegK1, are the most well-characterized (305, 306). While the mechanism of action of LnaB remains unclear, the coiled-coil domain is required for the induction of NFκB activation (305). Meanwhile, LegK1 mimics the action of IKK by phosphorylating host IκB, leading to translocation of the NFκB subunit p65 into the nucleus (306). Deletion of both *lnaB* and *legK1* does not lead to a significant reduction in bacterial replication, consistent with the presence of multiple Dot/Icm effectors that can induce prolonged NFκB activation (305).

However, while the activation of NFκB increased the level of transcript of anti-apoptotic genes, another study showed that the level of these proteins were not altered, perhaps due to the translation inhibition by *L. pneumophila* (307). Furthermore, in addition to the BCL2 family proteins, the pro-apoptotic protein BNIP3 is also influenced by NFκB. Another Dot/Icm effector, SidF, was shown to reduce apoptosis during infection of murine macrophages through interaction with the pro-apoptotic proteins BNIP3 and BCL-RAMBO (308). However, this phenotype is not reproducible, as another study demonstrated that loss of SidF does not affect host cell apoptosis or bacterial burden during infection by *L. pneumophila.* Furthermore, the loss of pro-apoptotic proteins BNIP3, BCL-RAMBO, Bax, or Bak did not influence host apoptosis and *L. pneumophila* burden, thus further emphasising the dispensability of SidF during infection (268).

The inhibition of translation by *L. pneumophila* Dot/Icm effector proteins may also contribute to host cell death, as translation inhibition leads to the loss of the rapidly-turned over anti-apoptotic protein MCL1 in murine BMDMs, thus sensitising the cells to BCL-XL anti-apoptotic activity. Consistently, inhibition of BCL-XL increases host cell death and reduces *L. pneumophila* burden (307). Nonetheless another study later showed that

cell death due to translation inhibition was more likely to be pyroptosis rather than apoptosis (268). Therefore, more studies are required to clarify the inhibition of host cell death by *L. pneumophila*.

Intriguingly, *L. pneumophila* can also enhance host apoptosis at later stage of infection, which may facilitate bacterial egress (147, 148). In dendritic cells (DCs), five Dot/Icm effectors, VipD, LegS2, Lem12, Ceg18, and Lpg0716, induce caspase-3-mediated apoptosis. LegS2, Lem12, and Ceg18 localize to the mitochondria, although their exact mechanisms of caspase 3 activation are unknown. On the other hand, through its phospholipase activity, VipD generates lysophospholipids and fatty acids which trigger mitochondrial damage and the release of cytochrome-c (309). Although VipD does not induce caspase-3 in macrophages at early time points (309), the relevance of these effectors at later timepoints has not been determined.

Taken together, these show that the Dot/Icm effectors are important modulators of the host processes which enable the intracellular replication of *L. pneumophila*. Multiple Dot/Icm effectors may target the same pathways, and may act either synergistically or antagonistically with each other, which exemplifies the complexity of the effector network.

1.10 Aims of this study

The Dot/Icm T4SS is critically important to the ability of *L. pneumophila* to replicate in all host cells. The T4SS secretes over 330 effectors into the host cells that manipulate a wide range of host processes. However, the majority of the effector repertoire remains uncharacterized, owing to the large number of effectors and functional redundancy, where multiple effectors target the same pathway. Therefore, the broad aim of this study is to identify Dot/Icm effectors important for *L. pneumophila* virulence traits. To bypass the challenges of studying the Dot/Icm effectors, large genomic region mutants of *L. pneumophila* strain 130b were generated in this study. Using these mutants, we aimed to characterize Dot/Icm effectors important for bacterial survival both *in vitro* and *in vivo*.

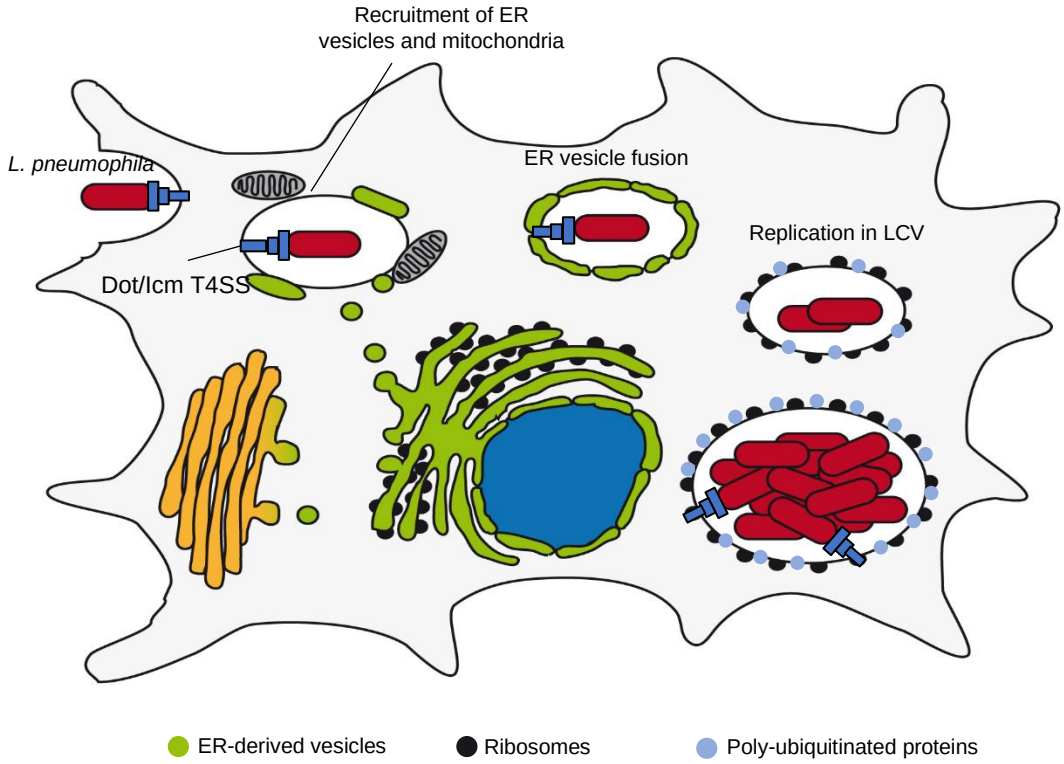

Figure 1.1. The intracellular lifestyle of *L. pneumophila*.

Following phagocytosis, *L. pneumophila* avoids lysosomal acidification and recruits ER-derived vesicles, mitochondria, leading to the formation of an ER-like vacuole termed *Legionella*-containing vacuole (LCV) where the bacteria replicates. The LCV is associated with ER-derived proteins, ribosomes, and poly-ubiquitinated proteins. After exhausting the nutrients in the host cells, *L. pneumophila* lyses cells to egress from the host cell. Image is adapted from (310).

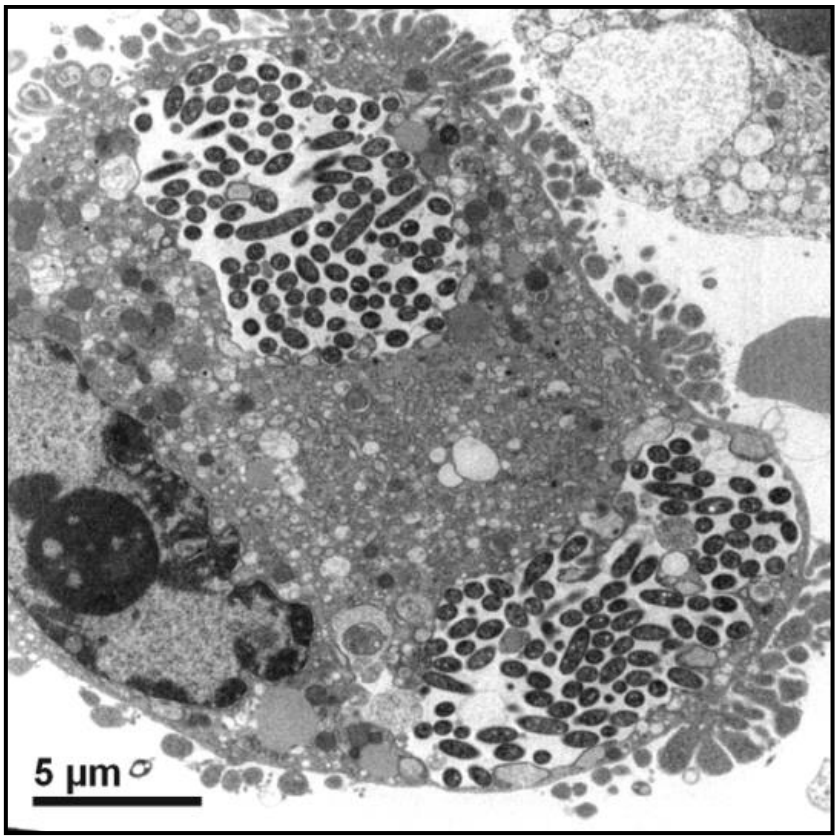

Figure 1.2. Electron micrograph of *L. pneumophila*-infected macrophage.

L. pneumophila (rod-shaped bacteria) replicates inside the *Legionella*-containing vacuole (LCV). Two LCVs are shown in this image. Image was created by Vicki Bennett-Wood.

Chapter 2
Materials and Methods

2.1 Chemicals and reagents

Unless otherwise stated, all chemicals and reagents used in this study were purchased from Sigma-Aldrich, Merck, Astral Scientific, Ajax Finechem, or Chem Supply. Bacteriological media components were purchased from Oxoid, BD Difco, Merck, or Sigma-Aldrich. Antibiotics were purchased from either Astral Scientific or Sigma-Aldrich. Tissue culture media were obtained from HyClone, Bovogen, Sigma-Aldrich, or Life Technologies.

2.2 Bacterial strains, media, and growth conditions

All bacterial strains and plasmids used in this study are listed in **Table 2.1** and **Table 2.2** respectively. *E. coli* was grown in either Luria-Bertani (LB, 1% (w/v) tryptone, 1% (w/v) NaCl, 0.5% (w/v) yeast extract) broth or agar. LB agar was made by adding 2% bacteriological agar to LB broth. Whenever required, either chloramphenicol or kanamycin was added at respectively 25 μg/mL or 100 μg/mL. For culturing *L. pneumophila*, either buffered charcoal yeast extract (BCYE) agar or N-(2-acetamido)-2-aminoethanesulfonic acid (ACES)-buffered yeast extract broth (1% (w/v) ACES buffer, 1% (w/v) yeast extract, pH 6.9) supplemented with 1 mM iron(III) nitrate ($Fe(NO_3)_3$) and 1 mM L-cysteine hydrochloride was used. Chloramphenicol (6.25 μg/mL), kanamycin (25 μg/mL), isopropyl β-d-1-thiogalactopyranoside (IPTG, 10 mM), or sucrose (5%) was added as required. All *L. pneumophila* agar media were purchased from the media preparation unit (MPU) at the Peter Doherty Institute (PDI).

All *E. coli* agar cultures were grown at 37°C for 1 day, whereas *L. pneumophila* agar cultures were grown at 37°C for 3 days. Liquid cultures for both *E. coli* and *L. pneumophila* were grown at 37°C for 18-20 h with agitation at 180-200 rpm. Long-term storage of all bacterial strains used in this study was done in 50% glycerol broth at -

80°C. All bacterial media used for growth and storage were sterilized at 121°C for at least 20 minutes at 15 kPa.

2.3 DNA isolation, purification, and sequencing

2.3.1 Bacterial genomic DNA (gDNA) extraction

Genomic DNA was extracted from proteinase-K treated *L. pneumophila* using the Quick-gDNA^{TM} MiniPrep kit (Zymo Research) according to manufacturer's protocol.

2.3.2 Plasmid DNA extraction

Plasmid DNA extraction was done using the Qiaprep Spin Miniprep kit (Qiagen) according to the manufacturer's protocol.

2.3.3 DNA purification

DNA purification and gel clean-up were performed using the ZymoClean^{TM} DNA purification or gel purification kit (Zymo Research) according to the manufacturer's protocol.

2.3.4 Quantification of DNA concentration

DNA concentration was determined using NanoDrop spectrophotometer (Thermo Fisher) according to manufacturer's instructions.

2.3.5 DNA sequencing

Sanger sequencing for plasmid DNA was done using the ABI PRISM BigDye Terminator (Applied Biosystems) according to manufacturer's instruction (**Table 2.5**). Sample purification and capillary electrophoresis were performed by either Australian Genome

Research Facility (AGRF), Monash High Throughput Platform (MHTP) Medical Genomics Facility, or Micromon Genomics. DNA sequence analysis was performed using either Sequencher® v 5.0 software (Gene Codes Corporation), or a combination of Chromas (Technelysium) and Serial Cloner v 2.6.1 (Serial Basics).

2.4 DNA manipulation

2.4.1 Polymerase Chain Reaction (PCR)

All oligonucleotides used for PCR were purchased from either Sigma-Aldrich or IDT. A list of oligonucleotides used in this study can be found on **Table 2.3**. Thermocycler reactions used in this study can be found in **Table 2.4**. PCR was done using either G-Storm GS482 Thermal Cycler (G-STORM), LifeTouch Thermal Cycler (Bioer), or T100 Thermal Cycler (Bio-Rad). Amplification of DNA fragments from bacterial gDNA was performed using Pfu Ultra II (Agilent Technologies) according to the manufacturer's protocol (**Table 2.4**). Overlap PCR was performed using Phusion-HF DNA polymerase (NEB) as detailed in **Table 2.4.** For colony PCR, GoTaq® Mastermix (Promega) was used (**Table 2.4**). Colonies were picked using sterile pipette tips or toothpicks and used as templates for the PCR reaction.

2.4.2 DNA gel electrophoresis

Agarose gel electrophoresis was used to separate and analyze DNA fragments. Agarose gel (Bioline) was made up to 1% (w/v) concentration in 1xTris-Acetate Ethylenediamine tetraacetic Acid/EDTA (1x TAE, **Table 2.5**) buffer containing 0.01% (v/v) SYBR-Safe DNA gel stain (Invitrogen). The DNA samples were mixed with 6x loading dye (NEB) and ran alongside NEB 1-kb ladder. Gels were visualized using the fluorescence mode of AI600 Imager (GE).

2.4.3 DNA restriction digest and ligation

Restriction digest was done at 37°C for at least 3 hours using the appropriate enzymes in 20 μL reactions. All restriction enzymes were obtained from NEB. DNA ligation was done in 20 μL reaction using T4 ligase from NEB either for 2 hours at room temperature or overnight at either 4°C or 16°C.

2.4.4 Transformation of E. coli

2.4.4.1 Preparation of chemically competent E. coli strains

The appropriate *E. coli* strains were grown in LB broth without any antibiotics for overnight at 37°C with shaking (180-200 rpm). Overnight culture was sub-inoculated 1:100 in 50 mL Super Optimal Broth (SOB, 2% (w/v) tryptone, 0.5% (w/v) yeast extract, 10 mM NaCl, 2.5 mM KCl, 10 mM Mg_2SO_4, 10 mM $MgCl_2$) and incubated with shaking (180-200 rpm) at either 37°C for 4-6 hours or 16°C for 40-60 hours to an OD_{600} of 0.4-0.8. After incubating the cells on ice for 10 minutes, the culture was spun down at 2,500 rpm for 15 minutes at 4°C. The pellet was then resuspended in ice-cold transformation buffer (**Table 2.5**). After adding DMSO, the suspension was frozen in aliquots at -80°C.

2.4.4.2 Transformation of E. coli

The appropriate plasmid DNA was added into an aliquot of chemically competent *E. coli*. The mixture was then incubated on ice for 20-30 minutes, followed by heat shock at 42°C for 90 seconds. After standing on ice for 2-3 minutes, the bacteria were recovered in 0.9 mL Super Optimal Broth with Catabolic Repression (SOC, SOB plus 20 mM glucose) for 1.5-2 h before plating on LB agar plates supplemented with the appropriate antibiotics.

2.5 Genetic manipulation of *L. pneumophila*

2.5.1 Transformation of L. pneumophila

A loopful of bacteria was added into 1 mL PBS and pelleted at 13,300 rpm for 1 minute. The pellet was then washed twice in ice-cold sterile H_2O and spun down at 13,300 rpm for 1 minute at 4°C. After one wash with ice-cold sterile 10% glycerol in H_2O, the pellet was resuspended in 0.5 mL ice-cold 10% glycerol and aliquoted in 0.1 mL. Plasmid DNA was mixed with each aliquot and transferred to chilled 0.2 cm electroporation cuvette (Cell Projects). Electroporation was then done at 2.3 μF. ACES broth was immediately added to the electroporated bacteria and the culture was allowed to recover for 4-5 h at 37°C with shaking (180-200 rpm). Culture was then plated on BCYE plates supplemented with the appropriate antibiotics.

2.5.2 L. pneumophila mutants construction

The 5' and 3' flanking sequences of the region to be deleted were first amplified from *L. pneumophila* gDNA using primers as indicated in **Table 2.3** and combined using overlap PCR. The resulting product was run on 1% agarose gel, and the band with correct size was excised. After gel purification, the DNA was digested using the appropriate restriction enzymes as indicated in **Table 2.3** and ligated into pSR47s suicide vector. The construct was then transformed into Pir2 *E. coli*. Positive transformants were identified using colony PCR with primers pSR47s-F and R. Finally, plasmid was then extracted from the positive transformants and confirmed by Sanger sequencing. To ensure that the overlap PCR has combined the two flanking regions properly, internal sequencing primers (B seq-I seq, **Table 2.3**) were also used for sequencing in addition to the pSR47s-F and R primers.

L. pneumophila mutants construction was conducted in two steps. In the first step, the suicide vectors (pSR47s:ΔA-ΔI, **Table 2.2**) were transformed into *L. pneumophila* strain 130b. Positive transformants which have undergone the first homologous recombination event were selected using kanamycin (25 μg/mL) and identified with colony PCR. The second homologous recombination was induced by single streaking the positive colonies obtained from the first step onto BCYE plates supplemented with 5% sucrose. Positive colonies were firstly screened with colony PCR using the primers as indicated in **Table 2.3**. Finally, the mutants were confirmed using whole genome sequencing.

2.5.3 Ectopic expression of effector proteins in L. pneumophila

2.5.3.1 Expression of TEM-1-tagged ralF

The TEM-1 fusion protein overexpression construct pXDC61:*ralF* was previously created by Dr Ralf Schuelein. The gene encoding for *ralF* was amplified from the gDNA of *L. pneumophila* strain 130b, This plasmid was transformed into all *L. pneumophila* large genomic region mutants (ΔA-ΔI) and plated onto BCYE plates plus 6.25 μg/mL chloramphenicol. Positive colonies were screened with colony PCR using pMMB207c F and R primers (**Table 2.3**).

2.5.3.2 Expression of legC4

To create the overexpression construct pMMB207c_4xHA:*legC4*, the gene encoding for *legC4* was amplified from the gDNA of *L. pneumophila* strain 130b using primers LegHA F and LegHA R (**Table 2.3**). On the other hand, for the complementation vector pMMB207c:*plegC4*, in addition to the gene encoding for LegC4, the 312-bp region upstream of *legC4* was amplified from the gDNA of *L. pneumophila* strain 130b. After confirming that the right fragments had been amplified using gel electrophoresis, the DNA was purified and digested using the appropriate restriction enzymes. DNA purification was again performed followed by ligation into pMMB207c:4xHA or pMMB207c vector. The constructs were then transformed into XL1 Blue *E. coli* (**Table 2.1**) and plated onto LB plates supplemented with 25 μg/mL chloramphenicol. Colony PCR was performed using primers pMMB207c F and R to screen for positive colonies. Plasmid extraction from positive colonies was then done, followed by sequencing with primers pMMB207c F and R. The plasmids for ectopic expression of LegC4 were transformed into *L. pneumophila* strain 130b and plated onto BCYE plates containing 6.25 μg/mL chloramphenicol. Positive colonies were screened with colony PCR using pMMB207c F and R primers (**Table 2.3**).

2.6 Whole genome sequencing of *L. pneumophila*

Sequencing of *L. pneumophila* WT and mutants gDNA was performed by Dr Sacha Pidot (PDI, The University of Melbourne) using an Illumina NextSeq platform. Sequencing library was made using Nextera XT according to the manufacturer's instructions. Snippy v 3.2 was used to call single-nucleotide polymorphisms (SNPs) with the WT *L. pneumophila* 130b genome as reference (311). SPAdes v 3.7.1 was used to assemble the sequenced reads when required (312).

2.7 Growth curve of *L. pneumophila*

L. pneumophila was grown in ACES broth for approximately 18 h with agitation. This culture was then adjusted to OD_{600} of 0.01 and loaded onto flat-bottom 96-well plate (Corning) wells in triplicate. The OD_{600} of each well was measured every 5 minutes for 40 h using ClarioStar® microplate reader (BMG Labtech). Throughout the reading, the microplate reader was set to agitate at 200 rpm and temperature was maintained at 37°C. To ease analysis, only data points measured at two-hour intervals were included. The mean OD_{600} of triplicate for each sample was then plotted in each experiment.

2.8 Cell culture

THP1 monocytes were sustained in Roswell Park Memorial Institute (RPMI) supplemented with 10% heat-inactivated Fetal Bovine Serum (FBS, HyClone Technologies, Utah, USA). All cells were maintained at 37°C, 5% CO_2 and passaged whenever 90% confluency was reached. For cryogen long-term storage, cells were kept in FBS containing 10% (v/v) DMSO.

Acanthamoeba castellanii Neff strain (ATCC30010) was maintained at room temperature in Peptone Yeast Glucose (PYG, 2% peptone, 0.1% sodium citrate, 0.1% yeast extract) medium supplemented with 0.1 M glucose, 0.4 mM $CaCl_2$, 2.5 mM KH_2PO_4, 4 mM $MgSO_4$, 2.5 mM Na_2HPO_4, 0.05 mM $Fe_4O_{21}P_6$). Cells were passaged every 3 days, and discarded once the passage number exceeds 30. *L. pneumophila* infection was performed

in the minimal medium (PYG without glucose, yeast extract, and peptone) at 37°C, 5% CO_2. For long term storage, cells were stored in PYG plus 10% (v/v) DMSO.

2.9 *L. pneumophila* replication assay

2.9.1 L. pneumophila replication assay in THP1 macrophages

Prior to infection, THP1 monocytes were differentiated into macrophages by adding 50 ng/mL phorbol 12-myristate 13-acetate (PMA) and seeded at $5x10^5$ cells per well in duplicates in 24-well plates. The cells were then allowed to differentiate at 37°C, 5% CO_2 prior to infection for 3 days after seeding. When IFNγ treatment was required, at approximately 18 h before infection, media was replaced with RPMI containing 100 ng/mL IFNγ and 50 ng/mL PMA.

Infection was performed at a MOI of 10 using *L. pneumophila* grown from either BCYE plates or liquid ACES broth. Cells were incubated at 37°C, 5% CO_2 for 2 hours, followed by gentamicin treatment (100 μg/mL) for 1 h at the same condition. After removing gentamicin, cells were washed to completely remove the gentamicin and fresh media was added to all wells, except t=3 h. To all wells in this plate, 0.05% (w/v) digitonin was added to lyse the cells. Lysis was performed at room temperature for 5 minutes. Lysed cells were then scraped, harvested in ACES broth, and serially diluted in PBS. The appropriate dilutions were then plated on BCYE plates. For later timepoints, infection media was collected to account for bacteria that have escaped the host cells. Cells were then lysed, harvested, and pooled with the collected media, prior to serial dilution and plating in a similar manner to the first timepoint. Plates were then incubated at 37°C for 3 days, and the bacterial colony-forming unit (CFU) was quantified.

2.9.2 L. pneumophila replication assay in A. castellanii

A. castellanii were seeded at $2x10^5$ cells/well in 24-well plates and incubated in PYG media at RT for 24 h. Prior to infection, non-adherent cells were removed by washing

with minimal medium. *L. pneumophila* infection was then performed at a MOI of 2. Cells were incubated at 37°C, 5% CO_2 for 2 h, followed by gentamicin treatment (100 μg/mL) for 1 h at the same condition. After removing gentamicin, cells were maintained in minimum media until the desired time points. At each time point, amoebae were lysed by vigorous vortexing. Serial dilutions of the lysate were then plated on BCYE agar at 37°C for 3 days to enable enumeration of bacterial CFU.

2.10 TEM-1 β-lactamase translocation assay

WT and mutant *L. pneumophila* strains carrying TEM-1 β-lactamase-tagged RalF were grown in ACES broth containing 6.25 μg/mL chloramphenicol and 10 mM IPTG for 18 h at 37°C with agitation at 180-200 rpm. These strains were then used to infect PMA-differentiated THP1 macrophages at an MOI of 40. In this assay, the THP1 macrophages were seeded in triplicate on black 96-well plate (Corning) instead of clear 24-well plates to enable accurate fluorescence reading. After addition of bacteria, the plates were spun at 1200 rpm for 10 minutes to synchronize the infection before incubating at 37°C, 5% CO_2 for 1 hour. Cells were then washed with 1x Hank's Balanced Salt Solution (HBSS) supplemented with 5% HEPES before addition of 100 μL of CCF2-AM LiveBLAzer™ (Thermo Scientific) solution prepared according to manufacturer's protocol. The cells were then incubated for 1 h and 45 minutes at room temperature in the dark. Prior to reading the assay in the ClarioStar® microplate reader, the CCF2-AM solution in each well was replaced with 100 μL 1x HBSS. The microplate reader was set to excite at 410 nm and the fluorescence at 450 nm and 520 nm were measured. The background reading from no cell control at each wavelength was subtracted from the results. The triplicate mean ratio of 520 nm to 450 nm was then calculated. This ratio was then compared to the sample infected by WT *L. pneumophila* carrying empty pXDC61 to determine the level of RalF translocation.

2.11 Cell viability assay

THP1 macrophages were infected by WT or mutant *L. pneumophila* strains at MOI 10 as described in section 2.9. In this assay, THP1 macrophages were seeded in triplicate on

black 96-well plates to enable accurate measurement of fluorescence. At either 24 h or 48 h post-infection, cells were washed with PBS and fixed with ice-cold methanol on ice for 10 minutes. Cells were then stained by adding 100 μL of CellTag700 (Licor) diluted in PBS at 1:10,000, and incubated at room temperature in the dark while shaking at 200 rpm for 20 minutes. After staining, cells were subjected to three 5 min washes with PBS plus 10% Tween-20 (PBST). Finally, 100 μL PBS was added to each well, and the fluorescence at 700 nm was measured using Odyssey Imaging System (Licor). The results for each sample was normalized by subtracting the background fluorescence obtained from no cell control from the reading results. Afterwards, the mean fluorescence of each triplicate was compared to the uninfected samples to obtain percentage of viable cells in each experiment.

2.12 Immunofluorescence

THP1 monocytes were differentiated by PMA addition as described in section 2.9 and seeded on coverslips in 24-well plates. Three days later, cells were infected at an MOI of 10 by *L. pneumophila* strains carrying either empty pMMB207c_4xHA or pMMB207c_4xHA:*legC4* grown overnight in ACES broth plus 6.25 μg/mL chloramphenicol and 10 mM IPTG. After the addition of bacteria, plates were spun at 1200 rpm for 10 minutes to synchronise infection. At 6 hours post-infection, cells were washed with PBS and fixed with 4% paraformaldehyde (PFA) for 12 minutes on ice. After three washes with PBS, the aldehyde was quenched by the addition of 50 mM NH_4Cl for 20 minutes at room temperature. Cells were then permeabilized by the addition of 0.2% Triton X-100 (Sigma-Aldrich) for three minutes at room temperature. After three washes with PBS, non-specific interaction was blocked by incubating the cells with 3% Bovine Serum Albumin (BSA, Sigma-Aldrich) in PBS. Cells were then incubated with 1:200 mouse-anti-haemagglutinin (HA) epitope tag (BioLegend) and 1:1,000 rabbit-anti-*L. pneumophila* (Meridian Bioscience) diluted in 3% BSA. After 1 h of incubation at room temperature in the dark, cells were subjected to three times five-minute washes with PBS and incubated with Alexa Fluor™ 488-conjugated goat-anti-mouse (Thermo Fisher) and Alexa Fluor™ 568-conjugated goat-anti rabbit (Thermo Fisher) secondary antibodies, both of which were diluted at 1:2,000 in 3% BSA, for 20 minutes at room

temperature in the dark. Following this, cells were incubated with 1:4,000 Hoechst (Sigma Aldrich) for 10 minutes at room temperature in the dark. Finally, cells were mounted onto microscope slides using ProLong Gold mounting medium (Life Technologies). Images were then obtained using Olympus FV1200 confocal microscope with 60x oil immersion objective and analysed using FIJI.

2.13 Quantitative real time (QRT)-PCR

THP1 monocytes were differentiated into macrophages by PMA addition and seeded on 24-well plates as described in section 2.9. Cells were then infected at MOI 10 with *L. pneumophila* strains grown in ACES broth overnight. Plates were then spun at 1200 rpm for 10 minutes to synchronise the infection and incubated at 37°C, 5% CO_2. Two hours after infection, the media was replaced with RPMI containing 100 μg/mL gentamicin and incubated at 37°C, 5% CO_2 for 1 h. After washing the gentamicin from the wells, RPMI plus FBS was added to the cells and incubated at 37°C, 5% CO_2. At 6 h post-infection, RNA was extracted and DNase-treated using the ISOLATE II RNA Mini Kit (Bioline) according to manufacturer's protocol. The RNA yield was then quantified using NanoDrop spectrophotometer. Following this, cDNA synthesis was performed using SuperScript II Reverse Transcriptase (Invitrogen) according to manufacturer's protocol.

cDNA was analysed using either non-quantitative or quantitative real time-PCR (QRT-PCR). For non-quantitative PCR, cDNA was amplified using GoTaq Green Mastermix using either the Gapdh F/R primer set or Actb F/R primer set (**Table 2.3, Table 2.4**). The PCR product was then run on 3% (w/v) Ultrapure Agarose containing 0.01% (v/v) SybrSafe DNA stain in 1x TAE buffer. Gel was then visualized using the fluorescence mode of AI600 Gel Imager. QRT-PCR was performed in 10 μL reactions in triplicate using Power SYBR® Green Master Mix (Thermo Fisher) according to the manufacturer's protocol. In each 10 μL reaction, 0.5 μM primers and 1 μL of cDNA were used. Primer pairs Gapdh F/R and Actb F/R (**Table 2.3**) were used. QRT-PCR was then performed using QuantStudio 6 Flex Real-Time PCR System (Thermo Fisher). The relative mRNA level of *GAPDH* was measured and normalized to the level of housekeeping gene *ACTB*.

The relative expression of *GAPDH* mRNA in WT- or mutant-infected cells were then compared to uninfected samples.

2.14 RNA sequencing

Infection of THP1 macrophages with WT or mutant *L. pneumophila* strains were conducted as described in section 2.10.1. At 6 h post-infection, RNA was harvested and DNase-treated using ISOLATE II RNA Mini Kit (Bioline). RNA sequencing was then performed by AGRF. Here, RNA quality was then assessed using Agilent 2100 Bioanalyzer (Agilent Technologies). Poly-A-tailed mRNA purification, cDNA synthesis, and library preparation were done using the TruSeq Stranded mRNA sample preparation kit (Illumina) as per manufacturer's instructions. Following this, sequencing was performed using NovaSeq 6000 system (Illumina).

Genome alignment and read counts generation were performed by Dr Dane Vassiliadis. The sequenced reads were aligned to the *Homo sapiens* genome (GRCh38.90) using Tophat2 v 2.1.1 and read counts were generated using featureCounts v 1.5.0. Principal component analysis (PCA) and differential expression analysis were performed using the R software package DeSeq2 (313). Volcano plots were created using Microsoft Excel. Genes that showed significant $\log_2$ fold change (LFC) of $-1 \leq LFC \leq 1$ were considered to be significantly upregulated or downregulated. Venn diagram was generated using Venny 2.1.0 to identify genes upregulated in all mutant-infected cells relative to WT-infected cells (314). The PANTHER gene list analysis was used to group these genes based on the biological process (315). Additionally, GO analysis was performed using the Generic GO::Term Finder tool to identify enriched biological processes using a hypergeometric distribution that takes into account the bias in the sample population (316). P-value was adjusted using the Bonferroni correction.

2.15 Animals and animal experiments

2.15.1 Mice

All mice were bred and maintained under specific pathogen free condition either in the Animal Resource Centre (ARC) or Bio21 Molecular Science and Biotechnology Institute. All mice experiments were conducted at the Bio21 Molecular Science and Biotechnology Institute under ethics approved by the University of Melbourne Animal Ethics Committee.

2.15.2 Intranasal infection and organ harvesting

A-strain mice or C57BL/6 mice were infected intranasally with WT or mutant strains of *L. pneumophila* 130b at $2.5x10^6$ cfu per animal as previously described (317). Bacterial inoculum was prepared at $5x10^7$ cfu/mL in PBS. During infection, animals were put under isofluorane anasthesia. Mice were then handled by the scruff and 50 μL of the inoculum was administered via droplet into one nostril.

After infection, animal body weights were monitored daily as prescribed by the ethics requirements. At either day 1 or day 3 post-infection, mice were euthanized via CO_2 inhalation in a Perspex container. The skin was then sterilized with 80% ethanol prior to dissection with forceps and scissors. For CFU counting, either the right lung or both lungs were harvested into 2.5 mL PBS as indicated in text. For flow cytometry analysis, the left lung was harvested into 3 mL FACS buffer (**Table 2.4**).

2.15.3 Preparation of lungs for CFU counting

Harvested lungs were homogenized using ULTRA-TURRAX® homogenizer (IKA). The homogenate was then permeabilized by adding 2.5 μL of 10% (w/v) saponin (Sigma-Aldrich) to 250 μL homogenate followed by incubation at 37°C for 30 minutes. Samples were then serially diluted, spotted onto BCYE plates, and incubated at 37°C for 3 days to enumerate bacterial CFU. The leftover non-permeabilized samples were frozen at -80°C for future cytokine analysis.

2.16 Flow cytometry

2.16.1 Preparation of cell suspension

Lungs were minced finely using scissors, collected in 3.5 mL digestion buffer (**Table 2.4**), and incubated at 37°C for 30 minutes with occasional mixing every 5 minutes. Cells were filtered using 70 μm cell strainers (Miltenyi Biotech). Strainers were then rinsed with FACS buffer. Cells were then pelleted at 600 rcf at 4°C. Finally, the cells were resuspended in 1 mL FACS buffer and stained with 1:1,000 APC-eFluor 780-conjugated viability dye (eBioscience, catalog 65-0865-14).

2.16.2 Staining of phagocyte panel

After staining with viability dye, cells were washed in FACS buffer, and incubated with primary antibodies from the phagocyte staining panel as described in **Table 2.5** for 30 minutes at 4°C. Red blood cells were then lysed using 1x BD FACS Lysing solution (BD Biosciences) for 7 minutes at room temperature. Cells were then fixed with 1x Fixation/Permeabilisation buffer (eBioscience) for 30 minutes at room temperature and permeabilised with 1x Permeabilisation buffer (eBioscience) to allow staining of intracellular *L. pneumophila*. After permeabilisation, cells were incubated with 1:1,000 FITC-conjugated anti-*L. pneumophila* antibody (ViroStat, catalog 6053) diluted in 1x permeabilization buffer for 30 minutes at 4°C. After washing with the staining buffer, cells were stored in FACS buffer at 4°C in the dark. Prior to analysis with BD LSR Fortessa II, $2x10^5$ APC-labelled beads were added to each sample to allow enumeration of cells.

2.16.3 Staining of lymphocyte panel

After staining with viability dye, cells were washed in FACS buffer, and incubated with primary antibodies from the lymphocyte staining panel as described in **Table 2.6** for 30 minutes at 4°C. Red blood cells were then lysed using 1x BD FACS Lysing solution (BD Biosciences) for 7 minutes at room temperature. Cells were then fixed with 2% PFA for

30 minutes. After washing off the PFA, cells were stored in FACS buffer and stored at 4°C in the dark prior to analysis on BD LSR Fortessa II.

2.17 Cytometric bead array (CBA)

After murine infection, lung harvest, and lung homogenization as described in section 2.15, lung homogenate was spun down at 10,000 rcf for 5 minutes to remove debris. The CBA Mouse Flex Set Kit (BD Biosciences) was used to quantify the concentration of pro-inflammatory cytokines as per manufacturer's instructions. Analysis was then performed on BD LSR Fortessa II.

2.18 Bioinformatics prediction and phylogenetic analysis

The genome sequences of *L. pneumophila* 130b and Philadelphia-1 were obtained from NCBI. Mapping of effector-encoding and secretion system-encoding genes to the genome was done using Artemis (318). Annotated *L. pneumophila* 130b genome was then visualized using DNAPlotter (319). The NCBI BLAST+ suite v 2.9.0 was used to compare the homology of each gene in *L. pneumophila* strain 130b and *L. pneumophila* strain Philadelphia-1 (320). Bacterial genomes were viewed using Artemis, whereas visualization of the alignment of the genomic regions in *L. pneumophila* strain 130b to the *L. pneumophila* strain Philadelphia-1 was done using Artemis Comparison Tool (ACT) (318, 321).

Domain prediction was performed through all databases available in the InterPro Scan web server (322). In addition, structural homology was predicted using HHPred, Phyre2 (intensive mode), Robetta, RaptorX, and i-TASSER web servers (323-326). The presence of coiled-coil region was predicted using the Parcoil2 web server (327). To identify orthologs of *lpw_04861* and *legC4*, protein BLAST (BLASTp) was performed. Sequences of orthologous genes were then retrieved from NCBI and aligned using MUSCLE (328). Finally, a maximum likelihood tree was constructed using MEGA v 10.1.7.

2.19 Data analysis

Analysis of flow cytometry data was done using BD FACSDiva™ or FlowJo v 10.0.7. Other data analyses were performed using GraphPad Prism 8 and Microsoft Excel. When required, statistical analysis was performed using either two-tailed unpaired t-test, Mann-Whitney test, or one-way ANOVA as indicated in text.

Table 2.1. Bacterial strains used in this study

Strains	Characteristics	Sources/References
E. coli XL1-Blue	*supE44 hsdR17 recA1 endA1 gyrA46 thi relA1 lac- F' [proAB+ lacIq lacZM15 Tn10 (TetR)]*	Novagen
E. coli PIR2	*F-Δlac169 rpoS(Am) robA1 creC510 hsdR514 endA recA1 uidA(ΔMluI)::pir*	Invitrogen
L. pneumophila 130b (ATCC BAA-744)	Clinical isolate	(329)
Δ*dotA*	130b Δ*dotA* deletion mutant	(330)
ΔA	130b ΔA deletion mutant	This study
ΔB	130b ΔB deletion mutant	This study
ΔC	130b ΔC deletion mutant	This study
ΔD	130b ΔD deletion mutant	This study
ΔE	130b ΔE deletion mutant	This study
ΔF	130b ΔF deletion mutant	This study
ΔG	130b ΔG deletion mutant	This study
ΔH	130b ΔH deletion mutant	This study
ΔI	130b ΔI deletion mutant	This study
ΔFGHI	130b ΔFGHI deletion mutant	This study
ΔDFGHI	130b ΔDFGHI deletion mutant	This study
Δ*lpw_04831*	130b Δ*lpw_04831* deletion mutant	This study
Δ*lpw_04841*	130b Δ*lpw_04841* deletion mutant	This study

Strains	Characteristics	Sources/References
Δ*lpw_04851*	130b Δ*lpw_04851* deletion mutant	This study
Δ*lpw_04861*	130b Δ*lpw_04861* deletion mutant	This study
ΔE1	130b ΔE1 deletion mutant	This study
ΔE2	130b ΔE2 deletion mutant	This study
ΔE3	130b ΔE3 deletion mutant	This study
ΔE4	130b ΔE4 deletion mutant	This study
ΔE2-1	130b ΔE2-1 deletion mutant	This study
ΔE2-2	130b ΔE2-2 deletion mutant	This study
ΔE2-3	130b ΔE2-3 deletion mutant	This study
Δ*legC4*	130b Δ*legC4* deletion mutant	This study

Table 2.2. Plasmids used in this study

Plasmids	Characteristics	Sources/References
pSR47s	*sacB* based suicide vector for mutagenesis	(331)
pSR47s:ΔA	Suicide vector to delete genomic region A	This study
pSR47s:ΔB	Suicide vector to delete genomic region B	This study
pSR47s:ΔC	Suicide vector to delete genomic region C	This study
pSR47s:ΔD	Suicide vector to delete genomic region D	This study
pSR47s:ΔE	Suicide vector to delete genomic region E	This study
pSR47s:ΔF	Suicide vector to delete genomic region F	This study
pSR47s:ΔG	Suicide vector to delete genomic region G	This study
pSR47s:ΔH	Suicide vector to delete genomic region H	This study
pSR47s:ΔI	Suicide vector to delete genomic region I	This study
pSR47s:Δ*lpw_04831*	Suicide vector to delete *lpw_04831*	This study
pSR47s:Δ*lpw_04841*	Suicide vector to delete *lpw_04841*	This study
pSR47s:Δ*lpw_04851*	Suicide vector to delete *lpw_04851*	This study
pSR47s:Δ*lpw_04861*	Suicide vector to delete *lpw_04861*	This study
pSR47s:ΔE1	Suicide vector to delete genomic region E1	This study
pSR47s:ΔE2	Suicide vector to delete genomic region E2	This study
pSR47s:ΔE2-1	Suicide vector to delete genomic region E2-1	This study
pSR47s:ΔE2-2	Suicide vector to delete genomic region E2-2	This study
pSR47s:ΔE2-3	Suicide vector to delete genomic region E2-3	This study

Plasmids	Characteristics	Sources/References
pSR47s:ΔE3	Suicide vector to delete genomic region E3	This study
pSR47s:ΔE4	Suicide vector to delete genomic region E4	This study
pSR47s:Δ*legC4*	Suicide vector to delete *legC4*	This study
pXDC61	N-terminal TEM-1 β-lactamase expression vector	(250)
pXDC61:*ralF*	130b *ralF* in pXDC61	(310)
pMMB207c_4xHA	N-terminal 4xHA expression vector	(310)
pMMB207c_4xHA:*legC4*	130b *legC4* in pMMB207c_4xHA	This study
pMMB207c:p*legC4*	130b *legC4* plus promoter in pMMB207c	This study

Table 2.3. Oligonucleotides used in this study

Name	Sequence (5'-3')	Purpose
pSR47s F	AGCTATGACCATGATTACGC	F- sequence pSR47s
pSR47s R	GTGAACGGCAGGTATATGT	R- sequence pSR47s
pMMB207c F	TTGACAATTAATCATCGGC	F- sequence pMMB207c-HAx4
pMMB207c R	AGGCAAATTCTGTTTTATC	R- sequence pMMB207c-HAx4
A5 F	GGACTAGTCGACACTCAAACCTCCACCC	F- amplify 5' flanking region of genomic region A. Contains SpeI site.
A5 R	AATAGAAGCCCCTTACCTCACAA	R- amplify 5' flanking region of genomic region A
A3 F	TTTTGTGAGGTAAGGGGCTTCTATTAAATGCCCCGCTTTCTGA	F- amplify 3' flanking region of genomic region A
A3 R	TTGCGGCCGCTTTTATCGGTGCTGTAATCTTGG	R- amplify 3' flanking region of genomic region A. Contains NotI site.
$A_{upstream}$	AAATCTGACCAATAGCCCAAGC	F- confirm the deletion of genomic region A
$A_{downstream}$	TTTGACGAAAAGGGAAACTGG	R- confirm the deletion of genomic region A
B5 F	CGAATTCCTGCAGCCCGGGGGATCCTGTCGGTTTCATTCAAATCCTC	F- amplify 5' flanking region of genomic region B. Contains BamHI site.
B5 R	TTCACCATATCCTGGCTCCAC	R- amplify 5' flanking region of genomic region B
B3 F	TGAGGTGGAGCCAGGATATGGTGAATGGTAATGACTCGCTCTGGG	F- amplify 3' flanking region of genomic region B
B3 R	CTAAAGGGAACAAAAGCTGGAGCTCCATGCTTTAGTTGCATAGGTTGTAT	R- amplify 3' flanking region of genomic region B. Contains SacI site.
B seq	GAAGTTGGTATGCGGGGTGC	Sequence pSR47s-ΔB

Name	Sequence (5'-3')	Purpose
$B_{upstream}$	CTCGGTCAATATCGCTCATAGG	F- confirm the deletion of genomic region B
$B_{downstream}$	CATCGCCCTTGTATCGTTTG	R- confirm the deletion of genomic region B
C5 F	TTGCGGCCGCTGCTCGCAGCGCATCA	F- amplify 5' flanking region of genomic region C. Contains NotI site.
C5 R	TCCTCGCAAAACCACCCA	R- amplify 5' flanking region of genomic region C
C3 F	TATGCATTGGGTGGTTTTGCGAGGAGTGAAAACAATAATTGCTTGAAACC	F- amplify 3' flanking region of genomic region C
C3 R	CGGAGCTCTCCCAGATAATAGCCGAGTGC	R- amplify 3' flanking region of genomic region C. Contains SacI site.
C seq	TTGCGGAACGAACCA	Sequence pSR47s-ΔC
$C_{upstream}$	GTGTCAGGACGGCATAGGG	F- confirm the deletion of genomic region C
$C_{downstream}$	TCATCGCCTGCTTATGCTTG	R- confirm the deletion of genomic region C
D5 F	CGGGATCCCTGCTTTAGCGGGGAACC	F- amplify 5' flanking region of genomic region D. Contains BamHI site.
D5 R	AGAATGTGATAGGACGGTAGAAAAT	R- amplify 5' flanking region of genomic region D
D3 F	ATTTTCTACCGTCCTATCACATTCTAACAAGCGATTCGACTGATAAAA	F- amplify 3' flanking region of genomic region D
D3 R	TTGCGGCCGCCTGAAGAGGTAGATGCTGGTCC	R- amplify 3' flanking region of genomic region D. Contains NotI site.
D seq	CAGCCATGTTGGGTGAC	Sequence pSR47s-ΔD
$D_{upstream}$	CTGCTTTAGCGGGGAACC	F- confirm the deletion of genomic region D
$D_{downstream}$	TGCGTGCCTTATGATTCGTT	R- confirm the deletion of genomic region D

Name	Sequence (5'-3')	Purpose
E5 F	GAGGGATCCGACCCT GTTGGCAGCTATC	F- amplify 5' flanking region of genomic region E. Contains BamHI site.
E5 R	TATCCCTACCTCTTGT GGAG	R- amplify 5' flanking region of genomic region E
E3 F	CTCCACAAGAGGTAG GGATAATGGCAGACA AATGTTAAGGAA	F- amplify 3' flanking region of genomic region E
E3 R	AGCGGCCGCCGGTTG GAGTAGTTTGGACA	R- amplify 3' flanking region of genomic region E. Contains NotI site.
E seq	AGCGGGTCCATATAA AATAGC	Sequence pSR47s-ΔE
$E_{upstream}$	GAACACGCGCTTGTA AGAAAA	F- confirm the deletion of genomic region E
$E_{downstream}$	AAATTGCAAAGATAA GATTGTACT	R- confirm the deletion of genomic region E
F5 F	CGAATTCCTGCAGCC CGGGGGATCCCAGTT TGCGGCCTCCACT	F- amplify 5' flanking region of genomic region F. Contains BamHI site.
F5 R	AGCAGCCTGTCGTCT ATTATTTTAC	R- amplify 5' flanking region of genomic region F
F3 F	GTAAAATAATAGACG ACAGGCTGCTTTGGC GGAAGTTGATGTCG	F- amplify 3' flanking region of genomic region F
F3 R	CTAAAGGGAACAAAA GCTGGAGCTCTGGCTT TCTCCACCAGGCT	R- amplify 3' flanking region of genomic region F. Contains SacI site.
F seq	CAAGGTCGAGGCAGA AAATG	Sequence pSR47s-ΔF
$F_{upstream}$	ATACGCCCTGATATG GGAAAT	F- confirm the deletion of genomic region F
$F_{downstream}$	GGCAAGAATAGTTCC TGTGCC	R- confirm the deletion of genomic region F
G5 F	CGGCGGCCGCCCCTG GCAATGTCACCTACC	F- amplify 5' flanking region of genomic region G. Contains NotI site.
G5 R	TACCTCCTGATTGTGG TTTTGTTT	R- amplify 5' flanking region of genomic region G

Name	Sequence (5'-3')	Purpose
G3 F	AAAACAAAACCACAATCAGGAGGTAATCCACTTCCCTATGTCATGATTT	F- amplify 3' flanking region of genomic region G
G3 R	CGCGAGCTCGGCGTAAGGAAACGACAGG	R- amplify 3' flanking region of genomic region G. Contains SacI site.
G seq	TTGAAGTCACATTTGCATATCC	Sequence pSR47s- ΔG
$G_{upstream}$	TATCGATGAAAAGCACAGGAG	F- confirm the deletion of genomic region G
$G_{downstream}$	AATTCCATCCATTTTGGCGATA	R- confirm the deletion of genomic region G
H5 F	CGGGATCCGGAAAAGGAGCATCAAAACAGT	F- amplify 5' flanking region of genomic region H. Contains BamHI site.
H5 R	ATTAAGGAAAACCGAGGCAAA	R- amplify 5' flanking region of genomic region H
H3 F	ATTTTTTGCCTCGGTTTTCCTTAATTAACAACTGCCCTCATTGCTTT	F- amplify 3' flanking region of genomic region H
H3 R	CGGCGGCCGCCCATAGGTGCTTGCGCTACA	R- amplify 3' flanking region of genomic region H. Contains NotI site.
H seq	GCATGCCATCAAAATCCAATT	Sequence pSR47s-ΔH
$H_{upstream}$	GAGCTATATTTGCCCTTGGTA	F- confirm the deletion of genomic region H
$H_{downstream}$	ATCAGACTTGGTTGAAATTGTG	R- confirm the deletion of genomic region H
I5 F	CGGGATCCAATGATTGTCACTTGCGATGG	F- amplify 5' flanking region of genomic region I. Contains BamHI site.
I5 R	CGATTTGAGAATTATTTGAGGAGC	R- amplify 5' flanking region of genomic region I
I3 F	AGCTCCTCAAATAATTCTCAAATCGTATTGCTTTTCCTCCTTGGTTT	F- amplify 3' flanking region of genomic region I
I3 R	CGGCGGCCGCTCTTGCTGCTTTGGCTGTATC	R- amplify 3' flanking region of genomic region I. Contains NotI site.

Name	Sequence (5'-3')	Purpose
I seq	TATCACGAAATGAGCAGACC	Sequence pSR47s-ΔI
$I_{upstream}$	AAAGAATAATTGGTTCGGCGA	F- confirm the deletion of genomic region I
$I_{downstream}$	ATTTCTCGCTCTCATTTGCAA	R- confirm the deletion of genomic region I
31-5 F	CGCGGATCCAGCAGGCGGTTGGGTTT	F- amplify 5' flanking region of *lpw4831*. Contains BamHI site.
31-5 R	CCATAGTAAAGATCGCTCTATTGGT	R- amplify 5' flanking region of *lpw4831*
31-3 F	ACCAATAGAGCGATCTTTACTATGGGTAAGCCTGACTTGTTTGGAGG	F- amplify 3' flanking region of *lpw4831*
31-3 R	CGCGAGCTCGGGATCTTGAGCAATACAGATTTT	R- amplify 3' flanking region of *lpw4831*. Contains SacI site.
$31_{upstream}$	TTTATCGGTTGCTCATTAGGGT	F- confirm the deletion of *lpw4831*
$31_{downstream}$	CGGGACGAGAACTCAAAGTAAG	R- confirm the deletion of *lpw4831*
41-5 F	CGCGGATCCTTGGCTTTATGGTAGGCTTCG	F- amplify 5' flanking region of *lpw4841*. Contains BamHI site.
41-5 R	CAAACAAGTCAGGCTTACTGCTCT	R- amplify 5' flanking region of *lpw4841*
41-3 F	TAGAGCAGTAAGCCTGACTTGTTTGTCGGACCTGTACTGAAATGAAAA	F- amplify 3' flanking region of *lpw4841*
41-3 R	CGCGAGCTCCCCGCAACAAACGATAGAATC	R- amplify 3' flanking region of *lpw4841*. Contains SacI site.
$41_{upstream}$	AGCCCTGCGAAAGTGGTTG	F- confirm the deletion of *lpw4841*
$41_{downstream}$	AAATGACAATATGATGGCGGTTA	R- confirm the deletion of *lpw4841*
51-5 F	CGCGGATCCAAGACAGCAAGGGGAGAACG	F- amplify 5' flanking region of *lpw4851*. Contains BamHI site.
51-5 R	CAGGTCCGATGCGAAAACA	R- amplify 5' flanking region of *lpw4851*

Name	Sequence (5'-3')	Purpose
51-3 F	CATATGATGTTTTCGC ATCGGACCTGCAGGT TAAGTTTAATAACCCC AGTT	F- amplify 3' flanking region of *lpw4851*
51-3 R	CGCGAGCTCCGATTTC AGGATATTGCTCGA	R- amplify 3' flanking region of *lpw4851*. Contains SacI site.
$51_{upstream}$	TGACTGTGAATACCG ATTTTGTTT	F- confirm the deletion of *lpw4851*
$51_{downstream}$	GCCAACGCCATAGCG ATTA	R- confirm the deletion of *lpw4851*
61-5 F	GGACTAGTTTCTCGG AGGGCTTGGTG	F- amplify 5' flanking region of *lpw4861*. Contains SpeI site.
61-5 R	CTGGGGTTATTAAACT TAACCTGTC	R- amplify 5' flanking region of *lpw4861*
61-3 F	GACAGGTTAAGTTTA ATAACCCCAGGCCTG GACAATTCAAGATAA CG	F- amplify 3' flanking region of *lpw4861*
61-3 R	CGCGAGCTCCAAAGC AAAGTTGGCAGAGC	R- amplify 3' flanking region of *lpw4861*. Contains SacI site.
$61_{upstream}$	CATTGGTTTGGGTGCT GTTT	F- confirm the deletion of *lpw4861*
$61_{downstream}$	TTTCTCAAGTGGCTTT ATTAGGG	R- confirm the deletion of *lpw4861*
E1-5 F	TCCTGCAGCCCGGGG GATCCCGCAAATTAT CAGCATCTACC	F- amplify 5' flanking region of region E1. Contains BamHI site.
E1-5 R	GTCAACACTGTGCCCT ATCCCTACCTC	R- amplify 5' flanking region of region E1
E1-3 F	AGGGCACAGTGTTGA CAATTGGCTCC	F- amplify 3' flanking region of region E1
E1-3 R	CTCCACCGCGGTGGC GGCCGCCGCCAGAGA ATGAGAATTG	R- amplify 3' flanking region of region E1. Contains NotI site.
$E1_{upstream}$	TCTTTTCCGAGCATTG ACGC	F- confirm the deletion of region E1
$E1_{downstream}$	ACCTGCGCATTTTGTT GTCT	R- confirm the deletion of region E1

Name	Sequence (5'-3')	Purpose
E2-5 F	TCCTGCAGCCCGGGG GATCCTCACTCTTGCA TTCAACG	F- amplify 5' flanking region of region E2. Contains BamHI site.
E2-5 R	CCGCAGTTTGGGAGC CAATTGTCAAC	R- amplify 5' flanking region of region E2
E2-3 F	GGCTCCCAAACTGCG GCCGGATCTTATTG	F- amplify 3' flanking region of region E2
E2-3 R	CTCCACCGCGGTGGC GGCCGCTGCTTGGGG ATTCTGGGTTAATAAC	R- amplify 3' flanking region of region E2. Contains NotI site.
$E2_{upstream}$	ACCTGCGCATTTTGTT GTCT	F- confirm the deletion of region E2
$E2_{downstream}$	TAGTGGTGCCTATTCC CAGC	R- confirm the deletion of region E2
E3-5 F	TCCTGCAGCCCGGGG GATCCGTCTGGATGG CTGGAAAAC	F- amplify 5' flanking region of region E3. Contains BamHI site.
E3-5 R	CTTCCCCAAGATCCG GCCGCAGTTTTATAA AAAAC	R- amplify 5' flanking region of region E3
E3-3 F	CCGGATCTTGGGGAA GACTTCGAATACATT G	F- amplify 3' flanking region of region E3
E3-3 R	CTCCACCGCGGTGGC GGCCGCGGTACGTCG CCATGTCAATTG	R- amplify 3' flanking region of region E3. Contains NotI site.
$E3_{upstream}$	TGCATTCCAGAAACA GGTCT	F- confirm the deletion of region E3
$E3_{downstream}$	TGATAATGGATGCTG GCAGTT	R- confirm the deletion of region E3
E4-5 F	TCCTGCAGCCCGGGG GATCCGCTTTCCACGT TCACTTG	F- amplify 5' flanking region of region E4. Contains BamHI site.
E4-5 R	TCTGCATCTGAGGTAT AAGAGGGCAG	R- amplify 5' flanking region of region E4
E4-3 F	TATACCTCAGATGCA GAAGAAATTTACTCC CC	F- amplify 3' flanking region of region E4
E4-3 R	CTCCACCGCGGTGGC GGCCGCGCTGCCTTG GTCGAGAAAG	R- amplify 3' flanking region of region E4. Contains NotI site.

Name	Sequence (5'-3')	Purpose
$E4_{upstream}$	AGCGCCAATTGTCCTTCTTC	F- confirm the deletion of region E4
$E4_{downstream}$	CATCATTACGGGGTTGCAGG	R- confirm the deletion of region E4
E2-1-5 F	TCCTGCAGCCCGGGGGATCCTCACTCTTGCATTCAACG	F- amplify 5' flanking region of region E2-1. Contains BamHI site.
E2-1-5 R	GGAGCTCTTGGGAGCCAATTGTCAAC	R- amplify 5' flanking region of region E2-1
E2-1-3 F	GGCTCCCAAGAGCTCCCGGTTTTGATG	F- amplify 3' flanking region of region E2-1
E2-1-3 R	CTCCACCGCGGTGGCGGCCGCCAGACGTATTGCTGCACC	R- amplify 3' flanking region of region E2-1. Contains NotI site.
$E2\text{-}1_{upstream}$	TGACCGTGGATGGACTCAAA	F- confirm the deletion of region E2-1
$E2\text{-}1_{downstream}$	GTGGGGTGGTATGACAAAGC	R- confirm the deletion of region E2-1
E2-2-5 F	TCCTGCAGCCCGGGGGATCCGCCCAAGTACGCAATGTC	F- amplify 5' flanking region of region E2-2. Contains BamHI site.
E2-2-5 R	TTGCACCACACAGGATCAAAACCGGGAGCTCTC	R- amplify 5' flanking region of region E2-2
E2-2-3 F	GGTTTTGATCCTGTGTGGTGCAAACTC	F- amplify 3' flanking region of region E2-2
E2-2-3 R	CTCCACCGCGGTGGCGGCCGCTCCTGTCGACTCGGTTTG	R- amplify 3' flanking region of region E2-2. Contains NotI site.
$E2\text{-}2_{upstream}$	CCTTGGGTGGTTTCCGACTT	F- confirm the deletion of region E2-2
$E2\text{-}2_{downstream}$	TACATCAATGAGCCCTGCGA	R- confirm the deletion of region E2-2
E2-3-5 F	TCCTGCAGCCCGGGGGATCCGCCACGGAAATCACTTGAG	F- amplify 5' flanking region of region E2-3. Contains BamHI site.
E2-3-5 R	ATCAAGCTTACACAGGGCTATACTTAGGGC	R- amplify 5' flanking region of region E2-3
E2-3-3 F	CCCTGTGTAAGCTTGATCTGGCCAATGC	F- amplify 3' flanking region of region E2-3

Name	Sequence (5'-3')	Purpose
E2-3-3 R	CTCCACCGCGGTGGC GGCCGCTGCTTGGGG ATTCTGGGTTAATAAC	R- amplify 3' flanking region of region E2C. Contains NotI site.
$E2\text{-}3_{upstream}$	GCCGCGCAACCATTA TTTTC	F- confirm the deletion of region E2-3
$E2\text{-}3_{downstream}$	GGCCATTTTGAGTAC GCGAT	R- confirm the deletion of region E2-3
Leg-5 F	TCCTGCAGCCCGGGG GATCCACCCGGATAT AACCACCAC	F- amplify 5' flanking region of *legC4.* Contains BamHI site.
Leg-5 R	TTACAGGCTTCTGACA AGCGAAATACAATG	R- amplify 5' flanking region of *legC4*
Leg-3 F	TTGTCAGAAGCCTGT AAGTACTGCATCG	F- amplify 3' flanking region of *legC4*
Leg-3 R	CTCCACCGCGGTGGC GGCCGCCCTCAAGTG ATTTCCGTG	R- amplify 3' flanking region of *legC4.* Contains NotI site.
$Leg_{upstream}$	AACGCTTACTGTTCCC GGTA	F- confirm the deletion of *legC4*
$Leg_{downstream}$	GCGTGCTTCCCAGTTC AAAA	R- confirm the deletion of *legC4*
LegHA F	GCGCGGGTACCCGGG GATCCAAACCCAATT TGTTTTACTTTG	F- amplify *legC4* to clone into pMMB207c_4xHA. Contains BamHI site.
LegHA R	GCCAAAACAGCCAAG CTTATCTAGATTATAG CTTCATACCAAAAGA TTC	R- amplify *legC4* to clone into pMMB207c_4xHA. Contains XbaI site.
pLegC4 F	CGGGGATCCCCCGAA AAGCCACTTATCCA	F- amplify *legC4* and promoter region. Contains BamHI site.
pLegC4 R	TTATCTAGATGTCAGA ACACTAGTATGCCAT	R- amplify *legC4* and promoter region. Contains XbaI site.
Gapdh-F	ACAACTTTGGTATCGT GGAAGG	F-QRT-PCR primer for GAPDH
Gapdh-R	GCCATCACGCCACAG TTTC	R-QRT-PCR primer for GAPDH
Actb-F	GCGAGAAGATGACCC AGATC	F-QRT-PCR primer for β-actin
Actb-R	CCAGTGGTACGGCCA GAGG	R-QRT-PCR primer for β-actin

Table 2.4. Thermocycler reactions used in this study

Name	Reaction Setup	Thermocycler Setup
Pfu Ultra II	100 ng gDNA 1 mM dNTP mix 0.2 µM each primer 1 µL DMSO 5 µL Pfu Ultra II buffer 1 µL Pfu Ultra II polymerase Nuclease-free dH_2O to 50 µL	95°C, 2 mins initial denaturation Start cycle 30x 95°C, 20s denaturation 50-55°C, 20s annealing 72°C, 15s/kb elongation End cycle 72°C, 3 mins final elongation
Phusion-HF	100 ng gDNA 1 mM dNTP mix 0.5 µM each primer 1.5 µL DMSO 10 µL Phusion-HF buffer 0.5 µL Phusion-HF polymerase Nuclease-free dH_2O to 50 µL	98°C, 30s initial denaturation Start cycle 35x 98°C, 10s denaturation Tann*, 30s annealing 72°C, 30s/kb elongation End cycle 72°C, 10 minutes final elongation
Phusion-HF Overlap step 1	50 ng 5' flank 50 ng 3' flank 1 mM dNTP mix 0.5 µM each primer 1.5 µL DMSO 10 µL Phusion-HF buffer 0.5 µL Phusion-HF polymerase Nuclease-free dH_2O to 50 µL	98°C, 1 min initial denaturation Start cycle 10x 98°C, 10s denaturation Tann*, 30s annealing 72°C, 30s elongation End cycle
Phusion-HF Overlap step 2	50 µL step 1 product 1 mM dNTP mix 0.5 µM each primer 1.5 µL DMSO 10 µL Phusion-HF buffer 0.5 µL Phusion-HF polymerase Nuclease-free dH_2O to 50 µL	98°C, 1 min initial denaturation Start cycle 35x 98°C, 10s denaturation Tann*, 20s annealing 72°C, 30s/kb elongation End cycle 72°C, 5 mins final elongation
GoTaq Green Colony PCR	10 µL GoTaq Green Mastermix 0.2 µM each primer Nuclease-free dH_2O to 20 µL	95°C, 2 mins initial denaturation Start cycle 35x 95°C, 30s denaturation 55°C, 30s annealing 72°C, 1 min/kb elongation End cycle 72°C, 5 mins final elongation
GoTaq Green RT-PCR	10 µL GoTaq Green Mastermix	94°C, 3 mins initial denaturation Start cycle 35x

Name	Reaction Setup	Thermocycler Setup
	0.2 μM each primer 0.5 μL cDNA Nuclease-free dH_2O to 20 μL	94°C, 30s denaturation 58°C, 30s annealing 72°C, 30s elongation End cycle 72°C, 3 mins final elongation
BigDye Terminator	1 μL BigDye 4 μL 5x BigDye buffer 0.1 μM each primer 400 ng DNA Nuclease-free dH_2O to 20 μL	98°C, 1 min initial denaturation Start cycle 25x 96°C, 10s denaturation 50°C, 5s annealing 60°C, 4 mins elongation End cycle

* Annealing temperature for Phusion-HF was determined using NEB Tm Calculator based on the template-annealing portion of primers

Table 2.5. Buffers used in this study

Buffer	Composition
1xTAE	40 mM Tris, 1 mM EDTA disodium salt, 0.114% glacial acetic acid (v/v), pH 8.3
1xTBS	50mM Tris-HCl pH 7.5, 150mM NaCl
TBST	50mM Tris-HCl pH 7.5, 150mM NaCl, 0.1% Tween-20
Transformation Buffer	10 mM PIPES, 15 mM $CaCl_2.2H_2O$, 250 mM KCl
FACS buffer	0.1% BSA, 2 mM EDTA in PBS
Lung digestion buffer	3% FCS, 1 mg/mL DNase-I, 1 mg/mL Collagenase-III in RPMI

Table 2.6. Antibodies for phagocyte staining panel

Antigen	Clone	Fluorochrome	Company	Reference
Ly6G	1A8	PerCP-Cy5.5	BD Pharmingen	560602
CD11c	HL3	PE-CF594	BD Biosciences	562454
FcεR1	MAR-1	PE-Cy7	eBioscience	25-5898-82
Siglec-F	E50-2440	BV421	BD Biosciences	562681
CD45	30-F11	V500	BD Pharmingen	561487
Ly6C	AL-21	BV605	BD Biosciences	563011
CD11b	M1/70	BV711	BioLegend	101242
CD64	X54-5/7.1	AlexaFluor® 647	BD Biosciences	558539
MHC-II	M5/114.15.2	AlexaFluor® 700	BioLegend	107622

Table 2.7. Antibodies for lymphocyte staining panel

Antigen	Clone	Fluorochrome	Company	Reference
CD3ε	145-2C11	PerCP-Cy5.5	BioLegend	100328
TCRγδ	GL3	PE	BD Pharmingen	553178
CD4	RM4-5	eFluor 450	eBioscience	48-0042-82
CD45	30-F11	V500	BD Pharmingen	561487
CD8α	53-6.7	BV711	BD Biosciences	563046
NK1.1	PK136	APC	BD Pharmingen	550627

Chapter 3
Identification of *L. pneumophila* 130b genes important for *in vitro* infection

3.1 Introduction

The Dot/Icm T4SS effectors play crucial roles throughout *L. pneumophila* intracellular replication. In addition, these effectors may also mediate novel modifications that further our understanding of host cell biology. However, to date, the majority of Dot/Icm T4SS effectors remain uncharacterised. The first challenge in studying the Dot/Icm T4SS effectors is the large effector repertoire. As there are over 330 predicted effectors of the Dot/Icm T4SS, this makes it difficult to identify effectors important for a particular phenotype. For instance, while it is known that *L. pneumophila* recruits PI(4)P-rich vesicles to the LCV, it is not known which effectors are responsible for the phenotype (111). The second challenge is the presence of functional redundancy among effectors, where the genetic deletion of one effector typically does not result in a significant replication defect. Thus far, only the single deletion of MavN, SdhA, RavY, and Lpg2505/MesI has led to a significant reduction in bacterial replication (332-334). Furthermore, as discussed in section 1.9, multiple Dot/Icm T4SS effectors target the same pathways, thus confirming the presence of functional redundancy. Finally, two or more effectors may display meta-effector relationships, where they regulate or act antagonistically against each other. For instance, the effector protein LubX mediates the degradation of SidH by ubiquitination, and subsequently degradation through the host proteasome (335). Another effector, MesI, binds to the effector SidI to reduce the host translation inhibition activity of SidI (336). Together, these challenges have complicated the characterisation of Dot/Icm effector functions.

Screening to identify effectors that contribute to a certain phenotype has previously been done through transfection of a library of tagged single effectors into the human epithelial cell line HEK293T cells (293, 305), perhaps due to the difficulty of achieving efficient transfection in macrophages. However, a limitation of this method is the discrepancy between epithelial, especially HEK293T cells, and macrophages cell lines. Secondly, synergistic or antagonistic effectors may not be identified by this method.

The advent of the high-throughput transposon sequencing (TnSeq), also known as insertion sequencing (INSeq) technology has been very powerful in tackling the large effector repertoire of *L. pneumophila* to provide answers to these questions. In this technique, a large library of mutants was used to infect host cells. Following this, the bacteria were recovered and the insertion sequences sequenced to determine the relative abundance of each mutant (337). Shames *et al* (334) utilised this technique to investigate which effector proteins are important for *L. pneumophila* strain Philadelphia-1 replication in both mammalian cells and the mouse lungs. After performing the transposon mutagenesis using a modified Mariner transposon to allow the insertion of a unique sequence, mutants with disruption in Dot/Icm effector-encoding genes, in addition to several control genes, were specifically selected and tested for replication *in vivo.* Using this technique, Dot/Icm effector proteins that contributed to infection in the mouse model were identified (334). While this method is very powerful, the number of mutants generated is enormous, thus, to investigate one phenotype, a high throughput screen is required. Further, the use of TnSeq/INSeq technology only results in the deletion of single genes, therefore, in the case of functional redundancy, where two or more gene products may execute the same function or act on the same pathway, this phenotype will not be identified.

In order to combat the challenge of functional redundancy, a novel screen which combined transposon-based mutagenesis with the RNA interference (iMAD screen) had been developed. In this study, RNAi was used to silence five GTPases known to be involved in cellular trafficking process in *Drosophila*. A *L. pneumophila* strain Philadelphia-1 transposon mutant library was then used to infect *Drosophila* cells. Using this method, the researchers were able to identify groups of effector proteins that cause a defect in replication when one or more GTPase was silenced. Combinatorial deletion of complementary groups of effector proteins then allowed the discovery of effector protein pairs that may be functionally redundant for infection in *Drosophila* cells (280). While this is an excellent method to unravel the complexity of Dot/Icm effector proteins function, it may be difficult to apply the RNAi technology in hosts with low genetic tractability, such as one of the natural hosts of *L. pneumophila, A. castellanii*.

In another study, using a transposon-site hybridisation (TraSH) screen, O'Connor *et al* (338) discovered seven regions in the *L. pneumophila* Philadelphia-1 genome that are devoid of genes important for bacterial viability but are enriched for Dot/Icm T4SS effectors. Following this, they also reported that the deletion of up to 31% of the bacterial genome is dispensable for both bacterial viability and replication in mammalian macrophages, but not in protozoan hosts. This study demonstrated the robustness and versatility of the *L. pneumophila* genome, as the loss of large genomic regions did not compromise bacterial viability, thus opening up the potential for making effector-less mutants, where regions enriched with Dot/Icm effectors are progressively deleted to yield a library of mutants with overlapping, cumulative deletions. Such mutants are then useful to identify Dot/Icm effector genes important for replication, as well as to investigate more specific questions, such as how Dot/Icm effectors influence host immunity, autophagy, translation inhibition, LCV formation, and so on.

In this study, we aimed to progressively delete regions of the *L. pneumophila* 130b genome enriched in effector proteins to hopefully uncover genes with novel functions. We mapped 34 large genomic regions and deleted 9 regions using a suicide vector approach to enable marker-less gene deletion. The deletion of these regions did not result in a significant defect in either bacterial growth rate or Dot/Icm T4SS functionality, thus ensuring that the phenotypes shown in the subsequent assays were the result of host-pathogen interactions and not just an artifact due to reduced mutants growth rate or a non-functional T4SS. While the mutants did not show a significant replication defect in THP1 macrophages, five out of nine mutants showed a severe replication defect in the protozoan host *A. castellanii,* thereby demonstrating the difference in requirements to infect and survive in different hosts.

3.2 Results

3.2.1 Towards an effector-less mutant library in L. pneumophila 130b

Several systematic genetic studies of Dot/Icm effectors in *L. pneumophila* have previously been done in the Philadelphia-1 strain (280, 334, 338). Due to the diversity of *L. pneumophila* strains, especially in the Dot/Icm effector repertoire, it is important to perform these studies in other strains. In this study, *L. pneumophila* strain 130b, a

prototype strain with different effector repertoire was used as it is a useful comparison to generalize about *L. pneumophila* virulence.

The clinical isolate *L. pneumophila* 130b strain has previously been sequenced. While this strain is not well-annotated, it displays a high degree of conservation to the Philadelphia-1 strain (69). As such, a comparison of the *L. pneumophila* 130b and the better-annotated Philadelphia-1 strain was performed using whole-genome BLASTp and BLASTn methods to better annotate the 130b genome.

Since the Dot/Icm T4SS is a major virulence factor during *L. pneumophila* infection, to target the effector proteins from this T4SS in our mutant library, a list of putative Dot/Icm effector-encoding genes identified *in silico* in *L. pneumophila* 130b was obtained from the literature and mapped onto the genome (69, 339, 340). Other secretion systems of *L. pneumophila* can also play a role during bacterial replication. As such, genes that encode for all secretion systems in *L. pneumophila* 130b strain were obtained from Schroeder et al (69) and mapped onto the genome.

After mapping the positions of effector-encoding genes, we observed that they were well-interspersed in the genome and did not naturally form clusters (**Figure 3.1**). Random allocation of the genes into large regions may have led to the deletion of either non-effector-encoding genes or secretion system components, which would confound the study's results. Therefore, customised grouping of these genes was required. To this end, effector-encoding genes were grouped based on their proximity. During this process, we strived to maximise the number of effector-encoding genes, and minimise the number of non-effector genes, in particular those that may be important for bacterial viability, such as metabolic genes and replication-related genes. When a potentially essential gene was located in close proximity to several effectors, the number of copies of this gene was checked by BLAST search against the 130b genome. Only in cases where multiple copies of the gene were present, was the gene included in the regions to be deleted. As all secretion systems of *L. pneumophila* play a role during the bacterial lifecycle, the genes that encode for the components of all secretion systems were excluded from the regions. Using this approach, the *L. pneumophila* 130b genome was divided into 34 regions, covering 229 effector protein-encoding genes collectively (**Table 3.1, Figure 3.1**).

3.2.2 Generation of marker-less deletion mutants

A suicide vector approach that does not leave a scar in the chromosome was chosen to delete the large genomic regions (341). Further, this approach has been used effectively to delete genes in *L. pneumophila* (338, 342). To enable homologous recombination at the targeted genomic regions, 2.5-3.5 kbp of sequences flanking the genomic region were amplified. These fragments were then combined using overlap PCR and cloned into the pSR47s suicide vector which carries a Kanamycin resistance gene and a counter-selectable marker *sacB* from *Bacillus subtilis* (**Figure 3.2(1)**). The suicide vector pSR47s has an R6K origin of replication (*ori*), as such, plasmid replication can only occur in the presence of *pir* gene, which encodes for the π Rep protein (343). BLASTx search of the *L. pneumophila* 130b genome using *E. coli pir* gene as query resulted in no homologue found, suggesting the absence of this gene. Therefore, this plasmid will not be passed to *L. pneumophila* progeny during bacteria replication.

The flanking regions cloned into the suicide vector enabled homologous recombination, leading to the formation of a mero-diploid (single crossover) and integration of the flanking regions into the chromosome (**Figure 3.2(2)**). Mero-diploid colonies were then selected using Kanamycin resistant media and confirmed using PCR (**Figure 3.2(3)**). The *sacB* gene encodes for levansucrase, an enzyme that converts sucrose into the toxic substance levan (344). Therefore, exposure to sucrose adds a selection pressure for the second homologous recombination event to occur, leading to either reversion to WT or deletion of the designated region (**Figure 3.2(4)**). PCR was again used to confirm the deletion of the designated region (data not shown).

In this study, 9 out of the 35 regions were successfully deleted (ΔA-ΔI, **Table 3.2, Appendix 1**), resulting in the deletion of 68 Dot/Icm effector-encoding genes and 139 other genes. In addition, we progressively deleted regions to generate mutants lacking several genomic regions. To date, deletion mutants lacking four- and five-regions (ΔFGHI and ΔDFGHI) were successfully created, leading to the collective deletion of 42 and 47 effector proteins, as well as 134 and 146 non-effector genes respectively. A list of the genes deleted in each cluster can be found in **Appendix 1**. To enable a more accurate comparison to the published literature, and to gain insight into how conserved these regions are, a comparison of regions A-I in the 130b strain and Philadelphia strain was visualised using Artemis Comparison Tool (ACT) (**Figure 3.3**).

Based on the alignment, most regions, as indicated in coloured shading, showed >80% similarity to their homologous counterpart in the Philadelphia-1 strain (**Figure 3.3**). However, there are variations between the two genomes. For instance, the 130b strain encodes for one extra member of the SidE-family genes (*lpw_23281*). In addition, several genes, such as *lpw_20011* and *lpg2525* were unique to either strains. Other genes, such as *lpw_20001* and *lpg1948* were homologs of genes located in a remote region (**Figure 3.3**). Together, this showed that while the two genomes share a considerably high level of conservation, some differences exist, which may contribute to different outcomes of infection.

To identify off-target effects such as the disruption of genes unrelated to the deleted regions and to confirm that the deletion was successful, whole genome sequencing was performed in each deletion mutants. It was revealed that the designated regions in all mutants were successfully deleted. However, single-nucleotide polymorphisms (SNPs) were found in seven mutants. SNPs in ΔA and ΔH occurred in intergenic regions (**Table 3.3**). Promoter prediction using Softberry BPROM revealed that the SNPs found in ΔA and ΔH did not interfere with the predicted promoters of the surrounding genes (345). Therefore, there should be no consequence of the SNPs in ΔA and ΔH. In mutants ΔC, ΔE, ΔG, ΔH, and ΔI, SNPs were found in the open reading frame (ORF) of a gene. These SNPs led to either an amino acid substitution or a premature stop codon. The gene *lpw_31381*, encoding for the phosphoenolpyruvate protein phosphotransferase PtsP, was disrupted in ΔC, ΔH and ΔI. SNPs in ΔC and ΔI led to a premature stop codon that terminated protein expression at amino acid 76. Meanwhile, a SNP in ΔH led to a missense mutation, changing glutamate 480 into alanine. Additionally, in ΔH, a SNP in the Lvh T4SS component *lvh1D4* occurred, leading to the substitution of alanine 68 with valine (**Table 3.3**). A base deletion in Δ*G* mutant led to a nonsense mutation in the gene encoding for the DNA-binding response regulator *letA* (*lpw_28981*).

3.2.3 Growth rate of mutant strains under axenic condition

Although genes predicted to be important for bacterial growth rate were excluded from the regions, several genes with unknown function were deleted in the mutants. In addition, SNPs were also found in the mutants (**Table 3.3**). Therefore, to ensure that the cluster

deletion did not lead to a severe reduction in bacterial growth rate, bacterial replication in axenic media was monitored over 40 hours.

Both WT *L. pneumophila* 130b and the mutant strains were grown axenically with a starting bacterial density (OD_{600}) of 0.01. The absorbance was then measured every 2 h for 40 h. Seven out of nine single mutants did not show any significant difference in bacterial numbers at all time points compared to WT (**Figure 3.4**). Additionally, the two strains of multiple-cluster mutants did not show any defect in viability compared to WT. Two single mutants; ΔA and ΔB, showed a slight delay in the log phase and the lag phase respectively, but ultimately managed to reach the same bacterial numbers as WT (**Figure 3.4**). Based on this result, we were confident that the deletion of selected large genomic regions had not majorly affected the ~~viability~~ growth rate of the bacteria.

3.2.4 Dot/Icm T4SS functionality in mutant strains

During the construction of the mutants, all known secretion system components-encoding genes had been excluded from the deleted regions. However, there remained a possibility of accidentally deleting a novel regulator of the Dot/Icm T4SS. Further, in mutant ΔH, a SNP was found in the *lvhD4* gene. The Lvh T4SS may aid in the translocation of Dot/Icm effector proteins when the Dot/Icm T4SS is disrupted (235), and may be altered in the presence of a SNP. Therefore, to ensure the functionality of the Dot/Icm secretion system, and to eliminate the possibility of accidentally deleting or introducing mutations to a novel component or regulator of the Dot/Icm secretion system, translocation of the Dot/Icm effector protein RalF by the mutants was examined using the beta-lactamase TEM1 method described in de Felipe *et al* (250).

In this assay, TEM1 beta-lactamase was fused to the N terminus of RalF to avoid disruption of the C-terminal signal sequence that is required for translocation by the Dot/Icm T4SS. Both WT and mutant strains carrying the TEM1-RalF fusion construct were then used to infect macrophages. Upon translocation of the tagged effector, cleavage of the substrate CCF-2AM could be observed as a shift in fluorescence from blue (520 nm) to green (450 nm). The 450nm/520nm fluorescence intensity ratio was then used as a measure of the level of translocation. At 2 h post-infection, the level of RalF translocation in the mutant strains was consistent with WT levels (**Figure 3.5**). The negative control, Δ*dotA*, which lacks an essential component of the Dot/Icm T4SS (246),

showed significantly reduced RalF translocation compared to WT. This suggested that all mutants were competent in translocating Dot/Icm effector proteins, and that none of the genes in the deleted regions or affected by SNP, act as novel component or regulator of the Dot/Icm T4SS. Therefore, the results of the subsequent assays were not compromised by a defective Dot/Icm T4SS.

3.2.5 Replication of L. pneumophila mutants in THP1 macrophages

After confirming that the mutants were able to grow at a similar rate to WT, and that the functionality of the Dot/Icm T4SS in the mutant strains was not disrupted, replication efficiency of the mutants was assessed in THP1 macrophages. Bacterial numbers at 3 h and 48 h after infection were enumerated to examine the mutants ability to replicate in THP1 macrophages. The 3 h timepoint was selected as a measure of bacterial entry into the host cells, whereas the 48 h timepoint was selected as this represents the endpoint of infection. At 3 h post-infection, ΔG showed a significant decrease in bacterial numbers compared to WT. However, this decrease was not observed in the multiple mutants ΔFGHI and ΔDFGHI. None of the other mutants showed any significant difference in either the bacterial numbers at 3 h after infection compared to WT, indicating that except for ΔG, the infectivity of the mutants was not altered by the deletion.

Consistent with the decrease in infectivity, at 48 h post-infection, only ΔG showed a modest decrease in bacterial numbers compared to WT (**Figure 3.6**). Despite the deletion of respectively 134 and 146 genes, both ΔFGHI and ΔDFGHI mutants did not show any defect in replication compared to WT (**Table 3.2, Figure 3.6**). These results demonstrate that the deletion of up to 68 effector protein-encoding genes, or 207 genes in total, did not have a significant effect on bacterial replication in human macrophages. Further, this also emphasised the likelihood of functional redundancy between the effectors of *L. pneumophila*.

3.2.6 Replication of L. pneumophila mutants in Acanthamoeba castellanii

L. pneumophila naturally infects a diverse range of protozoa. As *A. castellanii* is one of the known natural hosts of *L. pneumophila* (50, 346), replication of the mutant strains was examined during *A. castellanii* infection. As ΔDFGHI was created late in the course of the study, this mutant was not examined in this experiment, as well as any other

subsequent experiments presented in this thesis. Similar to the THP1 macrophages model, the bacterial numbers were quantified at 3 h and 48 h post-infection to examine the bacterial entry and replication endpoint respectively. At 3 h post-infection, none of the mutants showed a significant decrease in bacterial numbers compared to WT (**Figure 3.7**), demonstrating that the infectivity of the mutants in *A. castellanii* was unaffected. Unlike in the macrophage model, at 48 h post-infection, four mutants; ΔB, ΔE, ΔF, and ΔG, showed a significant reduction in bacterial numbers (**Figure 3.7**). Consistently, the multiple-region mutant ΔFGHI also displayed a significant reduction in bacterial numbers. This indicates that these regions are important for the bacterial replication in *A. castelllanii*, but not in a human macrophages cell line.

3.3 Discussion

Critical to *L. pneumophila* infection is the modulation of host processes by Dot/Icm T4SS effectors. To identify which effectors are important for *L. pneumophila* infection, a library of 35 mutants lacking Dot/Icm effector proteins was designed, and nine mutants from this library have been generated. Using these mutants, the roles of multiple Dot/Icm T4SS effectors during infection can be investigated. To date, thirteen mutants (ΔA-ΔI) have been constructed, covering 207 genes, 68 of which encode for Dot/Icm T4SS effectors. Additionally, multiple-cluster mutants (ΔFGHI and ΔDFGHI) were created to cover a larger region of 134 and 146 genes respectively. These mutants varied in their ability to replicate in the conditions as summarised in **Table 3.4**.

ΔG is the only mutant that showed reduced cfu in both THP1 macrophages and *A. castellanii*. Noteworthy, ΔG contained a SNP at the gene *lpw_28981* (*letA*), a member of the LetA/S two-component system (93), leading to a premature stop codon. Mutants deficient in LetA/S are known to be impaired in bacterial motility, macrophage infectivity and cytotoxicity, although bacterial replication in both bone marrow-derived macrophages and HL60-derived macrophages is unaffected (93, 94). ΔG showed an approximately 0.5 log-fold decrease in bacterial numbers compared to WT at 3 h after infection in THP1 macrophages, indicating lower infectivity in macrophages. Consistently, an approximately 0.5 log-fold reduction in bacterial numbers compared to WT at 48 h post-infection was observed. This implies that the reduction in ΔG bacterial numbers at 48 h may be due to the lower bacteria uptake rather than impaired replication,

thus supporting previously published observations. Neither ΔFGHI nor ΔDFGHI, both of which lacked region G but contained no SNP, displayed a reduced bacterial load at 3 h and 48 h in THP1 macrophages. This suggests that the phenotype of ΔG in THP1 macrophages may be due to the SNP in *letA*. However, complementation of *letA* to ΔG mutant is required to confirm this hypothesis.

Prior to this study, O'Connor *et al* (338) generated large genomic region mutants in the *L. pneumophila* Philadelphia-1 strain. Δ6a, which covers an overlapping homologous region with ΔG, proficiently replicates in either mammalian macrophages or *A. castellanii* (338). The genes in this region were highly conserved between the two strains, thus, it is likely that the SNP in *letA* caused the reduction in ΔG bacterial numbers.

Four single mutants, ΔB, ΔE, ΔF, and ΔI, showed a significant reduction in replication in *A. castellanii*, but not macrophages. Consistent with our results, Δ4, Δ5, and Δ7a mutants, which covered homologous region with ΔE, ΔF, and ΔI, also displayed a significant reduction in replication in *A. castellanii*, but not in bone marrow-derived macrophages (BMDMs) from A-strain mice (338).

ΔB also displayed a slight delay in the entry into log-phase. Our lab recently discovered that *lpw_04851* was responsible for the decrease in bacterial replication in the ΔB mutant at 48 hours after infection in *A. castellanii* (Pengfei Li, personal communication). Homology prediction suggested that *lpw_04851* encodes for a glutamate/gamma-aminobutyric acid (GABA) transporter (325). Glutamate is important for bacterial replication in nutrient broth and in *A. castellanii* but not in macrophages, as the deletion of host glutamate transporter SLC1A5 led to reduced bacterial replication in *A. castellanii*, but not macrophages (347). Thus, the reduction of ΔB replication in *A. castellanii* but not THP1 macrophages supports this observation. The deletion of *lpw_04851* may be responsible for the prolonged lag phase of ΔB in nutrient broth, as a metabolic phenotype is more likely to be contributed by non-effector genes. However, experimental evidence is required to confirm this.

Our results suggested that ΔE, ΔF, and ΔI showed a reduced replication in *A. castellanii*, but not THP-1 macrophages. However, as all three regions are over 30 kbp in size, it is difficult to complement these regions using plasmid. Therefore, deletion of smaller regions within regions E, F, or I can be performed to narrow down the gene(s) responsible

for this phenotype. Complementation can then be performed to confidently determine the gene(s) important for *L. pneumophila* replication in *A. castellanii.* This will also reveal whether the SNPs found in mutants ΔE and ΔI play a role during the mutants replication in amoebae.

ΔA, ΔC, ΔD, and ΔH did not show any significant defect in replication in either nutrient broth, THP1 macrophages or *A. castellanii*. Consistently, Δ2a and Δ6 generated by O'Connor *et al* (338), which covered an overlapping homologous region in the Philadelphia-1 strain with ΔC and ΔH, did not show any reduction in replication in either protozoan or mammalian hosts. On the other hand, Δ3 (338), which covered the region homologous to ΔD, displayed reduced replication in *A. castellanii,* but not macrophages. However, Δ3 also covers a larger region than ΔD, suggesting that the gene(s) responsible for this phenotype are located outside our region D.

Despite efficient replication in cells, ΔA displayed a significant delay during replication in axenic conditions. This lack of growth occurred in the log-phase, which takes place before the 20 h post-infection period during intracellular replication. Quantification of flagellated *L. pneumophila* in BMDMs from A-strain mice have shown that flagellated bacteria start appearing at 20-30 h after infection, marking the stationary phase during macrophage infection (138). Furthermore, egress from the LCV, which should occur in stationary phase, was reported to occur at 12-18 hours after infection in U937 macrophages and *A. polyphaga* models (135). Therefore, given that ΔA can reach similar bacterial numbers as WT at stationary phase, it is not surprising that the slight delay in log-phase *in vitro* growth of ΔA did not translate to a reduction in replication in either THP1 macrophages or *A. castellanii* at 48 h after infection, as the bacteria should already be past log-phase.

The large genomic region mutants generated in this study have allowed us to investigate the role of not just one gene, but multiple genes during infection, thereby bypassing some of the functional redundancy of the Dot/Icm T4SS effectors. Furthermore, in addition to replication phenotypes, various aspects of bacterial infection, such as LCV formation, translation inhibition, and unfolded protein response can be investigated using these mutants.

Overall, we found that none of the genomic regions A-I were essential for *L. pneumophila* replication in macrophages. Nonetheless, in this study, only the entry and replication endpoint were examined. As such, subtle delay at the middle stage of replication may be missed. Therefore, adding an extra timepoint between 3 h and 24 h may be performed to examine the replication of the mutants more thoroughly. While most genomic regions were not essential for replication in macrophages, at least four genomic regions were important for replication in *A. castellanii*. This observation is supported by other studies, which showed that some genes were important for bacterial replication in the protozoan, but not mammalian host (334, 338, 348). Further, the deletion of up to 31% of *L. pneumophila* strain Philadelphia-1 genome led to a reduced replication in the protozoan but not mammalian host (338). Conversely, a locus that contributes to *L. pneumophila* replication in macrophages, but not protozoan host was reported (349), although in this study, only one protozoan host was tested. These may suggest that macrophages are more susceptible to infection than amoebae. However, PMA-differentiated THP1 macrophages likely do not reflect infection of resident macrophages in mammalian hosts in the context of overall immune system. Naturally, the ability of macrophages to clear bacteria is enhanced in the presence of other cell types which may act either indirectly through cytokines or directly to clear the bacteria. As such, the goal of the following chapter is to examine the survival of the deletion mutants under immune pressure.

Table 3.1. List of designed genomic regions

Genes	Region		Size (kbp)
	Start	End	
lpw_00071-lpw_00221	10906	28922	18.017
lpw_00311-lpw_00791	38409	86857	48.449
lpw_01261-lpw_01361	137868	157558	134.565
lpw_02641-lpw_02861	280171	307298	27.128
lpw_02981-lpw_03361	321736	371744	50.009
lpw_03641-lpw_03751	400460	430582	30.123
lpw_04431-lpw_04721	482706	512790	30.085
lpw_04831-lpw_04861	520038	524801	4.764
lpw_05041-lpw_05201	540169	556383	16.215
lpw_06951-lpw_08111	728277	876371	148.095
lpw_09801-lpw_10551	1049210	1140049	90.84
lpw_11451-lpw_11581	1212455	1226841	14.387
lpw_11681-lpw_11901	1239133	1266373	27.241
lpw_11971-lpw_12401	1271839	1325399	53.561
lpw_14431-lpw_15181	1535544	1614553	79.01
lpw_16861-lpw_16971	1792794	1813545	20.752
lpw_17121-lpw_17411	1829498	1865067	35.57
lpw_17761-lpw_19161	1902451	2051954	149.504
lpw_19211-lpw_19721	2054909	2111600	56.692
lpw_19951-lpw_20201	2137369	2170480	33.112
lpw_20291-lpw_20431	2178969	2199685	20.717
lpw_23101-lpw_23561	2447737	2505304	57.568
lpw_23811-lpw_24091	2546616	2575782	29.167
lpw_24261-lpw_24611	2595555	2636837	41.283
lpw_25181-lpw_25561	2691462	2724014	32.553
lpw_26021-lpw_26191	2770465	2789322	18.858
lpw_26241-lpw_26431	2791756	2813633	21.878
lpw_26521-lpw_26861	2820995	2853452	32.458
lpw_27241-lpw_27551	2887964	2933051	45.088
lpw_27671-lpw_27911	2941383	2964125	22.743
lpw_28241-lpw_28891	2992466	3068467	76.002
lpw_29461-lpw_30041	3131377	3184099	52.723
lpw_30591-lpw_30921	3240876	3288724	47.849
lpw_31411-lpw_31571	3333394	3352075	18.682

Table 3.2. Location, size, and composition of the deleted genomic regions

Region (position)	Size (kbp)	Number of effector-encoding genes	Number of non-effector-encoding genes	Total number of genes
$A_{(10906..28922)}$	18.017	3	14	17
$B_{(520038..524801)}$	4.764	3	1	4
$C_{(1212455..1226841)}$	14.387	5	9	14
$D_{(1792794..1813545)}$	20.752	5	7	12
$E_{(2137369..2170480)}$	33.112	10	16	26
$F_{(2447737..2505304)}$	57.568	13	34	47
$G_{(2791756..2813633)}$	21.878	8	12	20
$H_{(2820995..2853452)}$	32.458	8	27	35
$I_{(2887964..2933051)}$	45.088	13	19	32
FGHI	156.992	42	92	134
DFGHI	177.744	47	99	146

Table 3.3. List of SNPs in *L. pneumophila* genomic region mutants

Region	Genomic Position	SNPs	Consequences
A	191,568	Intergenic region between *lpw_01691* (Lvh1 T4SS protein *lvr1A*) and *lpw_01701* (putative phage repressor *prpA1*)	Unknown. SNP occurred in neither the putative promoter nor RBS of the surrounding genes.
B	N/A	No SNP	N/A
C	3,329,340	Deletion of T at position 229 in *lpw_31381* (phosphoenolpyruvate protein phosphotransferase *ptsP*)	Premature stop codon in amino acid 76
D	N/A	No SNP	N/A
E	2,171,002	SNP at position 4 of *lpw_20211* (major outer membrane protein)	Point mutation, changing Thr2Ala
F	N/A	No SNP	N/A
G	3,080,422-3,080,430	Deletion of one T in the sequence "GTTTTTTTTA" *lpw_28981* (Response regulator *letA*)	Frameshift from amino acid 72 and premature stop codon at amino acid 76
H	179,426	SNP at position 203 of *lpw_01551* (Lvh1 T4SS protein *lvh1D4*)	Point mutation, changing Ala68Val
	191,450	Intergenic region between *lpw_01691* (Lvh1 T4SS protein *lvr1A*) and *lpw_01701* (putative phage repressor *prpA1*)	Unknown. SNP occurred in neither the putative promoter nor RBS of the surrounding genes.
	3,330,551	SNP at position 1,439 of *lpw_31381* (phosphoenolpyruvate protein phosphotransferase *ptsP*)	Point mutation, changing Glu480Ala
I	3,329,340	Deletion of T at position 229 in *lpw_31381* (phosphoenolpyruvate protein phosphotransferase ptsP)	Premature stop codon at amino acid position 76
FGHI	N/A	No SNP	N/A
DFGHI	N/A	No SNP	N/A

Table 3.4. Summary of *L. pneumophila* mutants replication phenotype

Mutant	Replication	
	THP1	***A. castellanii***
ΔA	+	+
ΔB	+	-
ΔC	+	+
ΔD	+	+
ΔE	+	-
ΔF	+	-
ΔG	-	-
ΔH	+	+
ΔI	+	-
ΔFGHI	+	-
ΔDFGHI	+	Untested*

+ Competent replication
- Reduced or incompetent replication

* ΔDFGHI was created late in the course of study, therefore it was only examined in the first two experiments, namely the growth under axenic condition and replication in THP-1 macrophages.

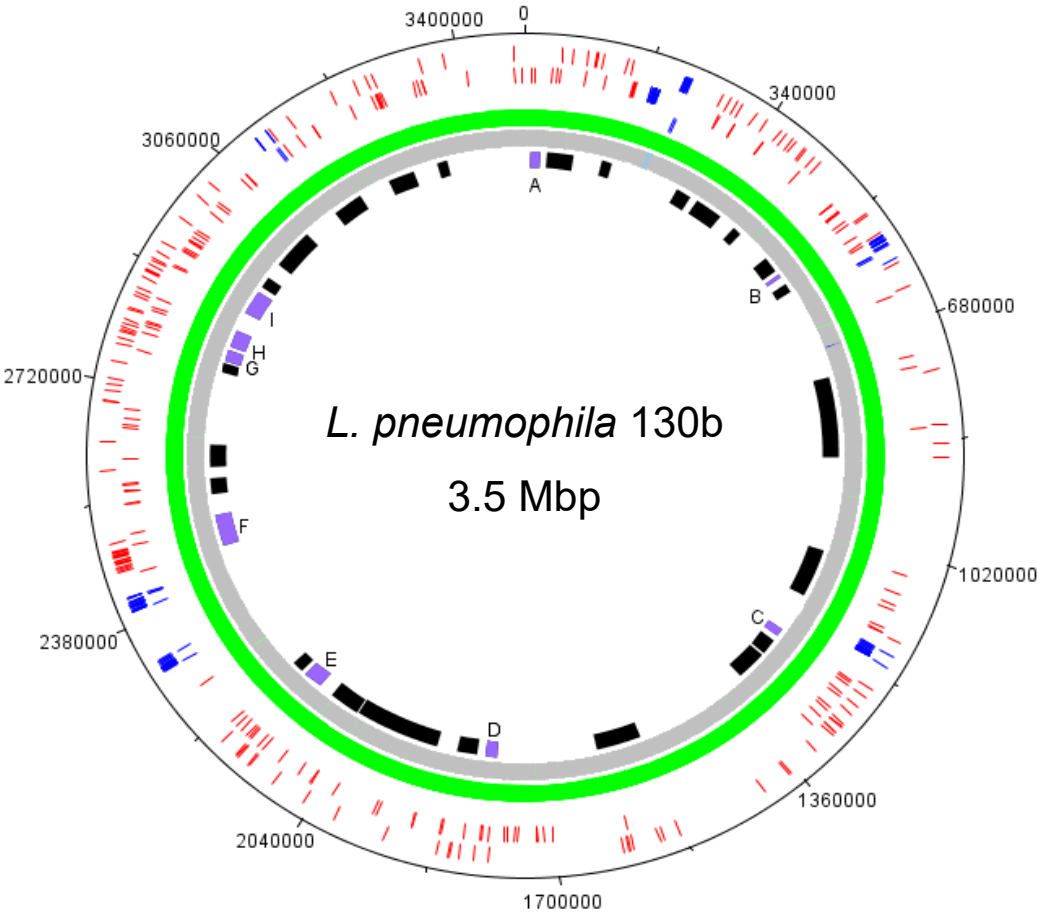

Figure 3.1. Effector-less mutant library design in *L. pneumophila* 130b genome.

Large genomic regions were assigned to cover as many effector-encoding genes as possible. **Red lines** indicate effector-encoding genes, while **blue lines** indicate secretion system-encoding genes. **Black bars** indicate genomic regions. **Light blue** bars indicate successfully deleted genomic regions**.**

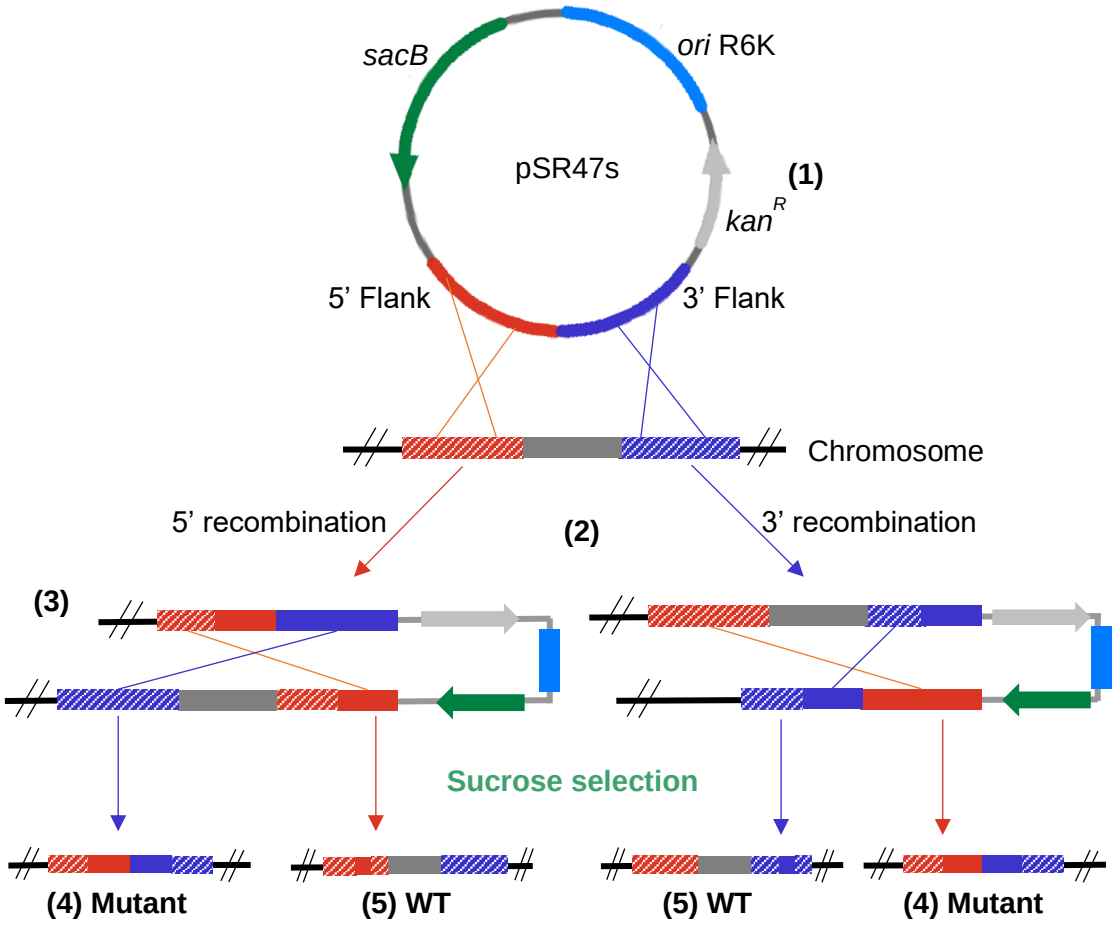

Figure 3.2. Generation of marker-less deletion mutants.

The suicide vector pSR47s was used to perform marker-less deletion of large genomic regions. The regions flanking the target gene (**dark grey**) were cloned into the suicide vector **(1)**. These flanks undergo either 5' (**red** arrow) or 3' (**blue** arrow) homologous recombination with the corresponding region (**red** or **blue** region with stripes) in the genomic DNA **(2),** resulting in merodiploid products **(3)**. After undergoing **sucrose selection**, a second homologous recombination either in the 5' (**red** line) or 3' (**blue** line) region occurs. This leads to either the deletion of target region **(4),** or reversion to WT **(5)**.

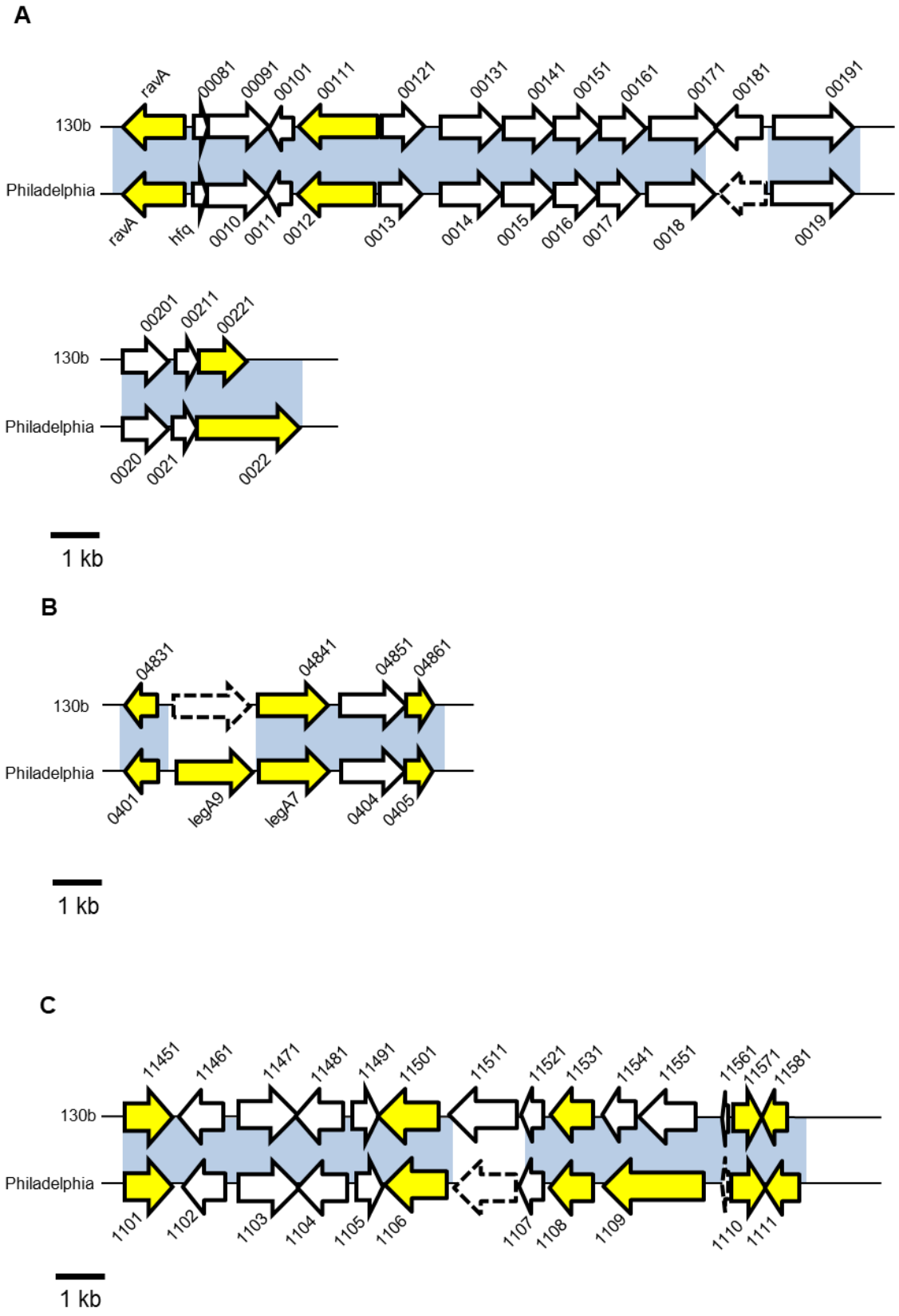
A
ravA
00081
00091
00101
00111
00121
00131
00141
00151
00161
00171
00181
00191
130b
Philadelphia
ravA
hfq
0010
0011
0012
0013
0014
0015
0016
0017
0018
0019
00201
00211
00221
130b
Philadelphia
0020
0021
0022
1 kb
B
04831
04841
04851
04861
130b
Philadelphia
0401
legA9
legA7
0404
0405
1 kb
C
11451
11461
11471
11481
11491
11501
11511
11521
11531
11541
11551
11561
11571
11581
130b
Philadelphia
1101
1102
1103
1104
1105
1106
1107
1108
1109
1110
1111
1 kb

D

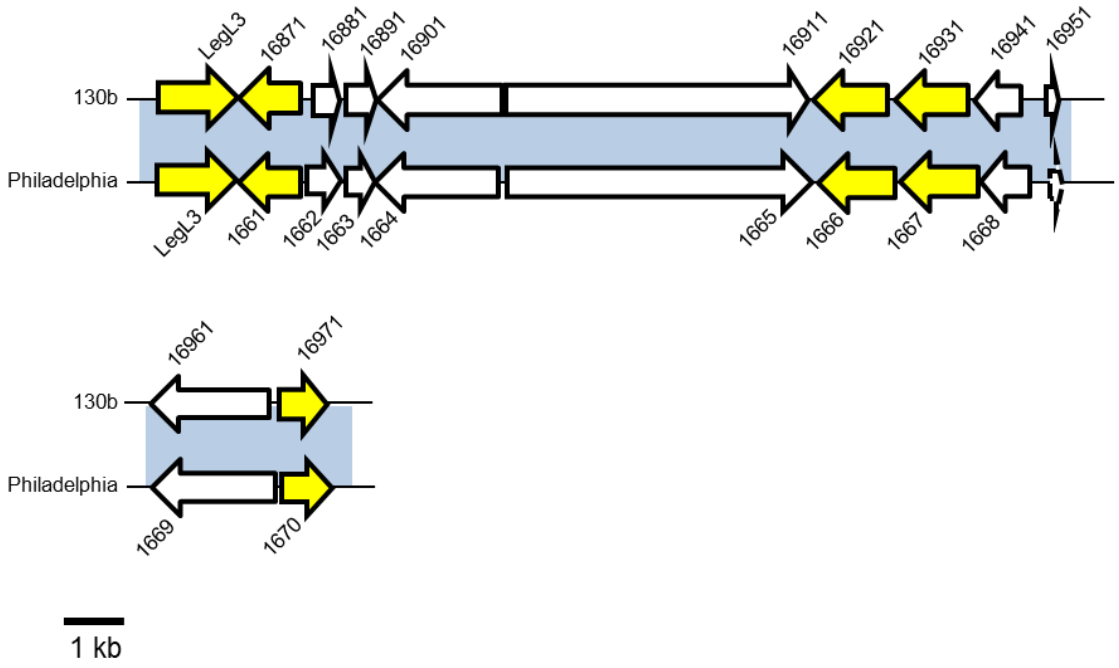
LegL3
16871
16881
16891
16901
16911
16921
16931
16941
16951
130b
Philadelphia
LegL3
1661
1662
1663
1664
1665
1666
1667
1668
16961
16971
130b
Philadelphia
1669
1670
1 kb

E

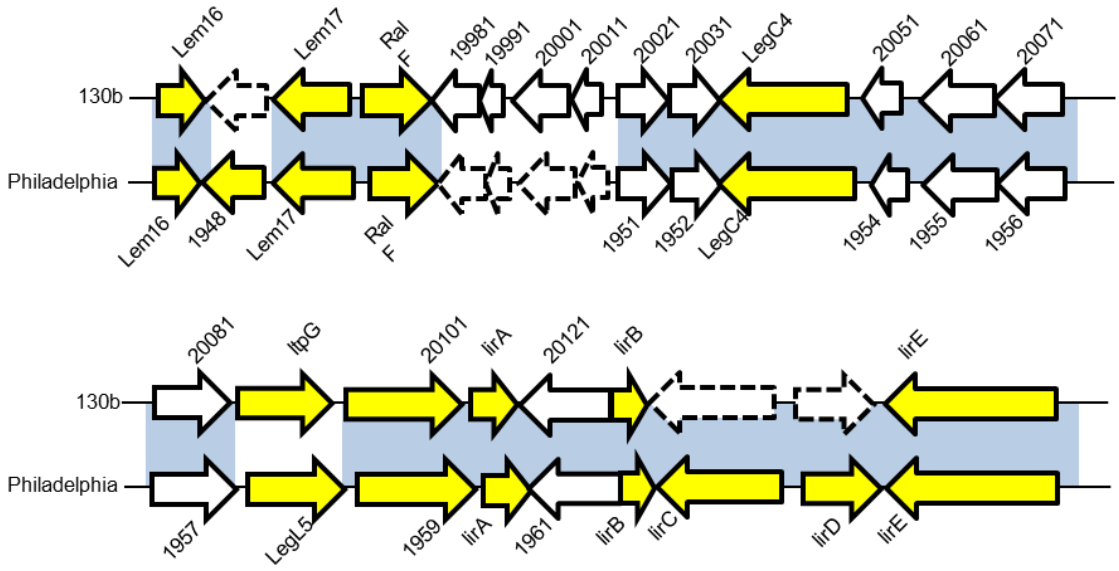
Lem16
Lem17
Ral F
19981
19991
20001
20011
20021
20031
LegC4
20051
20061
20071
130b
Philadelphia
Lem16
1948
Lem17
Ral F
1951
1952
LegC4
1954
1955
1956
20081
ltpG
20101
lirA
20121
lirB
lirE
130b
Philadelphia
1957
LegL5
1959
lirA
1961
lirB
lirC
lirD
lirE

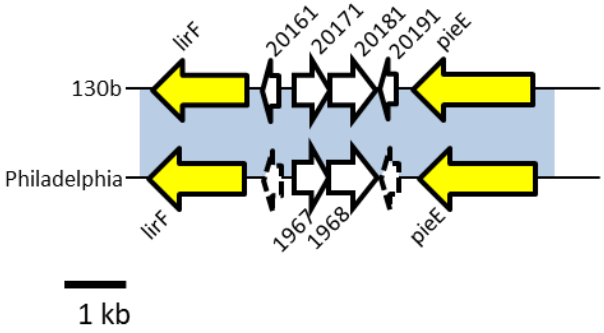
lirF
20161
20171
20181
20191
pieE
130b
Philadelphia
lirF
1967
1968
pieE
1 kb

F

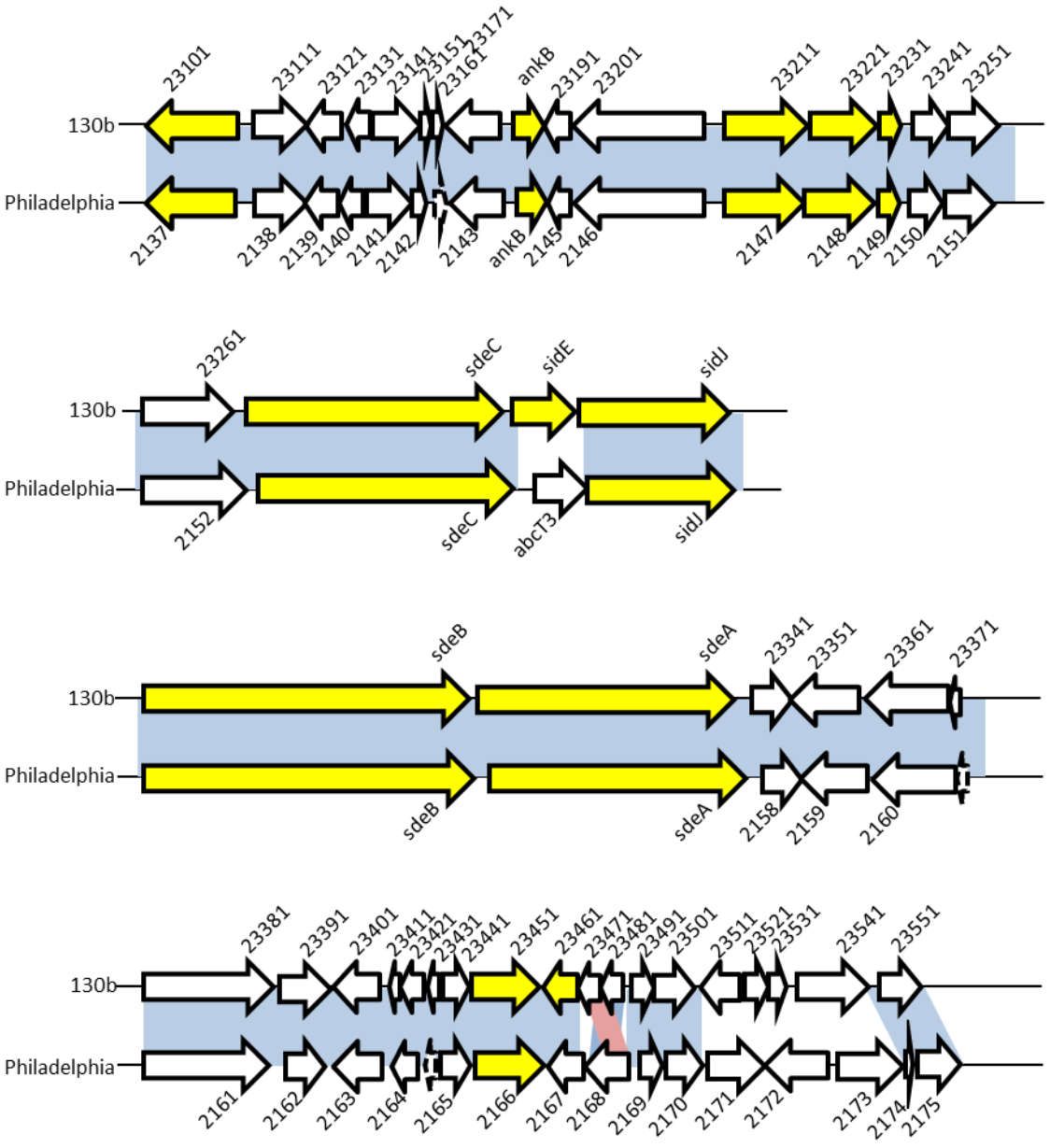
23101
23111
23121
23131
23141
23151
23161
23171
ankB
23191
23201
23211
23221
23231
23241
23251
130b
Philadelphia
2137
2138
2139
2140
2141
2142
2143
ankB
2145
2146
2147
2148
2149
2150
2151
23261
sdeC
sidE
sidJ
130b
Philadelphia
2152
sdeC
abcT3
sidJ
sdeB
sdeA
23341
23351
23361
23371
130b
Philadelphia
sdeB
sdeA
2158
2159
2160
23381
23391
23401
23411
23421
23431
23441
23451
23461
23471
23481
23491
23501
23511
23521
23531
23541
23551
130b
Philadelphia
2161
2162
2163
2164
2165
2166
2167
2168
2169
2170
2171
2172
2173
2174
2175

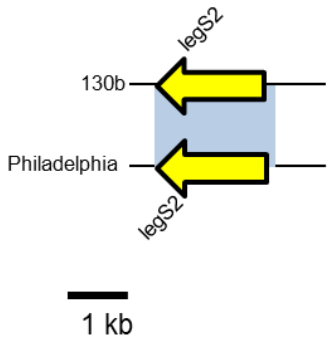
legS2
130b
Philadelphia
legS2
1 kb

G

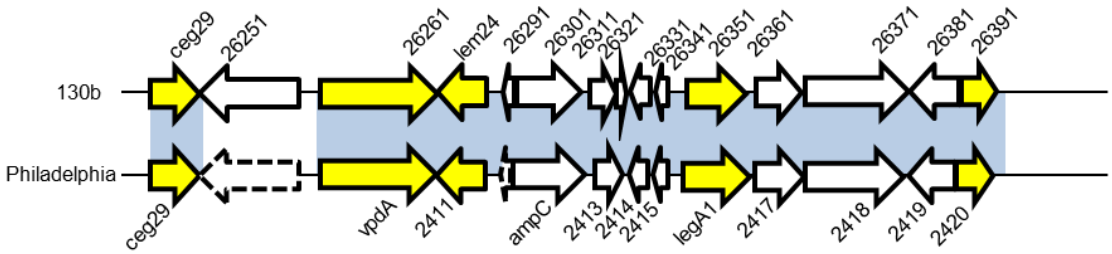
ceg29
26251
26261
lem24
26291
26301
26311
26321
26331
26341
26351
26361
26371
26381
26391
130b
Philadelphia
ceg29
vpdA
2411
ampC
2413
2414
2415
legA1
2417
2418
2419
2420

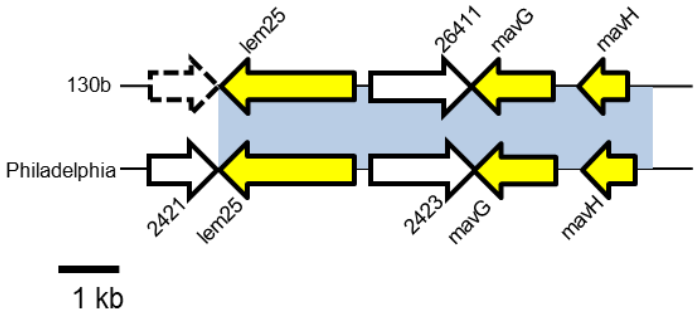
lem25
26411
mavG
mavH
130b
Philadelphia
2421
lem25
2423
mavG
mavH
1 kb

H

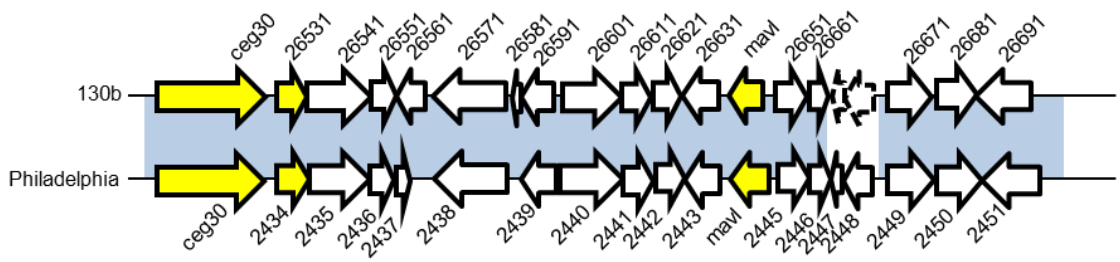
ceg30
26531
26541
26551
26561
26571
26581
26591
26601
26611
26621
26631
mavI
26651
26661
26671
26681
26691
130b
Philadelphia
ceg30
2434
2435
2436
2437
2438
2439
2440
2441
2442
2443
mavI
2445
2446
2447
2448
2449
2450
2451

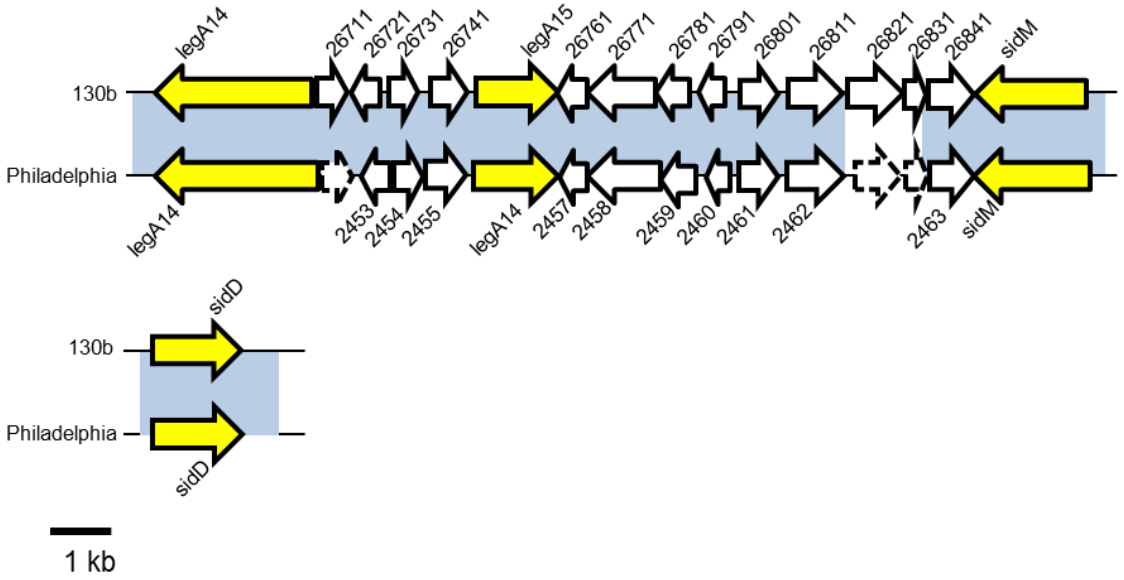
legA14
26711
26721
26731
26741
legA15
26761
26771
26781
26791
26801
26811
26821
26831
26841
sidM
130b
Philadelphia
legA14
2453
2454
2455
legA14
2457
2458
2459
2460
2461
2462
2463
sidM
sidD
130b
Philadelphia
sidD
1 kb

I

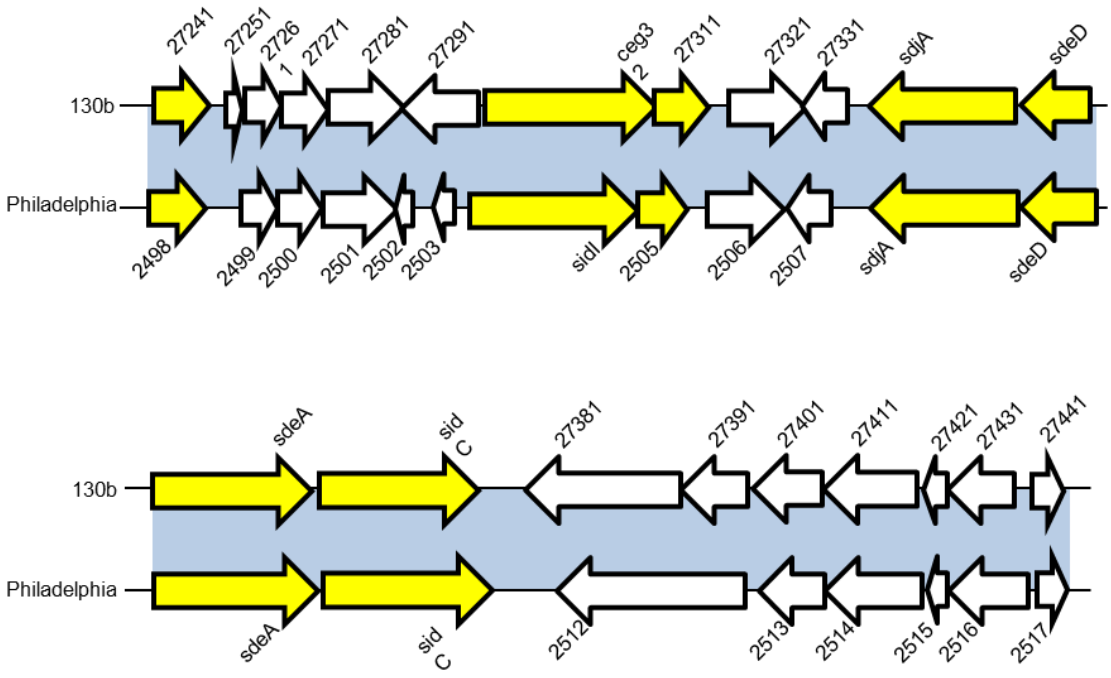
27241
27251
2726
1
27271
27281
27291
ceg3
2
27311
27321
27331
sdjA
sdeD
130b
Philadelphia
2498
2499
2500
2501
2502
2503
sidI
2505
2506
2507
sdjA
sdeD
sdeA
sid
C
27381
27391
27401
27411
27421
27431
27441
130b
Philadelphia
sdeA
sid
C
2512
2513
2514
2515
2516
2517

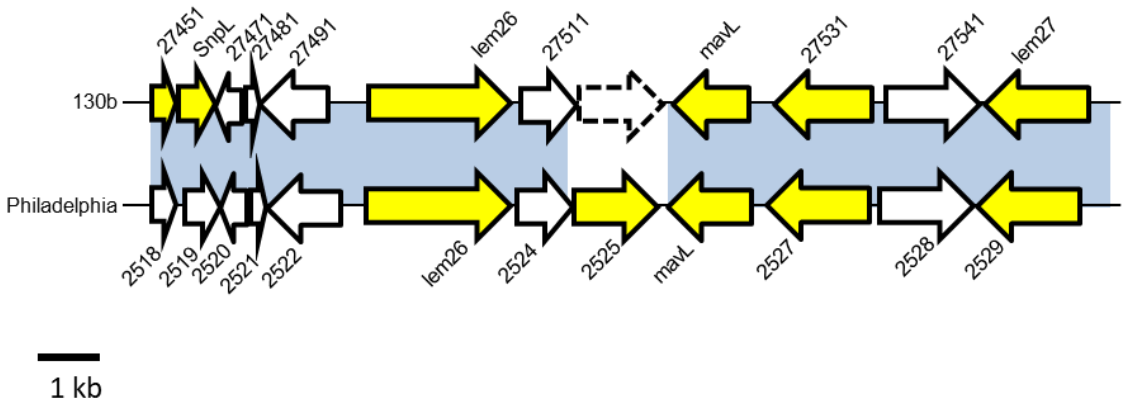

Figure 3.3. Comparison of deleted regions in 130b vs Philadelphia.

The deleted genomic regions in 130b was compared to Philadelphia and visualised using Artemis Comparison Tool (ACT). One centimeter corresponds to one kilobase (kb). Each arrow represents one gene. Numbers on each arrow indicate gene numbers in the corresponding strain. Yellow arrow indicates Dot/Icm effector-encoding genes, whereas white arrow indicates non-Dot/Icm effector-encoding genes. Arrow with dotted lines represents the absence of gene in the strain. Colour shading was used to show regions sharing over 80% protein sequence similarity.

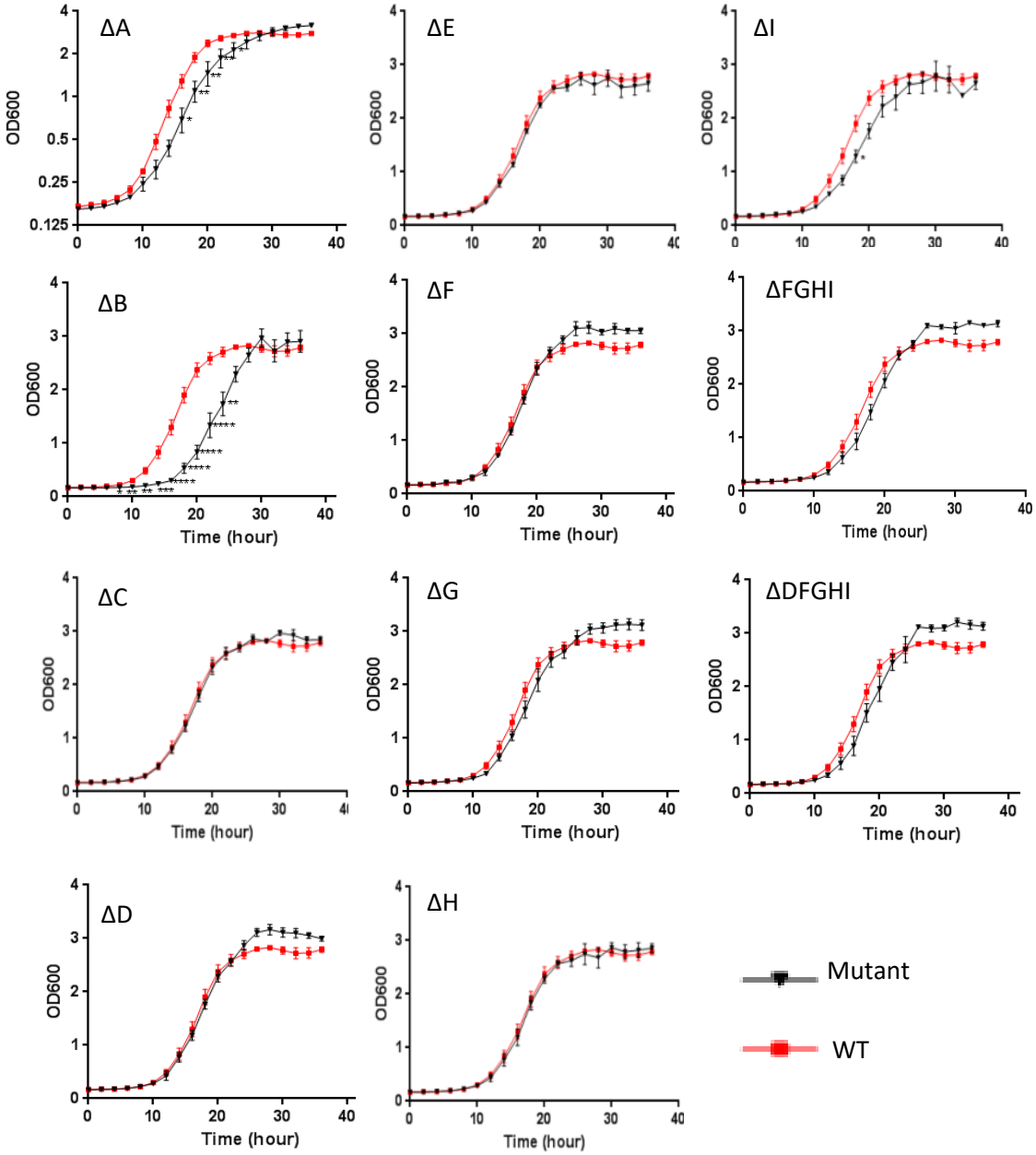

Figure 3.4. Growth rate of the mutants *in vitro*.

Absorbance at 600nm (A_{600}) of bacterial culture in supplemented Aces broth was measured every 2 hours over a 40-hour period (n=3). Each dot represents mean +/- SEM. Statistical significance was examined using one-way Anova. * $p \leq 0.05$, ** $p \leq 0.01$, *** $p \leq 0.001$, **** $p \leq 0.0001$.

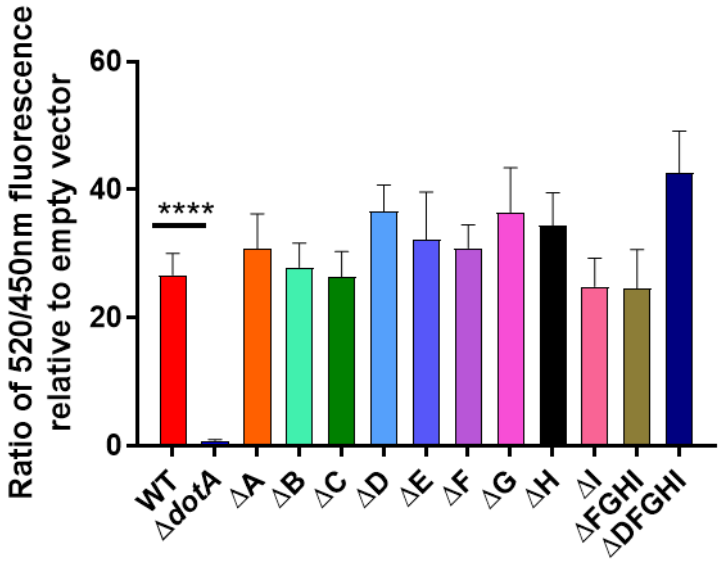

Figure 3.5. Functionality of the Dot/Icm T4SS in the mutants.

The ratio of 450/520 nm fluorescence was measured to quantify the level of translocation of beta-lactamase tagged RalF by each mutants. Each bar represents the mean +/- SEM. Statistical significance was determined using unpaired t-test. * $p \leq 0.05$, ** $p \leq 0.01$, *** $p \leq 0.001$, **** $p \leq 0.0001$.

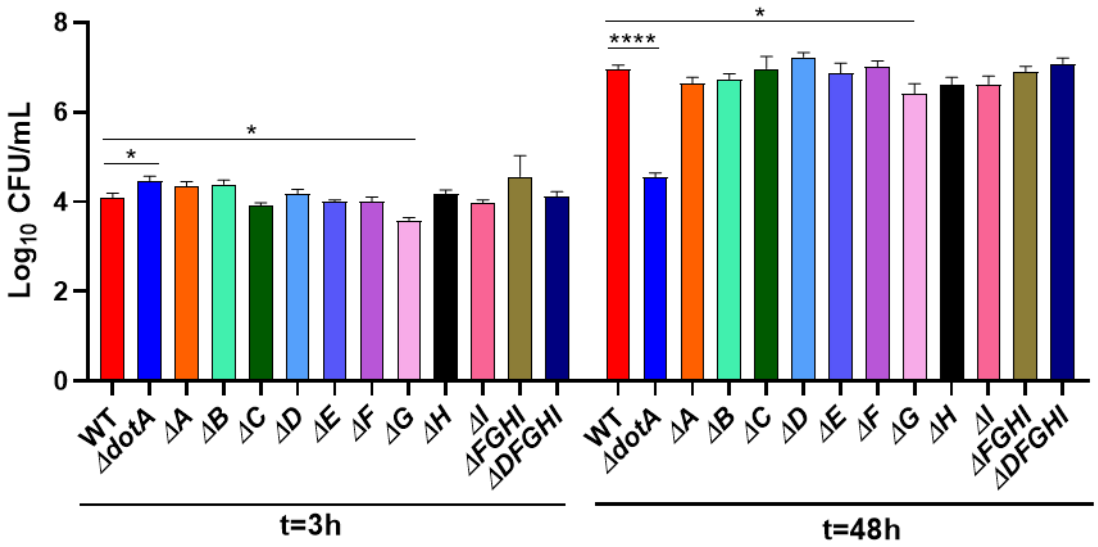

Figure 3.6. Replication of *L. pneumophila* mutants in THP1 macrophages.

The mutants bacterial CFU in THP1 macrophages was quantified at 3h and 48h after infection. Results from at least 3 independent experiments are presented. Each bar represents the mean +/- SEM. Statistical significance was determined using unpaired t-test. * $p \leq 0.05$, ** $p \leq 0.01$, *** $p \leq 0.001$, **** $p \leq 0.0001$

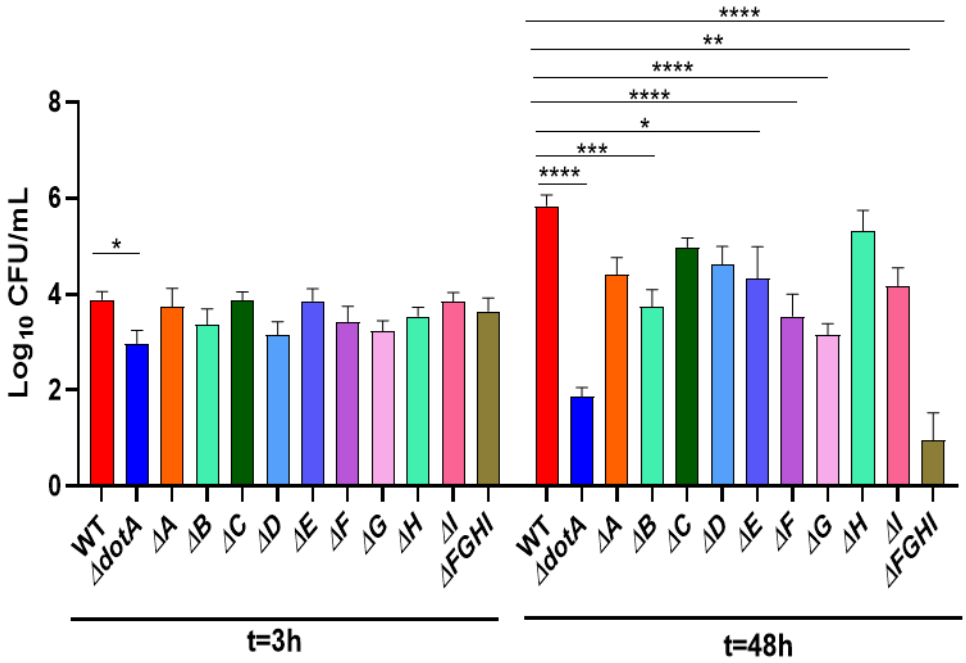

Figure 3.7. Replication of *L. pneumophila* mutants in *Acanthamoeba castellanii*.

The *L. pneumophila* mutants bacterial numbers recovered from *A. castellanii* at 3h and 48h after infection was enumerated. Results from at least 3 independent experiments are presented. Each bar represents the mean +/- SEM. Statistical significance was determined using unpaired t-test. * $p \leq 0.05$, ** $p \leq 0.01$, *** $p \leq 0.001$, **** $p \leq 0.0001$.

Chapter 4
Identification of *L. pneumophila* effector regions modulating survival under immune pressure

4.1 Introduction

The ability of *L. pneumophila* to infect macrophages is largely thought to be derived from the ability of the bacteria to infect protozoan hosts such as amoebae (62, 63). In the previous chapter, *L. pneumophila* mutants lacking up to 146 genes were found to proficiently replicate in THP1 macrophages, whereas many mutants were unable to sustain replication in *A. castellanii*. In another strain of *L. pneumophila*, deletion of up to 31% of the genome did not affect bacterial replication in macrophages, but severely attenuated replication in the protozoan hosts (338).

A potential contributing factor to the susceptibility of macrophages to *L. pneumophila* is that naïve macrophages or naïve macrophage cell lines are often used. Unlike the unicellular amoebae, macrophages function optimally in a cohesive response with other immune cells, which improve the clearance of bacteria through either direct bactericidal mechanisms or cytokine secretion. Cytokine secretion is important for optimal bactericidal activity of macrophages, as stimulation of macrophages with cytokines such as TNFα and IFNγ improves the resistance to *L. pneumophila* (194, 196-198, 350, 351). During *L. pneumophila* infection, infected macrophages have a restricted cytokine repertoire due to the inhibition of cytokine secretion by *L. pneumophila*. Under these conditions, infected cells are unable to make TNFα, and rely on cytokine production by bystander cells (177, 189). Furthermore, despite the importance of IFNγ to *L. pneumophila* clearance by macrophages, the majority of IFNγ is produced by the NK and T cells (185, 192, 352). Therefore, the addition of recombinant cytokine is ideally included in an *in vitro* model to approach optimal macrophage activation during *L. pneumophila* infection.

In vivo, cytokines also recruit other cell types which help in resolving the infection. During *in vivo* infection, *L. pneumophila* interacts with mononuclear phagocytes (MPC) such as alveolar macrophages (AMs) and monocytes, as well as polymorphonuclear (PMN) phagocytes such as neutrophils (78, 130, 353, 354). The translocation of Dot/Icm effectors also occurs in neutrophils (79), suggesting that *L. pneumophila* may modulate

cells other than macrophages during *in vivo* replication. Therefore, studying the Dot/Icm T4SS effectors exclusively in macrophages may not be sufficient, even though *L. pneumophila* is unable to replicate in neutrophils and neutrophils are imported for controlling infection.

Modulation of the host immune response can be performed by Dot/Icm T4SS effector proteins (305, 306, 355). For instance, the effector proteins MavC and RavD can dampen host NFκB response (292, 293), whereas other Dot/Icm effectors induce prolonged NFκB activation at the later stages of infection, resulting in an increase in the transcription of host anti-apoptotic genes (302-306). As cell death may improve bacterial clearance by removing susceptible cells, delaying this process allows better bacterial survival. Consequently, pharmacological induction of host apoptosis led to better clearance of *L. pneumophila* (307). Furthermore, at least seven Dot/Icm effectors (SidI, Lgt1-3, LegK4, SidL, and Lpg1489) inhibit host translation, leading to reduced cytokine secretion, and possibly influence host cell death (176, 268, 296-298, 307). These modulations may influence the pathogenesis of *L. pneumophila*, however to date, there is limited studies on the role of Dot/Icm effectors during *in vivo* infection.

Although studying the role of Dot/Icm effectors exclusively in macrophage cell lines may not be sufficient to detect any effects on overall disease, the use of animal models raises ethical and financial concerns, as the large effector repertoire means a large number of animals are required. As such, the majority of effectors characterised in mice have only been investigated after a phenotype has been observed *in vitro.* At the time of writing, there is only one study which has attempted to identify Dot/Icm effectors important for *L. pneumophila* survival in the *in vivo* model, where a library of pooled and tagged transposon mutants was used to infect mice. Sequencing was used to determine the proportion of each mutant to the entire pool before and after infection (334). Although this method is a powerful technique, a drawback is that it only allows the disruption of single genes, and therefore cannot identify functionally redundant effectors. Furthermore, more subtle phenotypes may be lost due to the high number of strains being competed in the transposon assay.

The large genomic region deletion mutants created in this study provided an opportunity to study Dot/Icm effectors in an alternate approach that may better detect any roles of

redundant or cooperative effectors. Therefore, using the large genomic region mutants, we aimed to identify Dot/Icm effectors that influence bacterial survival under immune pressure. While the mutants displayed only minor phenotypes in IFNγ-stimulated macrophages, they displayed either significant increases or decreases in bacterial CFU after infection of A-strain mice. Following this, Lpw_04861 was identified as one of the effectors responsible for the increase in bacterial survival *in vivo*. Additionally, three effector-rich regions were determined to be important for bacterial survival *in vivo.*

4.2 Results

4.2.1 Replication of L. pneumophila mutants in IFNγ-stimulated macrophages

The most potent mechanism of *L. pneumophila* restriction described in macrophages results from IFNγ stimulation. Therefore, the replication of genomic deletion mutant strains in IFNγ-stimulated THP1 macrophages was examined to investigate the role of the deleted effectors in modulating macrophage intrinsic immunity. In this experiment, following differentiation of THP1 monocytes into macrophages, cells were stimulated by addition of IFNγ (**Figure 4.1A**). 100 ng/ml IFNγ was used to stimulate THP1 cells as this was previously demonstrated to successfully stimulate THP1 macrophages without a significant loss of cell viability at 24 hours after treatment (356). To confirm that IFNγ stimulation was successful, the expression of a known IFNγ-responsive gene GBP5 (357) was examined using western blot before infection (t=0h), and at 3h, 24h, and 48h after infection (t=3h, t=24h, t=48h) (**Figure 4.1B**). A ~62 kDa band was observed in stimulated cells at all time-points tested, but not in unstimulated samples, suggesting IFNγ stimulation was successful. In contrast to the previous study (356), a reduction (~20%) in cell viability was observed when uninfected cells were treated with IFNγ compared to the untreated control (**Figure 4.2A, B**).

At 3 h post-infection, cells were lysed and the lysate was plated to determine bacterial CFU as a measure of uptake. Similarly, at 24 h and 48 h post-infection, bacterial CFU was enumerated to measure bacterial replication. At 3 h and 24 h post-infection, IFNγ treatment did not result in enhanced uptake or clearance of WT *L. pneumophila*. Similarly, all mutant-infected cells showed similar bacterial load as WT-infected cells at 3 h and 24 h post-infection (**Figure 4.1C**). At 48 h post-infection, a one log decrease in WT *L. pneumophila* CFU from stimulated cells compared to unstimulated cells was

observed, suggesting that IFNγ stimulation improved WT *L. pneumophila* clearance in THP1 macrophages (**Figure 4.1C**). Similarly, at 48 h post-infection, a decrease in bacterial load when cells were stimulated with IFNγ was observed for ΔA, ΔB, and ΔD mutants. Upon IFNγ treatment, ΔA mutant showed ~0.8 log lower bacterial load than WT, suggesting a lower survival in stimulated macrophages (**Figure 4.1C)**. In contrast, IFNγ stimulation did not significantly enhance the clearance of mutants ΔC, ΔE, and ΔFGHI at 48 h after infection, suggesting a role for these effector(s) in driving the susceptibility of *L. pneumophila* to immune pressure. However, no significant difference in bacterial CFU was observed between these mutants and WT, suggesting that these phenotypes were weak or variable (**Figure 4.1C**). Notably, there was no significant difference in the bacterial load of Δ*dotA* mutant in IFNγ-treated cells compared to untreated cells at all time points (**Figure 4.1C**), probably due to the inability of the mutant to replicate in THP1 macrophages.

4.2.2 Viability of THP1 macrophages infected with L. pneumophila mutants

During infection, host cells may initiate cell death to clear the bacteria or to prevent bacterial replication by eliminating infected cells. To understand the effect of the deletions in each mutant to the host, cell viability was examined after infection with each mutant either under naïve conditions or with IFNγ stimulation. Live THP1 macrophages maintain adherence to the wells, while dead cells become nonadherent. Therefore, dead cells were removed by washing, and the remaining cells were fixed. CellTag700 was then used to stain and quantify the number of cells in the well. Afterwards, the fluorescence intensity at 700 nm was measured and normalised to the uninfected untreated sample.

From 24 h post-infection, WT-infected cells began to display reduced fluorescence at 700 nm compared to uninfected cells, suggesting that WT infection led to a loss in cell viability. At 48 h post-infection, this reduction was more pronounced (**Figure 4.2A, B**). At 48 h after WT infection, IFNγ-treated cells showed higher fluorescence intensity than untreated cells, suggesting better viability, consistent with the IFNγ-mediated improvement of bacterial clearance (**Figure 4.2A, B**). Similar to WT infection, infection by mutants ΔA, ΔB, and ΔD resulted in an increase in fluorescence of IFNγ-treated cells compared to untreated cells (**Figure 4.2A, B**). This is also consistent with the enhanced clearance of these mutants (**Figure 4.1C**). Meanwhile, no significant increase in

fluorescence was observed for ΔC- and ΔFGHI-infected cells upon IFNγ treatment, again supporting the bacterial CFU data (**Figure 4.2A, B, Figure 4.1C**). Interestingly, unstimulated ΔE mutant-infected cells showed increased cell fluorescence compared to WT-infected cells, suggesting that one or more of the genes deleted in this region was important to induce host cell death (**Figure 4.2A, B**).

4.2.3 L. pneumophila mutants showed a variable phenotype in A-strain mice

During *L. pneumophila* infection *in vivo*, multiple cell types may aid in the bacterial clearance, leading to an alteration in the infection outcomes. Therefore, we decided to investigate the survival of the mutant strains in a mouse model to better understand if any of the deleted genes influenced bacterial persistence under immune pressure. Amongst inbred mice, only A-strain mice have been shown to facilitate WT *L. pneumophila* replication (353, 358). This susceptibility is due to a polymorphism in the *Naip5/Birc1e* gene, which reduces the capacity to recognise flagellin of these mice (359, 360). As such, to enable virulent studies of *L. pneumophila*, A-strain mice are typically used (361). As murine resistance towards *L. pneumophila* is mainly due to the recognition of bacterial flagellin by the NLRC4/Naip5 inflammasome, *Naip5*$^{-/-}$, *Nlrc4*$^{-/-}$ mice, or aflagellated (Δ*flaA*) *L. pneumophila* strains are also used (166, 168, 169). In this study, we examined the survival of the mutant strains during infection of A-strain mice.

Mice were infected intranasally, and at day 1 and day 3 after infection, lungs were harvested, homogenised, and plated to enumerate bacterial CFU. In contrast to isolated macrophages, this approach revealed distinct phenotypes for all mutant strains. Firstly, the mice infected with two mutants, ΔA and ΔB, showed significant increases in bacterial numbers compared to WT at day 1 and day 3 after infection (**Figure 4.3A**). Consistent with this, mice infected by ΔA or ΔB mutants showed significantly more weight loss compared to WT-infected mice in at least one of the time points tested (**Figure 4.3B**). Secondly, compared to WT, mice infected with ΔFGHI mutant displayed an increase in bacterial numbers at day 1 after infection that normalised by day 3 (**Figure 4.3A**). Mice infected by ΔFGHI mutant also showed a transient increase in weight loss relative to WT-infected mice, consistent with the transient increase in bacterial CFU (**Figure 4.3B**). Thirdly, mice infected with ΔE mutant displayed a significant reduction in bacterial numbers and significantly less weight loss at both day 1 and day 2 after infection (**Figure**

4.3A, B). Finally, ΔC-infected mice showed significantly more weight loss at day 3 after infection, despite showing similar bacterial CFU relative to WT (**Figure 4.3A, B**). As all mutants showed different phenotypes, to ensure that each strain was equally inoculated into the mice, the inoculum was retrospectively plated. No significant difference in the mutants inoculum CFU was observed compared to WT (**Figure 4.3C**), suggesting that the difference in bacterial numbers of the mutants was not due to unequal starting number.

4.2.4 L. pneumophila ΔFGHI mutant infection did not alter the host pulmonary immune response

To investigate why mice infected with ΔFGHI mutant exhibited an increase in bacterial load, after 1 day infection, the right lung was harvested and the homogenate was subjected to cytometric bead array (CBA) analysis to determine the host cytokine response. Additionally, the left lung was minced, digested, and stained to determine the immune cell profiles at day 1 after infection as previously described (317). No significant difference was observed for the level of any tested cytokines at day 1 after infection (**Figure 4.4**). While there was no significant difference in the recruitment of neutrophils and MCs into the lungs during ΔFGHI mutant infection compared to WT infection, a significant increase in *L. pneumophila*-containing neutrophils and MCs were observed, consistent with higher lung CFU for this mutant (**Figure 4.5**). No significant difference was observed for the abundance of other cell types (**Figure 4.5**). Hence the basis of increased CFU at day 1 after infection for ΔFGHI did not appear to be immune-based.

4.2.5 Lpw_04861 enhanced L. pneumophila clearance from the lungs

Four genes were deleted in ΔB mutant (**Appendix 1**). To understand why the deletion of region B led to an increase in bacterial load, deletion of single genes in this region was performed. These single-gene mutants were then used to infect A-strain mice and bacterial load was quantified at day 3 after infection. While there was no significant difference in the inoculum bacterial numbers, the single-gene mutants showed distinct phenotypes in mouse (**Figure 4.6A, C**). Δ*lpw_04861* was the only single-gene mutant that showed a significant increase in bacterial load compared to WT, suggesting that *lpw_04861* was responsible for the phenotype of ΔB (**Figure 4.6A**). Surprisingly, all of the other single-gene mutants (Δ*lpw_04831*, Δ*lpw_04841*, Δ*lpw_04851*) displayed significant reductions in bacterial load compared to WT (**Figure 4.6A**). In addition to the

reduced bacterial load, Δ*lpw_04841* infection led to a significantly less weight loss compared to WT (**Figure 4.6B**). These data suggest that Lpw_04861 may be masking the phenotypes of these three genes in the ΔB mutant.

Several Dot/Icm T4SS effectors induce host mammalian immune response. As such, we hypothesised that Lpw_04861 may enhance host immune responses, resulting in an enhanced bacterial load in the absence of this gene. To test this hypothesis, the lung homogenate was subjected to CBA assay. Infection with ΔB led to a modest but significant increase in the level of IL-1α and MCP1 (**Figure 4.7**), consistent with the increase in bacterial load. Infection with Δ*lpw_04861* led to an increase in IL-1α expression, similar to ΔB (**Figure 4.7**). However, infection with Δ*lpw_04861* also led to a significant reduction in the level of IFNγ relative to WT infection (**Figure 4.7**). In addition to the cytokine response, the immune cell abundance in the lungs was also examined using flow cytometry. Consistent with the increase in bacterial load, an increase in neutrophil and MC recruitment, as well as a higher percentage of infected cells were observed (**Figure 4.8**).

To investigate how Lpw_04861 might contribute to enhanced bacterial clearance in the lungs, basic bioinformatic analysis was performed on the amino acid sequence of Lpw_04861. While BLASTp search revealed that the homologues of this gene are all uncharacterised proteins, we also found that this gene was highly conserved amongst 57 species of *Legionella* (**Figure 4.9**) (362). Similar to BLASTp search, scanning for homologous proteins using all available databases on the Interpro server (322) resulted in no homologues found. Despite using different templates at a low sequence similarity, structural prediction using the HHPred (325, 363), Phyre2 (323), I-TASSER (324, 364, 365), SparksX (366), and RaptorX (326) webservers consistently predicted that Lpw_04861 contains multiple alpha-helices connected by linker regions. Alpha-helices may pack to form coiled-coil domains, commonly found amongst Dot/Icm effectors. Consistently, the coiled-coil prediction platform Parcoil2 predicted the presence of a coiled-coil domain between residues 112-141 (327). Lpw_04861 was predicted to be a Dot/Icm effector protein (339). Consistently, Lpg0405, a homologue of Lpw_04861, is translocated in a Dot/Icm dependent manner during *L. pneumophila* infection of U937 macrophages (254). Therefore, Lpw_04861 may be translocated to the host cytosol,

although the mechanism of action cannot be determined through basic bioinformatics alone.

To confirm that the deletion of *lpw_04861* was specific and did not alter other parts of the genome, whole genome sequencing was performed. This demonstrated that while the mutagenesis has specifically deleted *lpw_04861*, there were 10 SNPs in Δ*lpw_04861* compared to WT *L. pneumophila* as listed in **Table 4.1**. The consequences of these SNPs are currently unclear. ΔB did not have any SNPs compared to WT (**Table 3.3**), suggesting that SNPs were introduced during construction of the single gene mutant. Complementation of Lpw_04861 using the constitutively expressing pMIP vector did not restore the replication of Δ*lpw_04861* back to the level of WT *L. pneumophila* (**Figure 4.6A**). However, it is unclear whether Lpw_04861 was properly expressed during murine infection. Therefore, more studies are required to confirm the role of Lpw_04861 in the increase in bacterial load.

4.2.6 Regions E1, E3, and E4 were important for L. pneumophila survival in lungs

To narrow down the bacterial factors that caused a reduction in ΔE survival in A-strain mice lungs (**Figure 4.3A**), region E was divided into four smaller genomic regions, namely E1-E4 (**Table 4.2**). These smaller genomic regions were then deleted using the suicide vector approach, similar to the large genomic region mutants (**Figure 3.2**). Similar to ΔE, ΔE1, ΔE3, and ΔE4 displayed significant reductions in bacterial load compared to WT despite the inoculation of similar number of bacteria (**Figure 4.10A, C**). However, unlike ΔE-infected mice, mice infected with these mutants did not display a significant difference in weight loss compared to WT-infected mice (**Figure 4.10B**), perhaps suggesting that the phenotype of ΔE was an additive result of the deletion of these regions. Interestingly, ΔE2 displayed a significant increase in bacterial load (**Figure 4.10A**), contrary to the phenotype of ΔE, implying an interaction between genes in regions E1, E3, and E4, with gene(s) in region E2.

4.2.7 LegC4 enhanced host cytokine response against L. pneumophila infection in A-strain but not C57BL/6 mice

LegC4 is one of the effectors encoded in region E2. It was previously described that transposon disruption of *legC4* led to a significant increase in bacterial survival in

Nlrc4$^{-/-}$ mice (334), which could explain the increased CFU of ΔE2 in A-strain mice. Therefore, we examined the survival of Δ*legC4* strain in A-strain mice to confirm that LegC4 was responsible for the increase in survival of ΔE2. As with previous experiments, the number of bacteria inoculated into each mouse was retrospectively enumerated to be equal amongst the strains tested (**Figure 4.11C**). In contrast to the published finding (334), Δ*legC4* showed similar bacterial load to WT at day 3 after infection of A-strain mice (**Figure 4.11A**). Consistently, mice infected with Δ*legC4* showed a similar weight loss phenotype to WT-infected mice (**Figure 4.11B**). To rule out any other effects of mouse strain background, an aflagellated *L. pneumophila* (Δ*flaA*) strain was used to infect WT C57BL/6 mice. However, there was no significant difference in bacterial load at both day 1 and day 3 post-infection (**Figure 4.12A**). Infection by Δ*legC4* caused a significant increase in weight loss at day 3 post-infection (**Figure 4.12B**). Noteworthy, similar number of bacteria was inoculated for both strains (**Figure 4.12C**).

Infection with aflagellated Δ*legC4* strain was previously described to lead to reduced host TNFα and IL6, leading to a significant increase in bacterial load compared to WT in murine BMDMs (367). Thus, the lung cytokine response was measured to examine the host response towards Δ*legC4* infection. A significant reduction in IFNγ was observed during infection of Δ*legC4* in A-strain mice (**Figure 4.13**), suggesting that LegC4 enhanced IFNγ secretion during infection of A-strain mice, although this did not influence overall bacterial numbers. In contrast, there was no significant difference in the level of any pulmonary cytokine during aflagellated Δ*legC4* mutant infection of C57BL/6 mice (**Figure 4.14**). Hence, we could not reliably repeat the previous findings that LegC4 enhanced the cytokine response to *L. pneumophila* infection. This suggested that other genes encoded in the region deleted in ΔE2 were responsible for the phenotype observed.

4.3 Discussion

In this chapter, the large genomic mutants were used to investigate the effectors involved in bacterial survival in IFNγ-stimulated macrophages, host cell death, and *in vivo* pathogenesis. Strikingly, while all mutants were able to proficiently replicate in THP1 macrophages under either naïve or IFNγ stimulation conditions, various obvious phenotypes were observed in A-strain mice. Four out of six mutants tested displayed a significant increase in bacterial CFU, suggesting that genes deleted in these regions may

enhance the clearance of WT *L. pneumophila* from the murine lungs. *Lpw_04861*, the gene whose deletion is potentially responsible for the increase in CFU of ΔB, is well-conserved amongst *Legionella spp*, perhaps suggesting the importance of this gene in the environmental life cycle of *Legionella*. Deletion of region E led to a significant reduction in bacterial CFU, suggesting gene(s) within this region were important for pathogen persistence in the mammalian host. During the identification of genes responsible for the phenotype of the large genomic region mutants in A-strain mice, we observed a potential meta-effector relationship, as with the exception of *lpw_04861*, deletion of each gene in region B led to a significant reduction in bacterial CFU. Similarly, ΔE2 displayed a significant increase in bacterial CFU that was masked by other genes in ΔE.

While IFNγ is important for the clearance of *L. pneumophila*, IFNγ is primarily produced by lymphocytes (185, 192, 352). Therefore, in this study, we stimulated THP1 macrophages with IFNγ to represent a more optimal macrophage activation level. Despite the potent effect of IFNγ in the clearance of *L. pneumophila* in both murine and human models (194, 196-198, 350), surprisingly we saw little effects (~1 log fold change at 48 h post-infection only) on THP1 macrophages ability to clear *L. pneumophila*. Previous studies showed that IFNγ stimulation of human macrophages improved *L. pneumophila* clearance by at least 1 log fold at 24 h post-infection and more than 2 log fold at 48 h post-infection despite the use of similar or lower dose of IFNγ compared to this study (350, 351). Different cell lines may have different sensitivity to IFNγ treatment, therefore a higher dose may be required to impart the same level of inhibition in THP1 macrophages. Nonetheless, stimulation with 100 ng/ml of IFNγ reduced cell viability by ~20% in this study, and increasing the dose may further increase cell death. Previous studies on the effect of IFNγ to *L. pneumophila* clearance did not report whether there was any reduction in cell viability, therefore it is unclear whether excessive cell death has confounded their findings (350, 351). Together, these highlight the limitations of using macrophage cell lines to study *L. pneumophila* replication, especially under IFNγ stimulation.

Unlike in THP1 macrophages, the mutants displayed clear phenotypes during infection of A-strain mice. It may be argued that the differences in species is contributing to the differences in phenotype in THP1 macrophages and A-strain mice, as THP1 macrophages

are human cells (368). However, the deletion of orthologs of genes in regions C-I in *L. pneumophila* strain Philadelphia-1 also did not show a significant difference in mouse BMDMs (338), suggesting that the differences observed in this study were not simply due to differences in species. Rather, it is more likely that these differences arise from the lack of sensitivity of the *in vitro* model compared to *in vivo* model. *L. pneumophila* infection induces a robust pro-inflammatory response in the lung, such as the secretion of IL-6, IL-1β, and TNFα (369). In the *in vitro* model, these cytokines may improve bacterial clearance by improving macrophage antimicrobial activity if they are produced and can act back on the infected macrophage in an autocrine manner.

In addition to improving the macrophage antibacterial capacity, *in vivo* these cytokines recruit immune cells, such as neutrophils and monocytes, which subsequently differentiate into macrophage-like cells termed monocyte-derived cells (MCs), as well as NK cells and T cells, all of which contribute to bacterial clearance (370). Consistent with our results, another study showed that effectors that influence *L. pneumophila* replication in *NLRC4*$^{-/-}$ mice did not always influence the bacterial replication in *NLRC4*$^{-/-}$ mice BMDMs (334). This highlights the limitations of *in vitro* models to study the pathogenesis of *L. pneumophila*. These results show that screening for effector functions solely *in vitro* may not be accurate, as phenotypes found during *in vitro* infection may be completely different to *in vivo* phenotype. As such, screening of phenotypes should also be performed *in vivo*. A valid concern is the feasibility of this approach due to the large number of effectors. Genetic tools such as the large genomic region mutants used here or libraries of transposon mutants could provide a way to reduce the number of animals required.

Notably, we found that *L. pneumophila* contained at least four genomic regions that were detrimental to mammalian infection. For instance, despite losing 42 Dot/Icm effectors and 92 non-effector genes, ΔFGHI displayed a significant increase in bacterial CFU at day 1 after infection. Additionally, infection by ΔC led to increased weight loss compared to WT infection, despite showing similar bacterial burden, suggesting more severe disease. *Lpw_04861*, the gene in ΔB which enhanced the clearance of *L. pneumophila*, is well-conserved across 52 species in the genus *Legionella*, suggesting it has a key role in environmental persistence. Supporting our result, a recent paper reported that three Dot/Icm effectors, VpdA, MavW, and RavG, were important for *L. pneumophila*

replication in at least one of four natural protozoan host tested, but were disadvantageous for bacterial replication in U937 human macrophage-like cells (348). In addition, the effector protein LegS2 enhanced the cytokine secretion and subsequent clearance of *L. pneumophila* in BMDMs, although its involvement in the protozoan host is unknown (371). Together, these imply that there are many effectors detrimental to mammalian infection that are maintained to allow *L. pneumophila* survival in environmental hosts. The conservation of genes that are costly to mammalian infection is consistent with the lack of transmission and therefore selection for virulence during mammalian *L. pneumophila* infection.

The phenotype associated with Lpw_04861 is exciting as it is strong and can mask the phenotype of three other genes. However, more work needs to be done to understand this phenotype. Firstly, complementation of Δ*lpw_04861* is required to confirm that the increase in ΔB survival was indeed due to this putative effector protein. The introduction of N terminal tag may be helpful to ensure that Lpw_04861 is properly expressed in the complementation strain. Furthermore, the use of native promoter of *lpw_04861* may be better suited to the complementation compared to the use of constitutively high expressing *mip* promoter. Secondly, while the ortholog of Lpw_04861 in *L. pneumophila* strain Philadelphia-1, Lpg0405, was experimentally proven to be a Dot/Icm T4SS effector (254), investigation of the translocation of Lpw_04861 by the Dot/Icm T4SS is required to confirm this in *L. pneumophila* strain 130b.

Finally, another outstanding question is to understand how Lpw_04861 could potentially enhance bacterial clearance. To answer this, we attempted to elucidate whether Lpw_04861 also enhanced the cytokine and immune cell response against *L. pneumophila*. However, the results of cytokines and immune cell analysis did not explain the increase in bacterial load of Δ*lpw_04861*. Interestingly, a significant reduction in the level of lung IFNγ was observed after Δ*lpw_04861,* but not ΔB infection. Deletion of the three other genes in region B led to a reduced bacterial load compared to WT, suggesting possible interaction(s) which may mask the IFNγ reduction in the ΔB mutant. It is also possible the SNPs found in Δ*lpw_04861* may influence these phenotypes, therefore, trans-complementation of *lpw_04861* is required to confirm this phenotype. Nonetheless, ΔB displayed an increase in bacterial load without an apparent reduction in IFNγ, so reduction of this cytokine seems unlikely to be the cause of the increase in

bacterial load. Overall, based on the cytokine and immune cells examined in this study, it seems unlikely that Lpw_04861 enhanced the host immune response and subsequent bacterial clearance.

Bioinformatics was also employed to predict the function of Lpw_04861. Structure prediction predicts the presence of coiled-coil motif in Lpw_04861. This motif mediates protein-protein and protein-DNA interactions, and is associated with various functions, such as molecular spacer, transcription regulation, or ER-Golgi vesicle tethering to SNAREs (372). Therefore, while basic bioinformatics cannot predict the function of Lpw_04861, determination of the binding partner can be done in the future to characterise this effector protein.

Of the regions tested, the only region important for *L. pneumophila* survival in A-strain mice is region E. A clue to the reduced CFU of ΔE in mice may be the significant reduction in THP1 cell death induced by ΔE. In the later stages of infection, *L. pneumophila* lyse host cells to facilitate egress (135). The reduction in THP1 cell death during ΔE infection suggests either reduced or delayed egress. This can be examined by enumerating the bacterial numbers in the supernatant of infected host cells at 24 h and 48 h post-infection. We subsequently found that ΔE1, ΔE3, and ΔE4 led to a significant reduction in bacterial load, suggesting that multiple genes contributed to the ΔE phenotype. In a transposon study, disruption of *lem17*, a putative Dot/Icm effector deleted in ΔE1 led to a significant decrease in bacterial replication in *NLRC4*$^{-/-}$ mice, but not *NLRC4*$^{-/-}$ BMDMs, consistent with the phenotype of ΔE1 (334). As yet, none of the genes in region E3 and E4 have been characterised. Future studies will be required to identify the bacterial factors responsible for the phenotypes observed for the sub-deletion mutants here. Additionally, testing the sub-deletion mutants for the cell death phenotype should be done to determine the correlation between the two phenotypes.

Another interesting observation of this study is that sub-deletions sometimes led to a contradictory phenotype compared to the deletion of a larger region. While ΔB displayed a significant increase in bacterial load, Δ*lpw_04831,* Δ*lpw_04841*, and Δ*lpw_04851* showed a significant decrease in bacterial load. On the other hand, while ΔE exhibited a significant reduction in bacterial load, ΔE2 displayed a significant increase in bacterial load. These may suggest either a subtractive effect of genes, or meta-effector relationship,

where two or more effectors may counteract each other. For instance, the Dot/Icm effector MesI was previously described to reduce the translation inhibition mediated by another effector, SidI (336). A yeast-based screening of potential meta-effector partners has previously been done, however, this screen relied on one of the meta-effector partners being toxic to yeast, and so only a subset of effectors produced a phenotype (373). Unfortunately, all genes in region B, as well as most genes in region E2, are uncharacterised. Therefore, characterisation of the genes in ΔB, as well as the identification of gene that caused the phenotype of ΔE2 should be done to unravel the potential genetic interactions.

One of the effectors encoded in region E2, LegC4, was previously shown to enhance bacterial clearance from the lungs of *Nlrc4*$^{-/-}$ mice by enhancing host TNFα and IL-12 secretion (334), consistent with the increase in ΔE2 survival in A-strain mice. However, we were not able to reproduce this phenotype with Δ*legC4* mutant strains in either A-strain mice for WT *L. pneumophila* or C57BL/6 mice for Δ*flaA L. pneumophila*. This discrepancy may be due to the differences in *L. pneumophila* strain used, as well as differences in time points used. Additionally, the increase in Δ*legC4* replication was less than 1 log fold change (334), suggesting a weak phenotype. In this study, the authors were only able to complement the phenotype using competitive mixed infection, which is more sensitive to identify minor differences that monogenic infection (361). Furthermore, instead of pooling data obtained from all experiments, the authors only displayed representative data from 4 animals. Thus, it is questionable whether LegC4 is responsible for the overall phenotype of ΔE2. LegC4 was also shown to enhance host IL-12 production in *Nlrc4*$^{-/-}$ mice, as well as the production of TNFα and IL6 from BMDMs (334, 367). However, the TNFα and IL6 phenotypes were only present when LegC4 was expressed on a plasmid, as such this may simply be an effect of overexpression. In this study, we did not find any reduction in host IL-12, TNFα, or IL6 upon infection with Δ*legC4* mutant. We did find that the presence of LegC4 enhanced IFNγ production during infection of A-strain mice, but not C57BL/6 mice. IL-12 stimulates the production of IFNγ from NK cells and T cells (374), perhaps suggesting that LegC4 does enhance the host immune response. However, more studies are required to clarify the potential differences in inflammatory response present.

In summary, the results here demonstrate that large genomic region mutants can be an efficient tool to identify Dot/Icm T4SS effectors that influence infection outcomes. All mutants exhibited altered *in vivo* pathogenesis, which manifested in either bacterial burden or weight loss in infected mice. Four out of six mutants displayed an increase in bacterial load, suggesting many effectors are maintained by protozoan host selection to the detriment of mammalian infection. We implicated Lpw_04861, a well-conserved putative Dot/Icm T4SS effector with unknown function, in enhanced pulmonary clearance of *L. pneumophila*. Additionally, through the sub-deletions, we observed the presence of potential meta-effector relationships and functional redundancy. Further studies are required to elucidate the gene(s) responsible for the phenotypes in the cluster mutants generated, and to understand how the putative effectors Lpw_04861 and LegC4 influence *L. pneumophila* lung infection.

Table 4.1. List of SNPs in Δ*lpw_04861*

SNPs	Consequences
G > C substitution in *lpw_12441* (Kup2 low affinity potassium transport system	Synonymous mutation
C > A substitution in the intergenic region upstream of *lpw_13361* (hypothetical protein Lpg1326)	Change in predicted promoter region
G > A substitution in the intergenic region upstream of *lpw_14531* (hypothetical protein Lpg1453)	Alteration in predicted transcription factor binding site (rpoD17)
A > C substitution in *lpw_00671* (coiled-coil containing protein	Ile268Ser
A > T substitution in *lpw_27971* (hypothetical protein)	Synonymous mutation
G > C substitution between *lpw_26341* and *lpw_26351*	No alteration in predicted promoter region/transcription factor binding site
T > G substitution in the intergenic region between *lpw_27351* (sdeD) and *lpw_27361* (sdeA)	No alteration in predicted promoter region/transcription factor binding site
C > G substitution in the intergenic region upstream of *lpw_09611* (transporter)	No alteration in predicted promoter region/transcription factor binding site
T > C substitution in the intergenic region upstream of *lpw_14901*	No alteration in predicted promoter region/transcription factor binding site
T > G substitution in *lpw_08561* (hypothetical protein Lpg0766)	Ser366Arg

Table 4.2. Sub-regions of genomic region E.

Gene	Name	Sub-regions
LPW_19951	**lem16**	E1
LPW_19961	**lem17**	
LPW_19971	**ralF**	
LPW_19981		E2
LPW_19991		
LPW_20001		
LPW_20011		
LPW_20021		
LPW_20031		
LPW_20041	**legC4**	
LPW_20051		
LPW_20061		
LPW_20071		
LPW_20081		
LPW_20091	**ltpG**	
LPW_20101		E3
LPW_20111	**lirA**	
LPW_20121		
LPW_20131	**lirB**	
LPW_20141	**lirE/pieC**	
LPW_20151	**lirF/pieD**	
LPW_20161		E4
LPW_20171		
LPW_20181		
LPW_20191		
LPW_20201	**pieE**	

Genes encoding for Dot/Icm effectors are printed in **bold**.

A.

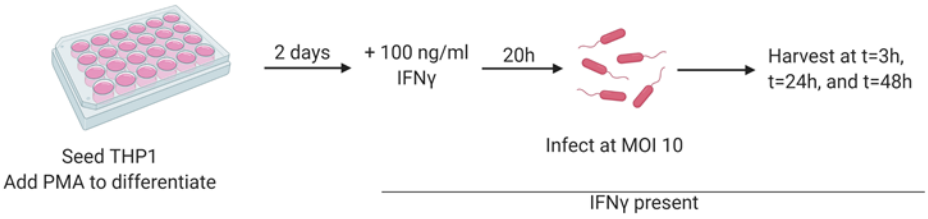
2 days
+ 100 ng/ml IFNγ
20h
Harvest at t=3h, t=24h, and t=48h
Seed THP1
Add PMA to differentiate
Infect at MOI 10
IFNγ present

B.

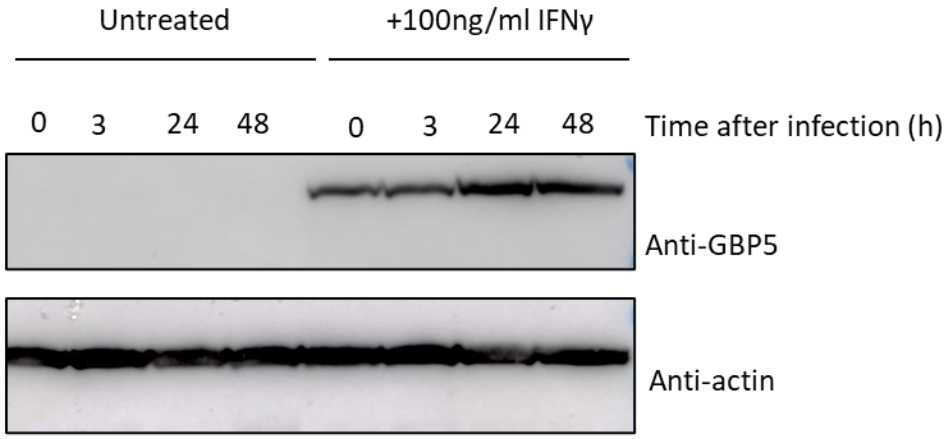
Untreated
+100ng/ml IFNγ
0 3 24 48 0 3 24 48
Time after infection (h)
Anti-GBP5
Anti-actin

C.

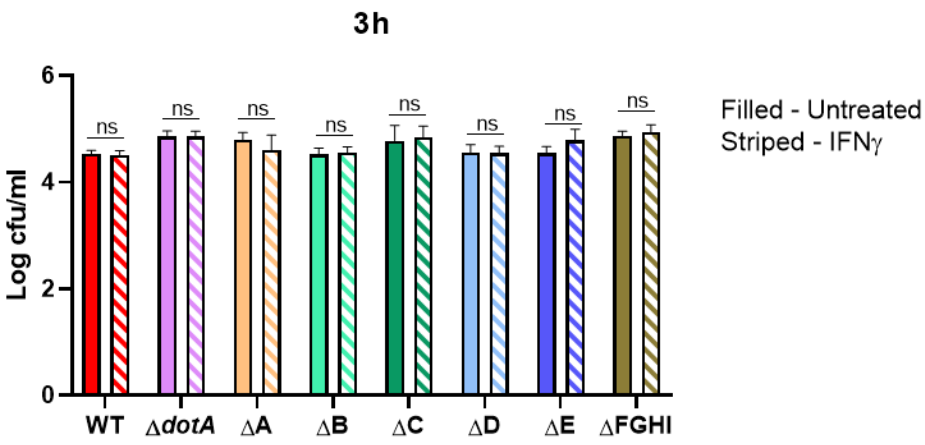
3h
Log cfu/ml
6
4
2
0
ns
WT
ΔdotA
ΔA
ΔB
ΔC
ΔD
ΔE
ΔFGHI
Filled - Untreated
Striped - IFNγ

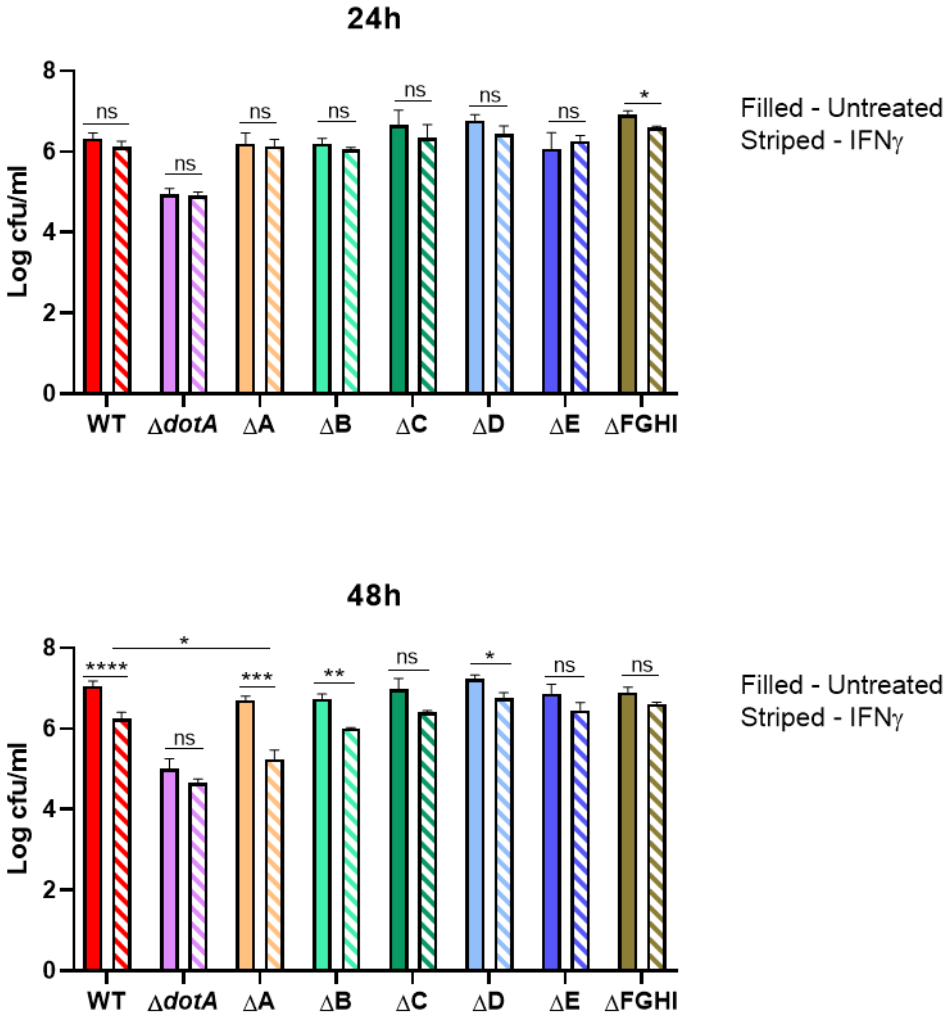

Figure 4.1. *L. pneumophila* mutants replicate proficiently in IFNγ-stimulated THP1 macrophages.

(A). Schematic of experiment design. (B). Immunoblot showing the expression of Gbp5. Image is representative of 3 independent experiments. Bacterial cfu of strains recovered from either unstimulated or IFNγ-stimulated cells at 3h, 24h, and 48h (C) after infection ($n \geq 3$). Each bar indicates the mean +/- SEM. Statistical significance was calculated using unpaired t-test (* $p \leq 0.05$, ** $p \leq 0.01$, *** $p \leq 0.001$, **** $p \leq 0.0001$).

A.

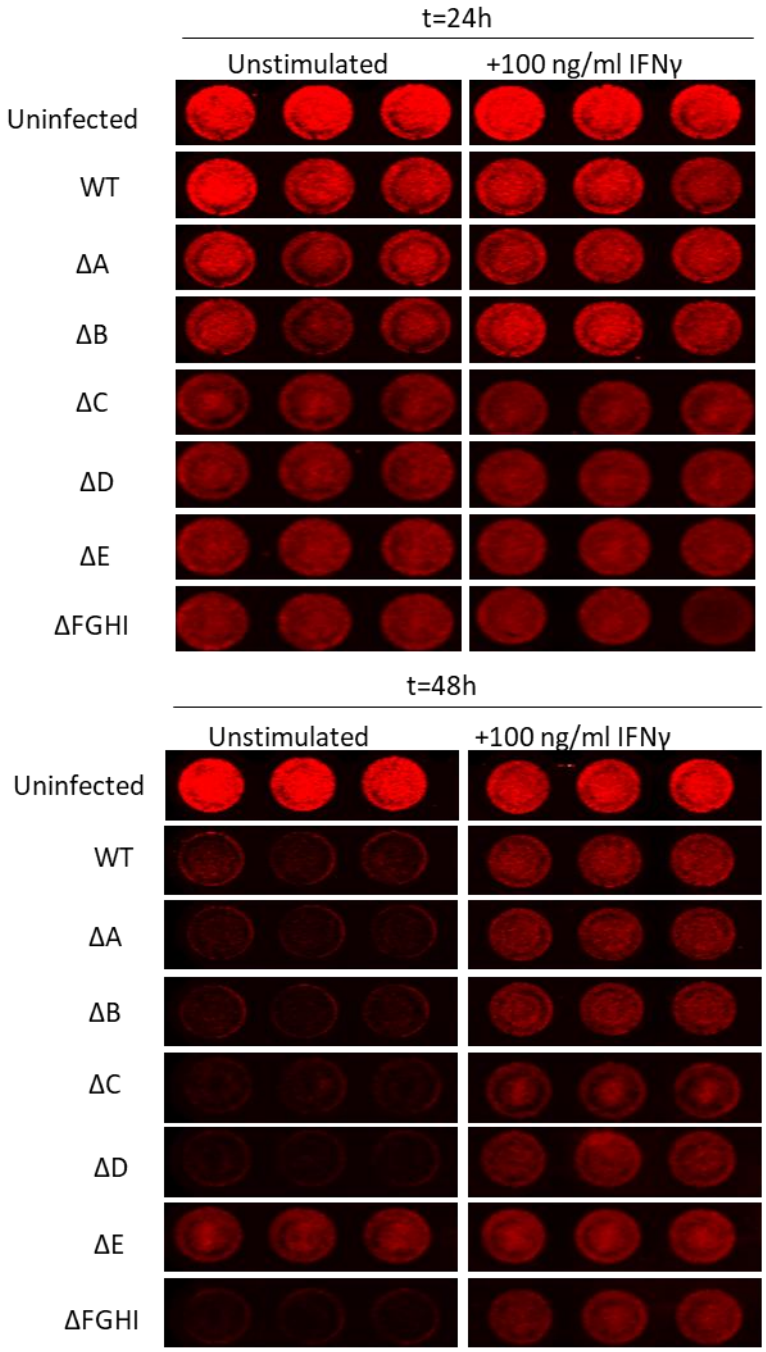
t=24h
Unstimulated
+100 ng/ml IFNγ
Uninfected
WT
ΔA
ΔB
ΔC
ΔD
ΔE
ΔFGHI
t=48h
Unstimulated
+100 ng/ml IFNγ
Uninfected
WT
ΔA
ΔB
ΔC
ΔD
ΔE
ΔFGHI

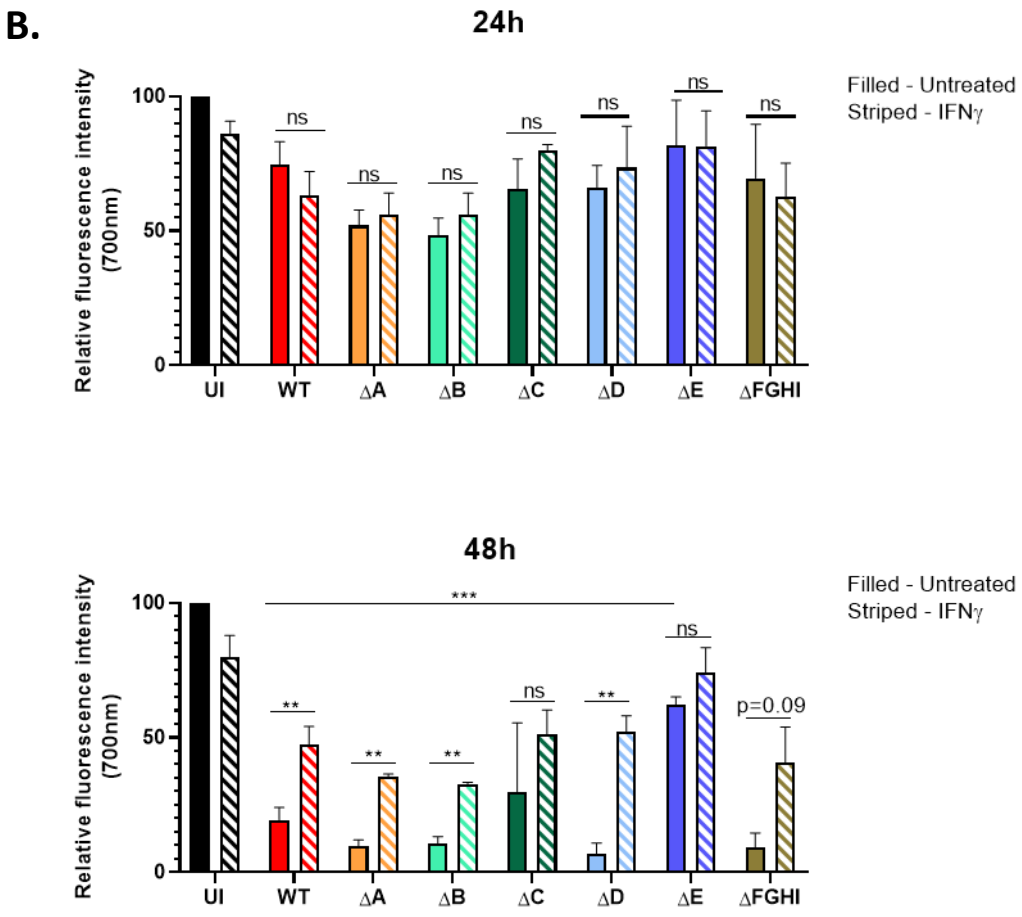

Figure 4.2. Cells infected with ΔE mutant showed enhanced viability at 48 h post-infection.

(A). In-cell Western-blot showing the density of cells in each 96-well plate well at 24 h (A) and 48 h post-infection. Cells were fixed and stained with CellTag 700, allowing fluorescence emission of stained nuclei at 700 nm. Image is representative of at least 3 independent experiments. Relative fluorescence intensity at 700 nm compared to untreated uninfected sample at 24 h and 48 h post-infection (B). Fluorescence intensity at 700 nm was quantified. After background subtraction, the intensity was normalized to the untreated uninfected sample. Each bar indicates the mean +/- SEM ($n \geq 3$). Statistical significance was determined using unpaired t-test (* $p \leq 0.05$, ** $p \leq 0.01$, *** $p \leq 0.001$, **** $p \leq 0.0001$).

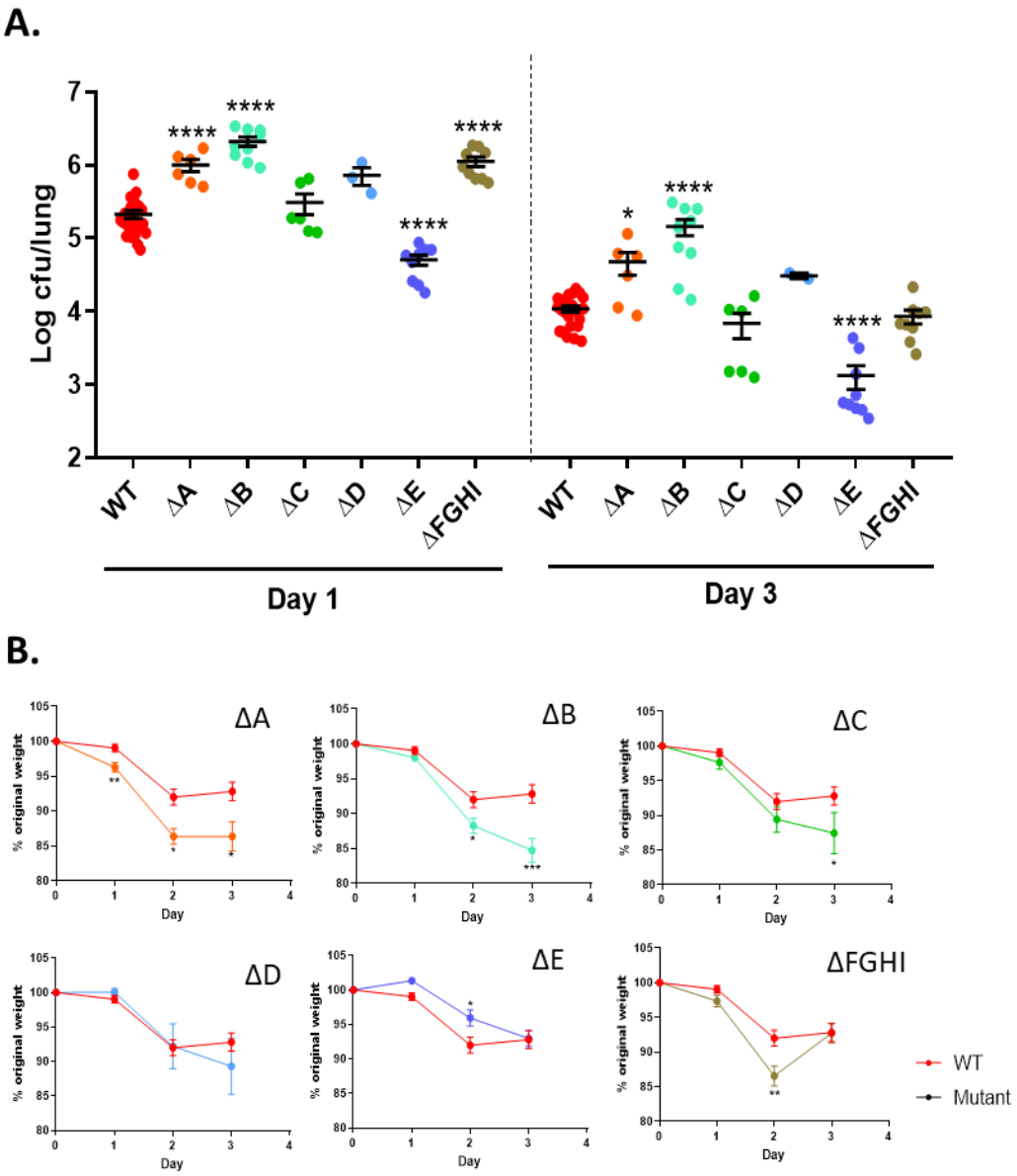
A.
Log cfu/lung
WT
ΔA
ΔB
ΔC
ΔD
ΔE
ΔFGHI
Day 1
Day 3
B.
ΔA
ΔB
ΔC
ΔD
ΔE
ΔFGHI
% original weight
Day
WT
Mutant

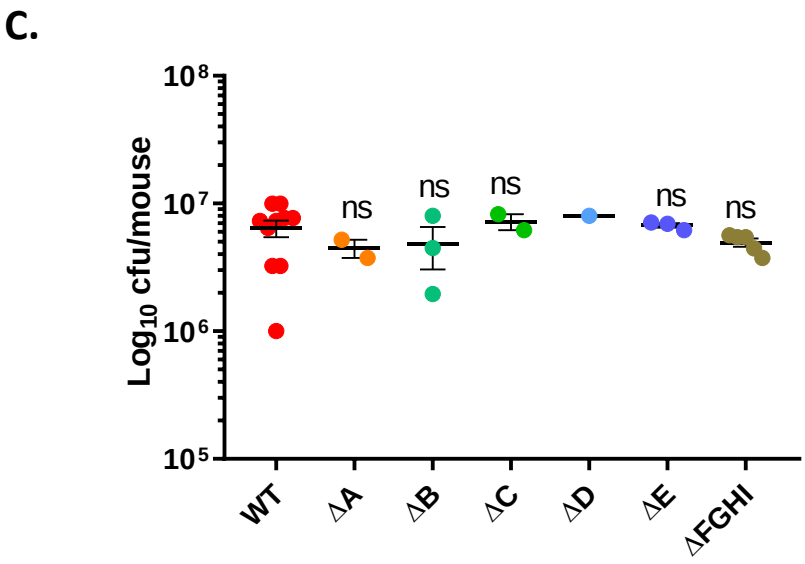

Figure 4.3. Mutants showed variable phenotypes in A-strain mice.

(A) At day 1 and 3 post-intranasal infection, mouse lungs were harvested. Bacterial CFU from A-strain lungs at day 1 and day 3 after intranasal infection was then enumerated. WEach dot represents data from one animal. Data was pooled from at least 2 independent experiments, except for ΔD (1 independent experiment). (B) Weight of mice after infection. Each point represents the mean +/- SEM of weight during the corresponding time point ($N \geq 6$). (C) Bacteria used to inoculate mice were retrospectively plated, and CFU was enumerated. Each dot represents data from one independent experiment. Except for ΔD (1 independent experiment), data from at least 2 independent experiments is presented. Statistical significance was determined using Mann-Whitney test. Unless otherwise indicated, asterisks indicate the statistical significance compared to WT (* $p \leq 0.05$, ** $p \leq 0.01$, *** $p \leq 0.001$, **** $p \leq 0.0001$).

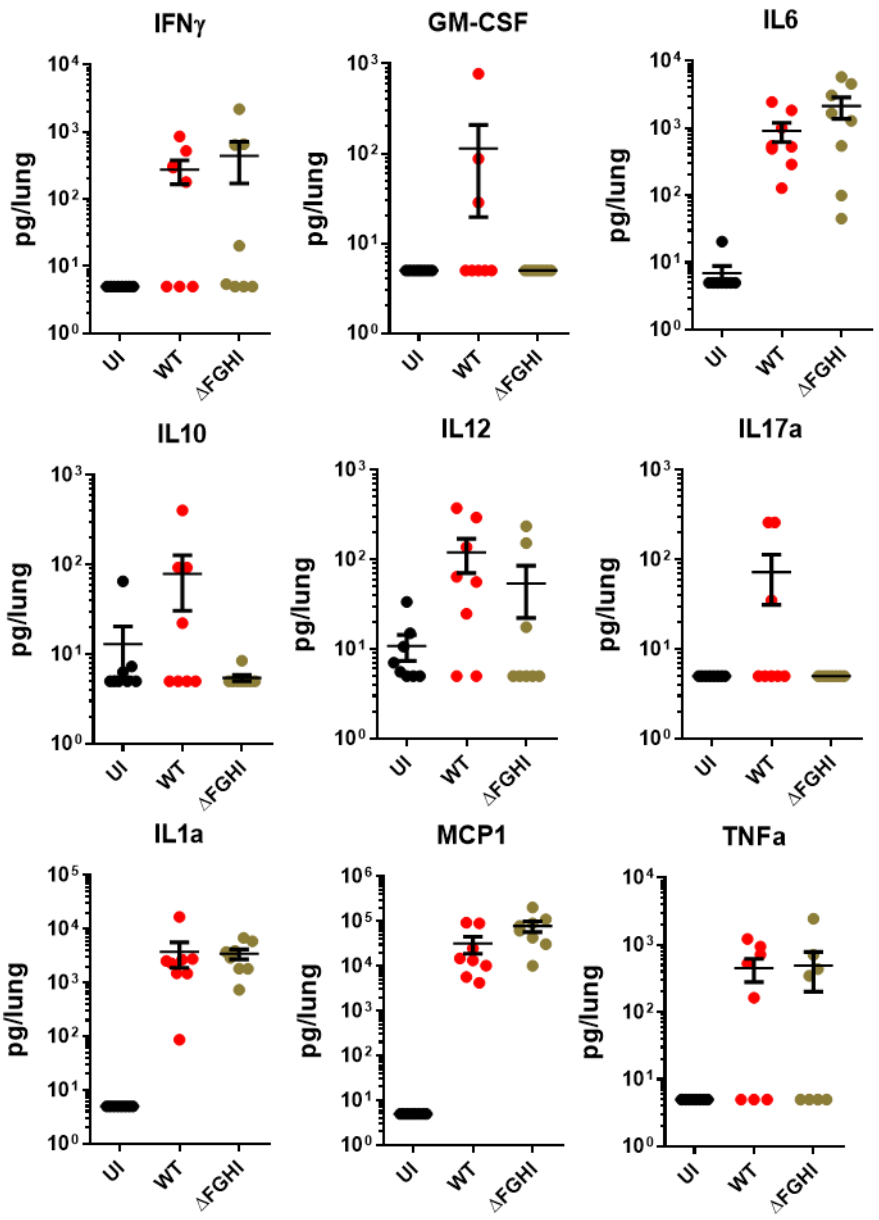

Figure 4.4. ΔFGHI infection resulted in similar host cytokine response compared to WT infection.

At day 1 after infection, the right lung was harvested and homogenised. Level of cytokines in the lung homogenate was determined with CBA flex kit. Each dot represents one animal (n=9). Data was pooled from 3 independent cohorts. Mean +/- SEM is represented by the lines. Statistical significance was performed using Mann-Whitney test (* $p \leq 0.05$, ** $p \leq 0.01$, *** $p \leq 0.001$, **** $p \leq 0.0001$).

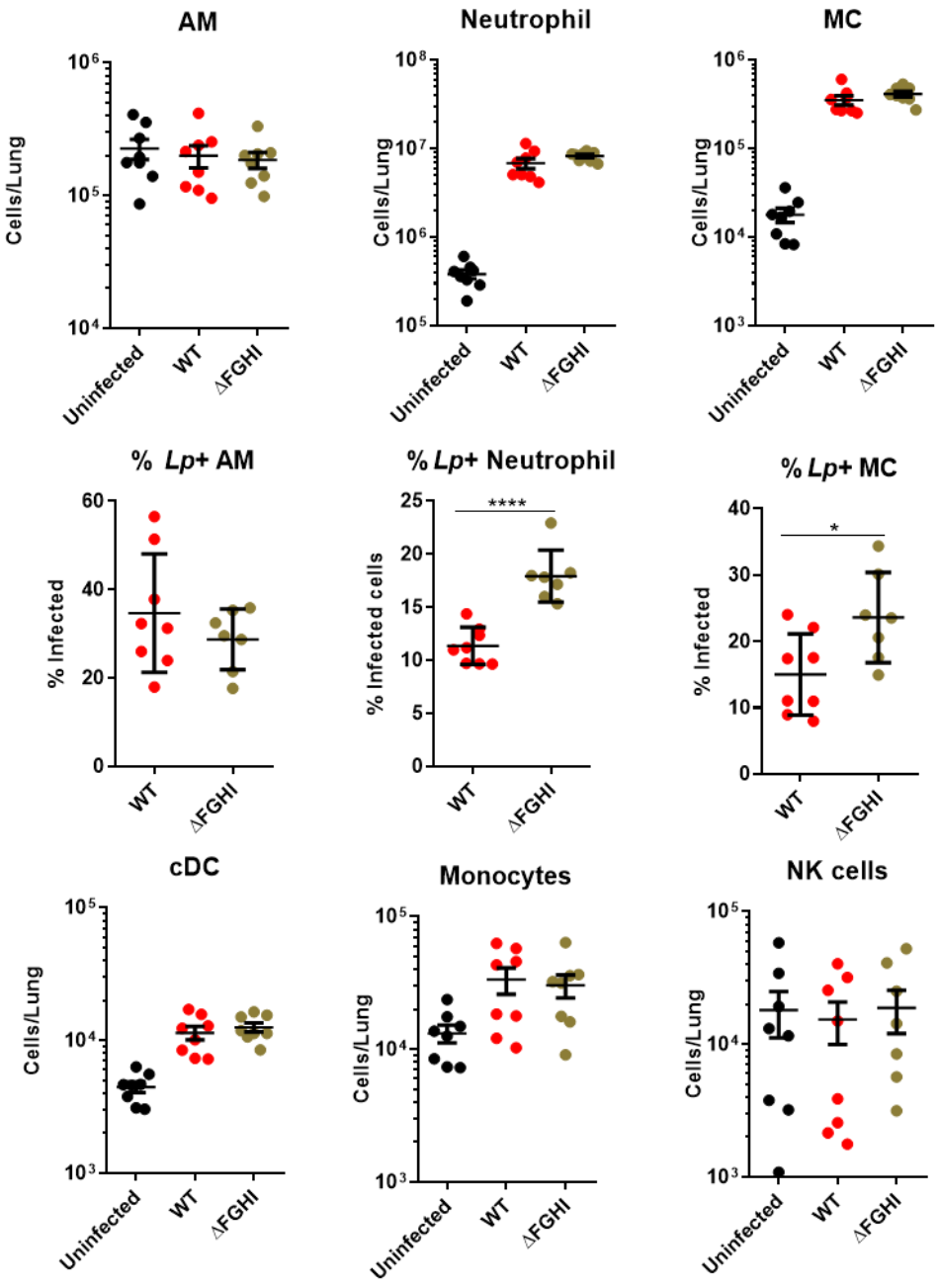
AM
Neutrophil
MC
Cells/Lung
Uninfected
WT
ΔFGHI
% Lp+ AM
% Lp+ Neutrophil
% Lp+ MC
% Infected
% Infected cells
****
*
cDC
Monocytes
NK cells

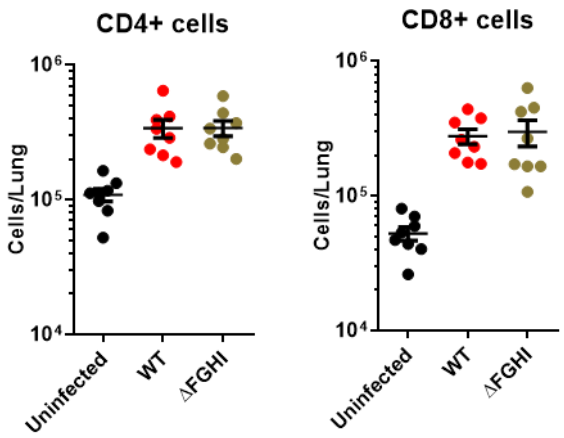

Figure 4.5. ΔFGHI displayed no alteration in lung immune response.

At day 1 after infection, left lung was harvested, minced, stained with the appropriate antibody, and analyzed using flow cytometry. Each dot represents one animal (n=9). Data was pooled from 3 independent cohorts. Mean +/- SEM is represented by the lines. Statistical significance was performed using Mann-Whitney test (* $p \leq 0.05$, ** $p \leq 0.01$, *** $p \leq 0.001$, **** $p \leq 0.0001$).

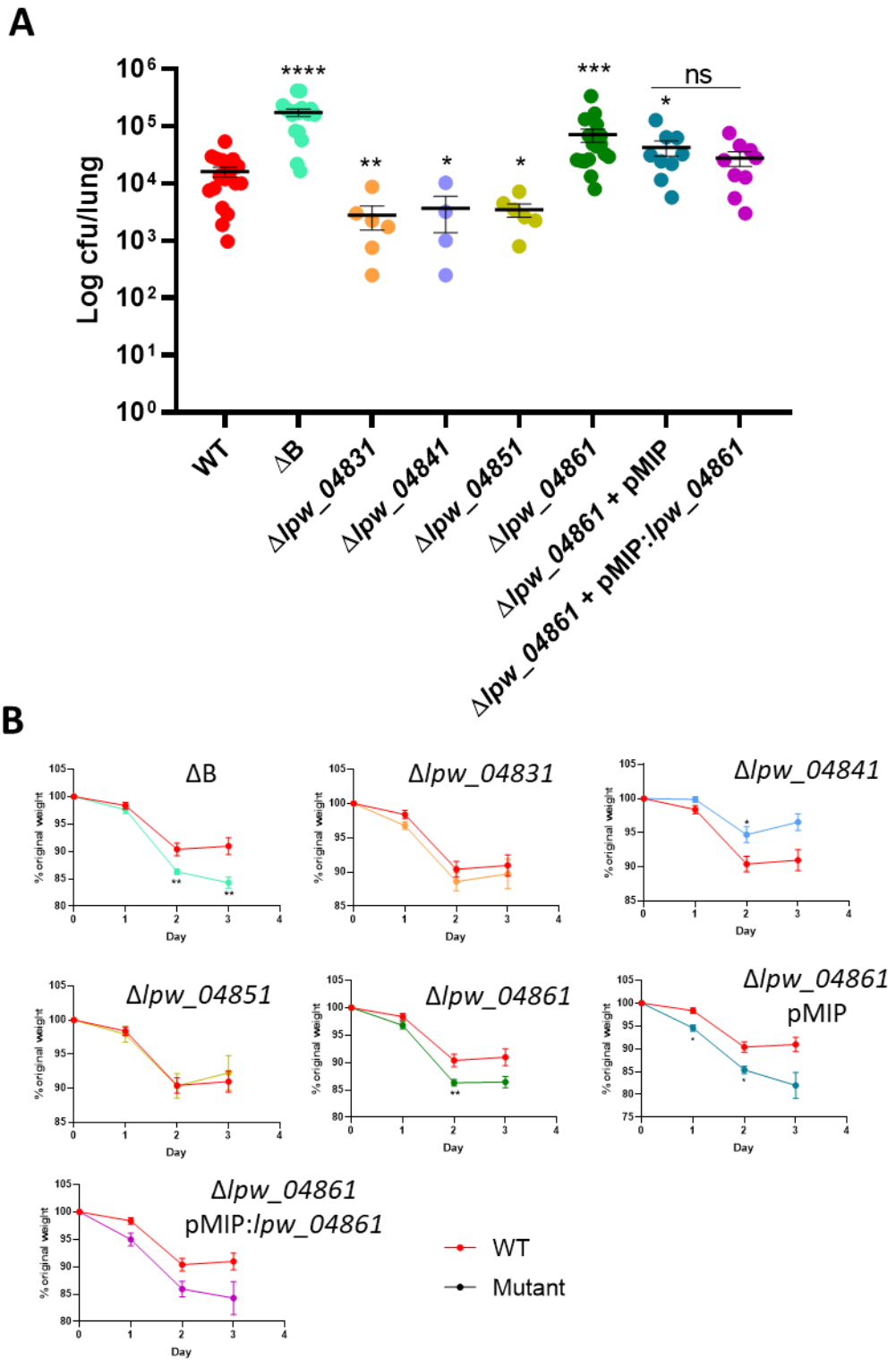
A
Log cfu/lung
WT
ΔB
Δlpw_04831
Δlpw_04841
Δlpw_04851
Δlpw_04861
Δlpw_04861 + pMIP
Δlpw_04861 + pMIP:lpw_04861
ns
B
ΔB
Δlpw_04831
Δlpw_04841
Δlpw_04851
Δlpw_04861
Δlpw_04861 pMIP
Δlpw_04861 pMIP:lpw_04861
% original weight
Day
WT
Mutant

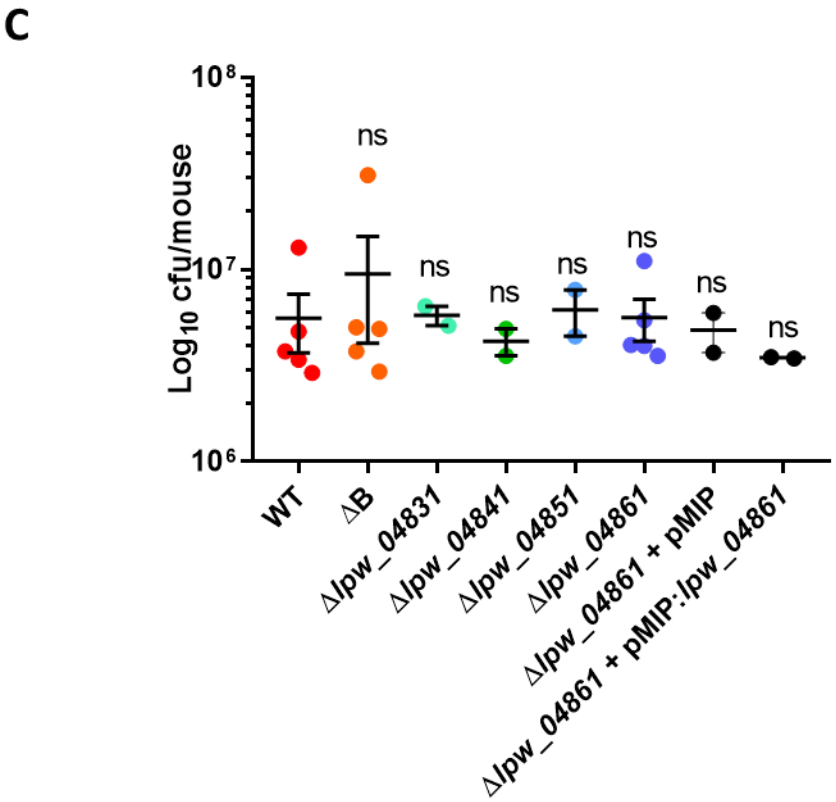

Figure 4.6. Lpw_04861 may influence the clearance of *L. pneumophila* from A-strain mice lungs.

(A) At day 3 post-intranasal infection, mouse lungs were harvested. Bacterial CFU from A-strain lungs at day 3 after intranasal infection. Each dot represents data from one animal. Data was pooled from at least 2 independent experiments. (B) Weight of mice after infection. Each point represents the mean +/- SEM of weight during the corresponding time point ($N \geq 6$). (C) Bacteria used to inoculate mice were retrospectively plated, and CFU was enumerated. Each dot represents data from one independent experiment. Data from at least 2 independent experiments are presented. Statistical significance was determined using Mann-Whitney test. Unless otherwise indicated, asterisks indicate the statistical significance compared to WT (* $p \leq 0.05$, ** $p \leq 0.01$, *** $p \leq 0.001$, **** $p \leq 0.0001$).

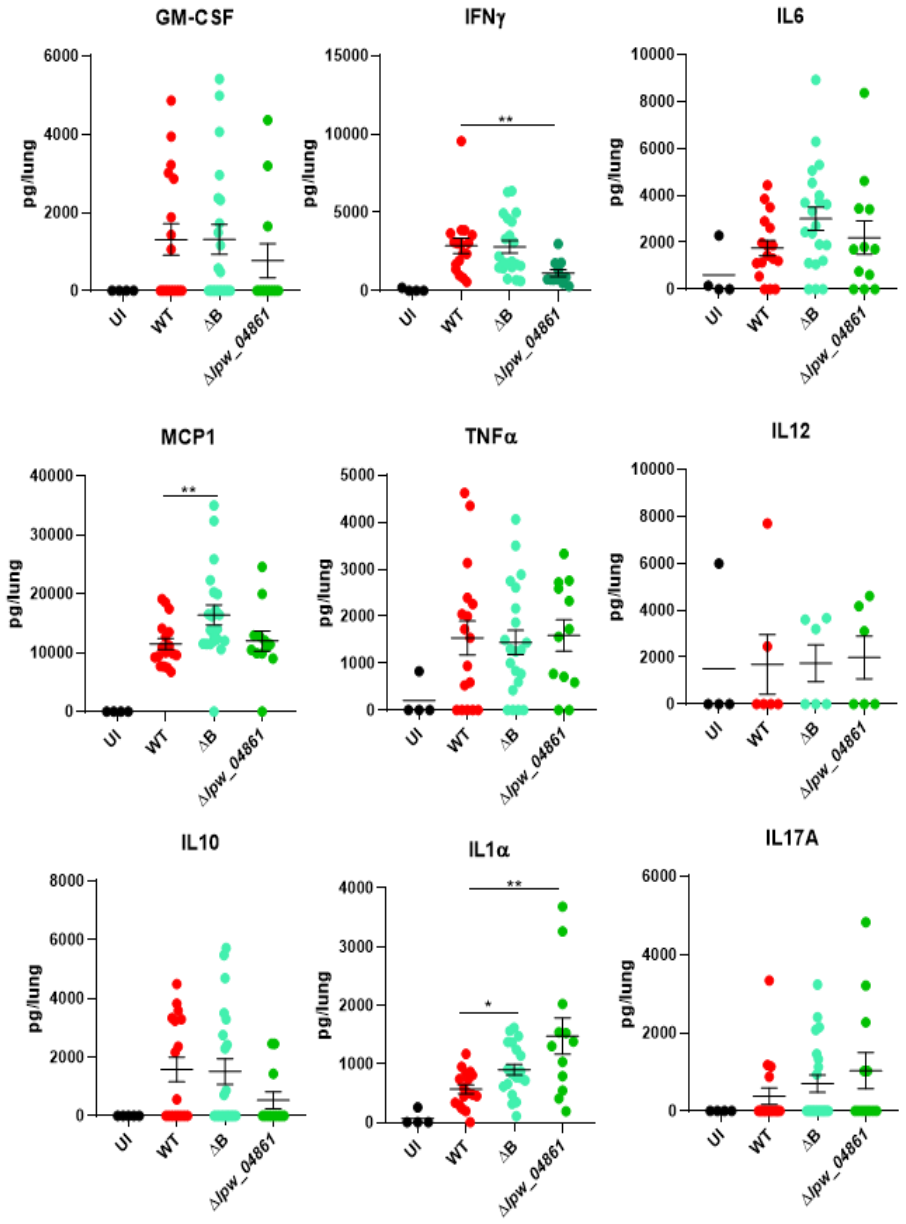

Figure 4.7. Lpw_04861 may influence host cytokine response.

At day 3 after infection, either the right lung or both lungs were harvested and homogenated. Lung homogenates were then analysed using CBA flex kit. When only one lung is used, number was multiplied by 2 to account for both lungs. Each dot represents one animal. Data was pooled from at least 2 independent cohorts. Mean +/- SEM is represented by the lines. Statistical significance was performed using Mann-Whitney test (* $p \leq 0.05$, ** $p \leq 0.01$, *** $p \leq 0.001$, **** $p \leq 0.0001$).

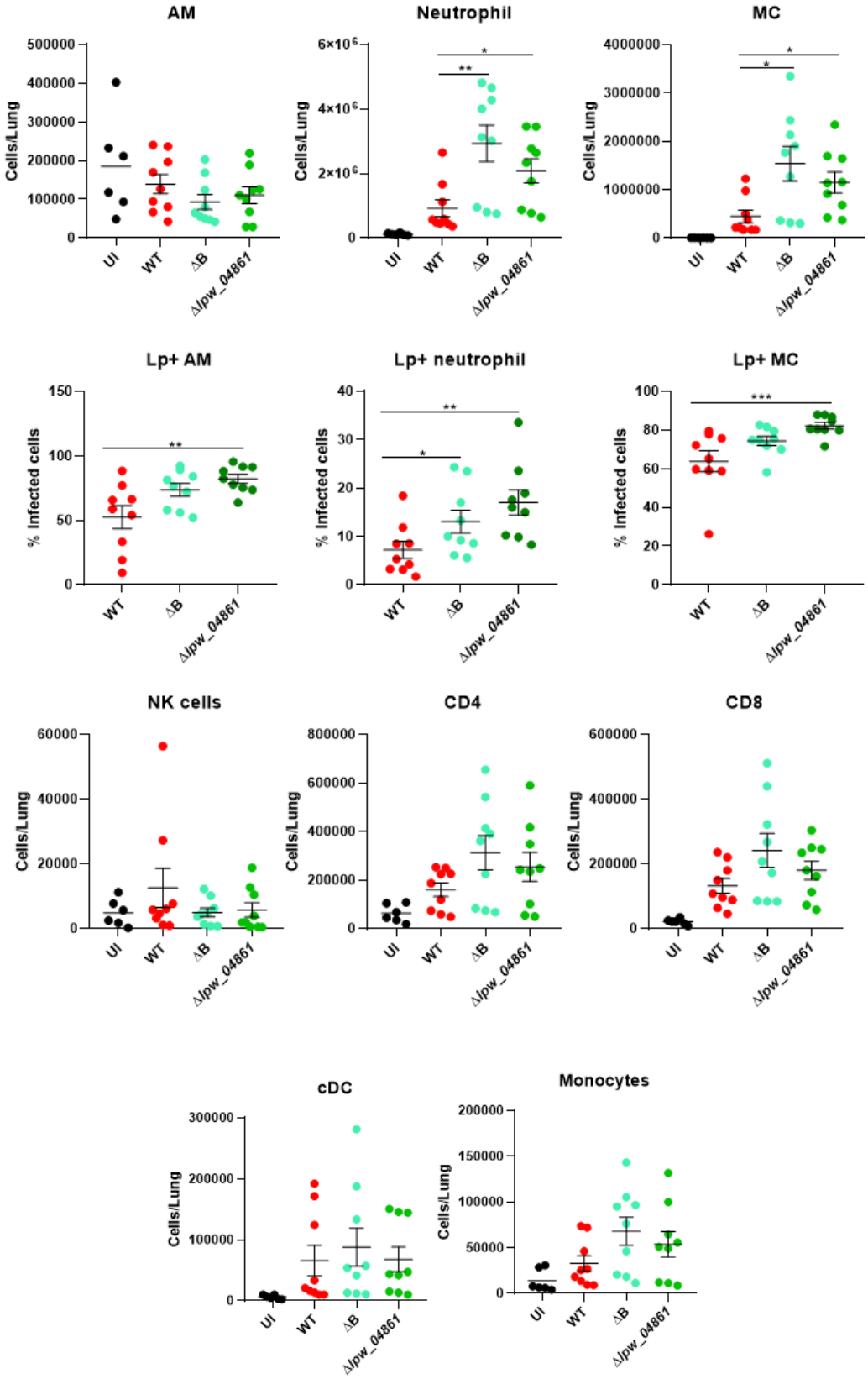
AM
Neutrophil
MC
Cells/Lung
500000
400000
300000
200000
100000
0
6×10^6
4×10^6
2×10^6
4000000
3000000
2000000
1000000
UI
WT
ΔB
Δlpw_04861
*
**
Lp+ AM
Lp+ neutrophil
Lp+ MC
% Infected cells
150
100
50
40
30
20
10
***
NK cells
CD4
CD8
60000
40000
20000
800000
600000
400000
200000
cDC
Monocytes
300000
150000

Figure 4.8. Infection with ΔB induced an increase in lung phagocyte infiltrate.

At day 3 after infection, left lung was harvested, minced, stained with the appropriate antibody, and analyzed using flow cytometry. Each dot represents one animal. Data was pooled from 2 independent cohorts. Mean +/- SEM is represented by the lines. Statistical significance was performed using Mann-Whitney test (* $p \leq 0.05$, ** $p \leq 0.01$, *** $p \leq 0.001$, **** $p \leq 0.0001$).

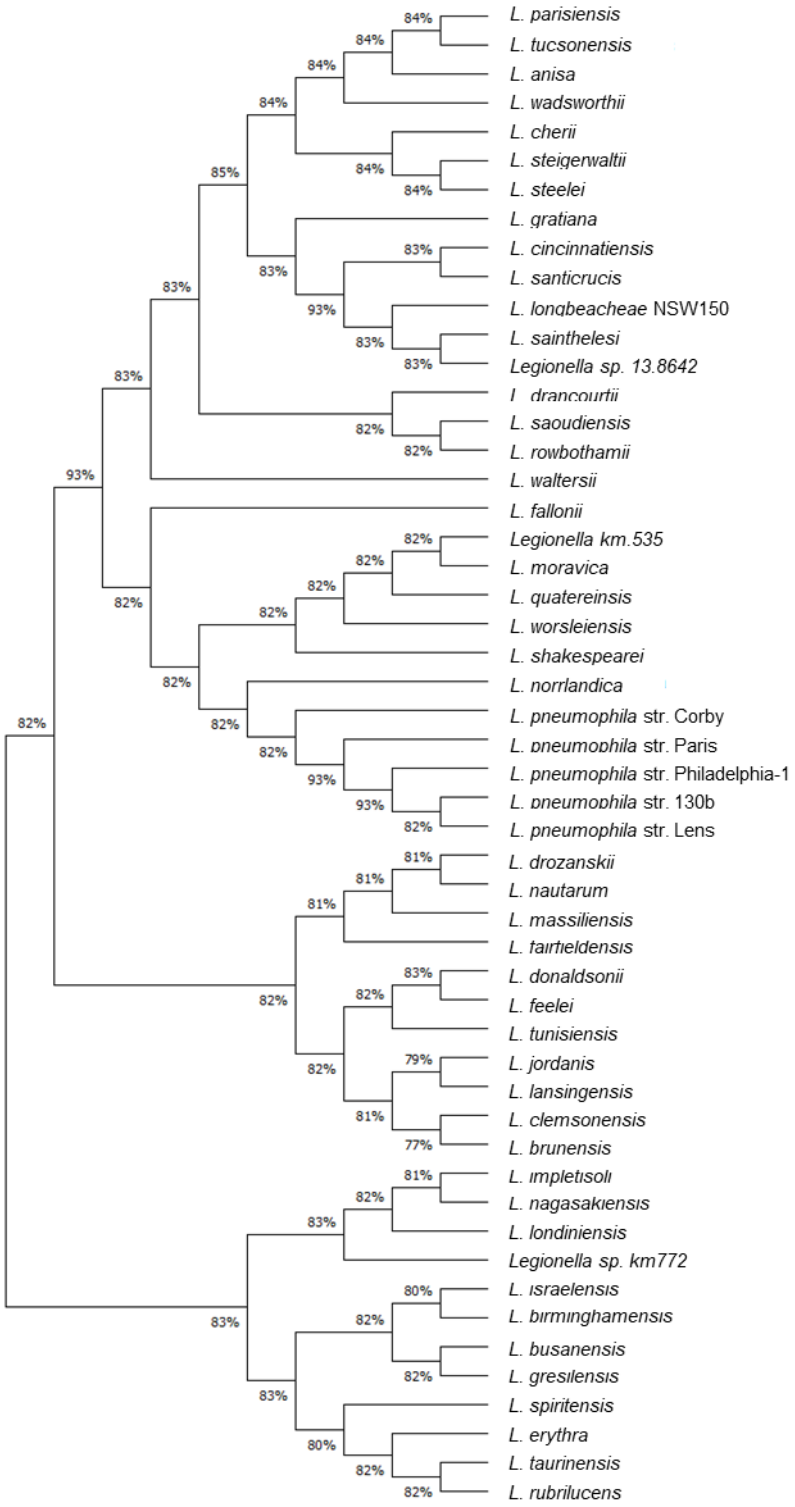
L. parisiensis
L. tucsonensis
L. anisa
L. wadsworthii
L. cherii
L. steigerwaltii
L. steelei
L. gratiana
L. cincinnatiensis
L. santicrucis
L. longbeacheae NSW150
L. sainthelesi
Legionella sp. 13.8642
L. drancourtii
L. saoudiensis
L. rowbothamii
L. waltersii
L. fallonii
Legionella km.535
L. moravica
L. quatereinsis
L. worsleiensis
L. shakespearei
L. norrlandica
L. pneumophila str. Corby
L. pneumophila str. Paris
L. pneumophila str. Philadelphia-1
L. pneumophila str. 130b
L. pneumophila str. Lens
L. drozanskii
L. nautarum
L. massiliensis
L. fairfieldensis
L. donaldsonii
L. feelei
L. tunisiensis
L. jordanis
L. lansingensis
L. clemsonensis
L. brunensis
L. impletisoli
L. nagasakiensis
L. londiniensis
Legionella sp. km772
L. israelensis
L. birminghamensis
L. busanensis
L. gresilensis
L. spiritensis
L. erythra
L. taurinensis
L. rubrilucens

Figure 4.9. Phylogeny of Lpw_04861.

Orthologs of Lpw_04861 amongst *Legionella* genus were identified using BLASTp. A maximum likelihood phylogenetic tree based on the amino acid sequences of the orthologs of Lpw_04861 was constructed using the software MEGA X. The percentage of trees in which the associated taxa clustered together is shown next to the branches (Bootstrap=500).

A.

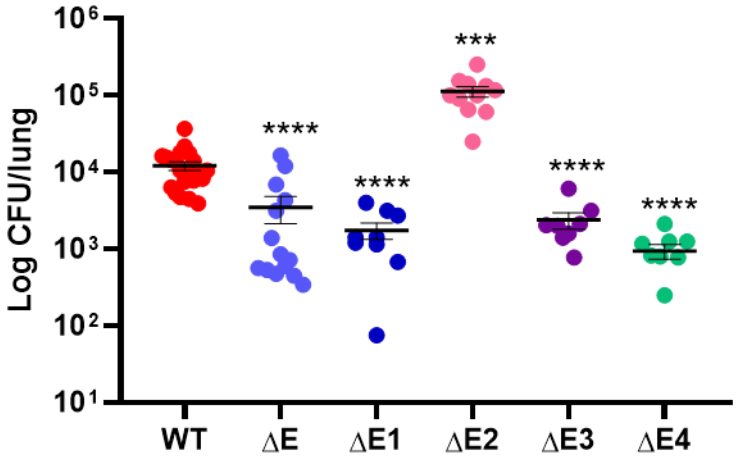
Log CFU/lung
10^6
10^5
10^4
10^3
10^2
10^1
***
****
****
****
****
WT
ΔE
ΔE1
ΔE2
ΔE3
ΔE4

B.

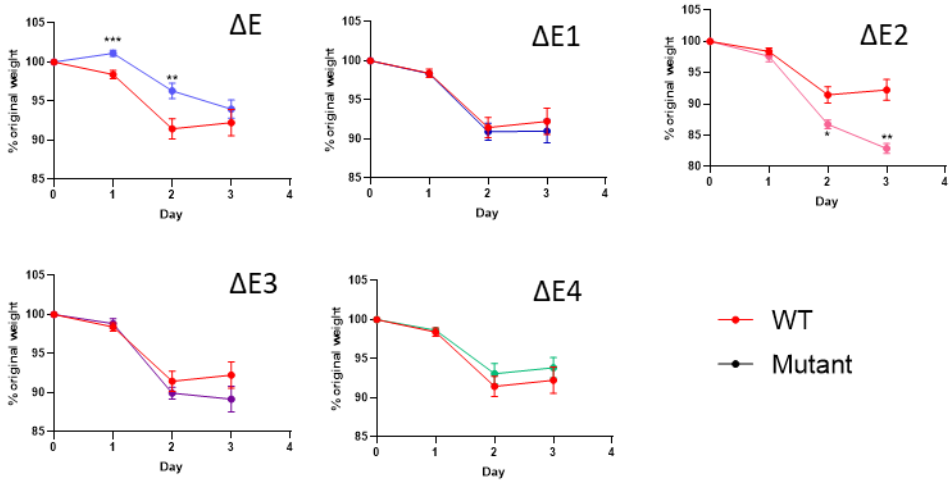
ΔE
ΔE1
ΔE2
ΔE3
ΔE4
% original weight
Day
WT
Mutant

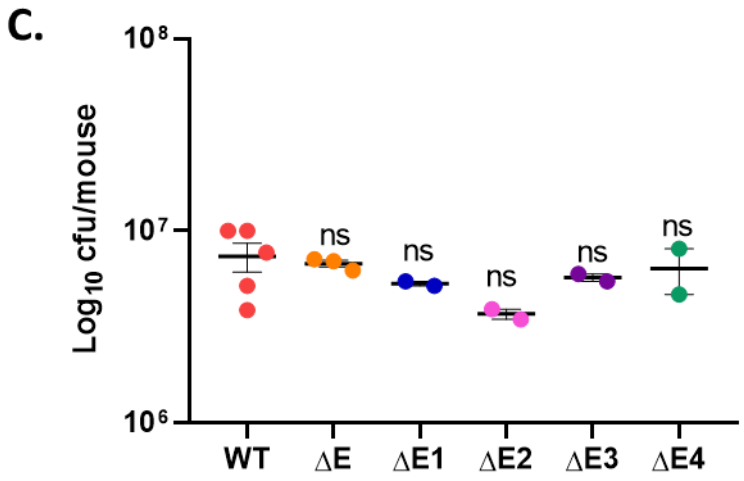

Figure 4.10. Regions E1, E3, and E4 were important for bacterial survival in lungs.

(A) At day 3 post-intranasal infection, mouse lungs were harvested. Bacterial CFU from A-strain lungs at day 3 after intranasal infection was then enumerated. Each dot represents data from one animal. Data was pooled from at least 3 independent experiments. (B) Weight of mice after infection. Each point represents the mean +/- SEM of weight during the corresponding time point ($N \geq 8$). (C) Bacteria used to inoculate mice were retrospectively plated, and CFU was enumerated. Each dot represents data from one independent experiment. Data from at least 2 independent experiments are presented. Statistical significance was determined using Mann-Whitney test. Unless otherwise indicated, asterisks indicate the statistical significance compared to WT (* $p \leq 0.05$, ** $p \leq 0.01$, *** $p \leq 0.001$, **** $p \leq 0.0001$).

A.

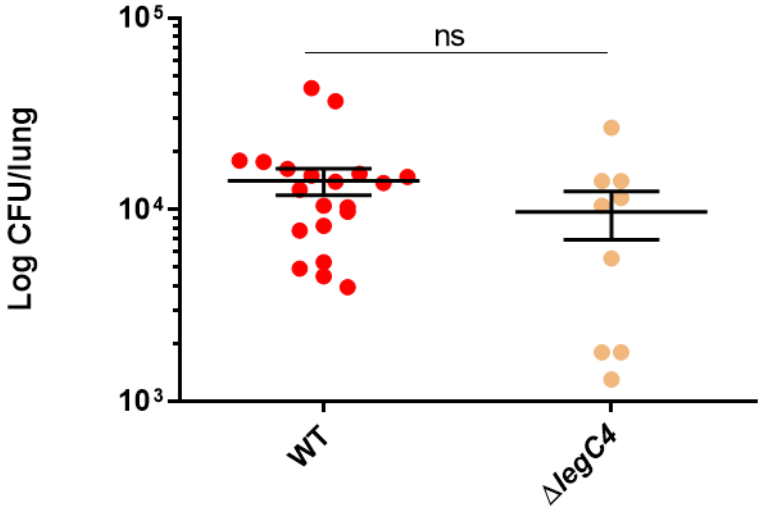
ns
Log CFU/lung
10^5
10^4
10^3
WT
ΔlegC4

B.

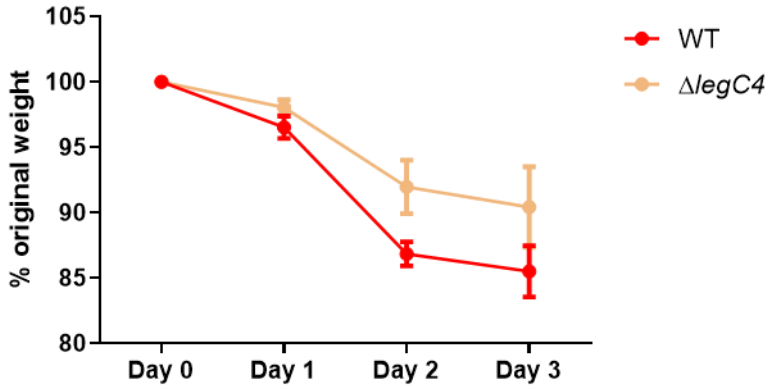
% original weight
105
100
95
90
85
80
Day 0
Day 1
Day 2
Day 3
WT
ΔlegC4

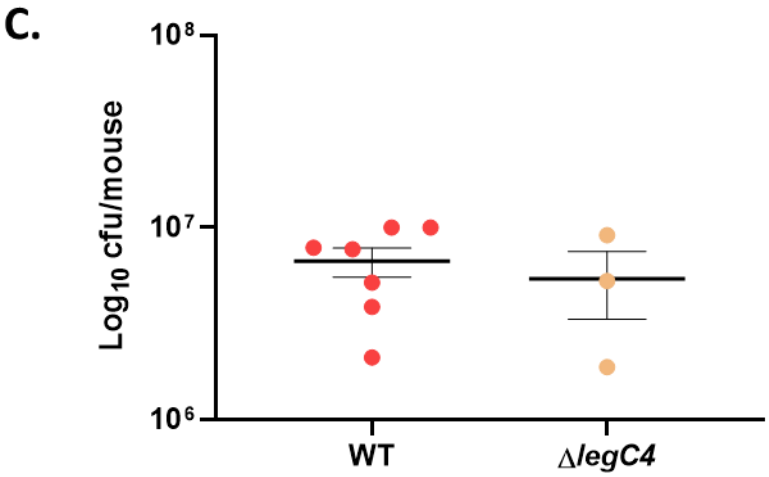

Figure 4.11. LegC4 did not alter *L. pneumophila* survival at day 3 post-infection in A-strain mice.

(A) At day 3 post-intranasal infection, mouse lungs were harvested. Bacterial CFU from A-strain lungs at day 1 and day 3 after intranasal infection was then enumerated. Each dot represents data from one animal. Data was pooled from at least 2 independent experiments. (B) Weight of mice after infection. Each point represents the mean +/- SEM of weight during the corresponding time point ($N \geq 6$). (C) Bacteria used to inoculate mice were retrospectively plated, and CFU was enumerated. Each dot represents data from one independent experiment. Data from at least 2 independent experiments are presented. Statistical significance was determined using Mann-Whitney test (* $p \leq 0.05$, ** $p \leq 0.01$, *** $p \leq 0.001$, **** $p \leq 0.0001$).

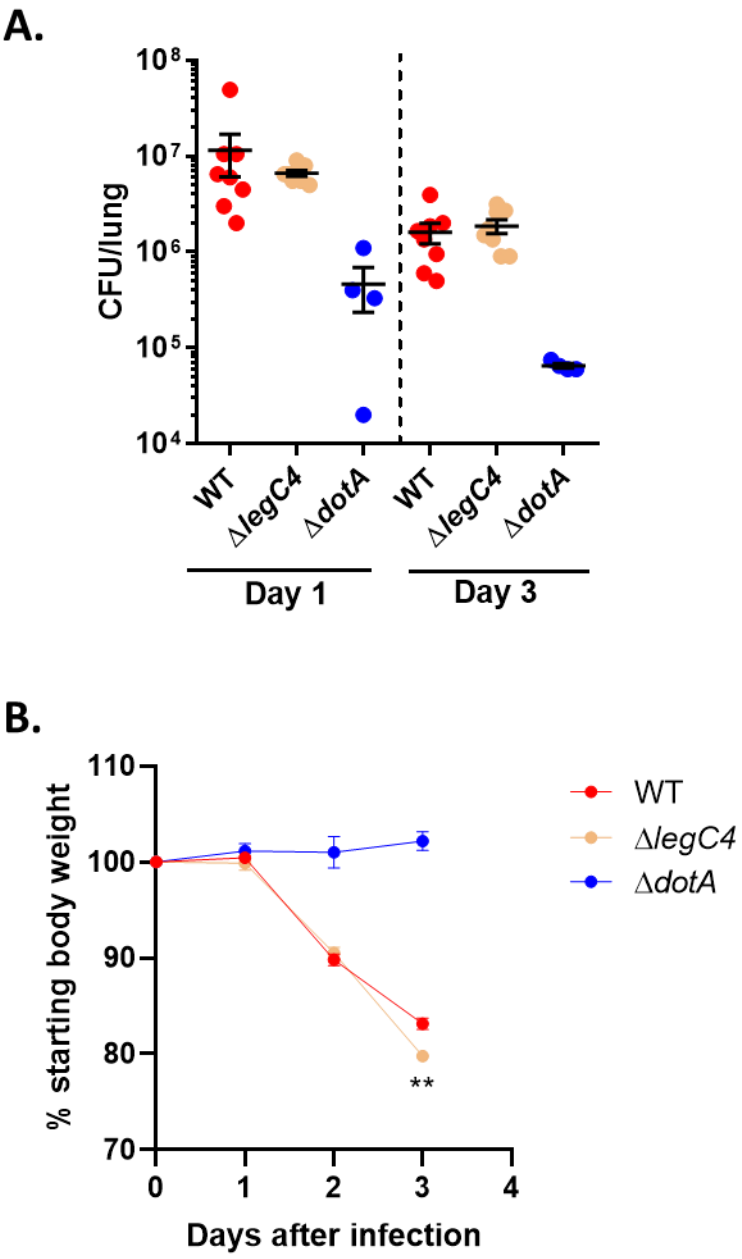
A.
CFU/lung
10^8
10^7
10^6
10^5
10^4
WT
ΔlegC4
ΔdotA
WT
ΔlegC4
ΔdotA
Day 1
Day 3
B.
% starting body weight
110
100
90
80
70
0
1
2
3
4
Days after infection
**
WT
ΔlegC4
ΔdotA

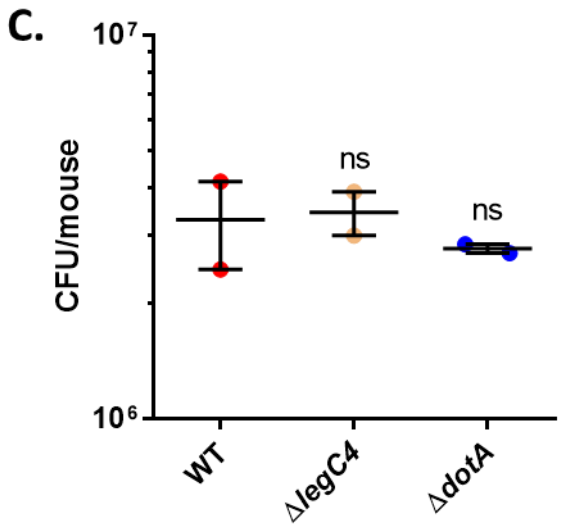

Figure 4.12. LegC4 did not alter aflagellated *L. pneumophila* survival in WT C57BL/6 mice

(A) At day 3 post-intranasal infection, mouse lungs were harvested. Bacterial CFU from WT mice lungs at day 1 and day 3 after intranasal infection was then enumerated. Each dot represents data from one animal. Data was pooled from at least 2 independent experiments. (B) Weight of mice after infection. Each point represents the mean +/- SEM of weight during the corresponding time point ($N \geq 6$). (C) Bacteria used to inoculate mice were retrospectively plated, and CFU was enumerated. Each dot represents data from one independent experiment. Statistical significance was determined using Mann-Whitney test (* $p \leq 0.05$, ** $p \leq 0.01$, *** $p \leq 0.001$, **** $p \leq 0.0001$).

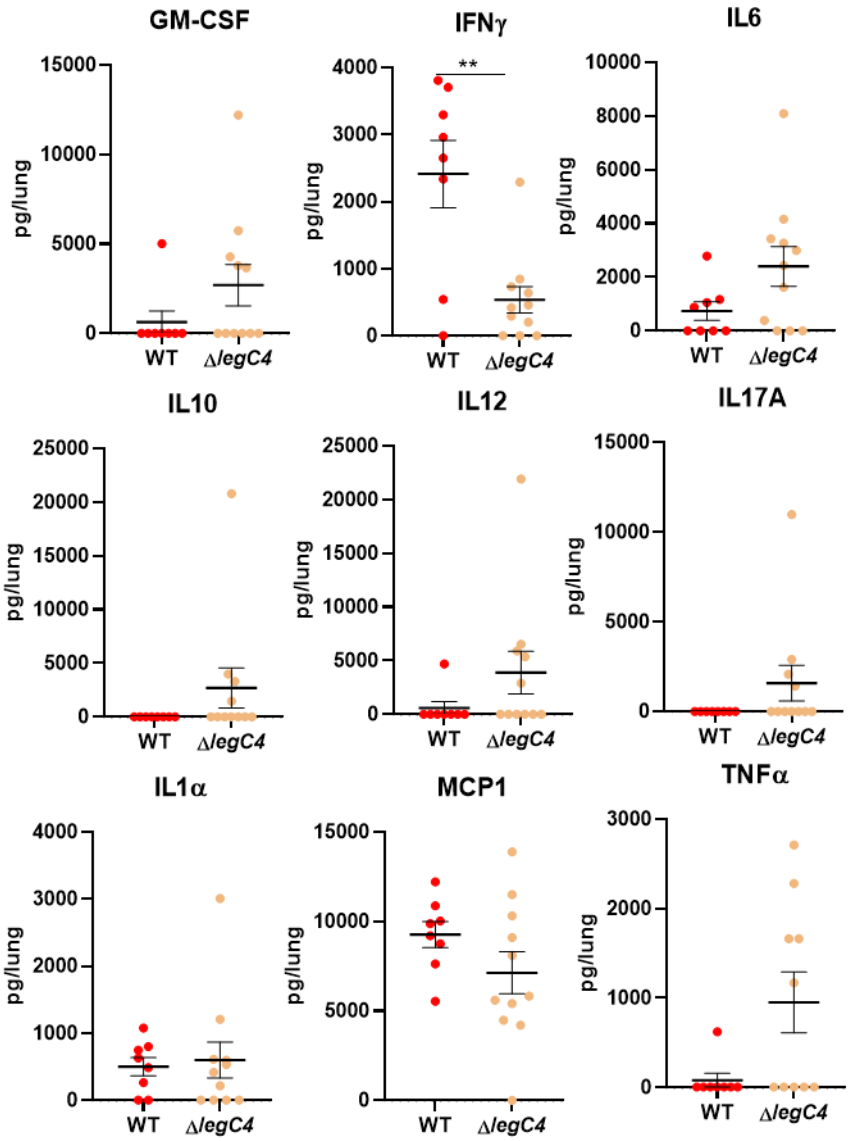

Figure 4.13. LegC4 enhanced host IFNγ production during infection of A-strain mice.

At day 3 after infection, either the right lung or both lungs were harvested and homogenised. Lung homogenates were then analysed using CBA flex kit. When only one lung is used, number was multiplied by 2 to account for both lungs. Each dot represents one animal. Data was pooled from at least 2 independent cohorts. Mean +/- SEM is represented by the lines. Statistical significance was performed using Mann-Whitney test (* $p \leq 0.05$, ** $p \leq 0.01$, *** $p \leq 0.001$, **** $p \leq 0.0001$).

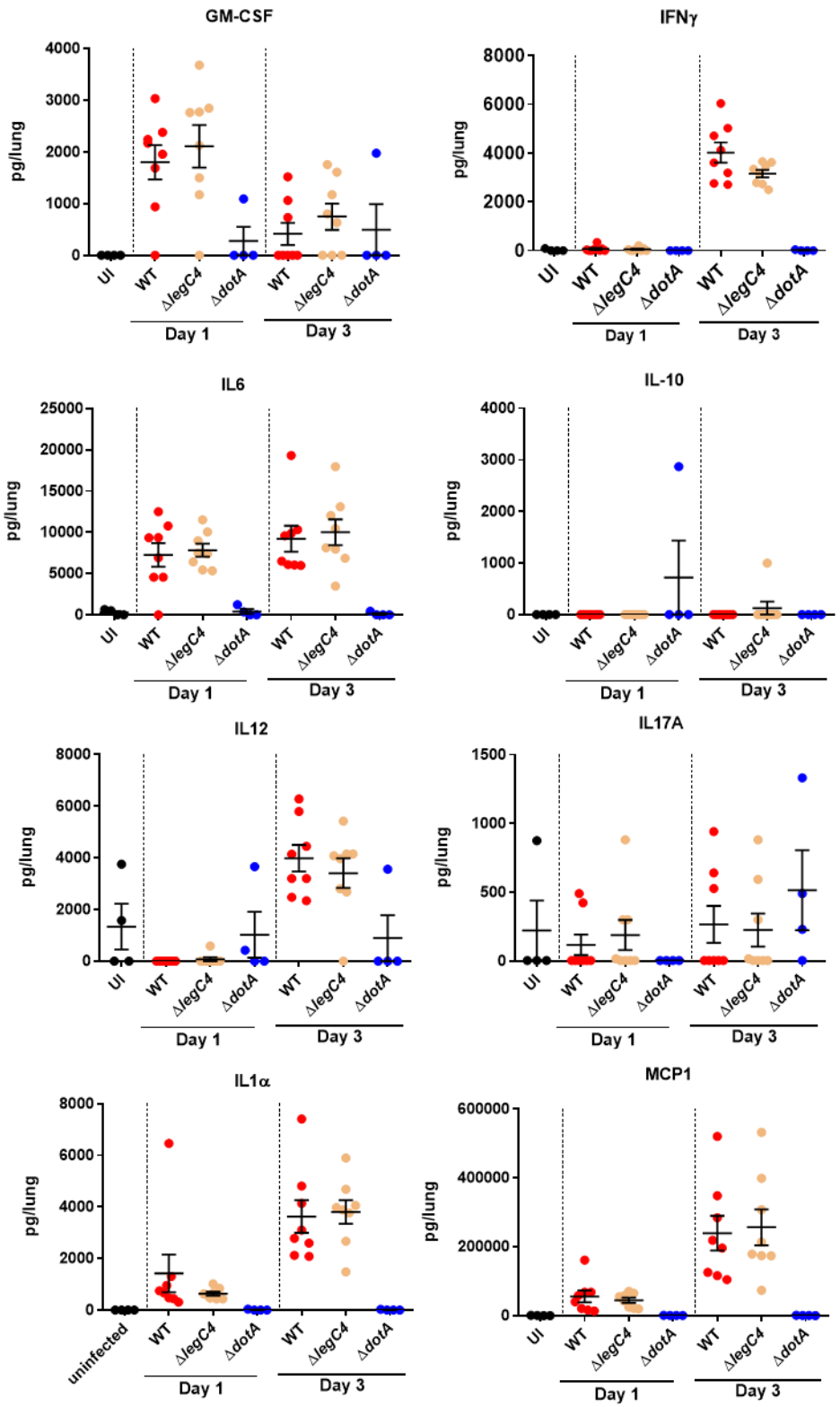
GM-CSF
pg/lung
4000
3000
2000
1000
0
UI
WT
ΔlegC4
ΔdotA
Day 1
Day 3
IFNγ
8000
6000
4000
2000
IL6
25000
20000
15000
10000
5000
IL-10
IL12
IL17A
1500
1000
500
IL1α
MCP1
600000
400000
200000
uninfected

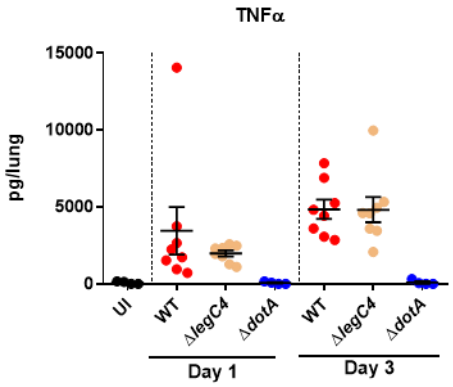

Figure 4.14. LegC4 did not influence host cytokine production during infection of WT C57BL/6 mice

At day 3 after infection, either the right lung or both lungs were harvested and homogenated. Lung homogenates were then analysed using CBA flex kit. When only one lung is used, number was multiplied by 2 to account for both lungs. Each dot represents one animal. Data was pooled from at least 2 independent cohorts. Mean +/- SEM is represented by the lines. Statistical significance was performed using Mann-Whitney test (* $p \leq 0.05$, ** $p \leq 0.01$, *** $p \leq 0.001$, **** $p \leq 0.0001$).

Chapter 5
Characterization of the *Legionella pneumophila* Dot/Icm T4SS-effector protein LegC4

5.1 Introduction

L. pneumophila infection has a major impact on the host transcriptome, resulting in a global increase in expression of various immune signaling pathways, consistent with activation of an immune response to infection (296, 375, 376). However, *L. pneumophila* infection also downregulates the expression of some genes involved in processes such as transcription, translation, and metabolism (375, 376). The Dot/Icm T4SS effectors may partly be responsible for the changes in host transcriptome, as three Dot/Icm effectors, SnpL, LegK7, and AnkH, have been described to increase host transcription (340, 377, 378). In contrast, another effector, RomA, represses the host transcriptional response (379). SnpL binds to the host DRB (5,6-dichloro-1-β-D-ribofuranosylbenzimidazole) sensitivity-inducing factor (DSIF) complex component Suppresor of Ty5 (SUPT5H), resulting in a global induction of host transcription and increased host cell death (340), although the connection between transcriptional induction and cell death is unclear. On the other hand, LegK7 alters the host transcriptional profile by mimicking the Hippo pathway kinase MST1 (378), involved in cell proliferation and development (380). LegK7 phosphorylates the Hippo protein MOB1, leading to the degradation of transcription regulators TAZ and YAP1 which alters the expression of genes regulated by the transcription factor PPARγ (378). AnkH interacts with host nuclear La-related protein 7 (LARP7), a component of the 7SK snRNP complex, which pauses transcription elongation by binding to to host transcription elongation factor P-TEFb (377). LARP7 prevents the degradation of 7SK snRNP by binding to the U-rich region (381-385). AnkH binding to LARP7 prevents the association with 7SK snRNP, to increase global transcription (377). Finally, the Dot/Icm effector RomA (Lpp1683) represses host transcription by the methylation of K14 in histone H3 (H3K14) via the SET domain. This modification affected a broad range of host promoters, suggesting a global repression of transcription (379). In contrast, a homolog of RomA, LegAS4, interacted with ribosomal DNA (rDNA) and increased the transcription of rRNA (386). The discrepancy in these findings has not yet been explained.

In this chapter, we describe a novel role for the *Legionella* effector protein LegC4 in altering the macrophage transcriptome during infection. We initially observed that WT *L. pneumophila* downregulated host *GAPDH* mRNA expression during infection in a Dot/Icm T4SS-dependent manner. Using the large genomic region mutants described in Chapters 3 and 4, we ultimately identified a single gene, *legC4*, which was required to downregulate host *GAPDH* mRNA. RNA sequencing analysis revealed that LegC4 downregulated a broader subset of host mRNAs that are highly enriched for enzymes, including *GAPDH*, involved in glycolysis and related metabolic pathways.

5.2 Results

5.2.1 LegC4 downregulates host GAPDH mRNA levels during L. pneumophila infection.

While measuring levels of *GAPDH* mRNA as a control for QRT-PCR, we unexpectedly observed that WT *L. pneumophila* infection of THP1 macrophages resulted in a significant decrease in host *GAPDH* mRNA expression compared to unifected (UI) and Δ*dotA* infected cells. At 6 h post-infection, *GAPDH* mRNA levels were determined by QRT-PCR and analysed by either agarose-gel electrophoresis (**Figure 5.1A**) or qPCR (**Figure 5.1B**) using β-actin mRNA as housekeeping gene control. This suggested that WT *L. pneumophila* inhibits *GAPDH* mRNA expression during infection in a Dot/Icm T4SS-dependent manner. Using the large genomic region deletion mutants strains of *L. pneumophila* previously described in chapter 3, we demonstrated that the ΔE mutant strain, reverted *GAPDH* mRNA expression to the levels observed in UI or *ΔdotA*-infected cells, suggesting that genes within this region of the genome were responsible for this phenotype (**Figure 5.1**). Infection with ΔG mutant also led to an increase in the *GAPDH* mRNA expression level, however, this phenotype is not always reproducible. In one out of three independent repeats, ΔG infection led to similar level of *GAPDH* mRNA to WT-infected cells (data not shown). Therefore, we decided to focus on identifying the gene whose deletion leads to the lack of *GAPDH* mRNA downregulation in ΔE mutant by creating sub-deletion mutants. Subsequent sub-deletions within genomic region E were then introduced into the *L. pneumophila* genome *(*ΔE2 and ΔE2-2) that ultimately

identified a single gene deletion, Δ*legC4*, sufficient to revert this phenotype (**Figure 5.2, Table 5.1**).

To confirm this phenotype, trans-complementation was performed by introducing a LegC4 protein expression plasmid (pMMB207c_4xHA:*legC4*) into the Δ*legC4* mutant strain. This strain was then used to infect THP-1 macrophages and the relative level of *GAPDH* mRNA was determined using QRT-PCR as above. Expression of LegC4 was sufficient to confer downregulation of *GAPDH* mRNA in the Δ*legC4* strain to levels observed in the WT strain (**Figure 5.3**). Together these data strongly suggest that the putative Dot/Icm effector LegC4 is responsible for the downregulation of host *GAPDH* mRNA during *L. pneumophila* infection.

5.2.2 GAPDH mRNA downregulation was not due to decreased bacterial fitness

It may be argued that the inability of Δ*legC4 L. pneumophila* to induce *GAPDH* mRNA degradation may be caused by a reduction in bacterial numbers during infection. Therefore, to examine the fitness of the Δ*legC4* strain, bacterial numbers during infection at 3h, 6h, 24h, and 48h post-infection were enumerated. At all timepoints tested, Δ*legC4* displayed similar bacterial load to WT *L. pneumophila* (**Figure 5.4**), suggesting that the deletion of *legC4* did not impair bacterial fitness and replication kinetics in THP1 macrophages.

5.2.3 LegC4 is translocated by the Dot/Icm T4SS into the host cytosol

LegC4 was previously predicted to be a Dot/Icm T4SS effector protein (339). To confirm the translocation of LegC4 translocation via the Dot/Icm T4SS and examine the sub-cellular localisation, 4xHA-epitope-tagged LegC4 (pMMB207c_4xHA:*legC4*) was introduced into both WT or Δ*dotA L. pneumophila* strains and used to infect THP-1 macrophages. At 6 h post-infection, THP1 macrophages were fixed and stained for LegC4 (anti-HA) and *L. pneumophila* (anti-*L. pneumophila*) as well as the cell nucleus stain (Hoescht) and analysed by confocal microscopy (**Figure 5.5**).

Infection by strains carrying the empty pMMB207c_4xHA led to the colocalisation of HA signal with the bacteria, suggesting the lack of translocation of HA peptide (**Figure 5.5**). Similarly, during infection by Δ*dotA L. pneumophila* carrying the 4xHA-tagged LegC4, HA-tagged LegC4 co-localised with the bacteria (**Figure 5.5**). In contrast, during infection by WT *L. pneumophila,* 4xHA-tagged LegC4 showed a diffuse staining pattern in the cytosol of THP1 macrophages (green) suggesting that it is translocated into the host cell cytosol (**Figure 5.5**). Interestingly, 4xHA-tagged LegC4 did not show strong accumulation to the nucleus (**Figure 5.5**), suggesting LegC4 may also modulates *GAPDH* gene expression in another cell compartment.

5.2.4 Bioinformatics analysis of LegC4

Bioinformatics analysis was employed to understand how LegC4 may cause the downregulation of host *GAPDH* mRNA. Using Blastp against non-*Legionella spp* genomes, no homolog was found. Domain prediction using InterPro Scan web server against all available databases revealed the presence of a coiled-coil motif near the C terminus (322). However, there is no domain predicted, suggesting the absence of known conserved domain. Structural homology prediction was then employed using HHPred web-server, which predicted the presence of an ankyrin domain at residues 380 to 744 with a ~95% confidence (325). Ankyrin domain is generally involved in protein-protein interaction, and can be associated with multiple distinct functions (387). As such, basic bioinformatics alone cannot reveal the mechanism of *GAPDH* mRNA downregulation by LegC4, suggesting that LegC4 may possess a novel domain.

5.2.5 LegC4 alters the host cell transcriptome during infection

Our data suggested that LegC4 downregulated *GAPDH* mRNA but not other mRNAs such as *ACTB* (β-actin) used as a control in these experiments (**Figure 5.1**). We therefore wanted to understand whether LegC4 specifically targets *GAPDH* mRNA expression or if it modulates the expression of a broader subset of host genes. To detect changes in the host transcriptome, RNA sequencing was performed on THP1 cells infected with WT *L. pneumophila,* as well as Δ*dotA*, ΔE, and Δ*legC4* mutant strains.

At 6 h post-infection, RNA was extracted from infected cells and purified prior to poly-adenylated RNA enrichment and RNA sequencing. The *Homo sapiens* genome was used to align the trimmed reads. Principal component analysis (PCA) plot was used to summarise and visualise the general similarities and differences between samples in each replicate (388). The data points clustered by sample type, instead of replicate, suggesting the reproducibility of the three replicates (**Figure 5.6A**). The gene expression of WT-, ΔE-, and Δ*legC4*-infected cells clustered together, whereas Δ*dotA*-infected samples were segregated, showing that gene expression of Δ*dotA*-infected cells was different compared to WT-, ΔE-, and Δ*legC4*-infected cells (**Figure 5.6A**). To clarify the differences between WT, ΔE, and Δ*legC4*, Δ*dotA* sample was excluded from the subsequent analysis. WT-infected samples were segregated from ΔE- and Δ*legC4*-infected samples, suggesting possible alteration of gene expression that depended on LegC4 (**Figure 5.6A**).

To identify genes that were differentially expressed, differential expression analysis was then performed for Δ*dotA*, ΔE or Δ*legC4* mutant strains versus WT *L. pneumophila* using the DeSeq2 R-package (313) and measured as $\log_2$ fold change (LFC) with a cut-off of $-1 \leq \text{LFC} \leq 1$. Statistical *p*-values were adjusted using the Benjamini-Hochberg method (PADJ), and samples with a PADJ value of less than 0.05 were considered significant. As summarised in the volcano plots (**Figure 5.6B**), 2526 genes were upregulated during infection by Δ*dotA*, compared to WT-infected cells, and 2695 genes were downregulated. In contrast, compared to WT-infected cells, the large genomic region mutant ΔE upregulated only 77 genes and downregulated two genes, and the Δ*legC4* mutant strain upregulated 91 genes and downregulated one gene (**Figure 5.6B**). *GAPDH* is included amongst the 91 upregulated genes in the Δ*legC4* mutant strain (LFC=1.80, PADJ=3.55×10^{-183}), thus supporting our earlier results. The observation that the Δ*legC4* and ΔE mutant strains primarily upregulated gene expression compared to WT-infected cells was consistent with a role for LegC4 in downregulating gene expression as observed for *GAPDH* mRNA above.

To identify the subset of genes regulated by LegC4 with a high degree of confidence, the 91 genes upregulated in Δ*legC4*-infected cells were compared to genes upregulated in both ΔE and Δ*dotA*-infected cells. As shown in the Venn diagram (**Figure 5.6C**), this

analysis identified 50 genes, including *GAPDH*, that were upregulated in each of the three mutant samples (Δ*dotA*, ΔE, and Δ*legC4*) compared to WT *L. pneumophila* infection. These 50 genes are listed in **Table 5.2**. Notably, the only gene that was downregulated in Δ*legC4*-infected cells, *RNU6-2*, was also downregulated in ΔE and Δ*dotA*-infected cells, strongly suggesting that LegC4 increases the expression of this gene (**Figure 5.6C, Table 5.2**). Together, these data indicate that WT *L. pneumophila* downregulates the expression of at least 50 host genes and upregulates the expression of one host gene in a LegC4-dependent manner.

5.2.6 LegC4 downregulates genes involved in glucose metabolism

To understand the biological impact of the downregulation of genes by LegC4, the 50 genes that were upregulated during Δ*legC4*, ΔE, and Δ*dotA* infection were subjected to gene ontology (GO) analysis. Using the PANTHER gene list analysis (389), approximately 70% of the genes were categorised into metabolic processes. In addition, 21.1% of these genes were involved in glycolysis (**Figure 5.7A**). Consistently, gene ontology (GO) term enrichment analysis using GO::Term Finder platform (316) also revealed enrichment for glycolysis, gluconeogenesis, pyruvate metabolism, ATP generation, and NAD metabolism (**Figure 5.7B**).

To further analyse the role of these genes, a heatmap of the $\log_2$ fold change (LFC) values of these genes in Δ*legC4*- compared to WT-infected cells was superimposed on the canonical glycolysis pathway adapted from the Kyoto Encyclopedia of Genes and Genomes (KEGG) database (390) (**Figure 5.8**). In mammalian cells, glycolysis generates energy (ATP and NADH) by converting glucose to pyruvate (or lactate) in the cytosol. Pyruvate is then the converted in the mitochondria to acetyl-CoA which enters the TCA cycle to generate more NADH and ATP via oxidative phosphorylation (OXPHOS). Many other metabolites such as amino-acids and nucleic acids are also generated from various intermediates in this pathway.

Six genes encoding enzymes involved in the central glycolysis or gluconeogenesis (reverse of glycolysis) pathways were significantly downregulated by LegC4; *HK1*

(hexokinase-1), *GPI* (glucose-6-phosphate isomerase), *PFK* (phosphofructokinase platelet isoform), *GAPDH*, *PGK1* (phosphoglyceratekinase-1) and *FBP1* (fructose-bisphosphatase-1) (**Figure 5.8, Table 5.2**). Furthermore, four genes encode for enzymes that contribute to the removal of metabolites from the glycolysis pathway, *G6PD* (glucose-6-phosphate dehydrogenase), *PDH* (pyruvate dehydrogenase), *LDH* (lactate dehydrogenase), *PHGDH* (phosphoglycerate dehydrogenase), were also downregulated (**Figure 5.8, Table 5.2**). This clearly showed that LegC4 downregulated the expression of many genes encoding essential enzymes involved in the glycolysis/gluconeogenesis pathway, suggesting that LegC4 is likely to significantly alter glucose metabolism during *L. pneumophila* infection of macrophages.

5.3 Discussion

In macrophages, glucose metabolism influences functionality. Exposure of macrophages (M0) to bacterial-derived LPS causes an increase in glycolysis in the cytoplasm and a reduction of mitochondrial respiration (OXPHOS), resulting in the transition to M1 macrophages which display enhanced anti-microbial and pro-inflammatory response (391). In contrast, anti-inflammatory cytokines such as IL-4 upregulate OXPHOS, resulting in an anti-inflammatory M2 phenotype (392). Therefore, glucose metabolism is not only essential for generating energy and other metabolites within the cell but also the function of immune cells during infection, or immunometabolism.

L. pneumophila induces host glycolysis early during infection of macrophages independent of the Dot/Icm T4SS (393, 394). This process is most likely due to macrophage activation via TLR signalling, as *Myd88*$^{-/-}$*/Nod1*$^{-/-}$*/Nod2*$^{-/-}$ macrophages did not show increased glycolysis during *L. pneumophila* infection, suggesting that macrophages upregulate glycolysis and pro-inflammatory response to the bacteria (394). However, virulent *L. pneumophila* infection resulted in reduced host-cell glycolysis compared to heat-killed or T4SS-deficient mutant, but the effector that contribute to this process is currently unknown (394). It has also been reported that mitochondrial respiration was inhibited in a T4SS-dependent manner during *Legionella* infection, in part

via the Dot/Icm effector MitF, which caused fragmentation of the mitochondria to enhance replication (19).

In this chapter, a reverse-genetic approach was used to define the role of the *L. pneumophila* effector protein, LegC4, and in downregulation of a specific subset of genes encoding enzymes involved in glycolysis and related metabolic pathways. We experimentally confirmed that LegC4 was efficiently translocated into the host cytoplasm in a Dot/Icm-dependent manner. Despite the ability of LegC4 to downregulate host mRNA, no conserved RNA-binding domain was found in the amino acid sequence of LegC4, suggesting that LegC4 may either possess a novel RNA binding motif or act indirectly to mediate the mRNA downregulation.

The downregulation in glycolysis gene mRNA by LegC4 may lead to reduced macrophage glycolysis and subsequent reduction in the pro-inflammatory M1 macrophage phenotypes. However, since the Δ*legC4* null mutant strain was able to proficiently replicate in human and mouse macrophages, LegC4-dependent targeting of glucose metabolism is dispensable for *L. pneumophila* replication within the macrophage host. One study reported that neither the inhibition nor induction of host glycolysis affected *L. pneumophila* replication in murine BMDMs, perhaps suggesting modulation of host glucose metabolism is dispensible for *in vitro* replication (394). However, dampening glycolysis may also affect the functionality of macrophages and subsequent recruitment and activation of other immune cells that aid in the clearance of pathogen (395), and this may be better represented *in vivo* rather than *in vitro*. Despite this, we did not observe any significant replication defect of Δ*legC4* during infection of either A-strain mice or C57BL/6 mice (previously discussed in chapter 4, **Figure 4.11, 4.12**). Hence the functional importance of LegC4 dampening of glycolysis during *L. pneumophila* infection is unclear. A previous study has shown that transposon disruption of *legC4* (*legC4::Tn*) within aflagellated *L. pneumophila* modestly increased bacterial load during C57BL/6 mouse lung infection. The authors also found that the overexpression of LegC4 modestly enhanced IL-12 production during pulmonary infection of mice (334). While we were unable to reproduce these phenotypes, we found that LegC4 enhanced host IFNγ secretion in A-strain mice, but not C57BL/6 mice (**Figure**

4.13, 4.14). This suggests that LegC4 may increase the pro-inflammatory response during infection and contradicts our hypothesis that LegC4 ineterferes with M1 macrophage activation by dampening host glycolysis. Therefore, to properly evaluate the role of LegC4 during *L. pneumophila* intracellular replication, more studies need to be conducted. Firstly, the downregulation of key glycolytic enzymes should be examined at the protein level. Additionally, the direct measurement of glycolytic activity of infected cells, such as using the Seahorse bioanalyzer or measuring lactate production, is needed to confirm the impact of LegC4 on host glycolysis. Secondly, whether LegC4 alters the macrophage inflammatory phenotype needs to be confirmed, for instance by measuring the level of pro-inflammatory cytokine secretion during infection of macrophages *in vitro*. Finally, whether LegC4 alters the activation status of key IFNγ producers such as NK and T cells should be investigated *in vivo* using flow cytometry.

Another outstanding question is how LegC4 downregulates host gene expression during infection. Although a number of Dot/Icm effector proteins have been shown to directly act on the transcriptional machinery within the host cell nucleus, LegC4 predominantly localised outside the nucleus. This implies that LegC4 is unlikely to target transcription but rather acts on cytosolic mRNA or cytosolic processes that lead to decreased levels of mRNA. Therefore, future studies should elucidate the mechanism of action of LegC4 by examining whether LegC4 directly binds and degrades mRNAs or acts indirectly on certain pathways that result in mRNA downregulation. The intracellular bacterial pathogen *Mycobacterium tuberculosis*, for example, restrains host glycolysis by modulating miRNA-21 (miR-21), a small RNA that regulates one of the central enzymes involved in glycolysis, phosphofructokinase (PFK) (396) (**Figure 5.8**).

In addition to the upregulation of metabolic genes, one gene, *RNU6-2* was downregulated during Δ*legC4* infection, suggesting that WT *L. pneumophila* upregulates this host gene through LegC4. *RNU6-2* encodes for U6 snRNA-2, a small nuclear RNA (snRNA) that belongs to the U6 snRNA family. U6 snRNA is a vital component of the spliceosome that coordinates Mg^{2+} ion to perform the splicing chemistry (397). There are more than 900 U6 snRNA copies in the human genome, but only four are actively transcribed, including U6 snRNA 2 (398, 399). Notably, instead of being poly-adenylated, U6 snRNA has a

short oligo-uridyl (oligo-U) tail (4-7 nucleotides) upon transcription termination (400). As poly-A-tail RNA enrichment was performed before RNA sequencing, this gene should not have been present in the sequenced samples. However, U6 snRNA may be poly-adenylated at the 3' end post-transcriptionally, potentially leading to the degradation of U6 snRNA via the exosome (401, 402). As such, it is possible that instead of increasing the expression of U6 snRNA, LegC4 increased the abundance of poly-adenylated U6 snRNA species, perhaps leading to a reduced abundance of the spliceosome, which may impact splicing and RNA biogenesis. However, none of the other spliceosome components were differentially expressed in Δ*legC4* compared to WT. As such, investigation into the impact of LegC4 on the host spliceosome can be done to further understand this phenotype.

In summary, using the large genomic region deletion mutants, we identified LegC4 as a Dot/Icm effector protein that mediates the downregulation host *GAPDH* mRNA, as well as 90 other genes. The deletion of *legC4* did not result in a significant reduction of replication, which is not surprising for a single Dot/Icm T4SS effector. LegC4 was translocated to the host cell cytosol by the Dot/Icm T4SS, suggesting its potential action in the host cytosol. Of the 91 host genes, there was an enrichment of genes involved in the glycolysis/gluconeogenesis pathway. In addition to these, LegC4 also upregulated a component of the spliceosome complex. These findings may provide clues to the action of LegC4. Overall, while this data is very exciting, more studies are required to understand fully the action and impact of LegC4 during *L. pneumophila* infection.

Table 5.1. Sub-deletions of region E2

Gene	Name	Sub-region
LPW_19981		E2-1
LPW_19991		
LPW_20001		
LPW_20011		
LPW_20021		E2-2
LPW_20031		
LPW_20041	**legC4**	
LPW_20051		
LPW_20061		E2-3
LPW_20071		
LPW_20081		
LPW_20091	**LtpG**	

Genes encoding for Dot/Icm effectors are printed in **bold**.

Table 5.2. List of genes commonly upregulated in Δ*legC4*, ΔE, and Δ*dotA*

Gene Name	Gene description	Δ*legC4*		ΔE		Δ*dotA*	
		LFC	PADJ	LFC	PADJ	LFC	PADJ
GAPDHP72	glyceraldehyde-3-phosphate dehydrogenase pseudogene 72	2.00	2.28E-16	2.13	7.95E-19	1.79	9.98E-15
LDHBP2	lactate dehydrogenase B pseudogene 2	2.00	9.24E-27	1.90	3.30E-24	1.66	3.41E-20
EXOSC5	exosome component 5	1.91	1.45E-24	1.93	3.04E-25	1.76	1.28E-22
FBP1	fructose-bisphosphatase 1	1.91	3.06E-16	1.99	8.36E-18	1.35	2.57E-09
LDHB	lactate dehydrogenase B	1.83	4.11E-84	1.84	1.65E-84	1.55	1.13E-61
SLC25A4	solute carrier family 25 member 4	1.82	1.93E-19	1.73	1.25E-17	1.93	1.10E-24
GAPDH	glyceraldehyde-3-phosphate dehydrogenase	1.80	3.35E-183	1.73	1.45E-169	1.47	1.21E-124
NDUFA9	NADH:ubiquinone oxidoreductase subunit A9	1.74	4.32E-26	1.59	8.09E-22	1.77	4.26E-30
PDHB	pyruvate dehydrogenase E1 beta subunit	1.70	7.41E-87	1.70	1.22E-87	2.09	1.51E-140
PECR	peroxisomal trans-2-enoyl-CoA reductase	1.63	1.81E-12	1.49	2.06E-10	1.21	5.12E-08
PHGDH	phosphoglycerate dehydrogenase	1.59	2.51E-57	1.56	3.51E-55	1.03	2.34E-25
CCT7	chaperonin containing TCP1 subunit 7	1.58	1.21E-180	1.43	2.91E-148	1.57	1.11E-184
IFI27	interferon alpha inducible protein 27	1.56	1.02E-05	1.62	3.48E-06	2.15	4.17E-12
SLC25A5	solute carrier family 25 member 5	1.56	8.24E-167	1.52	4.70E-159	1.24	1.43E-108
IFI27L2	interferon alpha inducible protein 27 like 2	1.56	1.98E-14	1.56	1.26E-14	1.25	1.44E-10
PGK1	phosphoglycerate kinase 1	1.53	1.06E-74	1.46	9.43E-68	1.38	1.77E-62
SLC25A11	solute carrier family 25 member 11	1.53	2.93E-53	1.52	1.13E-52	1.49	1.34E-53
HPRT1	hypoxanthine phosphoribosyltransferase 1	1.50	1.42E-46	1.47	2.06E-44	1.39	4.50E-42
TKFC	triokinase and FMN cyclase	1.46	5.61E-11	1.38	8.98E-10	1.39	2.61E-11
HADH	hydroxyacyl-CoA dehydrogenase	1.46	2.53E-53	1.34	8.86E-45	1.51	7.88E-61
ABCG2	ATP binding cassette subfamily G member 2	1.44	2.16E-10	1.18	5.89E-07	2.36	4.63E-31
ABHD4	abhydrolase domain containing 4	1.43	4.75E-80	1.37	5.64E-73	1.67	7.85E-115

Gene Name	Gene description	Δ*legC4*		ΔE		Δ*dotA*	
		LFC	PADJ	LFC	PADJ	LFC	PADJ
AC010618.1	6-phosphogluconolactonase	1.42	6.75E-28	1.40	3.77E-27	1.14	1.55E-19
ALDH3B1	aldehyde dehydrogenase 3 family member B1	1.40	7.84E-20	1.21	1.38E-14	1.17	1.90E-15
CBR4	carbonyl reductase 4	1.36	1.18E-14	1.11	1.11E-09	2.39	3.65E-52
UNC45A	unc-45 myosin chaperone A	1.34	2.96E-27	1.28	6.73E-25	1.61	1.98E-42
SERHL2	serine hydrolase like 2	1.32	2.12E-17	1.43	1.01E-20	1.70	8.90E-33
JUP	junction plakoglobin	1.32	6.18E-05	1.39	1.60E-05	1.79	3.34E-10
LANCL1	LanC like 1	1.29	2.37E-34	1.17	3.10E-28	2.15	9.88E-105
STOML2	stomatin like 2	1.27	1.01E-55	1.20	4.99E-50	1.52	2.75E-86
LAS1L	LAS1 like, ribosome biogenesis factor	1.25	3.89E-49	1.15	4.37E-41	1.32	7.86E-60
AC006064.4	novel transcript, antisense to GAPDH	1.25	6.50E-04	2.07	1.53E-10	1.52	1.00E-06
SFXN3	sideroflexin 3	1.22	7.40E-51	1.22	3.78E-51	1.42	1.15E-72
G6PD	glucose-6-phosphate dehydrogenase	1.20	1.24E-27	1.07	5.93E-22	1.13	1.60E-26
COPG2	coatomer protein complex subunit gamma 2	1.18	6.24E-22	1.14	8.89E-21	1.58	6.24E-44
PARVA	parvin alpha	1.16	9.43E-23	1.06	3.68E-19	1.26	1.45E-29
UROD	uroporphyrinogen decarboxylase	1.16	8.92E-53	1.12	4.57E-50	1.34	5.31E-77
NT5DC1	5'-nucleotidase domain containing 1	1.15	2.30E-17	1.12	1.28E-16	1.42	1.64E-29
GPI	glucose-6-phosphate isomerase	1.13	8.94E-34	1.04	1.24E-28	1.24	6.17E-43
DCTN2	dynactin subunit 2	1.13	5.08E-60	1.04	1.89E-50	1.16	1.10E-67
MPI	mannose phosphate isomerase	1.12	4.97E-20	1.21	6.94E-24	1.51	1.19E-41
FH	fumarate hydratase	1.11	2.75E-34	1.00	8.79E-28	1.30	3.64E-50
KPNB1	karyopherin subunit beta 1	1.10	9.38E-76	1.01	6.73E-64	1.56	1.51E-158
PYCR2	pyrroline-5-carboxylate reductase 2	1.10	9.60E-45	1.10	3.09E-45	1.48	8.34E-89
HK1	hexokinase 1	1.08	1.62E-08	1.16	5.97E-10	1.74	1.47E-25
NCKAP1L	NCK associated protein 1 like	1.08	6.25E-71	1.08	9.71E-72	1.12	6.78E-79

Gene Name	Gene description	Δ*legC4*		ΔE		Δ*dotA*	
		LFC	PADJ	LFC	PADJ	LFC	PADJ
SLC25A20	solute carrier family 25 member 20	1.06	1.28E-20	1.18	5.15E-26	1.53	3.92E-48
SDSL	serine dehydratase like	1.04	5.98E-08	1.14	1.44E-09	1.22	2.39E-12
FES	FES proto-oncogene, tyrosine kinase	1.00	3.52E-09	1.22	1.45E-13	1.11	1.97E-12
RAP1GDS1	Rap1 GTPase-GDP dissociation stimulator 1	1.00	9.71E-28	1.00	6.73E-28	1.30	3.33E-50

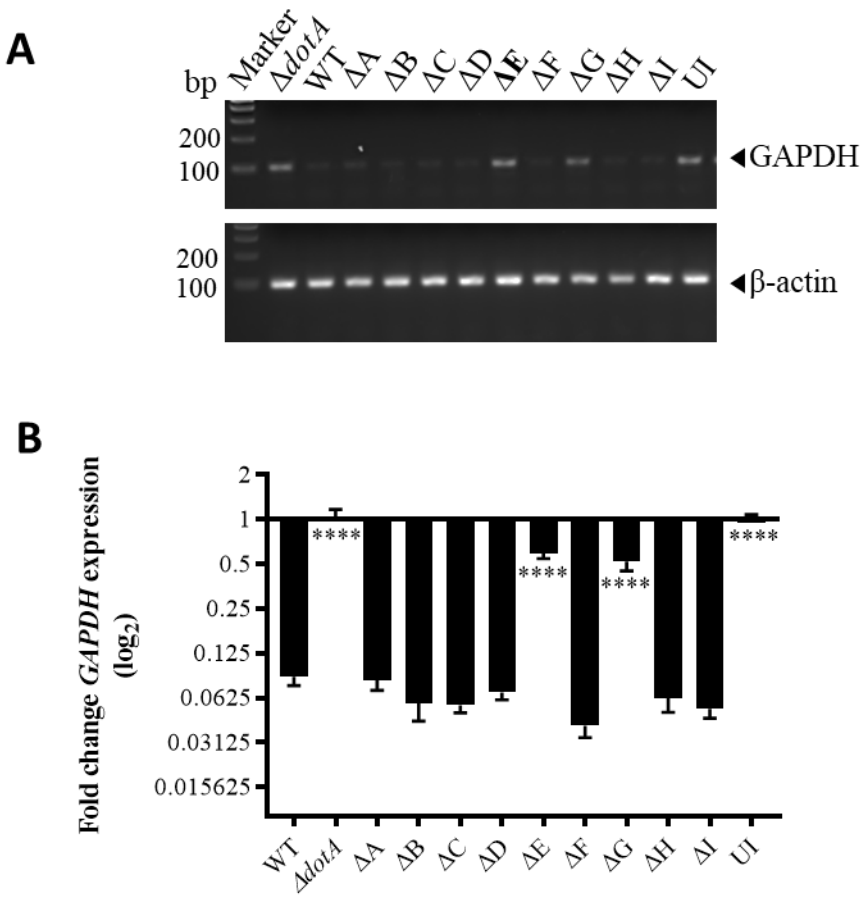

Figure 5.1. Downregulation of host *GAPDH* mRNA during *L. pneumophila* infection.

(A) cDNA from uninfected cells and cells infected with WT or mutant strains were amplified using either *GAPDH* or β-actin primers. PCR product was run on 3% agarose gel and visualized. Image is representative of 3 independent repeats. (B) Level of *GAPDH* mRNA quantified using QRT-PCR. Data was normalized using β-actin as housekeeping gene control. Bars represent mean +/- SEM. Statistical significance was determined by one-way ANOVA, with multiple comparison performed against WT (* $p < 0.05$, ** $p < 0.01$, *** $p < 0.001$, **** $p < 0.0001$).

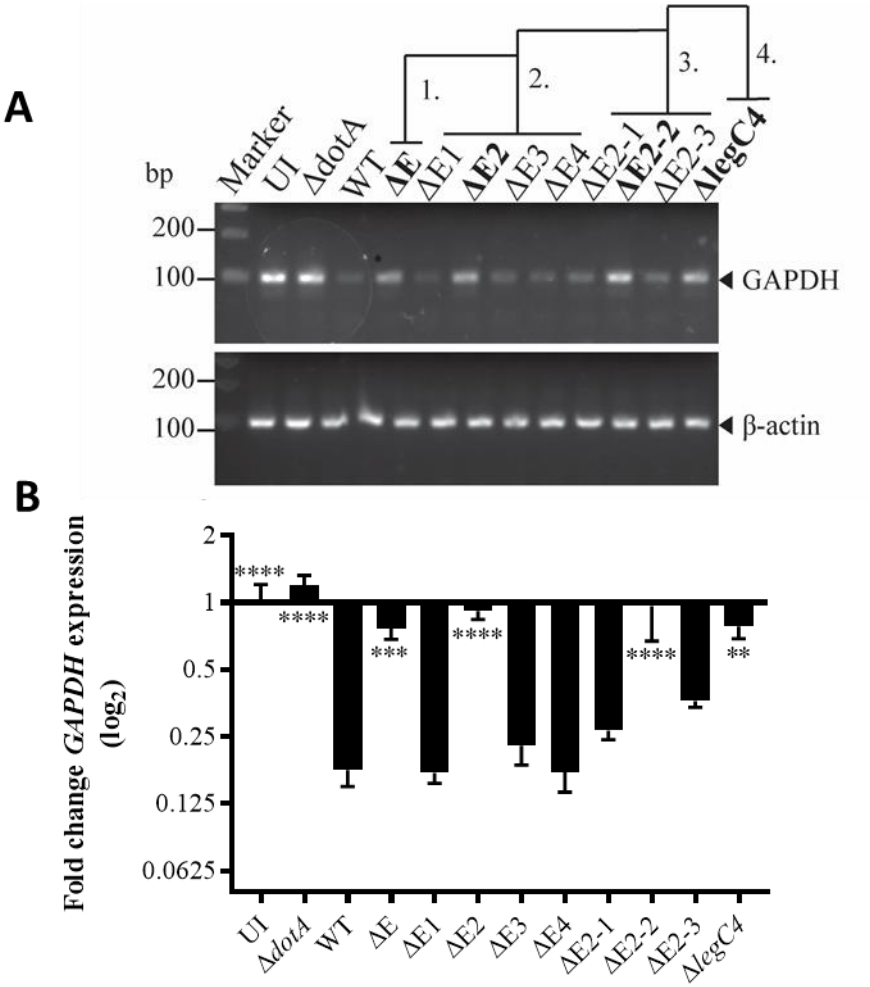

Figure 5.2. LegC4 downregulates host *GAPDH* mRNA during infection.

(A) cDNA from uninfected cells and cells infected with WT or mutant strains were amplified using either *GAPDH* or β-actin primers. PCR product was run on 3% agarose gel and visualized. Image is representative of 3 independent repeats. Numbers on top of the figure indicates the hierarchy of sub-deletion mutants. First, the entire region E was deleted (1). Second, region E is divided into four regions E1, E2, E3, and E4 (2). Third, region E2 was divided into three regions E2-1, E2-2, and E2-3 (3). Finally, a single gene from region E2-2 was deleted (4). (B) Level of *GAPDH* mRNA quantified using quantitative RT-PCR (qRT-PCR). Data was normalized using β-actin as housekeeping gene control. Bars represent mean +/- SEM. Statistical significance was determined by one-way ANOVA with multiple comparison against WT (* $p < 0.05$, ** $p < 0.01$, *** $p < 0.001$, **** $p < 0.0001$).

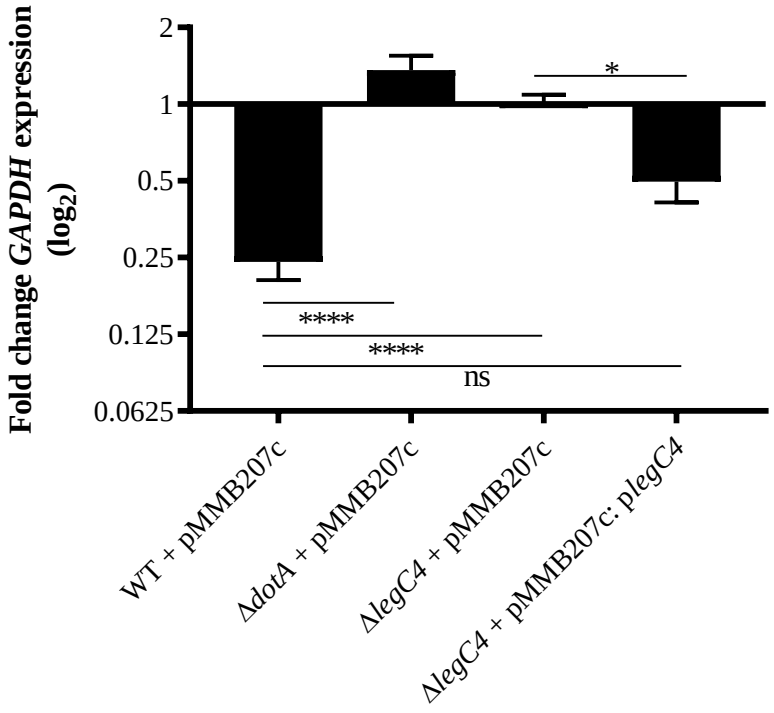

Figure 5.3. Trans-complementation of LegC4 rescued *GAPDH* downregulation phenotype.

Level of *GAPDH* mRNA in cells infected with WT, Δ*dotA*, Δ*legC4*, and Δ*legC4* expressing plasmid-borne *legC4* determined by qRT-PCR. Data was normalized to β-actin as housekeeping gene control. Log_2 fold change of expression compared to uninfected samples were plotted. Bars represent mean +/- SEM, and statistical significance was determined using one-way ANOVA (* $p < 0.05$, ** $p < 0.01$, *** $p < 0.001$, **** $p < 0.0001$).

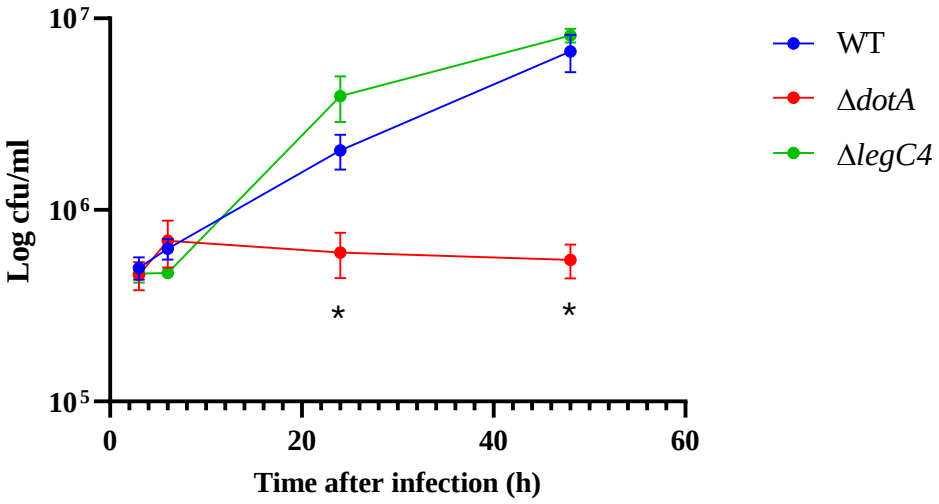

Figure 5.4. Δ*legC4* efficiently replicates in THP1 macrophages.

Bacterial CFU was quantified after infection of THP1 macrophages at 3 h, 6 h, 24 h, and 48 h post-infection. Each data point represents mean +/- SEM, and statistical significance was determined using unpaired t-test (* $p < 0.05$, ** $p < 0.01$, *** $p < 0.001$, **** $p < 0.0001$).

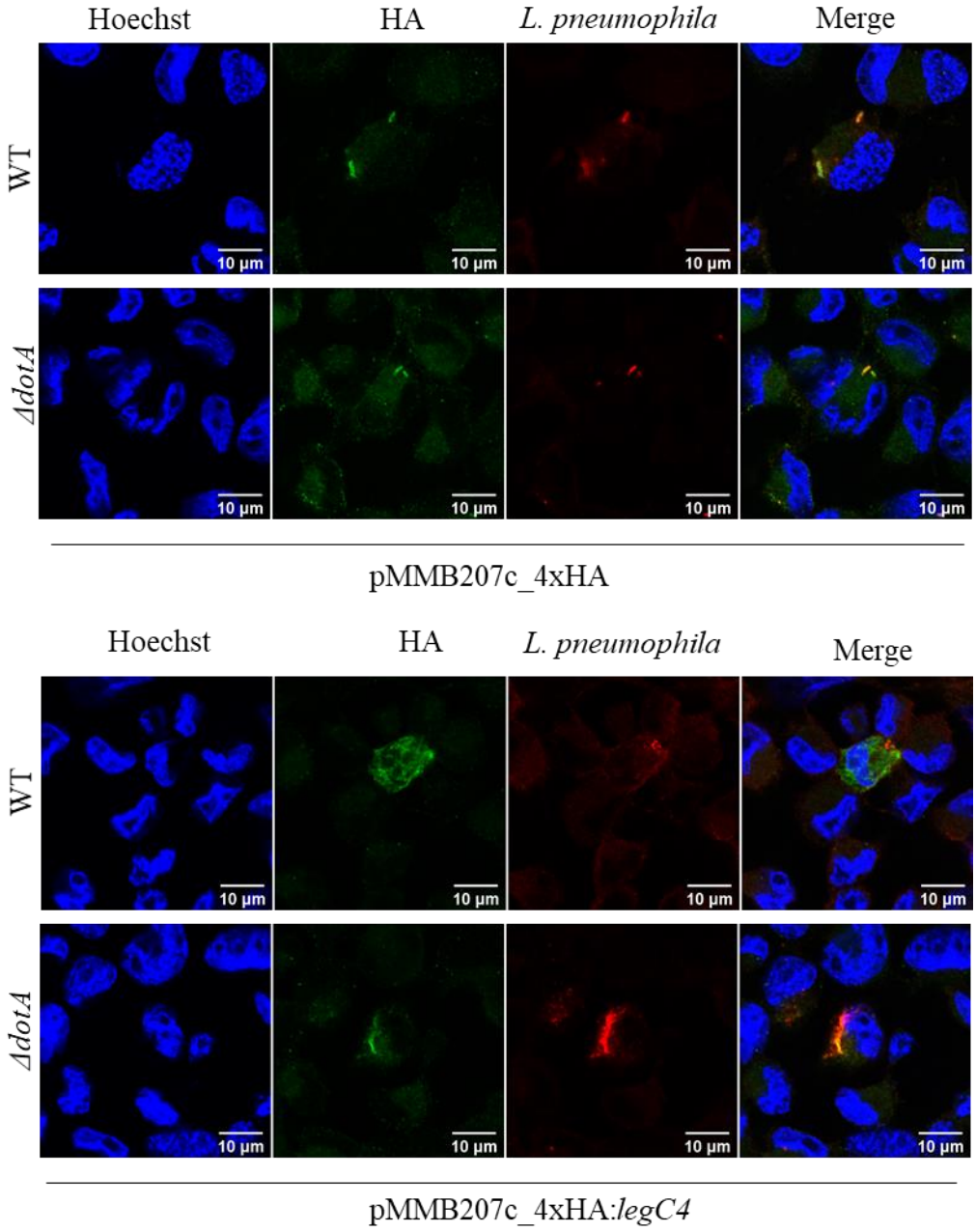

Figure 5.5. LegC4 was translocated to host cytosol by the Dot/Icm T4SS.

Immunofluorescence (IF) of cells infected by either WT or Δ*dotA* strain carrying empty pMMB207c_4xHA vector or pMMB207c_4xHA:*legC4*. Cells were fixed with 4% PFA, permeabilized with Triton X-100, and stained with anti-HA antibody (green), anti-*L. pneumophila* antibody (red), and Hoechst (blue). Images are representative of 3 independent repeats.

A

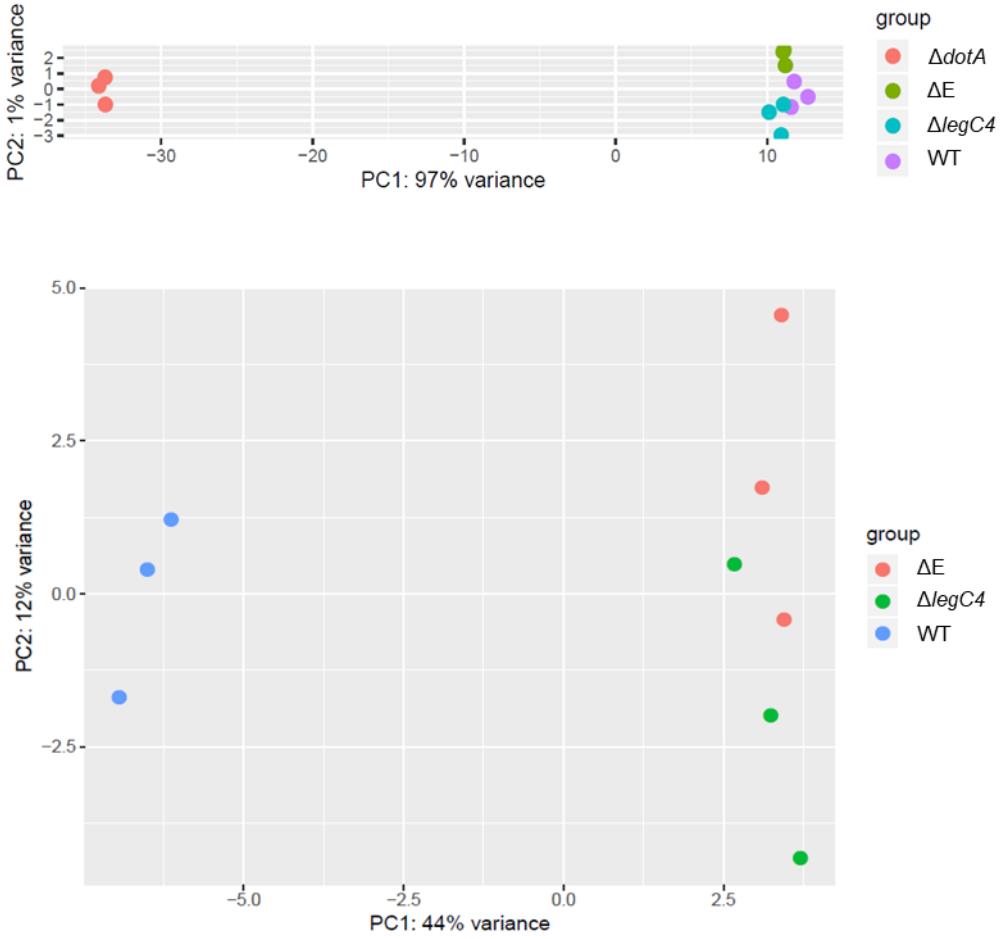
PC2: 1% variance
PC1: 97% variance
group
ΔdotA
ΔE
ΔlegC4
WT
PC2: 12% variance
PC1: 44% variance
group
ΔE
ΔlegC4
WT

B

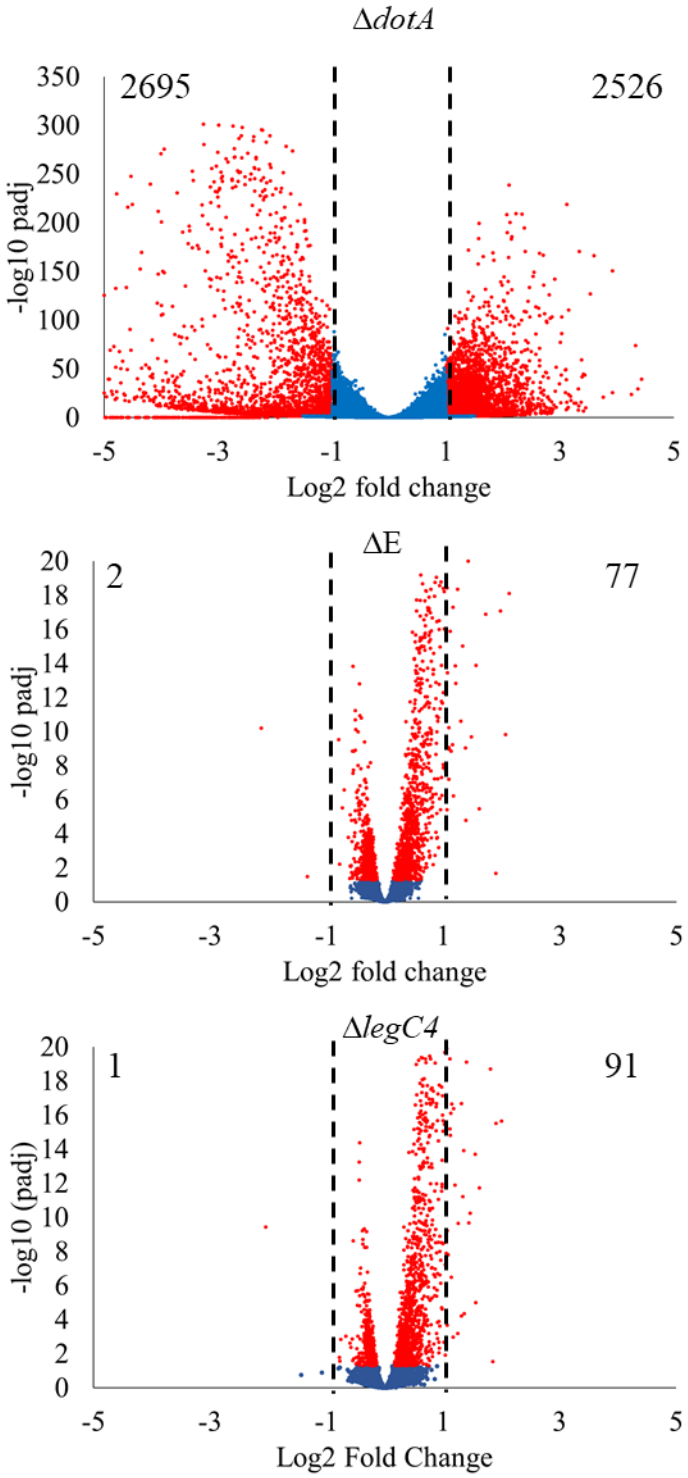
ΔdotA
2695
2526
-log10 padj
Log2 fold change
ΔE
2
77
-log10 padj
Log2 fold change
ΔlegC4
1
91
-log10 (padj)
Log2 Fold Change

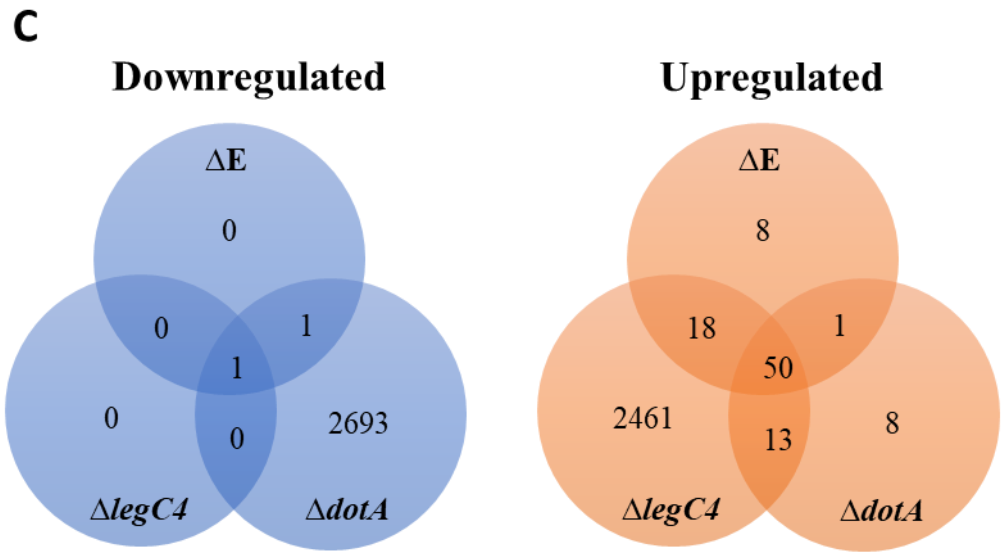

Figure 5.6. *L. pneumophila* alters host transcriptome dependently on LegC4.

(A) Principal component analysis (PCA) plot to visualize the differences of each sample. (B) Differential gene expression of mutant-infected cells compared to WT-infected cells were visualized in volcano plots. Blue dots represent data points with adjusted p-value (PADJ) > 0.05, whereas red dots represent data points with PADJ < 0.05. The dotted lines marked $\log_2$ fold change at -1 and 1. (C) Diagram showing the numbers of differentially expressed genes in each mutant-infected cells compared to WT-infected cells.

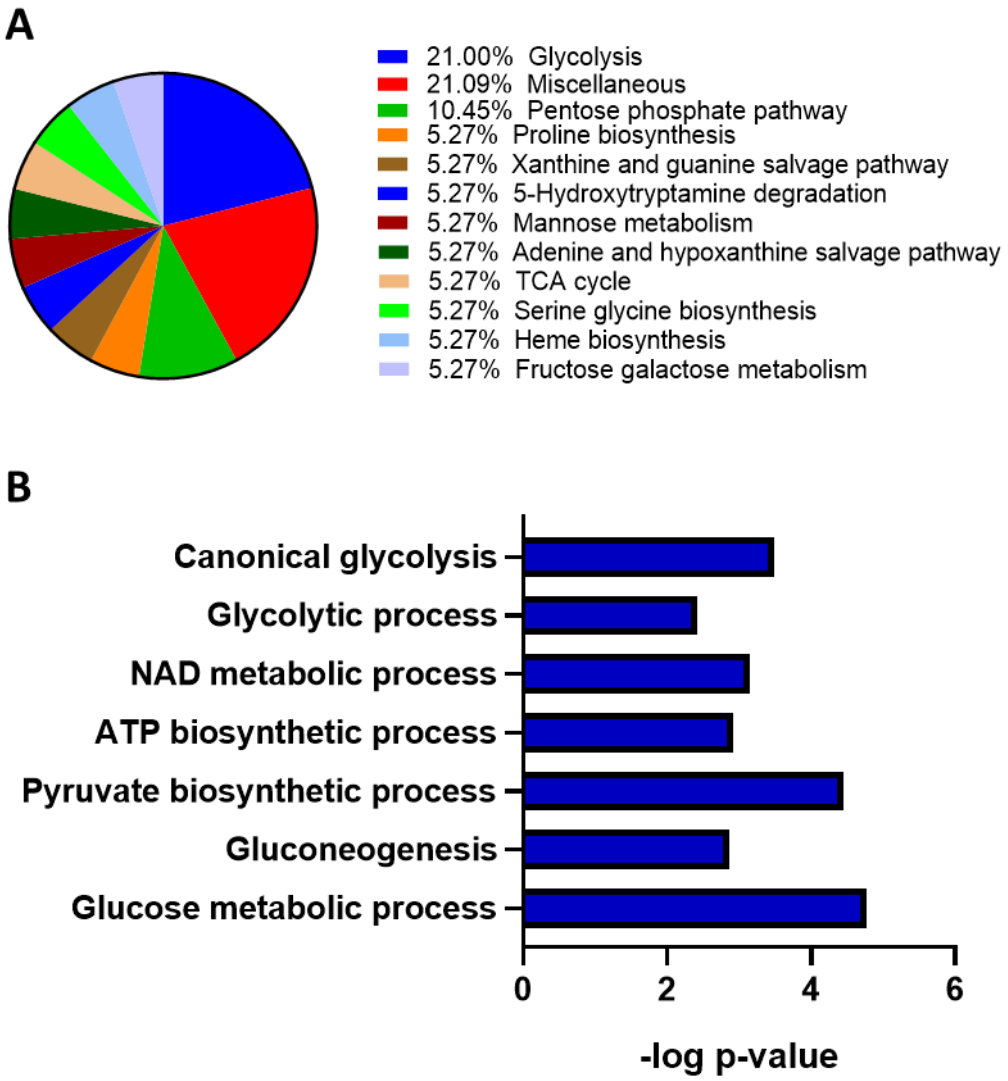

Figure 5.7. Genes involved in glucose metabolism were upregulated in mutant-infected cells.

(A) Genes upregulated in mutant-infected cells compared to WT-infected cells were deposited using PANTHER gene list analysis. Pie chart illustrated the molecular processes where genes were categorized. (B) Gene ontology (GO) term enriched amongst the upregulated genes were identified using GO Term::Finder and plotted against the –log p-value after correction with Bonferroni correction.

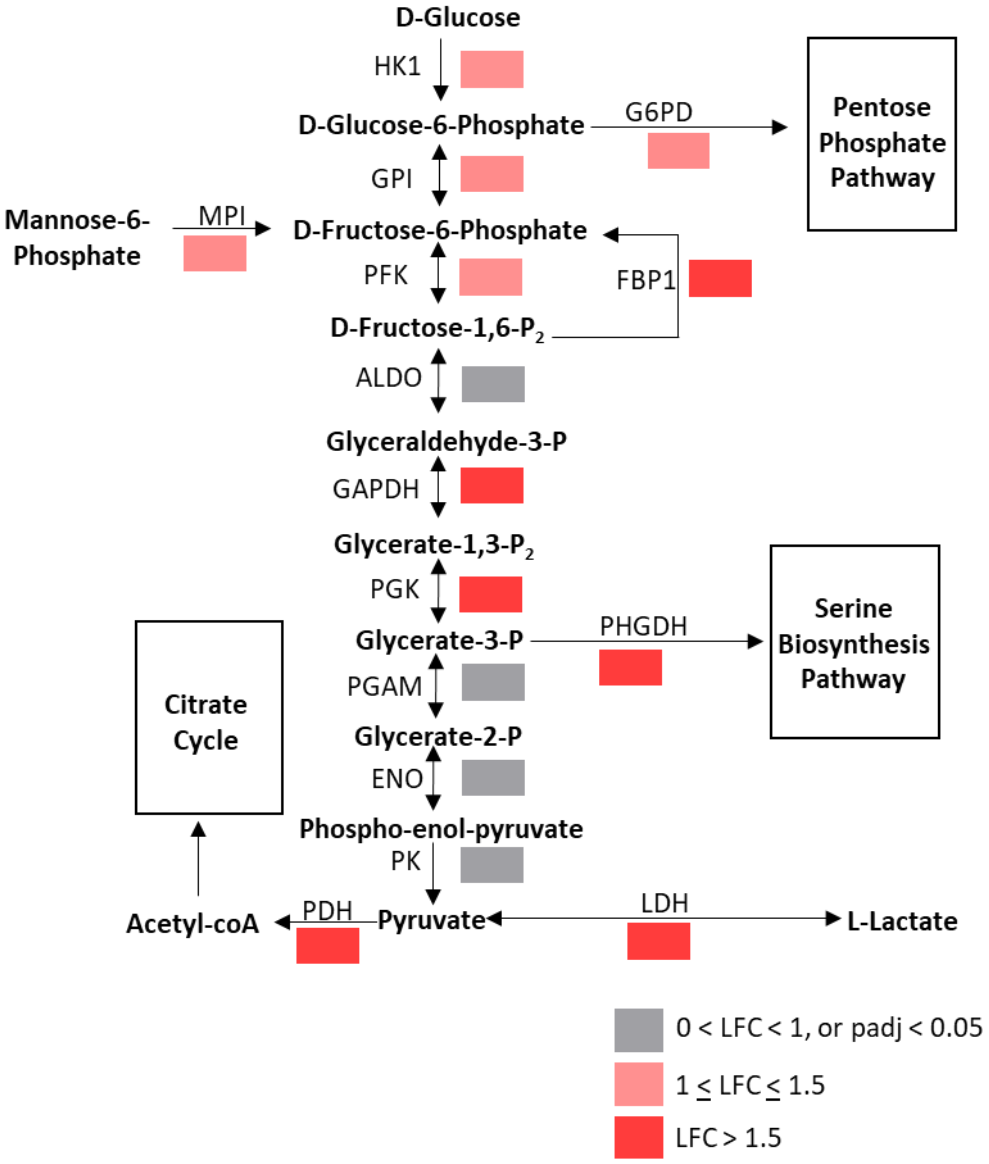

Figure 5.8. Genes involved in host glycolysis/gluconeogenesis pathway were upregulated in Δ*legC4*-infected cells.

Log_2 fold change (LFC) of genes involved in glycolysis/gluconeogenesis pathway in Δ*legC4* infected cells compared to WT-infected cells were superimposed with the glycolysis/gluconeogenesis pathway. Coloured boxes indicate the LFC value as shown in the legend.

Chapter 6
Perspective

L. pneumophila is an accidental human pathogen that causes a severe pneumonia in immunocompromised people, termed Legionnaires' disease (1, 2). Naturally, to survive predation and persist in the environment, *L. pneumophila* replicates in multiple species of amoebae. These protozoan hosts protect the bacteria from environmental stresses such as nutrient starvation, chlorine-based disinfectant and antibiotics (60, 62, 403), which has helped *L. pneumophila* to emerge as a human pathogen. This evolution and relationship with protozoan hosts has allowed *L. pneumophila* to also infect and replicate in human macrophages (63, 348). Indeed, macrophages show some remarkable similarities to amoeba. Not only are macrophages motile and capable of distinguishing self from non-self, they also share some cell surface receptors with amoebae and can phagocytose microbes (404). Thus, microbes that survive in amoebae, such as *Legionella*, *Mycobacteria*, *Burkholderia*, and *Pseudomonas*, often also survive in macrophages. Consistently, the intracellular life cycle of *L. pneumophila* is considered very similar in mammalian and protozoan hosts (62, 255). Furthermore, LCV proteomics studies have revealed that during infection of macrophages and the protozoan host *D. discoideum*, host proteins involved in similar processes were recruited to the LCV (134, 286-289), suggesting that *L. pneumophila* manipulates similar host pathways to allow bacterial survival.

Central to the survival of *L. pneumophila* in both amoebae and macrophages is the Dot/Icm T4SS (208, 238, 239). The Dot/Icm T4SS is very well-conserved amongst 58 sequenced *Legionella* species, confirming its importance for bacterial survival (72, 74). The Dot/Icm T4SS secretes over 330 effectors into the host cells that manipulate host processes and enable bacterial replication. Given the large effector repertoire, deletion of one effector gene often does not result in a significant reduction in virulence, which is frequently attributed to functional redundancy. This makes the identification of effectors important for the manipulation of host processes and bacterial replication challenging.

To circumvent this problem, in this study, we generated large genomic region deletion mutants to allow the identification of effectors important for bacterial replication in three different host models: THP1 human macrophage cell line, *A. castellanii*, and A-strain

mice. We found that using macrophage cell line *in vitro* was insufficient to identify Dot/Icm effectors implicated during *L. pneumophila* replication. No phenotype was observed in THP1 macrophages for any of the deletion mutants, whereas multiple phenotypes were found in A-strain mice. Deletion of homologous genomic regions in the *L. pneumophila* Philadelphia-1 strain also led to no difference during infection of BMDMs derived from A-strain mice (338), thus eliminating species differences as a contributing factor.

Importantly, here we showed that the ΔE mutant displayed a significant reduction in bacterial load in A-strain mice and *A. castellanii*, possibly hinting at the importance of this genomic region to sustain bacterial replication in these hosts, and supporting the hypothesis that virulence factors that evolved to allow bacterial replication in amoebae also enable replication in mammals. However, we found different outcomes of infection in mammalian compared to protozoan host as summarized in **Table 6.1**. This result corroborates other studies, which showed different phenotypes in mammalian compared to protozoan hosts. For instance, different sets of genes were important for replication in *A. castellanii*, compared to *NLRC4*$^{-/-}$ mice or *NLRC4*$^{-/-}$ mice-derived BMDMs (334). Furthermore, different sets of *L. pneumophila* genes were expressed upon infection of mammalian hosts compared to protozoan hosts (405).

These differences likely reflect different requirements for replication in different hosts. Amoebae are unicellular organisms that alternate between a metabolically active trophozoite and dormant cyst to survive unfavourable conditions (406). As such, *L. pneumophila* may require different strategies to survive in these distinct environments, a requirement that is absent in macrophages. On the other hand, unlike amoebae, macrophages exist in a network with other cell types as part of the host innate immune response. In this network, secondary messenger molecules such as cytokines and chemokines exist to allow immune cell recruitment and to mediate cell to cell communications, a feature that is not required in a unicellular organism such as amoebae. Consistently, the transcriptome of macrophages infected with *L. pneumophila* showed a significant enrichment in genes involved in the host innate immune response (296, 375, 376), whereas the transcriptome of *D. discoideum* after infection with *L. pneumophila* reflects the manipulation of host metabolism and vesicular trafficking (407). This

suggests despite some similarities, *L. pneumophila* still require different resources to successfully infect different hosts.

Another difference between amoebae and macrophages is that targeting the same host pathway may lead to different consequences in the different hosts. In this study, we identified that LegC4, a Dot/Icm effector, downregulated the mRNA of genes involved in glucose metabolism. Our lab also showed that LegC4 downregulated *GAPDH* mRNA during infection of *A. castellanii* (Dr Kathleen McCaffrey, personal communication). Downregulation of glucose metabolism in the protozoan host may lead to an increase in glucose availability which can then be taken up and utilized by *L. pneumophila*. In addition to increasing glucose availability, the downregulation of glucose metabolism in macrophages may alter the host inflammatory status (408). Silencing of enzymes involved in glucose metabolism is linked with reduced pro-inflammatory macrophage response (409, 410). However, contrary to this, we also found that infection with Δ*legC4* led to a significant reduction in pulmonary IFNγ level, suggesting that LegC4 may enhance the host immune response. Thus, more studies are required to unravel this paradox. Regardless of how LegC4 enhanced pulmonary pro-inflammatory response while also downregulating host glycolysis gene mRNAs, it seems that downregulation of glucose metabolism in protozoan host should result in different outcomes. The immune response in amoebae is primitive and far less complex compared to mammals (30). Therefore, targeting the same pathways in different host can lead to different consequences.

These differences between hosts translate to a requirement for distinct virulence factors to survive. In addition to the acquisition of virulence factors, specialization to infect another host may involve the loss of genomic regions. *Bordetella parapertussis*, *Bordetella bronchiseptica*, and *Bordetella pertussis* form a monophyletic group, suggesting a common ancestor (411). *B. pertussis* has undergone genome reduction, and hence specialisation to infect humans, which led to a loss in ability to utilise amoebae as a host, whereas, similar to *L. pneumophila*, *B. bronchiseptica* and *B. parapertussis* maintain the ability to replicate in protozoan hosts (411). This suggests that genes important for replication in protozoan hosts may not be beneficial to allow mammalian infection.

To date, studies suggest that *L. pneumophila* may not be well adapted to infecting macrophages, and remains an accidental pathogen of humans. For instance, there is no evidence of any genome reduction in *L. pneumophila* upon genome comparison with other *Legionella* species that only infect amoebae (72, 74). Additionally, a mutant lacking 31% of the genome displayed a severe replication defect in protozoa, but not macrophages (338). Consistently, all our mutants were able to efficiently replicate in THP1 macrophages, whereas four of these mutants displayed a severe reduction in replication in *A. castellanii*. This may suggest that certain genomic regions that were evolved to aid replication in protozoa may not be important for replication in macrophages. Even more strikingly, genes essential for replication in protozoa may be deleterious to bacterial replication in mammalian hosts (334, 348). In our study, four out of six tested genomic regions appeared disadvantageous for *L. pneumophila* replication during lung infection of A-strain mice. Infection by mutants lacking these regions also led to more severe weight loss. Of the four regions, three were important for *L. pneumophila* replication in *A. castellanii*. Δ*lpw_04861*, that showed an increase in survival in A-strain mice, lacked a Dot/Icm effector that is well-conserved amongst at least 52 species in the *Legionella* genus. Hence, while replication in protozoa may have allowed greater bacterial survival in macrophages, *L. pneumophila* is better adapted to infecting amoebae. What may trigger the specialisation of a bacterial pathogen to adapt to a human host remains unclear. *L. pneumophila* possesses a highly plastic genome that enables the acquisition of virulence factors. However, humans are a dead-end host for *L. pneumophila* as only one potential person-to-person transmission case has ever been reported (412). Thus, the evolution of *L. pneumophila* to adapt to human transmission is unlikely to occur. Together, these highlight the importance of protozoa as the reservoir of *L. pneumophila* in the environment. Therefore, to prevent Legionnaires' disease, proper measures to control levels of environmental bacteria and amoebae should be implemented at all times.

The treatment of *L. pneumophila* as an opportunistic intracellular pathogen relies on the effectiveness of broad range antimicrobials such as macrolides, floroquinolones, and rifampicin (31). Recently, the emergence of antimicrobial resistance in *L. pneumophila* has called for the development of novel therapeutics (31, 413). Our study suggests that some genes maintained in the *L. pneumophila* genome are deleterious to bacterial replication in mammalian hosts. These genes are not restricted to Dot/Icm effectors. For

example, mutants deficient in lysine biosynthesis genes *lysA/B* are unable to replicate in *A. castellanii,* but displayed an enhanced virulence in the murine BMDMs (414). Furthermore, flagella are important for bacterial survival in *A. castellanii*, however flagellin is deleterious in murine infection by activating the NLRC4 inflammasome (170). We have not yet discovered the genes responsible for the increase in survival of ΔA, ΔD, and ΔFGHI, but, in addition to the Dot/Icm effectors, there are transporters of unknown function, bacterial cell wall components, and efflux system components deleted in these mutants (**Appendix 1**). Therefore, the genes responsible for the increase in survival during murine infection need to be identified, to avoid targeting these genes for novel therapeutics, as this may inadvertently increase bacterial burden.

In summary, the ability of *L. pneumophila* to survive in protozoa likely allows replication of the pathogen in alveolar macrophages. However, *L. pneumophila* is less adapted to infecting macrophages due to the presence of genes deleterious for bacterial replication in mammalian tissues, suggesting that protozoa remain the most important reservoir of *L. pneumophila*. This highlights the need to control environmental sources of the bacteria. The identification of genes disadvantageous to replication in mammalian tissues need to be done in order to prevent targeting these genes for novel therapeutics and to monitor the adaptation of *L. pneumophila* to infecting mammalian hosts.

Table 6.1. Comparison of *L. pneumophila* mutants phenotypes in different hosts

Mutant	THP1	*A. castellanii*	A-strain mice
ΔA	No difference	No difference	Increased CFU
ΔB	No difference	Reduced CFU	Increased CFU
ΔC	No difference	No difference	No difference
ΔD	No difference	No difference	Increased CFU
ΔE	No difference	Reduced CFU	Reduced CFU
ΔF	No difference	Reduced CFU	Not tested
ΔG	No difference	Reduced CFU	Not tested
ΔH	No difference	No difference	Not tested
ΔI	No difference	Reduced CFU	Not tested
ΔFGHI	No difference	Reduced CFU	Increased CFU, reduced CFU at later time point

REFERENCES

1. Fraser DW, Tsai TR, Orenstein W, Parkin WE, Beecham HJ, Sharrar RG, Harris J, Mallison GF, Martin SM, McDade JE, Shepard CC, Brachman PS. 1977. Legionnaires' disease: description of an epidemic of pneumonia. N Engl J Med 297:1189-97.
2. McDade JE, Shepard CC, Fraser DW, Tsai TR, Redus MA, Dowdle WR. 1977. Legionnaires' disease: isolation of a bacterium and demonstration of its role in other respiratory disease. N Engl J Med 297:1197-203.
3. Brenner DJ, Steigerwalt AG, McDade JE. 1979. Classification of the Legionnaires' disease bacterium: *Legionella pneumophila*, genus novum, species nova, of the family *Legionella*ceae, familia nova. Ann Intern Med 90:656-8.
4. Glick TH, Gregg MB, Berman B, Mallison G, Rhodes WW, Jr., Kassanoff I. 1978. Pontiac fever. An epidemic of unknown etiology in a health department: I. Clinical and epidemiologic aspects. Am J Epidemiol 107:149-60.
5. Kaufmann AF, McDade JE, Patton CM, Bennett JV, Skaliy P, Feeley JC, Anderson DC, Potter ME, Newhouse VF, Gregg MB, Brachman PS. 1981. Pontiac fever: isolation of the etiologic agent (*Legionella pneumophilia*) and demonstration of its mode of transmission. Am J Epidemiol 114:337-47.
6. Rodgers FG. 1979. Ultrastructure of *Legionella pneumophila*. J Clin Pathol 32:1195-202.
7. Rodgers FG, Greaves PW, Macrae AD. 1979. Flagella and fimbriae on *Legionella* organisms. Lancet 2:753-4.
8. Chandler FW, Thomason BM, Hebert GA. 1980. Flagella on Legionnaires' disease bacteria in the human lung. Ann Intern Med 93:715-6.
9. Coil DA, Anne J. 2009. Twitching motility in *Legionella pneumophila*. FEMS Microbiol Lett 293:271-7.
10. Wu HY, Yan H, Zheng ML, Sun MM, Wang Q, Hu CM, Zhan XY, Yuan MG, Qu PH, Hu CH. 2019. *Legionella qingyii sp. nov.*, isolated from water samples in China. Int J Syst Evol Microbiol 69:2017-2022.
11. Miyashita N, Higa F, Aoki Y, Kikuchi T, Seki M, Tateda K, Maki N, Uchino K, Ogasawara K, Kiyota H, Watanabe A. 2020. Distribution of *Legionella* species and serogroups in patients with culture-confirmed *Legionella* pneumonia. J Infect Chemother doi:10.1016/j.jiac.2019.12.016.
12. Parte AC. 2018. LPSN - List of Prokaryotic names with Standing in Nomenclature (bacterio.net), 20 years on. Int J Syst Evol Microbiol 68:1825-1829.
13. Centers for Disease Control and Prevention, (CDC). 2018. Legionnaires' disease surveillance summary report, United States 2014-2015. U.S. Department of Health and Human Services, Centers for Disease Control and Prevention, Atlanta, GA.
14. Dooling KL, Toews KA, Hicks LA, Garrison LE, Bachaus B, Zansky S, Carpenter LR, Schaffner B, Parker E, Petit S, Thomas A, Thomas S, Mansmann R, Morin C, White B, Langley GE. 2015. Active Bacterial Core Surveillance for Legionellosis - United States, 2011-2013. MMWR Morb Mortal Wkly Rep 64:1190-3.
15. Muder RR, Yu VL. 2002. Infection due to *Legionella* species other than *L. pneumophila*. Clin Infect Dis 35:990-8.

16. Yu VL, Plouffe JF, Pastoris MC, Stout JE, Schousboe M, Widmer A, Summersgill J, File T, Heath CM, Paterson DL, Chereshsky A. 2002. Distribution of *Legionella* species and serogroups isolated by culture in patients with sporadic community-acquired legionellosis: an international collaborative survey. J Infect Dis 186:127-8.
17. Graham FF, White PS, Harte DJ, Kingham SP. 2012. Changing epidemiological trends of legionellosis in New Zealand, 1979-2009. Epidemiol Infect 140:1481-96.
18. National Notifiable Diseases Surveillance System Working Group. 2019. Australia's notifiable disease status, 2015: Annual report of the National Notifiable Diseases Surveillance System. Communicable Diseases Intelligence 43.
19. Doleans A, Aurell H, Reyrolle M, Lina G, Freney J, Vandenesch F, Etienne J, Jarraud S. 2004. Clinical and environmental distributions of *Legionella* strains in France are different. J Clin Microbiol 42:458-60.
20. Kruse EB, Wehner A, Wisplinghoff H. 2016. Prevalence and distribution of *Legionella spp* in potable water systems in Germany, risk factors associated with contamination, and effectiveness of thermal disinfection. Am J Infect Control 44:470-4.
21. De Filippis P, Mozzetti C, Messina A, D'Alo GL. 2018. Prevalence of *Legionella* in retirement homes and group homes water distribution systems. Sci Total Environ 643:715-724.
22. Dilger T, Melzl H, Gessner A. 2018. *Legionella* contamination in warm water systems: A species-level survey. Int J Hyg Environ Health 221:199-210.
23. Llewellyn AC, Lucas CE, Roberts SE, Brown EW, Nayak BS, Raphael BH, Winchell JM. 2017. Distribution of *Legionella* and bacterial community composition among regionally diverse US cooling towers. PLoS One 12:e0189937.
24. Phin N, Parry-Ford F, Harrison T, Stagg HR, Zhang N, Kumar K, Lortholary O, Zumla A, Abubakar I. 2014. Epidemiology and clinical management of Legionnaires' disease. Lancet Infect Dis 14:1011-21.
25. Ibranosyan M, Beraud L, Lemaire H, Ranc AG, Ginevra C, Jarraud S, Descours G. 2019. The clinical presentation of *Legionella* arthritis reveals the mode of infection and the bacterial species: case report and literature review. BMC Infect Dis 19:864.
26. Lowry PW, Tompkins LS. 1993. Nosocomial legionellosis: a review of pulmonary and extrapulmonary syndromes. Am J Infect Control 21:21-7.
27. Desgranges F, Coste AT, Wernly D, Dufour J, Opota O, Meylan S. 2020. Immunosuppressed gardener pricked by roses grows *Legionella longbeachae*. Lancet 395:604.
28. Young JS, Farber BF, Pupovac SS, Graver LM. 2019. Prosthetic Valve *Legionella* Endocarditis. Ann Thorac Surg 108:e271-e272.
29. Thurneysen C, Boggian K. 2014. *Legionella pneumophila* serogroup 1 septic arthritis with probable endocarditis in an immunodeficient patient. J Clin Rheumatol 20:297-8.
30. Cunha BA, Burillo A, Bouza E. 2016. Legionnaires' disease. Lancet 387:376-385.
31. National Academies of Sciences E, Medicine, Health, Medicine D, Division on E, Life S, Board on Population H, Public Health P, Board on Life S, Water S,

Technology B, Committee on Management of *Legionella* in Water S. 2019. Management of *Legionella* in Water Systems doi:10.17226/25474. National Academies Press (US).

32. Wolff C, Lange H, Feruglio S, Vold L, MacDonald E. 2019. Evaluation of the national surveillance of Legionnaires' disease in Norway, 2008-2017. BMC Public Health 19:1624.
33. Mercante JW, Winchell JM. 2015. Current and emerging *Legionella* diagnostics for laboratory and outbreak investigations. Clin Microbiol Rev 28:95-133.
34. Gramegna A, Sotgiu G, Di Pasquale M, Radovanovic D, Terraneo S, Reyes LF, Vendrell E, Neves J, Menzella F, Blasi F, Aliberti S, Restrepo MI, Group GS. 2018. Atypical pathogens in hospitalized patients with community-acquired pneumonia: a worldwide perspective. BMC Infect Dis 18:677.
35. Berendt RF. 1980. Survival of *Legionella pneumophila* in aerosols: effect of relative humidity. J Infect Dis 141:689.
36. Hambleton P, Broster MG, Dennis PJ, Henstridge R, Fitzgeorge R, Conlan JW. 1983. Survival of virulent *Legionella pneumophila* in aerosols. J Hyg (Lond) 90:451-60.
37. Dennis PJ, Lee JV. 1988. Differences in aerosol survival between pathogenic and non-pathogenic strains of *Legionella pneumophila* serogroup 1. J Appl Bacteriol 65:135-41.
38. Wadowsky RM, Wolford R, McNamara AM, Yee RB. 1985. Effect of temperature, pH, and oxygen level on the multiplication of naturally occurring *Legionella pneumophila* in potable water. Appl Environ Microbiol 49:1197-205.
39. Lanternier F, Tubach F, Ravaud P, Salmon D, Dellamonica P, Bretagne S, Couret M, Bouvard B, Debandt M, Gueit I, Gendre JP, Leone J, Nicolas N, Che D, Mariette X, Lortholary O, Research Axed on Tolerance of Biotherapies G. 2013. Incidence and risk factors of *Legionella pneumophila* pneumonia during anti-tumor necrosis factor therapy: a prospective French study. Chest 144:990-998.
40. Collier SA, Stockman LJ, Hicks LA, Garrison LE, Zhou FJ, Beach MJ. 2012. Direct healthcare costs of selected diseases primarily or partially transmitted by water. Epidemiol Infect 140:2003-13.
41. Cassini A, Colzani E, Pini A, Mangen MJ, Plass D, McDonald SA, Maringhini G, van Lier A, Haagsma JA, Havelaar AH, Kramarz P, Kretzschmar ME, On Behalf Of The BC. 2018. Impact of infectious diseases on population health using incidence-based disability-adjusted life years (DALYs): results from the Burden of Communicable Diseases in Europe study, European Union and European Economic Area countries, 2009 to 2013. Euro Surveill 23.
42. Skaliy P, McEachern HV. 1979. Survival of the Legionnaires' disease bacterium in water. Ann Intern Med 90:662-3.
43. Shaheen M, Scott C, Ashbolt NJ. 2019. Long-term persistence of infectious *Legionella* with free-living amoebae in drinking water biofilms. Int J Hyg Environ Health 222:678-686.
44. Taylor M, Ross K, Bentham R. 2009. *Legionella*, protozoa, and biofilms: interactions within complex microbial systems. Microb Ecol 58:538-47.
45. Conza L, Pagani SC, Gaia V. 2013. Presence of *Legionella* and free-living Amoebae in composts and bioaerosols from composting facilities. PLoS One 8:e68244.

46. Scheikl U, Sommer R, Kirschner A, Rameder A, Schrammel B, Zweimuller I, Wesner W, Hinker M, Walochnik J. 2014. Free-living amoebae (FLA) co-occurring with *Legionellae* in industrial waters. Eur J Protistol 50:422-9.
47. Valcina O, Pule D, Malisevs A, Trofimova J, Makarova S, Konvisers G, Berzins A, Krumina A. 2019. Co-Occurrence of Free-Living Amoeba and *Legionella* in Drinking Water Supply Systems. Medicina (Kaunas) 55:492.
48. Murga R, Forster TS, Brown E, Pruckler JM, Fields BS, Donlan RM. 2001. Role of biofilms in the survival of *Legionella pneumophila* in a model potable-water system. Microbiology 147:3121-6.
49. Vatansever C, Turetgen I. 2015. Survival of biofilm-associated *Legionella pneumophila* exposed to various stressors. Water Environ Res 87:227-32.
50. Rowbotham TJ. 1980. Preliminary report on the pathogenicity of *Legionella pneumophila* for freshwater and soil amoebae. J Clin Pathol 33:1179-83.
51. Steinert M, Emody L, Amann R, Hacker J. 1997. Resuscitation of viable but nonculturable *Legionella pneumophila* Philadelphia JR32 by *Acanthamoeba castellanii*. Appl Environ Microbiol 63:2047-53.
52. Dietersdorfer E, Kirschner A, Schrammel B, Ohradanova-Repic A, Stockinger H, Sommer R, Walochnik J, Cervero-Arago S. 2018. Starved viable but non-culturable (VBNC) *Legionella* strains can infect and replicate in amoebae and human macrophages. Water Res 141:428-438.
53. Epalle T, Girardot F, Allegra S, Maurice-Blanc C, Garraud O, Riffard S. 2015. Viable but not culturable forms of *Legionella pneumophila* generated after heat shock treatment are infectious for macrophage-like and alveolar epithelial cells after resuscitation on Acanthamoeba polyphaga. Microb Ecol 69:215-24.
54. Cervero-Arago S, Schrammel B, Dietersdorfer E, Sommer R, Luck C, Walochnik J, Kirschner A. 2019. Viability and infectivity of viable but nonculturable *Legionella pneumophila* strains induced at high temperatures. Water Res 158:268-279.
55. Cervero-Arago S, Sommer R, Araujo RM. 2014. Effect of UV irradiation (253.7 nm) on free *Legionella* and *Legionella* associated with its amoebae hosts. Water Res 67:299-309.
56. Dupuy M, Mazoua S, Berne F, Bodet C, Garrec N, Herbelin P, Menard-Szczebara F, Oberti S, Rodier MH, Soreau S, Wallet F, Hechard Y. 2011. Efficiency of water disinfectants against *Legionella pneumophila* and Acanthamoeba. Water Res 45:1087-94.
57. Storey MV, Winiecka-Krusnell J, Ashbolt NJ, Stenstrom TA. 2004. The efficacy of heat and chlorine treatment against thermotolerant Acanthamoebae and *Legionella*e. Scand J Infect Dis 36:656-62.
58. Berk SG, Ting RS, Turner GW, Ashburn RJ. 1998. Production of respirable vesicles containing live *Legionella pneumophila* cells by two Acanthamoeba spp. Appl Environ Microbiol 64:279-86.
59. Bouyer S, Imbert C, Rodier MH, Hechard Y. 2007. Long-term survival of *Legionella pneumophila* associated with *Acanthamoeba castellanii* vesicles. Environ Microbiol 9:1341-4.
60. Rowbotham TJ. 1986. Current views on the relationships between amoebae, *Legionellae* and man. Isr J Med Sci 22:678-89.

61. Brown MR, Barker J. 1999. Unexplored reservoirs of pathogenic bacteria: protozoa and biofilms. Trends Microbiol 7:46-50.
62. Escoll P, Rolando M, Gomez-Valero L, Buchrieser C. 2013. From amoeba to macrophages: exploring the molecular mechanisms of *Legionella pneumophila* infection in both hosts. Curr Top Microbiol Immunol 376:1-34.
63. Molmeret M, Horn M, Wagner M, Santic M, Abu Kwaik Y. 2005. Amoebae as training grounds for intracellular bacterial pathogens. Appl Environ Microbiol 71:20-8.
64. Cirillo JD, Falkow S, Tompkins LS. 1994. Growth of *Legionella pneumophila* in *Acanthamoeba castellanii* enhances invasion. Infect Immun 62:3254-61.
65. Smirnov AV, Chao E, Nassonova ES, Cavalier-Smith T. 2011. A revised classification of naked lobose amoebae (Amoebozoa: lobosa). Protist 162:545-70.
66. Brieland JK, Fantone JC, Remick DG, LeGendre M, McClain M, Engleberg NC. 1997. The role of *Legionella pneumophila*-infected Hartmannella vermiformis as an infectious particle in a murine model of Legionnaire's disease. Infect Immun 65:5330-3.
67. Cazalet C, Rusniok C, Bruggemann H, Zidane N, Magnier A, Ma L, Tichit M, Jarraud S, Bouchier C, Vandenesch F, Kunst F, Etienne J, Glaser P, Buchrieser C. 2004. Evidence in the *Legionella pneumophila* genome for exploitation of host cell functions and high genome plasticity. Nat Genet 36:1165-73.
68. Chien M, Morozova I, Shi S, Sheng H, Chen J, Gomez SM, Asamani G, Hill K, Nuara J, Feder M, Rineer J, Greenberg JJ, Steshenko V, Park SH, Zhao B, Teplitskaya E, Edwards JR, Pampou S, Georghiou A, Chou IC, Iannuccilli W, Ulz ME, Kim DH, Geringer-Sameth A, Goldsberry C, Morozov P, Fischer SG, Segal G, Qu X, Rzhetsky A, Zhang P, Cayanis E, De Jong PJ, Ju J, Kalachikov S, Shuman HA, Russo JJ. 2004. The genomic sequence of the accidental pathogen *Legionella pneumophila*. Science 305:1966-8.
69. Schroeder GN, Petty NK, Mousnier A, Harding CR, Vogrin AJ, Wee B, Fry NK, Harrison TG, Newton HJ, Thomson NR, Beatson SA, Dougan G, Hartland EL, Frankel G. 2010. *Legionella pneumophila* strain 130b possesses a unique combination of type IV secretion systems and novel Dot/Icm secretion system effector proteins. J Bacteriol 192:6001-16.
70. D'Auria G, Jimenez-Hernandez N, Peris-Bondia F, Moya A, Latorre A. 2010. *Legionella pneumophila* pangenome reveals strain-specific virulence factors. BMC Genomics 11:181.
71. Glockner G, Albert-Weissenberger C, Weinmann E, Jacobi S, Schunder E, Steinert M, Hacker J, Heuner K. 2008. Identification and characterization of a new conjugation/type IVA secretion system (trb/tra) of *Legionella pneumophila* Corby localized on two mobile genomic islands. Int J Med Microbiol 298:411-28.
72. Gomez-Valero L, Rusniok C, Carson D, Mondino S, Perez-Cobas AE, Rolando M, Pasricha S, Reuter S, Demirtas J, Crumbach J, Descorps-Declere S, Hartland EL, Jarraud S, Dougan G, Schroeder GN, Frankel G, Buchrieser C. 2019. More than 18,000 effectors in the *Legionella* genus genome provide multiple, independent combinations for replication in human cells. Proc Natl Acad Sci U S A 116:2265-2273.
73. Joseph SJ, Cox D, Wolff B, Morrison SS, Kozak-Muiznieks NA, Frace M, Didelot X, Castillo-Ramirez S, Winchell J, Read TD, Dean D. 2016. Dynamics of genome change among *Legionella* species. Sci Rep 6:33442.

74. Burstein D, Amaro F, Zusman T, Lifshitz Z, Cohen O, Gilbert JA, Pupko T, Shuman HA, Segal G. 2016. Genomic analysis of 38 *Legionella* species identifies large and diverse effector repertoires. Nat Genet 48:167-75.
75. Coscolla M, Comas I, Gonzalez-Candelas F. 2011. Quantifying nonvertical inheritance in the evolution of *Legionella pneumophila*. Mol Biol Evol 28:985-1001.
76. Sanchez-Buso L, Comas I, Jorques G, Gonzalez-Candelas F. 2014. Recombination drives genome evolution in outbreak-related *Legionella pneumophila* isolates. Nat Genet 46:1205-11.
77. Bohlin J, Brynildsrud OB, Sekse C, Snipen L. 2014. An evolutionary analysis of genome expansion and pathogenicity in Escherichia coli. BMC Genomics 15:882.
78. Nash TW, Libby DM, Horwitz MA. 1984. Interaction between the legionnaires' disease bacterium (*Legionella pneumophila*) and human alveolar macrophages. Influence of antibody, lymphokines, and hydrocortisone. J Clin Invest 74:771-82.
79. Copenhaver AM, Casson CN, Nguyen HT, Fung TC, Duda MM, Roy CR, Shin S. 2014. Alveolar macrophages and neutrophils are the primary reservoirs for *Legionella pneumophila* and mediate cytosolic surveillance of type IV secretion. Infect Immun 82:4325-36.
80. Solomon JM, Isberg RR. 2000. Growth of *Legionella pneumophila* in Dictyostelium discoideum: a novel system for genetic analysis of host-pathogen interactions. Trends Microbiol 8:478-80.
81. Horwitz MA. 1984. Phagocytosis of the Legionnaires' disease bacterium (*Legionella pneumophila*) occurs by a novel mechanism: engulfment within a pseudopod coil. Cell 36:27-33.
82. Rittig MG, Burmester GR, Krause A. 1998. Coiling phagocytosis: when the zipper jams, the cup is deformed. Trends Microbiol 6:384-8.
83. Payne NR, Horwitz MA. 1987. Phagocytosis of *Legionella pneumophila* is mediated by human monocyte complement receptors. J Exp Med 166:1377-89.
84. Merle NS, Noe R, Halbwachs-Mecarelli L, Fremeaux-Bacchi V, Roumenina LT. 2015. Complement System Part II: Role in Immunity. Front Immunol 6:257.
85. Reynolds HY, Newball HH. 1974. Analysis of proteins and respiratory cells obtained from human lungs by bronchial lavage. J Lab Clin Med 84:559-73.
86. Bolger MS, Ross DS, Jiang H, Frank MM, Ghio AJ, Schwartz DA, Wright JR. 2007. Complement levels and activity in the normal and LPS-injured lung. Am J Physiol Lung Cell Mol Physiol 292:L748-59.
87. Araki N, Johnson MT, Swanson JA. 1996. A role for phosphoinositide 3-kinase in the completion of macropinocytosis and phagocytosis by macrophages. J Cell Biol 135:1249-60.
88. Tachado SD, Samrakandi MM, Cirillo JD. 2008. Non-opsonic phagocytosis of *Legionella pneumophila* by macrophages is mediated by phosphatidylinositol 3-kinase. PLoS One 3:e3324.
89. Harada T, Tanikawa T, Iwasaki Y, Yamada M, Imai Y, Miyake M. 2012. Phagocytic entry of *Legionella pneumophila* into macrophages through phosphatidylinositol 3,4,5-trisphosphate-independent pathway. Biol Pharm Bull 35:1460-8.
90. Khelef N, Shuman HA, Maxfield FR. 2001. Phagocytosis of wild-type *Legionella pneumophila* occurs through a wortmannin-insensitive pathway. Infect Immun 69:5157-61.

91. Weber SS, Ragaz C, Reus K, Nyfeler Y, Hilbi H. 2006. *Legionella pneumophila* exploits PI(4)P to anchor secreted effector proteins to the replicative vacuole. PLoS Pathog 2:e46.
92. Dreyfus LA. 1987. Virulence associated ingestion of *Legionella pneumophila* by HeLa cells. Microb Pathog 3:45-52.
93. Hammer BK, Tateda ES, Swanson MS. 2002. A two-component regulator induces the transmission phenotype of stationary-phase *Legionella pneumophila*. Mol Microbiol 44:107-18.
94. Gal-Mor O, Segal G. 2003. The *Legionella pneumophila* GacA homolog (LetA) is involved in the regulation of icm virulence genes and is required for intracellular multiplication in *Acanthamoeba castellanii*. Microb Pathog 34:187-94.
95. Rasis M, Segal G. 2009. The LetA-RsmYZ-CsrA regulatory cascade, together with RpoS and PmrA, post-transcriptionally regulates stationary phase activation of *Legionella pneumophila* Icm/Dot effectors. Mol Microbiol 72:995-1010.
96. Cirillo SL, Bermudez LE, El-Etr SH, Duhamel GE, Cirillo JD. 2001. *Legionella pneumophila* entry gene rtxA is involved in virulence. Infect Immun 69:508-17.
97. Cirillo SLG, Lum J, Cirillo JD. 2000. Identification of novel loci involved in entry by *Legionella pneumophila*. Microbiology 146 (Pt 6):1345-1359.
98. Cirillo SLG, Yan L, Littman M, Samrakandi MM, Cirillo JD. 2002. Role of the *Legionella pneumophila* rtxA gene in amoebae. Microbiology 148:1667-1677.
99. Newton HJ, Sansom FM, Dao J, McAlister AD, Sloan J, Cianciotto NP, Hartland EL. 2007. Sel1 repeat protein LpnE is a *Legionella pneumophila* virulence determinant that influences vacuolar trafficking. Infect Immun 75:5575-85.
100. Newton HJ, Sansom FM, Bennett-Wood V, Hartland EL. 2006. Identification of *Legionella pneumophila*-specific genes by genomic subtractive hybridization with *Legionella micdadei* and identification of lpnE, a gene required for efficient host cell entry. Infect Immun 74:1683-91.
101. Ridenour DA, Cirillo SL, Feng S, Samrakandi MM, Cirillo JD. 2003. Identification of a gene that affects the efficiency of host cell infection by *Legionella pneumophila* in a temperature-dependent fashion. Infect Immun 71:6256-63.
102. Christensen LM, Sule P, Strain M, Cirillo JD. 2019. *Legionella pneumophila* p45 element influences host cell entry and sensitivity to sodium. PLoS One 14:e0218941.
103. Garin J, Diez R, Kieffer S, Dermine JF, Duclos S, Gagnon E, Sadoul R, Rondeau C, Desjardins M. 2001. The phagosome proteome: insight into phagosome functions. J Cell Biol 152:165-80.
104. Kinchen JM, Ravichandran KS. 2008. Phagosome maturation: going through the acid test. Nat Rev Mol Cell Biol 9:781-95.
105. Horwitz MA. 1983. The Legionnaires' disease bacterium (*Legionella pneumophila*) inhibits phagosome-lysosome fusion in human monocytes. J Exp Med 158:2108-26.
106. Horwitz MA, Maxfield FR. 1984. *Legionella pneumophila* inhibits acidification of its phagosome in human monocytes. J Cell Biol 99:1936-43.
107. Kagan JC, Roy CR. 2002. *Legionella* phagosomes intercept vesicular traffic from endoplasmic reticulum exit sites. Nat Cell Biol 4:945-54.

108. Clemens DL, Lee BY, Horwitz MA. 2000. Deviant expression of Rab5 on phagosomes containing the intracellular pathogens Mycobacterium tuberculosis and *Legionella pneumophila* is associated with altered phagosomal fate. Infect Immun 68:2671-84.
109. Falkenburger BH, Jensen JB, Dickson EJ, Suh BC, Hille B. 2010. Phosphoinositides: lipid regulators of membrane proteins. J Physiol 588:3179-85.
110. Weber S, Wagner M, Hilbi H. 2014. Live-cell imaging of phosphoinositide dynamics and membrane architecture during *Legionella* infection. mBio 5:e00839-13.
111. Weber S, Steiner B, Welin A, Hilbi H. 2018. *Legionella*-Containing Vacuoles Capture PtdIns(4)P-Rich Vesicles Derived from the Golgi Apparatus. mBio 9.
112. Brombacher E, Urwyler S, Ragaz C, Weber SS, Kami K, Overduin M, Hilbi H. 2009. Rab1 guanine nucleotide exchange factor SidM is a major phosphatidylinositol 4-phosphate-binding effector protein of *Legionella pneumophila*. J Biol Chem 284:4846-56.
113. Kubori T, Kitao T, Ando H, Nagai H. 2018. LotA, a *Legionella* deubiquitinase, has dual catalytic activity and contributes to intracellular growth. Cell Microbiol 20:e12840.
114. Ragaz C, Pietsch H, Urwyler S, Tiaden A, Weber SS, Hilbi H. 2008. The *Legionella pneumophila* phosphatidylinositol-4 phosphate-binding type IV substrate SidC recruits endoplasmic reticulum vesicles to a replication-permissive vacuole. Cell Microbiol 10:2416-33.
115. Luo X, Wasilko DJ, Liu Y, Sun J, Wu X, Luo ZQ, Mao Y. 2015. Structure of the *Legionella* Virulence Factor, SidC Reveals a Unique PI(4)P-Specific Binding Domain Essential for Its Targeting to the Bacterial Phagosome. PLoS Pathog 11:e1004965.
116. Schwarz DS, Blower MD. 2016. The endoplasmic reticulum: structure, function and response to cellular signaling. Cell Mol Life Sci 73:79-94.
117. Haenssler E, Ramabhadran V, Murphy CS, Heidtman MI, Isberg RR. 2015. Endoplasmic Reticulum Tubule Protein Reticulon 4 Associates with the *Legionella pneumophila* Vacuole and with Translocated Substrate Ceg9. Infect Immun 83:3479-89.
118. Kotewicz KM, Ramabhadran V, Sjoblom N, Vogel JP, Haenssler E, Zhang M, Behringer J, Scheck RA, Isberg RR. 2017. A Single *Legionella* Effector Catalyzes a Multistep Ubiquitination Pathway to Rearrange Tubular Endoplasmic Reticulum for Replication. Cell Host Microbe 21:169-181.
119. Steiner B, Swart AL, Welin A, Weber S, Personnic N, Kaech A, Freyre C, Ziegler U, Klemm RW, Hilbi H. 2017. ER remodeling by the large GTPase atlastin promotes vacuolar growth of *Legionella pneumophila*. EMBO Rep 18:1817-1836.
120. Nagai H, Kagan JC, Zhu X, Kahn RA, Roy CR. 2002. A bacterial guanine nucleotide exchange factor activates ARF on *Legionella* phagosomes. Science 295:679-82.
121. Hutagalung AH, Novick PJ. 2011. Role of Rab GTPases in membrane traffic and cell physiology. Physiol Rev 91:119-49.
122. Lipatova Z, Tokarev AA, Jin Y, Mulholland J, Weisman LS, Segev N. 2008. Direct interaction between a myosin V motor and the Rab GTPases Ypt31/32 is required for polarized secretion. Mol Biol Cell 19:4177-87.

123. Kagan JC, Stein MP, Pypaert M, Roy CR. 2004. *Legionella* subvert the functions of Rab1 and Sec22b to create a replicative organelle. J Exp Med 199:1201-11.
124. Derre I, Isberg RR. 2004. *Legionella pneumophila* replication vacuole formation involves rapid recruitment of proteins of the early secretory system. Infect Immun 72:3048-53.
125. Kurokawa K, Nakano A. 2019. The ER exit sites are specialized ER zones for the transport of cargo proteins from the ER to the Golgi apparatus. J Biochem 165:109-114.
126. Arasaki K, Roy CR. 2010. *Legionella pneumophila* promotes functional interactions between plasma membrane syntaxins and Sec22b. Traffic 11:587-600.
127. Nichols BJ, Pelham HR. 1998. SNAREs and membrane fusion in the Golgi apparatus. Biochim Biophys Acta 1404:9-31.
128. Robinson CG, Roy CR. 2006. Attachment and fusion of endoplasmic reticulum with vacuoles containing *Legionella pneumophila*. Cell Microbiol 8:793-805.
129. Tilney LG, Harb OS, Connelly PS, Robinson CG, Roy CR. 2001. How the parasitic bacterium *Legionella pneumophila* modifies its phagosome and transforms it into rough ER: implications for conversion of plasma membrane to the ER membrane. J Cell Sci 114:4637-50.
130. Horwitz MA. 1983. Formation of a novel phagosome by the Legionnaires' disease bacterium (*Legionella pneumophila*) in human monocytes. J Exp Med 158:1319-31.
131. Price CT, Al-Quadan T, Santic M, Rosenshine I, Abu Kwaik Y. 2011. Host proteasomal degradation generates amino acids essential for intracellular bacterial growth. Science 334:1553-7.
132. Dorer MS, Kirton D, Bader JS, Isberg RR. 2006. RNA interference analysis of *Legionella* in Drosophila cells: exploitation of early secretory apparatus dynamics. PLoS Pathog 2:e34.
133. Ivanov SS, Roy CR. 2009. Modulation of ubiquitin dynamics and suppression of DALIS formation by the *Legionella pneumophila* Dot/Icm system. Cell Microbiol 11:261-78.
134. Bruckert WM, Abu Kwaik Y. 2015. Complete and ubiquitinated proteome of the *Legionella*-containing vacuole within human macrophages. J Proteome Res 14:236-48.
135. Molmeret M, Bitar DM, Han L, Kwaik YA. 2004. Disruption of the phagosomal membrane and egress of *Legionella pneumophila* into the cytoplasm during the last stages of intracellular infection of macrophages and Acanthamoeba polyphaga. Infect Immun 72:4040-51.
136. Alli OA, Gao LY, Pedersen LL, Zink S, Radulic M, Doric M, Abu Kwaik Y. 2000. Temporal pore formation-mediated egress from macrophages and alveolar epithelial cells by *Legionella pneumophila*. Infect Immun 68:6431-40.
137. Molmeret M, Alli OA, Zink S, Flieger A, Cianciotto NP, Kwaik YA. 2002. icmT is essential for pore formation-mediated egress of *Legionella pneumophila* from mammalian and protozoan cells. Infect Immun 70:69-78.
138. Byrne B, Swanson MS. 1998. Expression of *Legionella pneumophila* virulence traits in response to growth conditions. Infect Immun 66:3029-34.

139. Tiaden A, Spirig T, Carranza P, Bruggemann H, Riedel K, Eberl L, Buchrieser C, Hilbi H. 2008. Synergistic contribution of the *Legionella pneumophila* lqs genes to pathogen-host interactions. J Bacteriol 190:7532-47.
140. Molofsky AB, Shetron-Rama LM, Swanson MS. 2005. Components of the *Legionella pneumophila* flagellar regulon contribute to multiple virulence traits, including lysosome avoidance and macrophage death. Infect Immun 73:5720-34.
141. Bruggemann H, Hagman A, Jules M, Sismeiro O, Dillies MA, Gouyette C, Kunst F, Steinert M, Heuner K, Coppee JY, Buchrieser C. 2006. Virulence strategies for infecting phagocytes deduced from the in vivo transcriptional program of *Legionella pneumophila*. Cell Microbiol 8:1228-40.
142. Faucher SP, Mueller CA, Shuman HA. 2011. *Legionella pneumophila* Transcriptome during Intracellular Multiplication in Human Macrophages. Front Microbiol 2:60.
143. Portier E, Zheng H, Sahr T, Burnside DM, Mallama C, Buchrieser C, Cianciotto NP, Hechard Y. 2015. IroT/mavN, a new iron-regulated gene involved in *Legionella pneumophila* virulence against amoebae and macrophages. Environ Microbiol 17:1338-50.
144. O'Connor TJ, Zheng H, VanRheenen SM, Ghosh S, Cianciotto NP, Isberg RR. 2016. Iron Limitation Triggers Early Egress by the Intracellular Bacterial Pathogen *Legionella pneumophila*. Infect Immun 84:2185-2197.
145. Silveira TN, Zamboni DS. 2010. Pore formation triggered by *Legionella spp*. is an Nlrc4 inflammasome-dependent host cell response that precedes pyroptosis. Infect Immun 78:1403-13.
146. Kirby JE, Vogel JP, Andrews HL, Isberg RR. 1998. Evidence for pore-forming ability by *Legionella pneumophila*. Mol Microbiol 27:323-36.
147. Muller A, Hacker J, Brand BC. 1996. Evidence for apoptosis of human macrophage-like HL-60 cells by *Legionella pneumophila* infection. Infect Immun 64:4900-6.
148. Neumeister B, Faigle M, Lauber K, Northoff H, Wesselborg S. 2002. *Legionella pneumophila* induces apoptosis via the mitochondrial death pathway. Microbiology 148:3639-3650.
149. Alegre ML, Leemans J, Le Moine A, Florquin S, De Wilde V, Chong A, Goldman M. 2008. The multiple facets of toll-like receptors in transplantation biology. Transplantation 86:1-9.
150. Kawasaki T, Kawai T. 2014. Toll-like receptor signaling pathways. Front Immunol 5:461.
151. Pandey S, Kawai T, Akira S. 2014. Microbial sensing by Toll-like receptors and intracellular nucleic acid sensors. Cold Spring Harb Perspect Biol 7:a016246.
152. Shim HK, Kim JY, Kim MJ, Sim HS, Park DW, Sohn JW, Kim MJ. 2009. *Legionella* lipoprotein activates toll-like receptor 2 and induces cytokine production and expression of costimulatory molecules in peritoneal macrophages. Exp Mol Med 41:687-94.
153. Girard R, Pedron T, Uematsu S, Balloy V, Chignard M, Akira S, Chaby R. 2003. Lipopolysaccharides from *Legionella* and Rhizobium stimulate mouse bone marrow granulocytes via Toll-like receptor 2. J Cell Sci 116:293-302.
154. Newton CA, Perkins I, Widen RH, Friedman H, Klein TW. 2007. Role of Toll-like receptor 9 in *Legionella pneumophila*-induced interleukin-12 p40 production

in bone marrow-derived dendritic cells and macrophages from permissive and nonpermissive mice. Infect Immun 75:146-51.
155. Hawn TR, Berrington WR, Smith IA, Uematsu S, Akira S, Aderem A, Smith KD, Skerrett SJ. 2007. Altered inflammatory responses in TLR5-deficient mice infected with *Legionella pneumophila*. J Immunol 179:6981-7.
156. Zahringer U, Knirel YA, Lindner B, Helbig JH, Sonesson A, Marre R, Rietschel ET. 1995. The lipopolysaccharide of *Legionella pneumophila* serogroup 1 (strain Philadelphia 1): chemical structure and biological significance. Prog Clin Biol Res 392:113-39.
157. Akamine M, Higa F, Arakaki N, Kawakami K, Takeda K, Akira S, Saito A. 2005. Differential roles of Toll-like receptors 2 and 4 in in vitro responses of macrophages to *Legionella pneumophila*. Infect Immun 73:352-61.
158. Lettinga KD, Florquin S, Speelman P, van Ketel R, van der Poll T, Verbon A. 2002. Toll-like receptor 4 is not involved in host defense against pulmonary *Legionella pneumophila* infection in a mouse model. J Infect Dis 186:570-3.
159. Archer KA, Roy CR. 2006. MyD88-dependent responses involving toll-like receptor 2 are important for protection and clearance of *Legionella pneumophila* in a mouse model of Legionnaires' disease. Infect Immun 74:3325-33.
160. Hawn TR, Smith KD, Aderem A, Skerrett SJ. 2006. Myeloid differentiation primary response gene (88)- and toll-like receptor 2-deficient mice are susceptible to infection with aerosolized *Legionella pneumophila*. J Infect Dis 193:1693-702.
161. Hawn TR, Verbon A, Lettinga KD, Zhao LP, Li SS, Laws RJ, Skerrett SJ, Beutler B, Schroeder L, Nachman A, Ozinsky A, Smith KD, Aderem A. 2003. A common dominant TLR5 stop codon polymorphism abolishes flagellin signaling and is associated with susceptibility to legionnaires' disease. J Exp Med 198:1563-72.
162. Archer KA, Alexopoulou L, Flavell RA, Roy CR. 2009. Multiple MyD88-dependent responses contribute to pulmonary clearance of *Legionella pneumophila*. Cell Microbiol 11:21-36.
163. Mascarenhas DP, Pereira MS, Manin GZ, Hori JI, Zamboni DS. 2015. Interleukin 1 receptor-driven neutrophil recruitment accounts to MyD88-dependent pulmonary clearance of *Legionella pneumophila* infection in vivo. J Infect Dis 211:322-30.
164. Lamkanfi M, Dixit VM. 2009. The inflammasomes. PLoS Pathog 5:e1000510.
165. Malik A, Kanneganti TD. 2017. Inflammasome activation and assembly at a glance. J Cell Sci 130:3955-3963.
166. Amer A, Franchi L, Kanneganti TD, Body-Malapel M, Ozoren N, Brady G, Meshinchi S, Jagirdar R, Gewirtz A, Akira S, Nunez G. 2006. Regulation of *Legionella* phagosome maturation and infection through flagellin and host Ipaf. J Biol Chem 281:35217-23.
167. Molofsky AB, Byrne BG, Whitfield NN, Madigan CA, Fuse ET, Tateda K, Swanson MS. 2006. Cytosolic recognition of flagellin by mouse macrophages restricts *Legionella pneumophila* infection. J Exp Med 203:1093-104.
168. Ren T, Zamboni DS, Roy CR, Dietrich WF, Vance RE. 2006. Flagellin-deficient *Legionella* mutants evade caspase-1- and Naip5-mediated macrophage immunity. PLoS Pathog 2:e18.
169. Zamboni DS, Kobayashi KS, Kohlsdorf T, Ogura Y, Long EM, Vance RE, Kuida K, Mariathasan S, Dixit VM, Flavell RA, Dietrich WF, Roy CR. 2006. The Birc1e

cytosolic pattern-recognition receptor contributes to the detection and control of *Legionella pneumophila* infection. Nat Immunol 7:318-25.
170. Pereira MS, Morgantetti GF, Massis LM, Horta CV, Hori JI, Zamboni DS. 2011. Activation of NLRC4 by flagellated bacteria triggers caspase-1-dependent and -independent responses to restrict *Legionella pneumophila* replication in macrophages and in vivo. J Immunol 187:6447-55.
171. Akhter A, Gavrilin MA, Frantz L, Washington S, Ditty C, Limoli D, Day C, Sarkar A, Newland C, Butchar J, Marsh CB, Wewers MD, Tridandapani S, Kanneganti TD, Amer AO. 2009. Caspase-7 activation by the Nlrc4/Ipaf inflammasome restricts *Legionella pneumophila* infection. PLoS Pathog 5:e1000361.
172. Case CL, Shin S, Roy CR. 2009. Asc and Ipaf Inflammasomes direct distinct pathways for caspase-1 activation in response to *Legionella pneumophila*. Infect Immun 77:1981-91.
173. Mascarenhas DPA, Cerqueira DM, Pereira MSF, Castanheira FVS, Fernandes TD, Manin GZ, Cunha LD, Zamboni DS. 2017. Inhibition of caspase-1 or gasdermin-D enable caspase-8 activation in the Naip5/NLRC4/ASC inflammasome. PLoS Pathog 13:e1006502.
174. Goncalves AV, Margolis SR, Quirino GFS, Mascarenhas DPA, Rauch I, Nichols RD, Ansaldo E, Fontana MF, Vance RE, Zamboni DS. 2019. Gasdermin-D and Caspase-7 are the key Caspase-1/8 substrates downstream of the NAIP5/NLRC4 inflammasome required for restriction of *Legionella pneumophila*. PLoS Pathog 15:e1007886.
175. Ziltener P, Reinheckel T, Oxenius A. 2016. Neutrophil and Alveolar Macrophage-Mediated Innate Immune Control of *Legionella pneumophila* Lung Infection via TNF and ROS. PLoS Pathog 12:e1005591.
176. Barry KC, Fontana MF, Portman JL, Dugan AS, Vance RE. 2013. IL-1alpha signaling initiates the inflammatory response to virulent *Legionella pneumophila* in vivo. J Immunol 190:6329-39.
177. Copenhaver AM, Casson CN, Nguyen HT, Duda MM, Shin S. 2015. IL-1R signaling enables bystander cells to overcome bacterial blockade of host protein synthesis. Proc Natl Acad Sci U S A 112:7557-62.
178. Baskerville A, Fitzgeorge RB, Broster M, Hambleton P, Dennis PJ. 1981. Experimental transmission of legionnaires' disease by exposure to aerosols of *Legionella pneumophila*. Lancet 2:1389-90.
179. Brieland J, Freeman P, Kunkel R, Chrisp C, Hurley M, Fantone J, Engleberg C. 1994. Replicative *Legionella pneumophila* lung infection in intratracheally inoculated A/J mice. A murine model of human Legionnaires' disease. Am J Pathol 145:1537-46.
180. Casson CN, Doerner JL, Copenhaver AM, Ramirez J, Holmgren AM, Boyer MA, Siddarthan IJ, Rouhanifard SH, Raj A, Shin S. 2017. Neutrophils and Ly6Chi monocytes collaborate in generating an optimal cytokine response that protects against pulmonary *Legionella pneumophila* infection. PLoS Pathog 13:e1006309.
181. LeibundGut-Landmann S, Weidner K, Hilbi H, Oxenius A. 2011. Nonhematopoietic cells are key players in innate control of bacterial airway infection. J Immunol 186:3130-7.
182. Tateda K, Moore TA, Newstead MW, Tsai WC, Zeng X, Deng JC, Chen G, Reddy R, Yamaguchi K, Standiford TJ. 2001. Chemokine-dependent neutrophil

recruitment in a murine model of *Legionella* pneumonia: potential role of neutrophils as immunoregulatory cells. Infect Immun 69:2017-24.
183. Tateda K, Moore TA, Deng JC, Newstead MW, Zeng X, Matsukawa A, Swanson MS, Yamaguchi K, Standiford TJ. 2001. Early recruitment of neutrophils determines subsequent T1/T2 host responses in a murine model of *Legionella pneumophila* pneumonia. J Immunol 166:3355-61.
184. Cai S, Batra S, Langohr I, Iwakura Y, Jeyaseelan S. 2016. IFN-gamma induction by neutrophil-derived IL-17A homodimer augments pulmonary antibacterial defense. Mucosal Immunol 9:718-29.
185. Brown AS, Yang C, Fung KY, Bachem A, Bourges D, Bedoui S, Hartland EL, van Driel IR. 2016. Cooperation between Monocyte-Derived Cells and Lymphoid Cells in the Acute Response to a Bacterial Lung Pathogen. PLoS Pathog 12:e1005691.
186. Tsou CL, Peters W, Si Y, Slaymaker S, Aslanian AM, Weisberg SP, Mack M, Charo IF. 2007. Critical roles for CCR2 and MCP-3 in monocyte mobilization from bone marrow and recruitment to inflammatory sites. J Clin Invest 117:902-9.
187. Brieland JK, Remick DG, Freeman PT, Hurley MC, Fantone JC, Engleberg NC. 1995. In vivo regulation of replicative *Legionella pneumophila* lung infection by endogenous tumor necrosis factor alpha and nitric oxide. Infect Immun 63:3253-8.
188. Fujita M, Ikegame S, Harada E, Ouchi H, Inoshima I, Watanabe K, Yoshida S, Nakanishi Y. 2008. TNF receptor 1 and 2 contribute in different ways to resistance to *Legionella pneumophila*-induced mortality in mice. Cytokine 44:298-303.
189. Asrat S, Dugan AS, Isberg RR. 2014. The frustrated host response to *Legionella pneumophila* is bypassed by MyD88-dependent translation of pro-inflammatory cytokines. PLoS Pathog 10:e1004229.
190. Barry KC, Ingolia NT, Vance RE. 2017. Global analysis of gene expression reveals mRNA superinduction is required for the inducible immune response to a bacterial pathogen. Elife 6e:22707.
191. Casson CN, Shin S. 2013. Inflammasome-mediated cell death in response to bacterial pathogens that access the host cell cytosol: lessons from *Legionella pneumophila*. Front Cell Infect Microbiol 3:111.
192. Sporri R, Joller N, Albers U, Hilbi H, Oxenius A. 2006. MyD88-dependent IFN-gamma production by NK cells is key for control of *Legionella pneumophila* infection. J Immunol 176:6162-71.
193. Brieland JK, Remick DG, LeGendre ML, Engleberg NC, Fantone JC. 1998. In vivo regulation of replicative *Legionella pneumophila* lung infection by endogenous interleukin-12. Infect Immun 66:65-9.
194. Shinozawa Y, Matsumoto T, Uchida K, Tsujimoto S, Iwakura Y, Yamaguchi K. 2002. Role of interferon-gamma in inflammatory responses in murine respiratory infection with *Legionella pneumophila*. J Med Microbiol 51:225-230.
195. Yang C, McDermot DS, Pasricha S, Brown AS, Bedoui S, Lenz LL, van Driel IR, Hartland EL. 2020. IFNgamma receptor down-regulation facilitates *Legionella* survival in alveolar macrophages. J Leukoc Biol 107:273-284.
196. Akamine M, Higa F, Haranaga S, Tateyama M, Mori N, Heuner K, Fujita J. 2007. Interferon-gamma reverses the evasion of Birc1e/Naip5 gene mediated murine

macrophage immunity by *Legionella pneumophila* mutant lacking flagellin. Microbiol Immunol 51:279-87.
197. Bhardwaj N, Nash TW, Horwitz MA. 1986. Interferon-gamma-activated human monocytes inhibit the intracellular multiplication of *Legionella pneumophila*. J Immunol 137:2662-9.
198. Plumlee CR, Lee C, Beg AA, Decker T, Shuman HA, Schindler C. 2009. Interferons direct an effective innate response to *Legionella pneumophila* infection. J Biol Chem 284:30058-66.
199. Pilla-Moffett D, Barber MF, Taylor GA, Coers J. 2016. Interferon-Inducible GTPases in Host Resistance, Inflammation and Disease. J Mol Biol 428:3495-513.
200. Naujoks J, Lippmann J, Suttorp N, Opitz B. 2018. Innate sensing and cell-autonomous resistance pathways in *Legionella pneumophila* infection. Int J Med Microbiol 308:161-167.
201. Price JV, Russo D, Ji DX, Chavez RA, DiPeso L, Lee AY, Coers J, Vance RE. 2019. IRG1 and Inducible Nitric Oxide Synthase Act Redundantly with Other Interferon-Gamma-Induced Factors To Restrict Intracellular Replication of *Legionella pneumophila*. mBio 10:e02629-19.
202. Case CL, Kohler LJ, Lima JB, Strowig T, de Zoete MR, Flavell RA, Zamboni DS, Roy CR. 2013. Caspase-11 stimulates rapid flagellin-independent pyroptosis in response to *Legionella pneumophila*. Proc Natl Acad Sci U S A 110:1851-6.
203. Liu BC, Sarhan J, Panda A, Muendlein HI, Ilyukha V, Coers J, Yamamoto M, Isberg RR, Poltorak A. 2018. Constitutive Interferon Maintains GBP Expression Required for Release of Bacterial Components Upstream of Pyroptosis and Anti-DNA Responses. Cell Rep 24:155-168 e5.
204. Pilla DM, Hagar JA, Haldar AK, Mason AK, Degrandi D, Pfeffer K, Ernst RK, Yamamoto M, Miao EA, Coers J. 2014. Guanylate binding proteins promote caspase-11-dependent pyroptosis in response to cytoplasmic LPS. Proc Natl Acad Sci U S A 111:6046-51.
205. Kayagaki N, Wong MT, Stowe IB, Ramani SR, Gonzalez LC, Akashi-Takamura S, Miyake K, Zhang J, Lee WP, Muszynski A, Forsberg LS, Carlson RW, Dixit VM. 2013. Noncanonical inflammasome activation by intracellular LPS independent of TLR4. Science 341:1246-9.
206. Feeley EM, Pilla-Moffett DM, Zwack EE, Piro AS, Finethy R, Kolb JP, Martinez J, Brodsky IE, Coers J. 2017. Galectin-3 directs antimicrobial guanylate binding proteins to vacuoles furnished with bacterial secretion systems. Proc Natl Acad Sci U S A 114:E1698-E1706.
207. Liles MR, Viswanathan VK, Cianciotto NP. 1998. Identification and temperature regulation of *Legionella pneumophila* genes involved in type IV pilus biogenesis and type II protein secretion. Infect Immun 66:1776-82.
208. Berger KH, Isberg RR. 1993. Two distinct defects in intracellular growth complemented by a single genetic locus in *Legionella pneumophila*. Mol Microbiol 7:7-19.
209. Jacobi S, Heuner K. 2003. Description of a putative type I secretion system in *Legionella pneumophila*. Int J Med Microbiol 293:349-58.
210. Tseng TT, Tyler BM, Setubal JC. 2009. Protein secretion systems in bacterial-host associations, and their description in the Gene Ontology. BMC Microbiol 9 Suppl 1:S2.

211. Mackman N, Nicaud JM, Gray L, Holland IB. 1986. Secretion of haemolysin by Escherichia coli. Curr Top Microbiol Immunol 125:159-81.
212. Lazdunski A, Guzzo J, Filloux A, Bally M, Murgier M. 1990. Secretion of extracellular proteins by Pseudomonas aeruginosa. Biochimie 72:147-56.
213. Stanley P, Koronakis V, Hughes C. 1998. Acylation of Escherichia coli hemolysin: a unique protein lipidation mechanism underlying toxin function. Microbiol Mol Biol Rev 62:309-33.
214. Heuner K, Dietrich C, Steinert M, Gobel UB, Hacker J. 2000. Cloning and characterization of a *Legionella pneumophila*-specific gene encoding a member of the LysR family of transcriptional regulators. Mol Gen Genet 264:204-11.
215. Ferhat M, Atlan D, Vianney A, Lazzaroni JC, Doublet P, Gilbert C. 2009. The TolC protein of *Legionella pneumophila* plays a major role in multi-drug resistance and the early steps of host invasion. PLoS One 4:e7732.
216. Nishida T, Nakagawa N, Watanabe K, Shimizu T, Watarai M. 2019. Attenuated *Legionella pneumophila* Survives for a Long Period in an Environmental Water Site. Biomed Res Int 2019:8601346.
217. Fuche F, Vianney A, Andrea C, Doublet P, Gilbert C. 2015. Functional type 1 secretion system involved in *Legionella pneumophila* virulence. J Bacteriol 197:563-71.
218. Cirillo SL, Lum J, Cirillo JD. 2000. Identification of novel loci involved in entry by *Legionella pneumophila*. Microbiology 146 (Pt 6):1345-59.
219. Cirillo SL, Yan L, Littman M, Samrakandi MM, Cirillo JD. 2002. Role of the *Legionella pneumophila* rtxA gene in amoebae. Microbiology 148:1667-77.
220. Johnson TL, Abendroth J, Hol WG, Sandkvist M. 2006. Type II secretion: from structure to function. FEMS Microbiol Lett 255:175-86.
221. Natale P, Bruser T, Driessen AJ. 2008. Sec- and Tat-mediated protein secretion across the bacterial cytoplasmic membrane--distinct translocases and mechanisms. Biochim Biophys Acta 1778:1735-56.
222. Rossier O, Cianciotto NP. 2005. The *Legionella pneumophila* tatB gene facilitates secretion of phospholipase C, growth under iron-limiting conditions, and intracellular infection. Infect Immun 73:2020-32.
223. Rossier O, Starkenburg SR, Cianciotto NP. 2004. *Legionella pneumophila* type II protein secretion promotes virulence in the A/J mouse model of Legionnaires' disease pneumonia. Infect Immun 72:310-21.
224. Cianciotto NP. 2009. Many substrates and functions of type II secretion: lessons learned from *Legionella pneumophila*. Future Microbiol 4:797-805.
225. Ghosal D, Kim KW, Zheng H, Kaplan M, Truchan HK, Lopez AE, McIntire IE, Vogel JP, Cianciotto NP, Jensen GJ. 2019. In vivo structure of the *Legionella* type II secretion system by electron cryotomography. Nat Microbiol 4:2101-2108.
226. Rossier O, Cianciotto NP. 2001. Type II protein secretion is a subset of the PilD-dependent processes that facilitate intracellular infection by *Legionella pneumophila*. Infect Immun 69:2092-8.
227. Polesky AH, Ross JT, Falkow S, Tompkins LS. 2001. Identification of *Legionella pneumophila* genes important for infection of amoebas by signature-tagged mutagenesis. Infect Immun 69:977-87.
228. DebRoy S, Dao J, Soderberg M, Rossier O, Cianciotto NP. 2006. *Legionella pneumophila* type II secretome reveals unique exoproteins and a

chitinase that promotes bacterial persistence in the lung. Proc Natl Acad Sci U S A 103:19146-51.
229. Liles MR, Edelstein PH, Cianciotto NP. 1999. The prepilin peptidase is required for protein secretion by and the virulence of the intracellular pathogen *Legionella pneumophila*. Mol Microbiol 31:959-70.
230. Hales LM, Shuman HA. 1999. *Legionella pneumophila* contains a type II general secretion pathway required for growth in amoebae as well as for secretion of the Msp protease. Infect Immun 67:3662-6.
231. Rossier O, Dao J, Cianciotto NP. 2008. The type II secretion system of *Legionella pneumophila* elaborates two aminopeptidases, as well as a metalloprotease that contributes to differential infection among protozoan hosts. Appl Environ Microbiol 74:753-61.
232. Rossier O, Dao J, Cianciotto NP. 2009. A type II secreted RNase of *Legionella pneumophila* facilitates optimal intracellular infection of Hartmannella vermiformis. Microbiology 155:882-90.
233. Tyson JY, Pearce MM, Vargas P, Bagchi S, Mulhern BJ, Cianciotto NP. 2013. Multiple *Legionella pneumophila* Type II secretion substrates, including a novel protein, contribute to differential infection of the amoebae *Acanthamoeba castellanii*, Hartmannella vermiformis, and Naegleria lovaniensis. Infect Immun 81:1399-410.
234. Tyson JY, Vargas P, Cianciotto NP. 2014. The novel *Legionella pneumophila* type II secretion substrate NttC contributes to infection of amoebae Hartmannella vermiformis and Willaertia magna. Microbiology 160:2732-44.
235. Segal G, Russo JJ, Shuman HA. 1999. Relationships between a new type IV secretion system and the icm/dot virulence system of *Legionella pneumophila*. Mol Microbiol 34:799-809.
236. Bandyopadhyay P, Lang EA, Rasaputra KS, Steinman HM. 2013. Implication of the VirD4 coupling protein of the Lvh type 4 secretion system in virulence phenotypes of *Legionella pneumophila*. J Bacteriol 195:3468-75.
237. Bandyopadhyay P, Liu S, Gabbai CB, Venitelli Z, Steinman HM. 2007. Environmental mimics and the Lvh type IVA secretion system contribute to virulence-related phenotypes of *Legionella pneumophila*. Infect Immun 75:723-35.
238. Marra A, Blander SJ, Horwitz MA, Shuman HA. 1992. Identification of a *Legionella pneumophila* locus required for intracellular multiplication in human macrophages. Proc Natl Acad Sci U S A 89:9607-11.
239. Horwitz MA. 1987. Characterization of avirulent mutant *Legionella pneumophila* that survive but do not multiply within human monocytes. J Exp Med 166:1310-28.
240. Swanson MS, Isberg RR. 1996. Identification of *Legionella pneumophila* mutants that have aberrant intracellular fates. Infect Immun 64:2585-94.
241. Komano T, Yoshida T, Narahara K, Furuya N. 2000. The transfer region of IncI1 plasmid R64: similarities between R64 tra and *Legionella* icm/dot genes. Mol Microbiol 35:1348-59.
242. Segal G, Purcell M, Shuman HA. 1998. Host cell killing and bacterial conjugation require overlapping sets of genes within a 22-kb region of the *Legionella pneumophila* genome. Proc Natl Acad Sci U S A 95:1669-74.

243. Vogel JP, Andrews HL, Wong SK, Isberg RR. 1998. Conjugative transfer by the virulence system of *Legionella pneumophila*. Science 279:873-6.
244. Isberg RR, O'Connor TJ, Heidtman M. 2009. The *Legionella pneumophila* replication vacuole: making a cosy niche inside host cells. Nat Rev Microbiol 7:13-24.
245. Kwak MJ, Kim JD, Kim H, Kim C, Bowman JW, Kim S, Joo K, Lee J, Jin KS, Kim YG, Lee NK, Jung JU, Oh BH. 2017. Architecture of the type IV coupling protein complex of *Legionella pneumophila*. Nat Microbiol 2:17114.
246. Ghosal D, Jeong KC, Chang YW, Gyore J, Teng L, Gardner A, Vogel JP, Jensen GJ. 2019. Molecular architecture, polar targeting and biogenesis of the *Legionella* Dot/Icm T4SS. Nat Microbiol 4:1173-1182.
247. Bardill JP, Miller JL, Vogel JP. 2005. IcmS-dependent translocation of SdeA into macrophages by the *Legionella pneumophila* type IV secretion system. Mol Microbiol 56:90-103.
248. Campodonico EM, Chesnel L, Roy CR. 2005. A yeast genetic system for the identification and characterization of substrate proteins transferred into host cells by the *Legionella pneumophila* Dot/Icm system. Mol Microbiol 56:918-33.
249. Shohdy N, Efe JA, Emr SD, Shuman HA. 2005. Pathogen effector protein screening in yeast identifies *Legionella* factors that interfere with membrane trafficking. Proc Natl Acad Sci U S A 102:4866-71.
250. de Felipe KS, Glover RT, Charpentier X, Anderson OR, Reyes M, Pericone CD, Shuman HA. 2008. *Legionella* eukaryotic-like type IV substrates interfere with organelle trafficking. PLoS Pathog 4:e1000117.
251. Burstein D, Zusman T, Degtyar E, Viner R, Segal G, Pupko T. 2009. Genome-scale identification of *Legionella pneumophila* effectors using a machine learning approach. PLoS Pathog 5:e1000508.
252. Huang L, Boyd D, Amyot WM, Hempstead AD, Luo ZQ, O'Connor TJ, Chen C, Machner M, Montminy T, Isberg RR. 2011. The E Block motif is associated with *Legionella pneumophila* translocated substrates. Cell Microbiol 13:227-45.
253. Gomez-Valero L, Rusniok C, Buchrieser C. 2009. *Legionella pneumophila*: population genetics, phylogeny and genomics. Infect Genet Evol 9:727-39.
254. Zhu W, Banga S, Tan Y, Zheng C, Stephenson R, Gately J, Luo ZQ. 2011. Comprehensive identification of protein substrates of the Dot/Icm type IV transporter of *Legionella pneumophila*. PLoS One 6:e17638.
255. Newton HJ, Ang DK, van Driel IR, Hartland EL. 2010. Molecular pathogenesis of infections caused by *Legionella pneumophila*. Clin Microbiol Rev 23:274-98.
256. Qiu J, Luo Z-Q. 2014. Effector Translocation by the *Legionella* Dot/Icm Type IV Secretion System, p 103-115. *In* Hilbi H (ed), Molecular Mechanisms in *Legionella* Pathogenesis, vol 376. Springer Berlin Heidelberg.
257. Michard C, Doublet P. 2015. Post-translational modifications are key players of the *Legionella pneumophila* infection strategy. Front Microbiol 6:87.
258. Xu L, Shen X, Bryan A, Banga S, Swanson MS, Luo ZQ. 2010. Inhibition of host vacuolar H+-ATPase activity by a *Legionella pneumophila* effector. PLoS Pathog 6:e1000822.
259. Harding CR, Mattheis C, Mousnier A, Oates CV, Hartland EL, Frankel G, Schroeder GN. 2013. LtpD is a novel *Legionella pneumophila* effector that binds phosphatidylinositol 3-phosphate and inositol monophosphatase IMPA1. Infect Immun 81:4261-70.

260. Jank T, Bohmer KE, Tzivelekidis T, Schwan C, Belyi Y, Aktories K. 2012. Domain organization of *Legionella* effector SetA. Cell Microbiol 14:852-68.
261. Levanova N, Mattheis C, Carson D, To KN, Jank T, Frankel G, Aktories K, Schroeder GN. 2019. The *Legionella* effector LtpM is a new type of phosphoinositide-activated glucosyltransferase. J Biol Chem 294:2862-2879.
262. Pike CM, Boyer-Andersen R, Kinch LN, Caplan JL, Neunuebel MR. 2019. The *Legionella* effector RavD binds phosphatidylinositol-3-phosphate and helps suppress endolysosomal maturation of the *Legionella*-containing vacuole. J Biol Chem 294:6405-6415.
263. Toulabi L, Wu X, Cheng Y, Mao Y. 2013. Identification and structural characterization of a *Legionella* phosphoinositide phosphatase. J Biol Chem 288:24518-27.
264. Gaspar AH, Machner MP. 2014. VipD is a Rab5-activated phospholipase A1 that protects *Legionella pneumophila* from endosomal fusion. Proc Natl Acad Sci U S A 111:4560-5.
265. Weber S, Stirnimann CU, Wieser M, Frey D, Meier R, Engelhardt S, Li X, Capitani G, Kammerer RA, Hilbi H. 2014. A type IV translocated *Legionella* cysteine phytase counteracts intracellular growth restriction by phytate. J Biol Chem 289:34175-88.
266. Dong N, Niu M, Hu L, Yao Q, Zhou R, Shao F. 2016. Modulation of membrane phosphoinositide dynamics by the phosphatidylinositide 4-kinase activity of the *Legionella* LepB effector. Nat Microbiol 2:16236.
267. Hsu F, Zhu W, Brennan L, Tao L, Luo ZQ, Mao Y. 2012. Structural basis for substrate recognition by a unique *Legionella* phosphoinositide phosphatase. Proc Natl Acad Sci U S A 109:13567-72.
268. Speir M, Vogrin A, Seidi A, Abraham G, Hunot S, Han Q, Dorn GW, 2nd, Masters SL, Flavell RA, Vince JE, Naderer T. 2017. *Legionella pneumophila* Strain 130b Evades Macrophage Cell Death Independent of the Effector SidF in the Absence of Flagellin. Front Cell Infect Microbiol 7:35.
269. Barlocher K, Hutter CAJ, Swart AL, Steiner B, Welin A, Hohl M, Letourneur F, Seeger MA, Hilbi H. 2017. Structural insights into *Legionella* RidL-Vps29 retromer subunit interaction reveal displacement of the regulator TBC1D5. Nat Commun 8:1543.
270. Swanson MS, Isberg RR. 1995. Association of *Legionella pneumophila* with the macrophage endoplasmic reticulum. Infect Immun 63:3609-20.
271. Ingmundson A, Delprato A, Lambright DG, Roy CR. 2007. *Legionella pneumophila* proteins that regulate Rab1 membrane cycling. Nature 450:365-9.
272. Machner MP, Isberg RR. 2006. Targeting of host Rab GTPase function by the intravacuolar pathogen *Legionella pneumophila*. Dev Cell 11:47-56.
273. Murata T, Delprato A, Ingmundson A, Toomre DK, Lambright DG, Roy CR. 2006. The *Legionella pneumophila* effector protein DrrA is a Rab1 guanine nucleotide-exchange factor. Nat Cell Biol 8:971-7.
274. Machner MP, Isberg RR. 2007. A bifunctional bacterial protein links GDI displacement to Rab1 activation. Science 318:974-7.
275. Schoebel S, Oesterlin LK, Blankenfeldt W, Goody RS, Itzen A. 2009. RabGDI displacement by DrrA from *Legionella* is a consequence of its guanine nucleotide exchange activity. Mol Cell 36:1060-72.

276. Muller MP, Peters H, Blumer J, Blankenfeldt W, Goody RS, Itzen A. 2010. The *Legionella* effector protein DrrA AMPylates the membrane traffic regulator Rab1b. Science 329:946-9.
277. Hsu F, Luo X, Qiu J, Teng YB, Jin J, Smolka MB, Luo ZQ, Mao Y. 2014. The *Legionella* effector SidC defines a unique family of ubiquitin ligases important for bacterial phagosomal remodeling. Proc Natl Acad Sci U S A 111:10538-43.
278. Qiu J, Sheedlo MJ, Yu K, Tan Y, Nakayasu ES, Das C, Liu X, Luo ZQ. 2016. Ubiquitination independent of E1 and E2 enzymes by bacterial effectors. Nature 533:120-4.
279. Neunuebel MR, Mohammadi S, Jarnik M, Machner MP. 2012. *Legionella pneumophila* LidA affects nucleotide binding and activity of the host GTPase Rab1. J Bacteriol 194:1389-400.
280. O'Connor TJ, Boyd D, Dorer MS, Isberg RR. 2012. Aggravating genetic interactions allow a solution to redundancy in a bacterial pathogen. Science 338:1440-4.
281. Neunuebel MR, Chen Y, Gaspar AH, Backlund PS, Jr., Yergey A, Machner MP. 2011. De-AMPylation of the small GTPase Rab1 by the pathogen *Legionella pneumophila*. Science 333:453-6.
282. Tan Y, Luo ZQ. 2011. *Legionella pneumophila* SidD is a deAMPylase that modifies Rab1. Nature 475:506-9.
283. Campanacci V, Mukherjee S, Roy CR, Cherfils J. 2013. Structure of the *Legionella* effector AnkX reveals the mechanism of phosphocholine transfer by the FIC domain. EMBO J 32:1469-77.
284. Mukherjee S, Liu X, Arasaki K, McDonough J, Galan JE, Roy CR. 2011. Modulation of Rab GTPase function by a protein phosphocholine transferase. Nature 477:103-6.
285. Tan Y, Arnold RJ, Luo ZQ. 2011. *Legionella pneumophila* regulates the small GTPase Rab1 activity by reversible phosphorylcholination. Proc Natl Acad Sci U S A 108:21212-7.
286. Hoffmann C, Finsel I, Otto A, Pfaffinger G, Rothmeier E, Hecker M, Becher D, Hilbi H. 2014. Functional analysis of novel Rab GTPases identified in the proteome of purified *Legionella*-containing vacuoles from macrophages. Cell Microbiol 16:1034-52.
287. Schmolders J, Manske C, Otto A, Hoffmann C, Steiner B, Welin A, Becher D, Hilbi H. 2017. Comparative Proteomics of Purified Pathogen Vacuoles Correlates Intracellular Replication of *Legionella pneumophila* with the Small GTPase Ras-related protein 1 (Rap1). Mol Cell Proteomics 16:622-641.
288. Shevchuk O, Batzilla C, Hagele S, Kusch H, Engelmann S, Hecker M, Haas A, Heuner K, Glockner G, Steinert M. 2009. Proteomic analysis of *Legionella*-containing phagosomes isolated from Dictyostelium. Int J Med Microbiol 299:489-508.
289. Urwyler S, Nyfeler Y, Ragaz C, Lee H, Mueller LN, Aebersold R, Hilbi H. 2009. Proteome analysis of *Legionella* vacuoles purified by magnetic immunoseparation reveals secretory and endosomal GTPases. Traffic 10:76-87.
290. Rothmeier E, Pfaffinger G, Hoffmann C, Harrison CF, Grabmayr H, Repnik U, Hannemann M, Wolke S, Bausch A, Griffiths G, Muller-Taubenberger A, Itzen A, Hilbi H. 2013. Activation of Ran GTPase by a *Legionella* effector promotes

microtubule polymerization, pathogen vacuole motility and infection. PLoS Pathog 9:e1003598.
291. Liu T, Zhang L, Joo D, Sun SC. 2017. NF-kappaB signaling in inflammation. Signal Transduct Target Ther 2.
292. Gan N, Nakayasu ES, Hollenbeck PJ, Luo ZQ. 2019. *Legionella pneumophila* inhibits immune signalling via MavC-mediated transglutaminase-induced ubiquitination of UBE2N. Nat Microbiol 4:134-143.
293. Wan M, Wang X, Huang C, Xu D, Wang Z, Zhou Y, Zhu Y. 2019. A bacterial effector deubiquitinase specifically hydrolyses linear ubiquitin chains to inhibit host inflammatory signalling. Nat Microbiol 4:1282-1293.
294. Kee Y, Huibregtse JM. 2007. Regulation of catalytic activities of HECT ubiquitin ligases. Biochem Biophys Res Commun 354:329-33.
295. Mu Y, Wang Y, Huang Y, Li D, Han Y, Chang M, Fu J, Xie Y, Ren J, Wang H, Zhang Y, Luo ZQ, Feng Y. 2020. Structural insights into the mechanism and inhibition of transglutaminase-induced ubiquitination by the *Legionella* effector MavC. Nat Commun 11:1774.
296. Fontana MF, Banga S, Barry KC, Shen X, Tan Y, Luo ZQ, Vance RE. 2011. Secreted bacterial effectors that inhibit host protein synthesis are critical for induction of the innate immune response to virulent *Legionella pneumophila*. PLoS Pathog 7:e1001289.
297. Moss SM, Taylor IR, Ruggero D, Gestwicki JE, Shokat KM, Mukherjee S. 2019. A *Legionella pneumophila* Kinase Phosphorylates the Hsp70 Chaperone Family to Inhibit Eukaryotic Protein Synthesis. Cell Host Microbe 25:454-462 e6.
298. Shen X, Banga S, Liu Y, Xu L, Gao P, Shamovsky I, Nudler E, Luo ZQ. 2009. Targeting eEF1A by a *Legionella pneumophila* effector leads to inhibition of protein synthesis and induction of host stress response. Cell Microbiol 11:911-26.
299. Clarke M, Lohan AJ, Liu B, Lagkouvardos I, Roy S, Zafar N, Bertelli C, Schilde C, Kianianmomeni A, Burglin TR, Frech C, Turcotte B, Kopec KO, Synnott JM, Choo C, Paponov I, Finkler A, Heng Tan CS, Hutchins AP, Weinmeier T, Rattei T, Chu JS, Gimenez G, Irimia M, Rigden DJ, Fitzpatrick DA, Lorenzo-Morales J, Bateman A, Chiu CH, Tang P, Hegemann P, Fromm H, Raoult D, Greub G, Miranda-Saavedra D, Chen N, Nash P, Ginger ML, Horn M, Schaap P, Caler L, Loftus BJ. 2013. Genome of *Acanthamoeba castellanii* highlights extensive lateral gene transfer and early evolution of tyrosine kinase signaling. Genome Biol 14:R11.
300. Fritz-Laylin LK, Prochnik SE, Ginger ML, Dacks JB, Carpenter ML, Field MC, Kuo A, Paredez A, Chapman J, Pham J, Shu S, Neupane R, Cipriano M, Mancuso J, Tu H, Salamov A, Lindquist E, Shapiro H, Lucas S, Grigoriev IV, Cande WZ, Fulton C, Rokhsar DS, Dawson SC. 2010. The genome of Naegleria gruberi illuminates early eukaryotic versatility. Cell 140:631-42.
301. Olie RA, Durrieu F, Cornillon S, Loughran G, Gross J, Earnshaw WC, Golstein P. 1998. Apparent caspase independence of programmed cell death in Dictyostelium. Curr Biol 8:955-8.
302. Losick VP, Isberg RR. 2006. NF-kappaB translocation prevents host cell death after low-dose challenge by *Legionella pneumophila*. J Exp Med 203:2177-89.
303. Abu-Zant A, Jones S, Asare R, Suttles J, Price C, Graham J, Kwaik YA. 2007. Anti-apoptotic signalling by the Dot/Icm secretion system of *L. pneumophila*. Cell Microbiol 9:246-64.

304. Bartfeld S, Engels C, Bauer B, Aurass P, Flieger A, Bruggemann H, Meyer TF. 2009. Temporal resolution of two-tracked NF-kappaB activation by *Legionella pneumophila*. Cell Microbiol 11:1638-51.
305. Losick VP, Haenssler E, Moy MY, Isberg RR. 2010. LnaB: a *Legionella pneumophila* activator of NF-kappaB. Cell Microbiol 12:1083-97.
306. Ge J, Xu H, Li T, Zhou Y, Zhang Z, Li S, Liu L, Shao F. 2009. A *Legionella* type IV effector activates the NF-kappaB pathway by phosphorylating the IkappaB family of inhibitors. Proc Natl Acad Sci U S A 106:13725-30.
307. Speir M, Lawlor KE, Glaser SP, Abraham G, Chow S, Vogrin A, Schulze KE, Schuelein R, O'Reilly LA, Mason K, Hartland EL, Lithgow T, Strasser A, Lessene G, Huang DC, Vince JE, Naderer T. 2016. Eliminating *Legionella* by inhibiting BCL-XL to induce macrophage apoptosis. Nat Microbiol 1:15034.
308. Banga S, Gao P, Shen X, Fiscus V, Zong WX, Chen L, Luo ZQ. 2007. *Legionella pneumophila* inhibits macrophage apoptosis by targeting pro-death members of the Bcl2 protein family. Proc Natl Acad Sci U S A 104:5121-6.
309. Zhu W, Hammad LA, Hsu F, Mao Y, Luo ZQ. 2013. Induction of caspase 3 activation by multiple *Legionella pneumophila* Dot/Icm substrates. Cell Microbiol 15:1783-95.
310. Ong SY. 2017. Investigation of host factors involved in *Legionella pneumophila* virulence. Doctor of Philosophy (PhD). The University of Melbourne, Melbourne, Australia.
311. Seemann T. 2015. Snippy: fast bacterial variant calling from NGS reads. https://github.com/tseemann/snippy. Accessed March 2020.
312. Bankevich A, Nurk S, Antipov D, Gurevich AA, Dvorkin M, Kulikov AS, Lesin VM, Nikolenko SI, Pham S, Prjibelski AD, Pyshkin AV, Sirotkin AV, Vyahhi N, Tesler G, Alekseyev MA, Pevzner PA. 2012. SPAdes: a new genome assembly algorithm and its applications to single-cell sequencing. J Comput Biol 19:455-77.
313. Love MI, Huber W, Anders S. 2014. Moderated estimation of fold change and dispersion for RNA-seq data with DESeq2. Genome Biol 15:550.
314. Oliveros JC. 2007. VENNY. An interactive tool for comparing lists with Venn Diagrams. https://bioinfogp.cnb.csic.es/tools/venny/index.html. Accessed January 2020
315. Thomas PD, Campbell MJ, Kejariwal A, Mi H, Karlak B, Daverman R, Diemer K, Muruganujan A, Narechania A. 2003. PANTHER: a library of protein families and subfamilies indexed by function. Genome Res 13:2129-41.
316. Boyle EI, Weng S, Gollub J, Jin H, Botstein D, Cherry JM, Sherlock G. 2004. GO::TermFinder--open source software for accessing Gene Ontology information and finding significantly enriched Gene Ontology terms associated with a list of genes. Bioinformatics 20:3710-5.
317. Ng GZ, Solomatina A, van Driel IR, Hartland EL. 2019. The Mouse as a Model for Pulmonary *Legionella* Infection. Methods Mol Biol 1921:399-417.
318. Carver T, Harris SR, Berriman M, Parkhill J, McQuillan JA. 2012. Artemis: an integrated platform for visualization and analysis of high-throughput sequence-based experimental data. Bioinformatics 28:464-9.
319. Carver T, Thomson N, Bleasby A, Berriman M, Parkhill J. 2009. DNAPlotter: circular and linear interactive genome visualization. Bioinformatics 25:119-20.

320. Camacho C, Coulouris G, Avagyan V, Ma N, Papadopoulos J, Bealer K, Madden TL. 2009. BLAST+: architecture and applications. BMC Bioinformatics 10:421.
321. Carver T, Berriman M, Tivey A, Patel C, Bohme U, Barrell BG, Parkhill J, Rajandream MA. 2008. Artemis and ACT: viewing, annotating and comparing sequences stored in a relational database. Bioinformatics 24:2672-6.
322. Mitchell AL, Attwood TK, Babbitt PC, Blum M, Bork P, Bridge A, Brown SD, Chang HY, El-Gebali S, Fraser MI, Gough J, Haft DR, Huang H, Letunic I, Lopez R, Luciani A, Madeira F, Marchler-Bauer A, Mi H, Natale DA, Necci M, Nuka G, Orengo C, Pandurangan AP, Paysan-Lafosse T, Pesseat S, Potter SC, Qureshi MA, Rawlings ND, Redaschi N, Richardson LJ, Rivoire C, Salazar GA, Sangrador-Vegas A, Sigrist CJA, Sillitoe I, Sutton GG, Thanki N, Thomas PD, Tosatto SCE, Yong SY, Finn RD. 2019. InterPro in 2019: improving coverage, classification and access to protein sequence annotations. Nucleic Acids Res 47:D351-D360.
323. Kelley LA, Mezulis S, Yates CM, Wass MN, Sternberg MJ. 2015. The Phyre2 web portal for protein modeling, prediction and analysis. Nat Protoc 10:845-58.
324. Roy A, Kucukural A, Zhang Y. 2010. I-TASSER: a unified platform for automated protein structure and function prediction. Nat Protoc 5:725-38.
325. Soding J, Biegert A, Lupas AN. 2005. The HHpred interactive server for protein homology detection and structure prediction. Nucleic Acids Res 33:W244-8.
326. Wang S, Li W, Liu S, Xu J. 2016. RaptorX-Property: a web server for protein structure property prediction. Nucleic Acids Res 44:W430-5.
327. McDonnell AV, Jiang T, Keating AE, Berger B. 2006. Paircoil2: improved prediction of coiled coils from sequence. Bioinformatics 22:356-8.
328. Edgar RC. 2004. MUSCLE: a multiple sequence alignment method with reduced time and space complexity. BMC Bioinformatics 5:113.
329. Edelstein PH. 1986. Control of *Legionella* in hospitals. J Hosp Infect 8:109-15.
330. Riedmaier P, Sansom FM, Sofian T, Beddoe T, Schuelein R, Newton HJ, Hartland EL. 2014. Multiple ecto-nucleoside triphosphate diphosphohydrolases facilitate intracellular replication of *Legionella pneumophila*. Biochem J 462:279-89.
331. Merriam JJ, Mathur R, Maxfield-Boumil R, Isberg RR. 1997. Analysis of the *Legionella pneumophila* fliI gene: intracellular growth of a defined mutant defective for flagellum biosynthesis. Infect Immun 65:2497-501.
332. Creasey EA, Isberg RR. 2012. The protein SdhA maintains the integrity of the *Legionella*-containing vacuole. Proc Natl Acad Sci U S A 109:3481-6.
333. Harding CR, Stoneham CA, Schuelein R, Newton H, Oates CV, Hartland EL, Schroeder GN, Frankel G. 2013. The Dot/Icm effector SdhA is necessary for virulence of *Legionella pneumophila* in Galleria mellonella and A/J mice. Infect Immun 81:2598-605.
334. Shames SR, Liu L, Havey JC, Schofield WB, Goodman AL, Roy CR. 2017. Multiple *Legionella pneumophila* effector virulence phenotypes revealed through high-throughput analysis of targeted mutant libraries. Proc Natl Acad Sci U S A 114:E10446-E10454.
335. Kubori T, Shinzawa N, Kanuka H, Nagai H. 2010. *Legionella* metaeffector exploits host proteasome to temporally regulate cognate effector. PLoS Pathog 6:e1001216.
336. Joseph AM, Pohl AE, Ball TJ, Abram TG, Johnson DK, Geisbrecht BV, Shames SR. 2020. The *Legionella pneumophila* metaeffector Lpg2505 (MesI) regulates

SidI-mediated translation inhibition and novel glycosyl hydrolase activity. Infect Immun doi:10.1128/IAI.00853-19.
337. Opijnen TV, Bodi KL, Camilli A. 2009. Tn-seq: high-throughput parallel sequencing for fitness and genetic interaction studies in microorganisms. Nat Methods 6:767-72.
338. O'Connor TJ, Adepoju Y, Boyd D, Isberg RR. 2011. Minimization of the *Legionella pneumophila* genome reveals chromosomal regions involved in host range expansion. Proc Natl Acad Sci U S A 108:14733-40.
339. Gomez-Valero L, Rusniok C, Cazalet C, Buchrieser C. 2011. Comparative and functional genomics of *Legionella* identified eukaryotic like proteins as key players in host-pathogen interactions. Front Microbiol 2:208.
340. Schuelein R, Spencer H, Dagley LF, Li PF, Luo L, Stow JL, Abraham G, Naderer T, Gomez-Valero L, Buchrieser C, Sugimoto C, Yamagishi J, Webb AI, Pasricha S, Hartland EL. 2018. Targeting of RNA Polymerase II by a nuclear *Legionella pneumophila* Dot/Icm effector SnpL. Cell Microbiol 20:e12852.
341. Schweizer HP. 2008. Bacterial genetics: past achievements, present state of the field, and future challenges. BioTechniques 44:633-641.
342. Andrews HL, Vogel JP, Isberg RR. 1998. Identification of linked *Legionella pneumophila* genes essential for intracellular growth and evasion of the endocytic pathway. Infect Immun 66:950-8.
343. Bowers LM, Kruger R, Filutowicz M. 2007. Mechanism of origin activation by monomers of R6K-encoded pi protein. J Mol Biol 368:928-38.
344. Gay P, Le Coq D, Steinmetz M, Ferrari E, Hoch JA. 1983. Cloning structural gene sacB, which codes for exoenzyme levansucrase of Bacillus subtilis: expression of the gene in Escherichia coli. J Bacteriol 153:1424-31.
345. Salamov VSA, Solovyevand AJM, its applications in agriculture. Nova Science Publishers H, NY, USA. 2011. Automatic annotation of microbial genomes and metagenomic sequences.61-78.
346. Fields BS. 1996. The molecular ecology of *Legionella*e. Trends Microbiol 4:286-90.
347. Wieland H, Ullrich S, Lang F, Neumeister B. 2005. Intracellular multiplication of *Legionella pneumophila* depends on host cell amino acid transporter SLC1A5. Mol Microbiol 55:1528-37.
348. Park JM, Ghosh S, O'Connor TJ. 2020. Combinatorial selection in amoebal hosts drives the evolution of the human pathogen *Legionella pneumophila*. Nat Microbiol doi:10.1038/s41564-019-0663-7.
349. Gao LY, Harb OS, Kwaik YA. 1998. Identification of macrophage-specific infectivity loci (mil) of *Legionella pneumophila* that are not required for infectivity of protozoa. Infect Immun 66:883-92.
350. Nash TW, Libby DM, Horwitz MA. 1988. IFN-gamma-activated human alveolar macrophages inhibit the intracellular multiplication of *Legionella pneumophila*. J Immunol 140:3978-81.
351. Watanabe M, Shimamoto Y, Yoshida S, Suga K, Mizuguchi Y, Kohashi O, Yamaguchi M. 1993. Intracellular multiplication of *Legionella pneumophila* in HL-60 cells differentiated by 1,25-dihydroxyvitamin D3 and the effect of interferon gamma. J Leukoc Biol 54:40-6.

352. Kusaka Y, Kajiwara C, Shimada S, Ishii Y, Miyazaki Y, Inase N, Standiford TJ, Tateda K. 2018. Potential Role of Gr-1+ CD8+ T Lymphocytes as a Source of Interferon-gamma and M1/M2 Polarization during the Acute Phase of Murine *Legionella pneumophila* Pneumonia. J Innate Immun 10:328-338.
353. Brieland J, Freeman P, Kunkel R, Chrisp C, Hurley M, Fantone J, Engleberg C. 1994. Replicative *Legionella pneumophila* lung infection in intratracheally inoculated A/J mice. A murine model of human Legionnaires' disease. Am J Pathol 145:1537-1546.
354. Horwitz MA, Silverstein SC. 1980. Legionnaires' disease bacterium (*Legionella pneumophila*) multiples intracellularly in human monocytes. J Clin Invest 66:441-50.
355. Fontana MF, Shin S, Vance RE. 2012. Activation of host mitogen-activated protein kinases by secreted *Legionella pneumophila* effectors that inhibit host protein translation. Infect Immun 80:3570-5.
356. Genin M, Clement F, Fattaccioli A, Raes M, Michiels C. 2015. M1 and M2 macrophages derived from THP-1 cells differentially modulate the response of cancer cells to etoposide. BMC Cancer 15:577.
357. Fujiwara Y, Hizukuri Y, Yamashiro K, Makita N, Ohnishi K, Takeya M, Komohara Y, Hayashi Y. 2016. Guanylate-binding protein 5 is a marker of interferon-gamma-induced classically activated macrophages. Clin Transl Immunology 5:e111.
358. Fitzgeorge RB, Baskerville A, Broster M, Hambleton P, Dennis PJ. 1983. Aerosol infection of animals with strains of *Legionella pneumophila* of different virulence: comparison with intraperitoneal and intranasal routes of infection. J Hyg (Lond) 90:81-9.
359. Diez E, Lee SH, Gauthier S, Yaraghi Z, Tremblay M, Vidal S, Gros P. 2003. Birc1e is the gene within the Lgn1 locus associated with resistance to *Legionella pneumophila*. Nat Genet 33:55-60.
360. Wright EK, Goodart SA, Growney JD, Hadinoto V, Endrizzi MG, Long EM, Sadigh K, Abney AL, Bernstein-Hanley I, Dietrich WF. 2003. Naip5 affects host susceptibility to the intracellular pathogen *Legionella pneumophila*. Curr Biol 13:27-36.
361. Brown AS, van Driel IR, Hartland EL. 2013. Mouse models of Legionnaires' disease. Curr Top Microbiol Immunol 376:271-91.
362. Altschul SF, Gish W, Miller W, Myers EW, Lipman DJ. 1990. Basic local alignment search tool. J Mol Biol 215:403-10.
363. Zimmermann L, Stephens A, Nam SZ, Rau D, Kubler J, Lozajic M, Gabler F, Soding J, Lupas AN, Alva V. 2018. A Completely Reimplemented MPI Bioinformatics Toolkit with a New HHpred Server at its Core. J Mol Biol 430:2237-2243.
364. Yang J, Yan R, Roy A, Xu D, Poisson J, Zhang Y. 2015. The I-TASSER Suite: protein structure and function prediction. Nat Methods 12:7-8.
365. Zhang Y. 2008. I-TASSER server for protein 3D structure prediction. BMC Bioinformatics 9:40.
366. Yang Y, Faraggi E, Zhao H, Zhou Y. 2011. Improving protein fold recognition and template-based modeling by employing probabilistic-based matching between predicted one-dimensional structural properties of query and corresponding native properties of templates. Bioinformatics 27:2076-82.

367. Ngwaga T, Hydock AJ, Ganesan S, Shames SR. 2019. Potentiation of Cytokine-Mediated Restriction of *Legionella* Intracellular Replication by a Dot/Icm-Translocated Effector. J Bacteriol 201:e00755-18.
368. Chanput W, Mes JJ, Wichers HJ. 2014. THP-1 cell line: an in vitro cell model for immune modulation approach. Int Immunopharmacol 23:37-45.
369. Susa M, Ticac B, Rukavina T, Doric M, Marre R. 1998. *Legionella pneumophila* infection in intratracheally inoculated T cell-depleted or -nondepleted A/J mice. J Immunol 160:316-21.
370. Brown AS, Yang C, Hartland EL, van Driel IR. 2017. The regulation of acute immune responses to the bacterial lung pathogen *Legionella pneumophila*. J Leukoc Biol 101:875-886.
371. Abu Khweek A, Kanneganti A, Guttridge DD, Amer AO. 2016. The Sphingosine-1-Phosphate Lyase (LegS2) Contributes to the Restriction of *Legionella pneumophila* in Murine Macrophages. PLoS One 11:e0146410.
372. Truebestein L, Leonard TA. 2016. Coiled-coils: The long and short of it. Bioessays 38:903-16.
373. Urbanus ML, Quaile AT, Stogios PJ, Morar M, Rao C, Di Leo R, Evdokimova E, Lam M, Oatway C, Cuff ME, Osipiuk J, Michalska K, Nocek BP, Taipale M, Savchenko A, Ensminger AW. 2016. Diverse mechanisms of metaeffector activity in an intracellular bacterial pathogen, *Legionella pneumophila*. Mol Syst Biol 12:893.
374. Gee K, Guzzo C, Che Mat NF, Ma W, Kumar A. 2009. The IL-12 family of cytokines in infection, inflammation and autoimmune disorders. Inflamm Allergy Drug Targets 8:40-52.
375. Fortier A, Faucher SP, Diallo K, Gros P. 2011. Global cellular changes induced by *Legionella pneumophila* infection of bone marrow-derived macrophages. Immunobiology 216:1274-85.
376. Price CT, Abu Kwaik Y. 2014. The transcriptome of *Legionella pneumophila*-infected human monocyte-derived macrophages. PLoS One 9:e114914.
377. Von Dwingelo J, Chung IYW, Price CT, Li L, Jones S, Cygler M, Abu Kwaik Y. 2019. Interaction of the Ankyrin H Core Effector of *Legionella* with the Host LARP7 Component of the 7SK snRNP Complex. mBio 10:e01942-19.
378. Lee PC, Machner MP. 2018. The *Legionella* Effector Kinase LegK7 Hijacks the Host Hippo Pathway to Promote Infection. Cell Host Microbe 24:429-438 e6.
379. Rolando M, Sanulli S, Rusniok C, Gomez-Valero L, Bertholet C, Sahr T, Margueron R, Buchrieser C. 2013. *Legionella pneumophila* effector RomA uniquely modifies host chromatin to repress gene expression and promote intracellular bacterial replication. Cell Host Microbe 13:395-405.
380. Meng Z, Moroishi T, Guan KL. 2016. Mechanisms of Hippo pathway regulation. Genes Dev 30:1-17.
381. Barboric M, Lenasi T, Chen H, Johansen EB, Guo S, Peterlin BM. 2009. 7SK snRNP/P-TEFb couples transcription elongation with alternative splicing and is essential for vertebrate development. Proc Natl Acad Sci U S A 106:7798-803.
382. He N, Jahchan NS, Hong E, Li Q, Bayfield MA, Maraia RJ, Luo K, Zhou Q. 2008. A La-related protein modulates 7SK snRNP integrity to suppress P-TEFb-dependent transcriptional elongation and tumorigenesis. Mol Cell 29:588-99.

383. Muniz L, Egloff S, Kiss T. 2013. RNA elements directing in vivo assembly of the 7SK/MePCE/Larp7 transcriptional regulatory snRNP. Nucleic Acids Res 41:4686-98.
384. Uchikawa E, Natchiar KS, Han X, Proux F, Roblin P, Zhang E, Durand A, Klaholz BP, Dock-Bregeon AC. 2015. Structural insight into the mechanism of stabilization of the 7SK small nuclear RNA by LARP7. Nucleic Acids Res 43:3373-88.
385. Xue Y, Yang Z, Chen R, Zhou Q. 2010. A capping-independent function of MePCE in stabilizing 7SK snRNA and facilitating the assembly of 7SK snRNP. Nucleic Acids Res 38:360-9.
386. Li T, Lu Q, Wang G, Xu H, Huang H, Cai T, Kan B, Ge J, Shao F. 2013. SET-domain bacterial effectors target heterochromatin protein 1 to activate host rDNA transcription. EMBO Rep 14:733-40.
387. Mosavi LK, Cammett TJ, Desrosiers DC, Peng ZY. 2004. The ankyrin repeat as molecular architecture for protein recognition. Protein Sci 13:1435-48.
388. Jolliffe IT, Cadima J. 2016. Principal component analysis: a review and recent developments. Philos Trans A Math Phys Eng Sci 374:20150202.
389. Mi H, Muruganujan A, Ebert D, Huang X, Thomas PD. 2019. PANTHER version 14: more genomes, a new PANTHER GO-slim and improvements in enrichment analysis tools. Nucleic Acids Res 47:D419-D426.
390. Kanehisa M, Goto S. 2000. KEGG: kyoto encyclopedia of genes and genomes. Nucleic Acids Res 28:27-30.
391. Rodriguez-Prados JC, Traves PG, Cuenca J, Rico D, Aragones J, Martin-Sanz P, Cascante M, Bosca L. 2010. Substrate fate in activated macrophages: a comparison between innate, classic, and alternative activation. J Immunol 185:605-14.
392. Van den Bossche J, Baardman J, de Winther MP. 2015. Metabolic Characterization of Polarized M1 and M2 Bone Marrow-derived Macrophages Using Real-time Extracellular Flux Analysis. J Vis Exp doi:10.3791/53424.
393. Escoll P, Song OR, Viana F, Steiner B, Lagache T, Olivo-Marin JC, Impens F, Brodin P, Hilbi H, Buchrieser C. 2017. *Legionella pneumophila* Modulates Mitochondrial Dynamics to Trigger Metabolic Repurposing of Infected Macrophages. Cell Host Microbe 22:302-316 e7.
394. Price JV, Jiang K, Galantowicz A, Freifeld A, Vance RE. 2018. *Legionella pneumophila* Is Directly Sensitive to 2-Deoxyglucose-Phosphate via Its UhpC Transporter but Is Indifferent to Shifts in Host Cell Glycolytic Metabolism. J Bacteriol 200:e00176-18.
395. Orecchioni M, Ghosheh Y, Pramod AB, Ley K. 2019. Macrophage Polarization: Different Gene Signatures in M1(LPS+) vs. Classically and M2(LPS-) vs. Alternatively Activated Macrophages. Front Immunol 10:1084.
396. Hackett EE, Charles-Messance H, O'Leary SM, Gleeson LE, Munoz-Wolf N, Case S, Wedderburn A, Johnston DGW, Williams MA, Smyth A, Ouimet M, Moore KJ, Lavelle EC, Corr SC, Gordon SV, Keane J, Sheedy FJ. 2020. *Mycobacterium tuberculosis* Limits Host Glycolysis and IL-1beta by Restriction of PFK-M via MicroRNA-21. Cell Rep 30:124-136 e4.
397. Wahl MC, Will CL, Luhrmann R. 2009. The spliceosome: design principles of a dynamic RNP machine. Cell 136:701-18.

398. Doucet AJ, Droc G, Siol O, Audoux J, Gilbert N. 2015. U6 snRNA Pseudogenes: Markers of Retrotransposition Dynamics in Mammals. Mol Biol Evol 32:1815-32.
399. Domitrovich AM, Kunkel GR. 2003. Multiple, dispersed human U6 small nuclear RNA genes with varied transcriptional efficiencies. Nucleic Acids Res 31:2344-52.
400. Brow DA, Guthrie C. 1990. Transcription of a yeast U6 snRNA gene requires a polymerase III promoter element in a novel position. Genes Dev 4:1345-56.
401. Chen Y, Sinha K, Perumal K, Reddy R. 2000. Effect of 3' terminal adenylic acid residue on the uridylation of human small RNAs in vitro and in frog oocytes. RNA 6:1277-88.
402. Zhang L, Wan Y, Huang G, Wang D, Yu X, Huang G, Guo J. 2015. The exosome controls alternative splicing by mediating the gene expression and assembly of the spliceosome complex. Sci Rep 5:13403.
403. Bozue JA, Johnson W. 1996. Interaction of *Legionella pneumophila* with *Acanthamoeba castellanii*: uptake by coiling phagocytosis and inhibition of phagosome-lysosome fusion. Infect Immun 64:668-73.
404. Yan L, Cerny RL, Cirillo JD. 2004. Evidence that hsp90 is involved in the altered interactions of *Acanthamoeba castellanii* variants with bacteria. Eukaryot Cell 3:567-78.
405. Mou Q, Leung PHM. 2018. Differential expression of virulence genes in *Legionella pneumophila* growing in *Acanthamoeba* and human monocytes. Virulence 9:185-196.
406. Lloyd D. 2014. Encystment in *Acanthamoeba castellanii*: a review. Exp Parasitol 145 Suppl:S20-7.
407. Farbrother P, Wagner C, Na J, Tunggal B, Morio T, Urushihara H, Tanaka Y, Schleicher M, Steinert M, Eichinger L. 2006. *Dictyostelium* transcriptional host cell response upon infection with *Legionella*. Cell Microbiol 8:438-56.
408. Recalcati S, Gammella E, Cairo G. 2019. Ironing out Macrophage Immunometabolism. Pharmaceuticals (Basel) 12:94.
409. Song G, Lu Q, Fan H, Zhang X, Ge L, Tian R, Wang S, Feng T, Pan J, Feng J, Xiao Y, Yi X, Ren N, Wang L. 2019. Inhibition of hexokinases holds potential as treatment strategy for rheumatoid arthritis. Arthritis Res Ther 21:87.
410. Tan Z, Xie N, Cui H, Moellering DR, Abraham E, Thannickal VJ, Liu G. 2015. Pyruvate dehydrogenase kinase 1 participates in macrophage polarization via regulating glucose metabolism. J Immunol 194:6082-9.
411. Taylor-Mulneix DL, Hamidou Soumana I, Linz B, Harvill ET. 2017. Evolution of Bordetellae from Environmental Microbes to Human Respiratory Pathogens: Amoebae as a Missing Link. Front Cell Infect Microbiol 7:510.
412. Correia AM, Ferreira JS, Borges V, Nunes A, Gomes B, Capucho R, Goncalves J, Antunes DM, Almeida S, Mendes A, Guerreiro M, Sampaio DA, Vieira L, Machado J, Simoes MJ, Goncalves P, Gomes JP. 2016. Probable Person-to-Person Transmission of Legionnaires' Disease. N Engl J Med 374:497-8.
413. Sharaby Y, Nitzan O, Brettar I, Hofle MG, Peretz A, Halpern M. 2019. Antimicrobial agent susceptibilities of *Legionella pneumophila* MLVA-8 genotypes. Sci Rep 9:6138.

414. Ensminger AW, Yassin Y, Miron A, Isberg RR. 2012. Experimental evolution of *Legionella pneumophila* in mouse macrophages leads to strains with altered determinants of environmental survival. PLoS Pathog 8:e1002731.

Appendix 1. List of genes deleted in each genomic region and their homologs in Philadelphia-1 strain.

A

Gene	Name	Homolog	E value*
LPW_00071	**Rav A**	**hypothetical protein lpg0008**	**0**
LPW_00081		host factor-I protein for bacteriophage Q beta	2.00E-58
LPW_00091		GTP binding protein HflX	0
LPW_00101		thiol-disulfide oxidoreductase	2.00E-114
LPW_00111	**CegC1**	**hypothetical protein lpg0012**	**0**
LPW_00121		pirin	0
LPW_00131		transmembrane protein	0
LPW_00141		multidrug resistance protein	0
LPW_00151		hypothetical protein lpg0016	0
LPW_00161		hypothetical protein lpg0017	0
LPW_00171		outer membrane efflux protein	0
LPW_00181		multidrug-efflux system transmembrane protein	3.2
LPW_00191		hemagglutinin/protease, zinc metalloprotease	0
LPW_00201		hypothetical protein lpg0020	0
LPW_00211		hypothetical protein lpg0021	1.00E-111
LPW_00221		**23S rRNA m(2)G2445 methyltransferase**	**0**

B

Gene	Name	Homolog	E value*
LPW_04831	**ankY/legA9**	**hypothetical protein lpg0401**	**3.00E-144**
LPW_04841	**ankG/an**	**ankyrin repeat-containing protein**	**0**
LPW_04851		amino acid antiporter	0
LPW_04861		**hypothetical protein lpg0405**	**3.00E-125**

C

Gene	Name	Homolog	E value*

LPW_11451	**Lem4**	**hypothetical protein lpg1101**	**0**
LPW_11461		hypothetical protein lpg1102	0
LPW_11471		hypothetical protein lpg1103	0
LPW_11481		hypothetical protein lpg1104	0
LPW_11491		methionine sulfoxide reductase B	1.00E-122
LPW_11501		**hypothetical protein lpg1106**	**0**
LPW_11511		amino acid permease	3.2
LPW_11521		transporter family protein	3.00E-91
LPW_11531	**ravL**	**lipase**	**0**
LPW_11541		hypothetical protein lpg1109	1.00E-142
LPW_11551		hypothetical protein lpg1109	0
LPW_11561		hypothetical protein lpg2171	1.80E+00
LPW_11571	**Lem5**	**hypothetical protein lpg1110**	**2.00E-154**
LPW_11581	**RavN**	**hypothetical protein lpg1111**	**3.00E-148**

D

Gene	Name	Homolog	E value*
LPW_16861	**legL3**	**hypothetical protein lpg1660**	**0**
LPW_16871		**hypothetical protein lpg1661**	**0**
LPW_16881		transporter	4.00E-106
LPW_16891		hypothetical protein lpg1663	4.00E-120
LPW_16901		penicillin binding protein 1C	0
LPW_16911		hypothetical protein lpg1665	0
LPW_16921		**hypothetical protein lpg1666**	**0**
LPW_16931		**hypothetical protein lpg1667**	**0**
LPW_16941		hypothetical protein lpg1668	0
LPW_16951		hypothetical protein lpg2087	0.55
LPW_16961		alpha-amylase	0
LPW_16971		**hypothetical protein lpg1670**	**0**

E

Gene	Name	Homolog	E value*
LPW_19951	**lem16**	**hypothetical protein lpg1947**	**7.00E-157**
LPW_19961	**lem17**	**hypothetical protein lpg1949**	**0.00E+00**
LPW_19971	**ralF**	**guanine nucleotide exchange protein**	**0.00E+00**
LPW_19981		mercuric reductase	2.30E+00
LPW_19991		hypothetical protein lpg1969	3.70E-01
LPW_20001		transposase (ISSod13)	6.00E-14
LPW_20011		hypothetical protein lpg1370	1.80E-01
LPW_20021		hypothetical protein lpg1951	0.00E+00
LPW_20031		3',5'-cyclic-nucleotide phosphodiesterase	0.00E+00
LPW_20041	**legC4**	**hypothetical protein lpg1953**	**0.00E+00**
LPW_20051		hypothetical protein lpg1954	1.00E-137
LPW_20061		permease	0.00E+00
LPW_20071		chloromuconate cycloisomerase	0.00E+00
LPW_20081		EbhA protein	0.00E+00
LPW_20091	**ltpG**	**ankyrin repeat-containing protein**	**4.30E-01**
LPW_20101		hypothetical protein lpg1959	0.00E+00
LPW_20111	**lirA**	**hypothetical protein lpg1960**	**0.00E+00**
LPW_20121		hypothetical protein lpg1961	0.00E+00
LPW_20131	**lirB**	**peptidyl-prolyl cis-trans isomerase**	**2.00E-132**
LPW_20141	**lirE/pieC**	**hypothetical protein lpg1965**	**0.00E+00**
LPW_20151	**lirF/pieD**	**hypothetical protein lpg1966**	**0.00E+00**
LPW_20161		malonyl CoA-ACP transacylase	1.80E-01
LPW_20171		TetR family transcriptional regulator	2.00E-131
LPW_20181		hypothetical protein lpg1968	2.00E-163
LPW_20191		hypothetical protein lpg1832	1.58E-01
LPW_20201	**pieE**	**hypothetical protein lpg1969**	**0.00E+00**

F

Gene	Name	Homolog	E value*
LPW_23101		**calmodulin-dependent protein kinase**	**0.00**
LPW_23111		LysR family transcriptional regulator	0.00
LPW_23121		pyridoxamine 5'-phosphate oxidase	3.00E-131
LPW_23131		MarR family transcriptional regulator	3.00E-87
LPW_23141		glucose-1-dehydrogenase	0.00
LPW_23151		hypothetical protein lpg2142	6.00E-32
LPW_23161		rhodanese domain-containing protein	4.70
LPW_23171		hypothetical protein lpg2143	0.00
LPW_23181		**F-box protein**	**4.00E-124**
LPW_23191		two component response regulator protein	2.00E-84
LPW_23201		response regulator TutC	0.00
LPW_23211		**hypothetical protein lpg2147**	**0.00**
LPW_23221		**hypothetical protein lpg2148**	**0.00**
LPW_23231		**hypothetical protein lpg2149**	**2.00E-79**
LPW_23241		hypothetical protein lpg2150	5.00E-118
LPW_23251		aminoglycoside 6-adenylyltransferase	0.00
LPW_23261		multidrug resistance ABC transporter ATP-binding	0.00
LPW_23271		**Sid related protein-like**	**0.00**
LPW_23281		**Sid related protein-like**	**0.00**
LPW_23291		**hypothetical protein lpg2155**	**0.00**
LPW_23301		**Sid related protein-like**	**0.00**
LPW_23311		N/A	
LPW_23321		N/A	
LPW_23331		**Sid related protein-like**	**0.00**
LPW_23341		hypothetical protein lpg2158	3.00E-150
LPW_23351		hydroxyneurosporene (C20) methyltransferase CrtF	0.00

LPW_23361		hypothetical protein lpg2160	0.00
LPW_23371		hypothetical protein lpg012	4.50
LPW_23381		hypothetical protein lpg2161	0.00
LPW_23391		hypothetical protein lpg2162	3.00E-151
LPW_23401		AraC family transcriptional regulator	0.00
LPW_23411		sensory box protein	0.75
LPW_23421		hypothetical protein lpg2164	6.00E-96
LPW_23431		sulfatase	0.68
LPW_23441		hypothetical protein lpg2165	2.00E-92
LPW_23451		**hypothetical protein lpg2166**	**0.00**
LPW_23461		**DeoR family transcriptional regulator**	**6.00E-161**
LPW_23471		acetyltransferase	1.00E-82
LPW_23481		acetyltransferase	1.00E-52
LPW_23491		hypothetical protein lpg2169	4.00E-89
LPW_23501		hypothetical protein lpg2170	5.00E-142
LPW_23511		LuxR family transcriptional regulator	2.00E-18
LPW_23521		conjugative transfer: assembly	0.15
LPW_23531		ribosomal large subunit (23S rRNA) pseudouridine	0.16
LPW_23541		hypothetical protein lpg2128	8.00E-05
LPW_23551		(2-pyrone-4,6-)dicarboxylic acid hydrolase	1.00E-173
LPW_23561		**sphingosine-1-phosphate lyase I**	**0.00**

G

Gene	Name	Homolog	E value*
LPW_26241	**ceg29**	**hypothetical protein lpg2409**	**0**
LPW_26251		sensor histidine kinase	1.00E-86
LPW_26261	**vpdA**	**patatin-like phospholipase**	**0**
LPW_26271		N/A	
LPW_26281	**lem24**	**hypothetical protein lpg2411**	**0**

LPW_26291		transposase (ISmav2)	0.59
LPW_26301		beta-lactamase	0
LPW_26311		hypothetical protein lpg2413	2.00E-103
LPW_26321		sulfate transporter	2.8
LPW_26331		hypothetical protein lpg2414	2.00E-65
LPW_26341		transmembrane protein	2.00E-35
LPW_26351	**legA1**	**ankyrin repeat-containing protein**	**0**
LPW_26361		hypothetical protein lpg2417	0
LPW_26371		penicillin-binding protein AmpH	0
LPW_26381		hypothetical protein lpg2419	0
LPW_26391		**hypothetical protein lpg2420**	**1.00E-131**
LPW_26401	**lem25**	**hypothetical protein lpg2422**	**0**
LPW_26411		hypothetical protein lpg2423	0
LPW_26421	**mavG**	**hypothetical protein lpg2424**	**0**
LPW_26431	**mavH**	**hypothetical protein lpg2425**	**2.00E-166**

H

Gene	Name	Homolog	E value*
LPW_26521	**ceg30**	**hypothetical protein lpg2433**	**0**
LPW_26531		**hypothetical protein lpg2434**	**1.00E-117**
LPW_26541		hypothetical protein lpg2435	0
LPW_26551		hypothetical protein lpg2436	2.00E-85
LPW_26561		hypothetical protein lpg0203	6.9
LPW_26571		florfenicol efflux pump	0
LPW_26581		Type IV secretory protein VirB4 components	2.4
LPW_26591		NADPH-dependent FMN reductase domain-containing pro	1.00E-134
LPW_26601		glutathione S-transferase	0
LPW_26611		DNA binding protein	2.00E-113
LPW_26621		PhnB protein	2.00E-100

LPW_26631		hypothetical protein lpg2443	5.00E-134
LPW_26641	**mavI**	**hypothetical protein lpg2444**	**1.00E-135**
LPW_26651		hypothetical protein lpg2445	5.00E-102
LPW_26661		hypothetical protein lpg2446	1.00E-60
LPW_26671		D-alanyl-D-alanine dipeptidase	7.00E-178
LPW_26681		hypothetical protein lpg2450	3.00E-150
LPW_26691		N-hydroxyarylamine O-acetyltransferase	0
LPW_26701	**legA14/ankF/ceg31**	**ankyrin repeat-containing protein**	**0**
LPW_26711		glycosyl transferase	1.6
LPW_26721		hypothetical protein lpg2453	7.00E-85
LPW_26731		acetyltransferase	7.00E-106
LPW_26741		hypothetical protein lpg2455	1.00E-128
LPW_26751	**legA15/ankD**	**ankyrin repeat-containing protein**	**0**
LPW_26761		two component response regulator	6.00E-93
LPW_26771		sensory box histidine kinase	0
LPW_26781		guanylate cyclase	1.00E-135
LPW_26791		hypothetical protein lpg2460	2.00E-90
LPW_26801		**hypothetical protein lpg2461**	**2.00E-145**
LPW_26811		hypothetical protein lpg2462	0
LPW_26821		major facilitator family transporter	1.00E-05
LPW_26831		drug:proton antiporter	7.00E-04
LPW_26841		peptide aspartate b-dioxygenase	5.00E-174
LPW_26851	**sidM/drrA**	**hypothetical protein lpg2464**	**0**
LPW_26861	**sidD**	**protein SidD**	**0**

I

Gene	Name	Homolog	E value*
LPW_27241	**mavJ**	**hypothetical protein lpg2498**	**0**
LPW_27251		hypothetical protein lpg1793	6.00E-05

LPW_27261		lysine decarboxylase	1.00E-138
LPW_27271		carbonic anhydrase Mig5	0
LPW_27281		multidrug resistance protein D	0
LPW_27291		hypothetical protein lpg2502	2.00E-51
LPW_27301	**ceg32/sidI**	**hypothetical protein lpg2504**	**0**
LPW_27311		**hypothetical protein lpg2505**	**0**
LPW_27321		sensor histidine kinase/response regulator LuxN	0
LPW_27331		hypothetical protein lpg2507	2.00E-174
LPW_27341	**sdjA**	**hypothetical protein lpg2508**	**0**
LPW_27351	**sdeD**	**hypothetical protein lpg2509**	**0**
LPW_27361	**sdcA**	**hypothetical protein lpg2510**	**0**
LPW_27371	**sidC**	**hypothetical protein lpg2511**	**0**
LPW_27381		RND multidrug efflux transporter MexF	2.00E-87
LPW_27391		RND multidrug efflux transporter MexF	0
LPW_27401		RND multidrug efflux membrane fusion protein	0
LPW_27411		outer membrane efflux protein	0
LPW_27421		structural toxin protein (hemagglutinin/hemolysin)	2.00E-70
LPW_27431		major facilitator family transporter	0
LPW_27441		AsnC family transcriptional regulator	6.00E-112
LPW_27451		**hypothetical protein lpg2518**	**7.00E-78**
LPW_27461	**SnpL**	**hypothetical protein lpg2519**	**2.00E-113**
LPW_27471		hypothetical protein lpg2520	8.00E-86
LPW_27481		hypothetical protein lpg2521	2.00E-31
LPW_27491		metal-activated pyridoxal enzyme	0
LPW_27501	**lem26**	**hypothetical protein lpg2523**	**0**
LPW_27511		LuxR family transcriptional regulator	0
LPW_27521	**mavL**	**hypothetical protein lpg2526**	**0**
LPW_27531		**hypothetical protein lpg2527**	**0**

LPW_27541		alpha-amylase	0
LPW_27551	**lem27**	**hypothetical protein lpg2529**	**0**

Dot/Icm effector-encoding genes were printed in **bold**.

* E value describes the possibility that the homolog in Philadelphia-1 strain was purely by chance.